

Over-expression of DNA methyltransferase MET1 in Arabidopsis creates novel
epi-alleles with heritable expression states

Samuel George Philip Brocklehurst

Submitted in accordance with the requirements for the degree of Doctor of Philosophy

The University of Leeds

School of Biology

September 2017

Intellectual Property and Publication Statement.

The candidate confirms that the work submitted is his own and that appropriate credit has been given where reference has been made to the work of others.

This copy has been supplied on the understanding that it is copyright material and that no quotation from the thesis may be published without proper acknowledgment.

© 2017 The University of Leeds and Samuel George Philip Brocklehurst

Acknowledgements

Firstly, I would like to thank my project supervisor Professor Peter Meyer for his invaluable advice and support, especially for organizing the transcription data. I will always be grateful for the time you have committed to me and the project.

I also wish to thank Iris Heidmann and her team, including Suzan Out and Marieke Ykeme. Their willingness to guide me during the collaboration made gathering data at Enza Zaden infinitely easier. I would especially like to thank Iris for the excellent pictures she captured for this thesis and her support while at Enza.

To the Bioinformatician Dr. Ian Carr for compiling all the transcription data and spending the time and energy required to explain the process and what the data means. Thank you.

Thank you to my fellow lab members past and present. Dr. Michael Watson for his guidance and patience, especially during the early years of my Ph.D. Associate Professor. Valya Vassileva, Dr. Matthew Gentry, Dr. Mohd Ahmad Mokhtar, Elizabeth Hollwey, Susan Marcus and Najiha Mohamed, whose knowledge and friendship, made working much more enjoyable.

I owe a great deal of thanks to my mum and sister Lorraine and Megan Brocklehurst for their love and encouragement. Most of all, thank you to my loving and patient partner Louise Frankland whose support during this Ph.D. is greatly appreciated.

Abstract

DNA methylation marks and histone modifications are important factors involved in regulating gene expression and genome structure. By destabilizing these vital factors we can create novel epi-alleles that are transgenerational. To investigate the potential of destabilizing an epigenetic function, we over-expressed DNA METHYLTRANSFERASE1 (MET1) in both *Arabidopsis* and tomato. In *Arabidopsis thaliana*, MET1 controls maintenance of cytosine methylation at symmetrical CG positions. At certain densely methylated loci, loss of MET1 causes the loss of all cytosine methylation marks. Over-expression of either the catalytically active or inactive versions of MET1 in *Arabidopsis* stochastically generates new epi-alleles at loci encoding transposable elements, non-coding RNAs, and proteins, which mainly results in increased expression. These altered expression states can be transmitted to the next generation, without the need for increased MET1 concentration, but long-term stability differs for individual loci. Destabilizing epigenetic factors in tomato appears to be more sensitive, causing lethality when levels of MET1 are increased at certain stages of development. The over-expression of MET1, or other epigenetic factors, offers an alternative strategy to create novel epi-alleles, identify phenotypes under epigenetic control and determine which genes are epigenetically regulated.

Table of Contents

1	General Introduction.....	12
1.1	An Introduction to Epigenetics	12
1.2	DNA Methylation	14
1.3	De novo DNA methylation	15
1.4	Maintenance of DNA methylation	18
1.5	DNA Demethylation	19
1.6	Histones	21
1.7	The biological function of DNA methylation.....	23
1.8	The structure and novel functions of MET1	25
1.9	Thesis objective.....	27
2	Over-expression of DNA methyltransferase MET1 in Arabidopsis thaliana generates new epialleles with heritable expression states.....	29
2.1	Introduction	29
2.2	Results.....	31
2.2.1	Generating MET1 over-expression lines	31
2.2.2	Phenotypic analysis of the MET1 over-expression lines.....	33
2.2.3	Transcript analysis of the MET1 over-expression lines.....	38
2.2.4	Bisulphite analysis of MET1 over-expression lines	42
2.2.5	Histone analysis of the MET1 over-expression lines.....	45
2.2.6	Heritability of epigenetic changes	48
2.2.7	Protein analysis of over-expressing MET1	52
2.2.8	Genetic analysis of AT5G34850	54
2.2.9	Investigating the phenotypic effects of the four candidate genes.....	55
2.3	Discussion.....	58
3	Investigating the application of over-expressing MET1 in tomato.....	65
3.1	Introduction	65
3.2	Results.....	67
3.2.1	Determining the structure of tomato MET1.....	67
3.2.2	Phenotypic analysis of the tomato ArMET1 over-expression lines	68
3.2.3	Transcript analysis of MET1 over-expression in tomato.....	73
3.3	Discussion.....	78
4	General discussion	80
4.1	Over-expression of MET1 induces heritable epigenetic diversity	80
4.2	Investigating the tomato epigenome	82
4.3	Outlook and open questions.....	83

4.3.1	Linking phenotypic change to alternatively expressed epi-alleles	83
4.3.2	Using an inducible system to over-express MET1	83
4.3.3	Investigating the protein interactions of MET1	84
4.3.4	The function of the MET1 homologs	85
4.3.5	Epigenetic changes induced by transformation	85
5	Materials and Methods.....	86
5.1	Materials	86
5.1.1	Arabidopsis material	86
5.1.2	Solanum lycopersicum material.....	87
5.1.3	Bacterial strains.....	87
5.2	Primer list.....	87
5.3	Construction of plasmids and plant transformation.....	89
5.3.1	Over-expression Constructs	89
5.3.2	Arabidopsis transformation by floral dip	89
5.3.3	Leaf disc transformation of Solanum lycopersicum.....	90
5.4	Agrobacterium protocols	91
5.4.1	Agrobacterium tumefaciens GV3101::pMP90 electro-competent cells.....	91
5.4.2	Binary plasmid electroporation Agrobacterium	91
5.4.3	Isolation of plasmid DNA from Agrobacterium tumefaciens GV3101::pMP90	91
5.5	E. coli protocols.....	92
5.5.1	Preparation of chemically competent E. coli	92
5.5.2	Heat-shock transformation	93
5.5.3	Mini-prep isolation of plasmid DNA from E.coli	93
5.6	Phenotypic analysis.....	94
5.6.1	Arabidopsis phenotyping	94
5.6.2	Tomato phenotyping.....	94
5.7	DNA Protocol.....	95
5.7.1	Isolation of genomic DNA from Arabidopsis.....	95
5.7.2	Restriction digest	95
5.7.3	Ligation reaction	95
5.7.4	Polymerase chain reaction (PCR)	96
5.7.5	Bisulphite analysis	96
5.7.6	DNA sequencing	97
5.7.7	Data analysis	97
5.8	RNA analysis.....	98
5.8.1	Isolation of RNA from plants.....	98

5.8.2	Semi-quantitative PCR	98
5.8.3	Quantitative RT-PCR assay	99
5.8.4	Sequencing and data analysis	99
5.9	Protein analysis	102
5.9.1	ChIP assay.....	102
5.9.2	Western blot assay.....	102
6	References	103
7	Supplementary data.....	122
	Supplementary Table 1	139
	Supplementary Table 2	141
	Supplementary Table 3	147
	Supplementary Table 4	148
	Supplementary Table 5	160
	Supplementary Table 6	163
	Supplementary Figure 1.....	164
	Supplementary Figure 2.....	165
	Supplementary Figure 3.....	166

List of Abbreviations.

5-aza	5-Azacytidine
A	Adenine
AGO	Argonaute
ArMET1	Arabidopsis Methyltransferase 1
BAH	Bromo-Adjacent homology
bp	base pairs
C	Cytosine
CaMV	Cauliflower Mosaic Virus
cDNA	Complementary Deoxyribonucleic acid
CHD	Chromo-Domain
CLE3	Clavata 3
CLE9	Clavata 9
CMT2	Chromomethyltransferase 2
CMT3	Chromomethyltransferase 3
Col	<i>Arabidopsis</i> Columbia
DCL	Dicer-Like
DCM	DNA Cytosine Methyltransferase
DDM1	Decrease in DNA Methylation 1
DME	Demeter
DML	Demeter-Like
DNA	Deoxyribonucleic acid

DNMT1	DNA Methyltransferase 1
DNMT3A	DNA Methyltransferase 3 A
DNMT3B	DNA Methyltransferase 3 B
DNMT3L	DNA Methyltransferase 3-Like
DRM2	Domains Re-Arranged Methyltransferase 2
ds	double stranded
E.coli	Escherichia coli
EDTA	Ethylenediaminetetraacetic acid
FWA	Flowering Wageningen
G	Guanine
GUS	β -Glucuronidase
H3K4me3	Histone 3 lysine 4 trimethylation
H3K9me2	Histone 3 lysine 2 dimethylation
H3K27ac	Histone 3 lysine 27 acetylation
H3K27me3	Histone 3 lysine 27 trimethylation
H4ac	Histone 4 acetylation
HDA6	Histone Deacetylase 6
IAA	Isoamyl Alcohol
KTF1	Kow Domain-Containing Transcription Factor 1
LB	liquid lysogeny broth
LINE	Long Interspersed Nuclear Element
mC	5-methyl-cytosine
MEA	MEDEA

MET1	Methyltransferase 1
met1-1RE	MET1 Restored
METo	Methyltransferase 1 over-expressioning
mRNA	messenger Ribonucleic acid
MS	Murashige and Skoog
NASC	Nottingham Arabidopsis Stock Centre
nc	non-coding
NCBI	National Center for Biotechnology Information
nt	nucleotide
PAP26	Purple Acid Phosphatase 26
PCNA	Proliferating Cell Nuclear Antigen
PCR	Polymerase Chain Reaction
PEV	position effect variegation
PGC	Primordial Germ Cells
pi	piwi-interacting
POLII	RNA Polymerase II
POLIV	RNA Polymerase IV
POLV	RNA Polymerase V
PTGS	Post-Transcriptional Gene Silencing
RdDM	RNA-directed DNA Methylation
rDNA	ribosomal DNA
RDR2	RNA-Dependent RNA Polymerase 2
RDR6	RNA-dependent RNA polymerase 6

RISC	RNA-Induced Silencing Complex
RNA	Ribonucleic acid
ROS	Repressor of Silencing
RPS	Repetitive Petunia Sequence
SAM	S-adenosyl methionine
SaM	Shoot apical Meristem
SDS	Sodium Dodecyl Sulphate
si	small interfering
SNP	Single Nucleotide Polymorphism
SP9D	Self-Pruning 9D
sq	semi-quantitative
SRA	Set and Ring Associated
sup	superman
SUVH4	Suppressor of Variegation 3-9 Homologue 4
T	Thymine
TAE	Tris-acetate-EDTA
T-DNA	Transfer-DNA
TE	Transposable Element
TGS	Transcriptional Gene Silencing
SIMET1	tomato Methyltransferase 1
VCN	Vegetative Cell Nucleus
WT	Wildtype
WUS	Wuschel

1 General Introduction

1.1 An Introduction to Epigenetics

From the beginning when DNA was first identified as a distinct molecule by the Swiss physician Friedrich Miescher in 1869 (Dahm, 2005), to the discovery of the molecular structure and function of DNA in 1953 by Watson and Crick (Watson and Crick, 1953), DNA has established itself as the universal language of life. This led to the founding of the central dogma of molecular biology which describes the transfer of information from DNA to RNA to protein, giving rise to a wide variety of functions. This simplistic view led many scientists to focus solely on protein encoding genes, disregarding over 90% of the human genome leading to the term junk DNA which was believed to have no function or purpose. However, new findings have brought to light the importance of DNA structure, not just DNA sequence, in determining gene expression and development. The importance of genotype determining phenotypic change during development and the interaction between the two led to the coining of the term 'epigenetics' (Waddington, 1942). At the time, however, it was not yet fully understood the significance of epigenetic control and its wider implications in cell development. One of the most powerful metaphors used to illustrate cellular development is the epigenetic landscape (Fig 1.1) introduced by Conrad Waddington (Waddington, 1957).

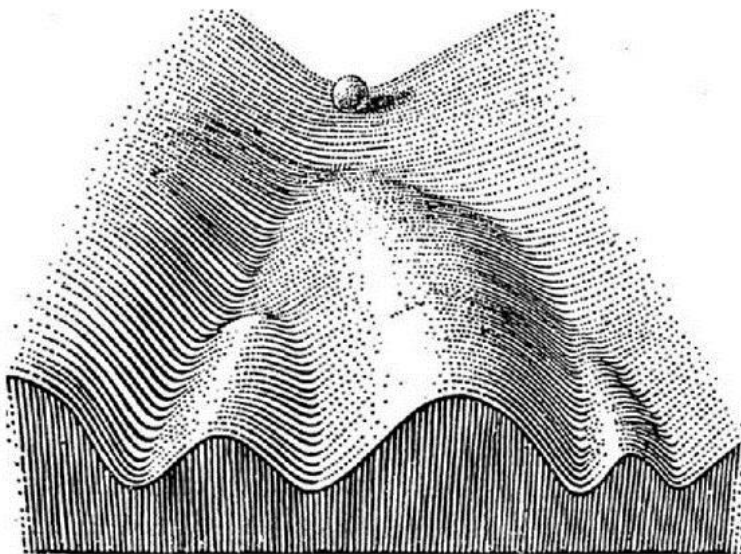


Figure 1.1: Waddington's classic model of an epigenetic landscape. At the top of the landscape is a ball which represents an undifferentiated totipotent cell, the troughs and peaks below portray the countless developmental pathways that the ball can traverse. The further the ball travels down a specific pathway, the more established it becomes in a particular developmental route until the cell becomes fully committed to its fate.

Over time the term epigenetics has been redefined as the study of internal factors and external stimuli leading to a heritable change in gene expression that is independent of alterations in the DNA sequence (Dupont *et al.*, 2009). This can occur as post-transcriptional gene silencing (PTGS) which involves the cleavage of mRNAs directed by short interfering RNA (siRNAs), or as transcriptional gene silencing (TGS). The mechanism of TGS is primarily regulated by the structural organisation of the genome. In eukaryotes, the genomic structure is comprised of an eight histone protein wound by DNA twice to form a nucleosome. This, in turn, forms the fundamental repeating unit that structures the genome. Covalent marks such as acetylation and methylation at the N-terminal tails of histone proteins have the ability to alter the structural conformation of chromatin into a tightly packed and repressed heterochromatic state, or a more open transcriptionally active euchromatic state. Methylation marks are another important layer of epigenetic control which involves the transfer of a methyl group (-CH₃) from S-adenosyl methionine (SAM) to a cytosine residue. These epigenetic modifications must adhere to two fundamental rules. The alteration must be reversible in the sense that the original structure can be recovered; conversely, the modifications should be heritable so that the epi-alleles generated are stable following cell division, and even span multiple generations. The ability of epigenetic modifications to work independently or coordinate between each other is essential genome regulation. This includes position effect variegation (PEV) (Muller, 1930), paramutations (Brink, 1959), transgene silencing (Napoli *et al.*, 1990; Meyer *et al.*, 1992) and imprinting (DeChiara *et al.*, 1991).

1.2 DNA Methylation

From Prokaryotes to Eukaryotic organisms the genetic code is highly conserved. However, the epigenetic strategies implemented to regulate the genome are often very different. For example, DNA methylation in bacteria occurs at nitrogen 6 of adenine (m^6A), carbon 5 of cytosine (m^5C) and in some cases nitrogen 4 of adenine (m^4A). DNA methylation in bacteria is used as a defence mechanism against foreign DNA. The methylated genome prevents cleavage from endonucleases, unlike unmethylated invading phage genomes which are readily degraded (Casadesus & Low, 2006).

In eukaryotes, the most prominent type of methylation is cytosine methylation, which in vertebrates accounts for nearly 100% of all methylated loci. In the mammalian system, methylation is found exclusively at the carbon 5 of cytosine, and this epigenetic modification is present throughout the whole genome. At gene promoters (Larsen *et al.*, 1992) and origins of replication (Antequera & Bird, 1999) unmethylated regions can be found with higher than average CG content called CpG islands (Cooper *et al.*, 1983) which function as a genomic platform for regulating transcription. In mammals, DNA methylation is located at cytosines in a CG sequence context, with the exception of embryonic stem cells, where methylation is found at cytosines in CA and CT sequence contexts (Ramsahoye *et al.*, 2000).

In plants, DNA methylation can occur in CG, CHG and CHH sequence contexts (where H represents A, C or T). Establishment and maintenance of methylation in these three specific contexts requires the particular action of one of three methyltransferases; *DOMAINS REARRANGED METHYLTRANSFERASE 2 (DRM2)*, *METHYLTRANSFERASE 1 (MET1)* and *CHROMOMETHYLASE 3 (CMT3)*. *DRM2* is a homologue of the mammalian DNA methyltransferase DNA METHYLTRANSFERASE 3 (*DNMT3*) and is responsible for *de novo* methylation in all sequence contexts (Cao *et al.*, 2003). *MET1* is a homolog of the mammalian DNA methyltransferase DNA METHYLTRANSFERASE 1 (*DNMT1*), that is responsible for maintenance of CG methylation during DNA replication (Jones *et al.*, 2001). *CMT3* is another maintenance methyltransferase that is plant specific and is required for CHG methylation (Lindroth *et al.*, 2001). While these enzymes seem to have specific roles, there are studies that demonstrate their ability to coordinate or compete at specific

genomic regions. One example would be the maintenance of non-CG methylation which is carried out by both CMT3 and DRM2 via small interfering RNA (siRNA) (Cao *et al.*, 2003). In a *met1* mutant, methylation is lost in all three sequence contexts (Stroud *et al.*, 2013). Though loss of CHG methylation is possibly due to the loss of chromatin marks required for CMT3 binding (Soppe *et al.*, 2002; Tariq *et al.*, 2003), the loss of CHH marks remain unclear, but may reflect a failed interaction between CMT3 and DRM2, or a direct role of MET1 in CHH methylation targeting.

1.3 De novo DNA methylation

De novo methylation is described as the addition of a methyl group to a cytosine base, that had been previously unmethylated. It was first identified from studies in tobacco when an RNA viroid containing a high level of secondary structures was shown to direct methylation to homologous transgenic sequences (Wassenegger *et al.*, 1994). In mammals, there is an escalation of *de novo* methylation that occurs during two stages of development. During early embryogenesis, there is a universal removal of epigenetic markers shortly after fertilisation. This mechanism allows for a wave of *de novo* methylation to generate new methylation patterns (Reik *et al.*, 2001), and silence one copy of the X-chromosome in females (Goto & Monk, 1998). During gametogenesis, there is a significant increase in the levels of *de novo* methylation which establishes DNA methylation at transposable elements (TE) and imprinted genes (Chen *et al.*, 2003). The majority of the *de novo* methylation processes are catalysed by DNA METHYLTRANSFERASE 3A (DNMT3A) and DNA METHYLTRANSFERASE 3B (DNMT3B) which are guided by PIWI-like ARGONAUTE (AGO) proteins and PIWI-interacting RNA (piRNA). Although DNMT3A & B play different roles, they both have the ability to catalyse both CG and non-CG methylation. The major role of DNMT3A is the establishment of genomic imprinting, while DNMT3B serves to catalyse *de novo* methylation of repetitive centromeric DNA to increase the stability of the genome.

Unlike mammals, plants do not undergo an extensive reprogramming of DNA methylation but appear to have a stable methylation pattern. Plants have two distinct pathways which they can employ to target cytosine residues for methylation. The two pathways that control *de novo* methylation are the RNA-directed DNA methylation pathway (RdDM) and the independent pathway. DOMAINS REARRANGED METHYLTRANSFERASE 2 (DRM2), a homologue of the mammalian methyltransferase DNMT3A is highly regulated by the RdDM pathway which is responsible for *de novo* methylation. The RdDM pathway utilises siRNA in order to target *de novo* methylation in a sequence-specific manner to regulate various epigenetic activities. The generation of a diverse range of siRNAs for targeting requires a variety of plant-specific proteins and enzymes. Precursor dsRNA is generated by plant-specific RNA-DEPENDENT RNA-POLYMERASE 2 (RDR2) which synthesises the complementary strand of RNA POLYMERASE IV (PolIV) transcripts. Furthermore, dsRNA can be produced by the RNA POLYMERASE II (PolII) which produces transcripts derived from inverted repeats or over-lapping antagonistic regions. The generated dsDNA is recognised by DICER-LIKE (DCL) for cleavage into siRNAs. In total plants contain four DCL proteins, the first being DCL1 which is associated with the production of microRNAs (miRNA) (Henderson *et al.*, 2006). DCL3 is the primary protein involved in cleavage of dsRNA into 21-24nt siRNAs, although DCL2 and DCL4 have some overlapping function (Xie *et al.*, 2004). These 21-24nt, small RNA duplexes are in turn stabilised by ribose methylation at the 3' terminal catalysed by the enzyme HEN1 methyltransferase (Yu *et al.*, 2005). It is believed this modification acts as a two-fold function: firstly to protect the siRNAs from degradation by exonucleases, and secondly, it may help with recognition and loading onto ARGONAUTE (AGO) complexes (Yu *et al.*, 2005). In *Arabidopsis*, there are ten AGO proteins present, of these, three (AGO4, AGO6 and AGO9) are known to associate with 24nt siRNAs and have a preference for siRNAs with a 5' terminal adenosine (Mi *et al.*, 2008; Havecker *et al.*, 2010). The mature siRNA is loaded onto an AGO4- RNA-induced silencing complex (RISC) or AGO6-RISC (Li *et al.*, 2006) which is facilitated by KOW DOMAIN-CONTAINING TRANSCRIPTION FACTOR 1 (KTF1) (He *et al.*, 2009). The AGO4 complex is then targeted to a specific site through the use of the PolIV scaffold complexes (Wierzbicki *et al.*, 2009), which allows the AGO4 complex to direct DRM2 to the particular site (Wierzbicki *et al.*, 2009), for targeted *de novo* methylation (Fig. 1.2).

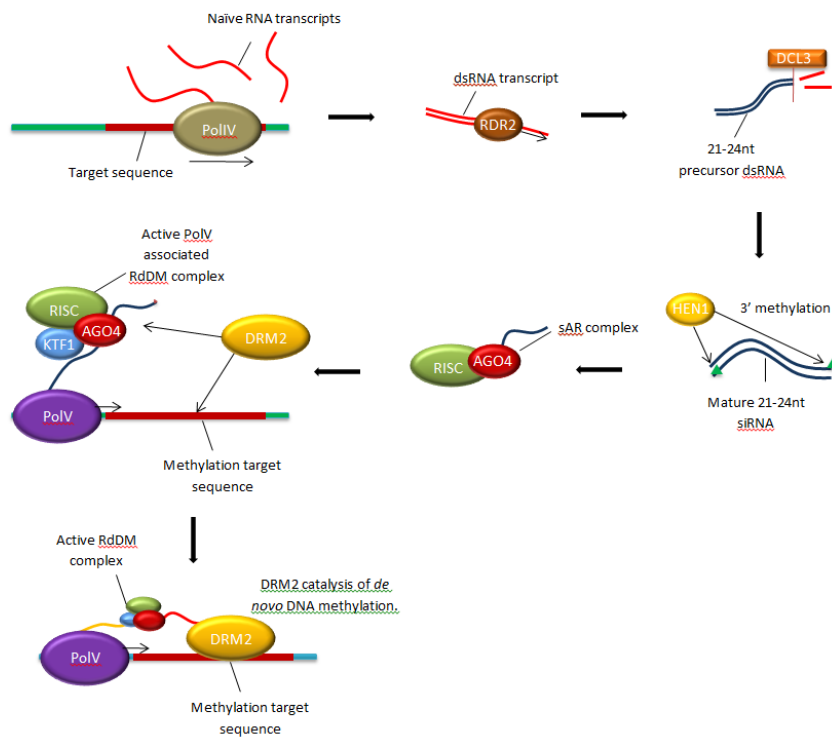


Figure 1.2: RNA dependent DNA *de novo* methylation. Pol IV transcribes ssRNA that is copied into a dsRNA by RDR2. DCL3 processes the dsRNA into 24-nucleotide siRNAs. HEN 1 then methylates the 3' ends of the siRNA to be incorporated into the AGO4-RISC complex. Pol V transcribes a scaffold that base-pairs with the AGO4-bound siRNAs. The AGO4-RISC complex is recruited via Pol V to create a complex with KTF1, which binds the non-coding nascent PolIV transcripts. AGO4 links DRM2, which catalyses *de novo* methylation of DNA.

Despite, RdDM pathways ability to direct *de novo* methylation at all three-sequence context, there is an alternate path independent of siRNAs that can *de novo* methylate at CHH sites.

This alternative pathway requires CMT2 (Zemach *et al.*, 2013). It is hypothesised that the targeting of CMT2 to CHH regions occurs through interaction with the dimethylation of lysine 9 on histone 3 (H3K9me2) via its chromodomain and not siRNA (Pikaard, 2013).

1.4 Maintenance of DNA methylation

Once methylation has been established, it must be maintained. In mammals, the responsibility of CG methylation maintenance is carried out by DNMT1. DNMT1's primary function is the maintenance of DNA methylation lost during semi-conservative replication. To ensure the faithful duplication of methylation patterns, a range of histone modifications and proteins have evolved allowing DNMT1 to actively associate with the replication foci during S-phase (Fig 1.3). DNMT1 functions to restore hemimethylated DNA during semi-conservative replication to its fully methylated state (Kim *et al.*, 2009). Studies have shown that the C-terminal catalytic domain of DNMT1 is recruited to the replication fork via PROLIFERATING CELL NUCLEAR ANTIGEN (PCNA) elements found at the replication foci (Chuang *et al.*, 1997). Other chromatin-associated proteins, such as the multi-domain protein UHRF1 assist in the stable association of DNMT1 to hemimethylated DNA during replication. The PCNA/ DNMT1 interaction along with the activity of UHRF1 enhances DNMT1 affinity for hemimethylated DNA. This function allows DNMT1 to recognise and replicate the methylation pattern from the parent strand to the daughter strand as they are generated during semi-conservative replication (Mortusewicz *et al.*, 2005).

Like DNMT1 the primary function of MET1 is the maintenance of methylation patterns during semi-conservative replication. The mechanism by which MET1 targets the replication foci is believed to be similar in manner to DNMT1 targeting (Fig 1.3). MET1 binds to hemimethylated DNA mediated by VARIANT IN METHYLATION (VIM) proteins. These contain the Set and Ring associated (SRA) domain that binds methylated Cytosine residues (Woo *et al.*, 2008). The VIM1 protein also interacts with histone modifications (H2B, H3, H4, and HTR12) suggesting that the protein acts as a DNA methylation-histone interface. At heterochromatic regions, an SWI/SNF family chromatin remodelling factor, DECREASE IN DNA METHYLATION 1 (DDM1) allows access to the target area allowing MET1 to bind (Woo

et al., 2007). Once MET1 has attached, the parent DNA strand is utilised during semi-conservative replication to reproduce the methylation pattern onto the newly synthesised daughter strand.

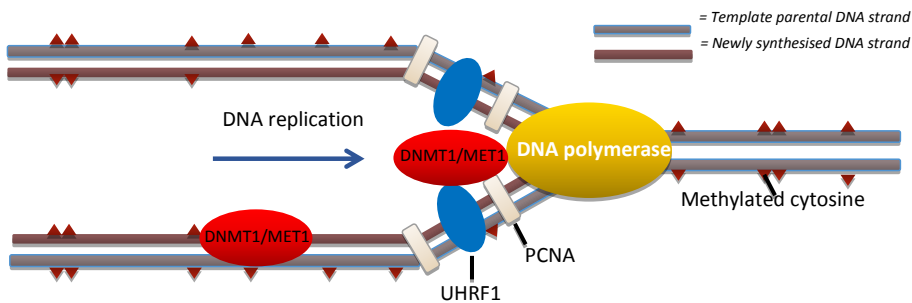


Figure 1.3: Model is depicting the maintenance of CG methylation during replication in both plants and mammals. DNMT1 is believed to be recruited to the replication foci through UHRF1 which specifically interacts with hemimethylated DNA as well as with PCNA. After being recruited, DNMT1 functions to maintain methylation patterns by restoring the hemimethylated DNA to a fully methylated state. In plants, MET1 and the VIM family of SRA domain proteins, which are homologues of DNMT1 and UHRF1, respectively, are likely to function in a similar manner to maintain CG methylation patterns.

1.5 DNA Demethylation

Epigenetic modifications must be reversible, but for such an important role there is little documentation how active demethylation is carried out and the underlying mechanisms that are involved. There are two ways methylation can be removed; passive demethylation and active demethylation. Passive demethylation of genomic regions occurs via the loss of

function of maintenance enzymes, leading to a global loss of methylation following cell division. An example of passive DNA demethylation can be observed in MET1 mutants which possess a global loss of methylation in all three sequence contexts (Kankel *et al.*, 2003). In plants, active demethylation removes methylated cytosines (5-mC) directly excised via the base excision repair process carried out by REPRESSOR OF SILENCING 1 (ROS1), DEMETER (DME), DEMETER like 2 (DML2) and DML3 (Penterman *et al.*, 2007; Zhu, 2009). Each of the four enzymes can remove 5-mC in all sequence contexts, although preferential removal of specific substrates is debated (Agius *et al.*, 2006; Gehring *et al.*, 2006; Morales-Ruiz *et al.*, 2006; Penterman *et al.*, 2007). In addition to hydrolysing the glycosidic bond between the cytosine and sugar-phosphate backbone, they can also nick the DNA backbone at the abasic site via apurinic/apyrimidinic (AP) lyase activity (Bruner *et al.*, 2000; Jiricny, 2002). During removal of 5-mC, these enzymes simultaneously glycosylates the 5-methylcytosine base and cleaves the DNA backbone, generating a single-nucleotide gap that induces the base excision repair pathway, eventually refilling it with an unmethylated cytosine.

In vegetative cells, ROS1, DML2 and DML3 remove DNA methylation at the 5' and 3' ends of genes in a sequence-specific context (Penterman *et al.*, 2007). ROS1 offsets the DNA methylation established by RdDM, to prevent hypermethylation and the spreading of DNA methylation via the self-reinforcement mechanisms that could lead to adverse gene silencing. DNA methylation and DNA methyltransferases may act as feedback mechanisms that play a role in establishing and regulating ROS1 demethylation (Mathieu *et al.*, 2007; Williams *et al.*, 2015). When DNA methylation levels are reduced in a *met1* mutant or treated with DNA methylation inhibitors, ROS1 levels are down-regulated (Mathieu *et al.*, 2007). However, it is still not fully understood how plant DNA glycosylases are targeted to specific sequences. One possibility is a RNA-based targeting system. It has been demonstrated that ROS1 co-localises with REPRESSOR OF SILENCING 3 (ROS3), which possesses RNA binding capacity (Zheng *et al.*, 2008).

During gametogenesis, DME is responsible for maternal allele DNA demethylation in the endosperm that establishes gene imprinting (Gehring *et al.*, 2006). Maternal DME also has the ability to change the endosperm methylation landscape completely, demethylating TEs and repeat sequences (Hsieh *et al.*, 2009). In the central cell during female gametogenesis, the levels of MET1 are reduced (Jullien *et al.*, 2008), and DME levels are increased (Choi *et*

al., 2002), culminating in the global loss of DNA methylation via both passive and active demethylation.

Although demethylation directly removes methylation modifications, it may also lead to modifications of the chromatin before or during the removal of 5-mC. A histone acetyltransferase INCREASED DNA METHYLATION 1 (IDM1) was identified as a regulator of DNA demethylation in *Arabidopsis* (Qian, W. *et al.*, 2012). IDM1 recognises chromatin regions with CG methylation and low histone 3 lysine 4 (H3K4). ROS1 and IDM1 interact with each other and appear to function in the same pathway for DNA demethylation, albeit only a portion of ROS1 targets are regulated by IDM1. Currently, it is uncertain how ROS1 is recruited to the modified chromatin, but the discovery that there is interplay between IDM1 and ROS1 suggests that histone modifications and chromatin structure may play a role in active DNA demethylation. Maintenance of CHG methylation can be impaired by INCREASE IN BONSAI METHYLATION 1 (IBM1), which is a histone demethylase that prevents H3K9 methylation (Saze *et al.*, 2008; Miura *et al.*, 2009), further supporting this theory.

1.6 Histones

Chromatin is made up of the basic structural unit, the nucleosome, which consists of a 146-bp fragment of DNA that's wrapped almost twice around a protein octamer which is comprised of a histone H3-H4 tetramer and two H2A-H2B dimers (Kornberg, 1974; Richmond *et al.*, 1999; Wolffe and Guschin, 2000). Each histone protein possesses an N-terminal tail which allows for a variety of modifications such as methylation, acetylation, ubiquitination or phosphorylation of specific amino acids which can alter the conformational state of chromatin, essential for gene regulation. An example of a histone modification creating a conformational change is acetylation of lysine residues. One of the primary 'active' modifications is acetylation of the N-terminal tail which neutralises the positive charge on the ϵ amino group which acts as a binding site for the bromodomain-containing proteins, leading to a more open and active euchromatic state (Taverna *et al.*, 2007).

Methylation of lysine residues are a more complex epigenetic mark, that can either silence transcription or activate chromatin domains, depending on which lysine residues are methylated and the degree of methylation. The overall charge of the histone tail is not

Commented [CW1]: Remove initials from refs

affected by lysine methylation, but an increase in hydrophobicity may allow intra- or intermolecular interactions between proteins or the modification alters the conformational structure allowing proteins to bind preferentially to the methylated domain (Du *et al.*, 2012; Lanouette *et al.*, 2014). Typically, histone H3K9 and H3K27 methylation are associated with repressed regions, whereas H3K4 methylation is associated with a more active open chromatin structure (Berger, 2007). In *Arabidopsis*, SET domain proteins are responsible for modulating lysine methylation, which can be classified into four distinct groups: SU(VAR)3–9, ENHANCER OF ZESTE (E(Z)) homologs, TRITHORAX (TRX) groups, and ABSENT, SMALL, OR HOMEOTIC DISCS 1 (ASH1) (Baumbusch *et al.*, 2001).

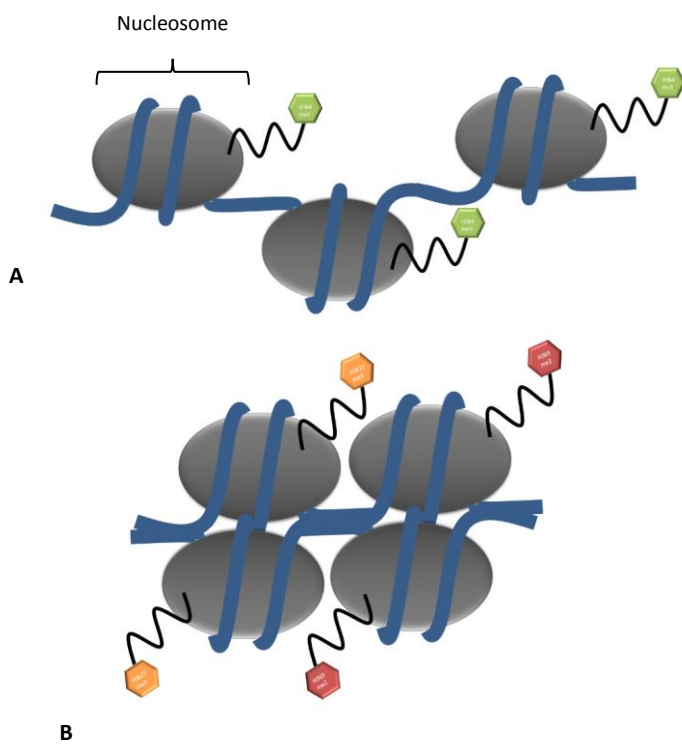


Figure 1.4: The different conformational structures of chromatin. A) Euchromatic structure of histones with the active modification H3K4me3 at the N-terminal tail. B) Heterochromatic structure of histone with the repressive marks H3K9me2 and H3K27me3.

It has been well documented that there is a complex interplay between DNA methylation and the methylated H3K9 modification. In *kyp/suvh4* mutants, H3K9me2 is reduced, leading to a loss of CHG methylation catalysed by CMT3 (Jackson *et al.*, 2002). Transposable elements were also identified as common targets for both KYP/SUVH4 and CMT3 using expression profiling (Tran *et al.*, 2005), and CHROMATIN IMMUNOPRECIPITATION (ChIP) analysis revealed a high correlation between H3K9me2 and CHG methylation (Bernatavichute *et al.*, 2008). These results indicate that maintenance of non-CG methylation requires H3K9 methylation and is critical for preservation of genome stability and transcriptional repression. DNA methylation can also reinforce histone methylation in a positive feedback loop. In a *met1* mutant where CG levels are diminished, a decrease in H3K9me2 is observed at 180bp centromeric repeats and transposable elements (Johnson *et al.*, 2002; Tariq *et al.*, 2003).

1.7 The biological function of DNA methylation

DNA methylation is essential for a number of cellular functions including gene expression, cell differentiation, regulation of transposable elements and even plant immunity (Choi *et al.*, 2002; Chan *et al.*, 2006; Agorio and Vera, 2007). DNA methylation present at gene promoters are commonly associated with transcriptional silencing, by directly obstructing transcription factors, and recruiting methyl-binding proteins that can modify the histone tail altering the chromatin structure. Methylation of DNA in all three-sequence context “dense methylation” is often found at TEs to prevent activation and mobilisation, which would disrupt the genome integrity by inserting into critical regions. One example would be the transposable element ATGP3, a class I TE in the gypsy family, which is not active in either a *cmt3* or *met1* mutant, but does occur in the *ddm1* and *met1 cmt3* double mutant

(Tsukahara *et al.*, 2009). This observation suggests a redundant function of CG and non-CG methylation in the transcriptional silencing of the TEs.

TEs should not be seen as just mobile deleterious mutagens, as they can also have positive regulatory roles. At regions with hypermethylated TEs, a lower meiotic recombination rate is observed compared to hypomethylated low copy number genes, which indicates that DNA methylation can influence the rate of recombination (Melamed-Bessudo & Levy, 2012). In the *ddm1* hypomethylated mutant's recombination rates were analysed in both euchromatin and heterochromatin. It was discovered that the rate of recombination between markers located in euchromatin increased, whereas recombination went unchanged between markers located in heterochromatin. Interestingly it is heterochromatic regions that are most affected by the loss of methylation in the *ddm1* mutant; this suggests that DNA methylation may only act as a repressor of meiotic recombination at euchromatic regions where the chromatin is tightly packed (Melamed-Bessudo & Levy, 2012).

Genomic imprinting a mechanism by which genes are expressed in a parent-specific manner is also mediated by DNA methylation. Imprinting is present throughout the plant kingdom and occurs in the endosperm during seed development (Jahnke & Scholten, 2009). There are many examples of imprinted genes in plants including the *Arabidopsis* *MEA*, *FIS2*, *FIE* (Luo *et al.*, 2000) and *FWA* (Kinoshita *et al.*, 2004) genes, which are all expressed from the maternal alleles of the endosperm. *FWA* is an imprinted gene that is by default, silenced via methylation (Choi *et al.*, 2002). Expression of *FWA* during endosperm development occurs via maternal-specific activation that is dependent on the removal of methylation by *DME*. However, the loss of *MET1* activity induces ectopic *FWA* expression causing late flowering. This observation indicates that maintenance of endosperm-specific and parent of origin-specific *FWA* expression depends on *MET1*. If hypomethylation of *FWA* occurs in embryonic lineages, the *fwa* epigenetic mutation and its associated late-flowering phenotype can be stably inherited over many generations.

Methylation also plays a crucial role in plant immunity by regulating immune response genes. In *Arabidopsis*, crown gall tumours increased levels of *MET1*, *DRM2*, *CMT3*, and *AGO4* transcripts were detected along with a global increase of methylation (Gohlke *et al.*, 2013). These findings indicate that enhanced expression of these epigenetic factors may be part of a plant-induced defence response to prevent *Agrobacterium*-induced tumour

Commented [CW2]: *Et al* in italics in this section

development. Six disease resistance genes carrying repeats in their vicinity were identified to be derepressed in *met1 nrpd2* mutants (Yu *et al.*, 2013). One of these genes, *RESISTANCE METHYLATED GENE 1* (RMG1) possesses two repeats in its promoter, a distal repeat that is strongly methylated in all mC contexts and a proximal repeat that is unmethylated in the wildtype but hypermethylated in *ros1* mutants (Zhu *et al.*, 2007). The hypermethylated repeat in the *ros1* mutant prevents transcriptional activation. This suggests that RMG1 is controlled by a dual and antagonistic mechanism. Basal expression of RMG1 is repressed via siRNA-directed DNA methylation, while active DNA demethylation maintains pathogen-triggered induction by regularly pruning DNA methylation at the boundaries of its proximal repeat, which may contain functional cis-regulatory elements (Deleris *et al.*, 2016).

Currently, the significance of DNA methylation found within the gene bodies is poorly understood. DNA methylation found within the gene is predominantly located in exons especially those found within genes that are longer than average and functionally more important. This observation supports the hypothesis that body methylation may function as a marker allowing enhanced accuracy for splicing, preventing aberrant transcription (Takuno & Gaut, 2012). Since methylation of DNA is considered a repressive mark especially on single copy genes and TEs, it may play a role in the silencing of cryptic promoters found within the gene body (Zilberman *et al.*, 2007).

1.8 The structure and novel functions of MET1

MET1 is structurally similar to that of the mammalian methyltransferase, DNMT1. Both MET1 and DNMT1 have a conserved methyltransferase domain but diverge at the N-terminus responsible for DNA targeting and regulation (Finnegan and Dennis, 1993). The N-terminal domain is connected to the C-terminus via a stretch of alternating glycine–lysine (GK) that acts as a nuclear import mechanism (Vanderkrol and Chua, 1991). Within the N-terminal of MET1, a slight hydrophobic region serves as a replication foci targeting sequence, assisting in MET1 localisation at the replication foci (Hermann *et al.*, 2004). MET1 also contains two BAH domains, that have been demonstrated to interact with histone deacetylase HDA6 and coordinate the maintenance of TE silencing (Liu *et al.*, 2012). The

methyltransferase domain of MET1 contains six highly conserved regions (Fig 1.5). Motifs I and X are responsible for the binding of the methyl donor SAM (Posfai *et al.*, 1989). Motif IV contains an invariable Pro-Cys dipeptide that is the catalytic site of all known C-5 cytosine-specific DNA methylases. Motif VI is responsible for the binding of the methyltransferase domain to the targeted cytosine (Jeltsch, 2006), while motif VIII is believed to negate the negative charge of the DNA backbone via nonspecific association with cytosine residues. Motif IX interacts with the target recognition domain (TRD) located between motif VII and IX. The variable TRD is thought to be responsible for nearly all base-specific interactions with the 5'-GCGC-3' target site (Lee *et al.*, 2002).

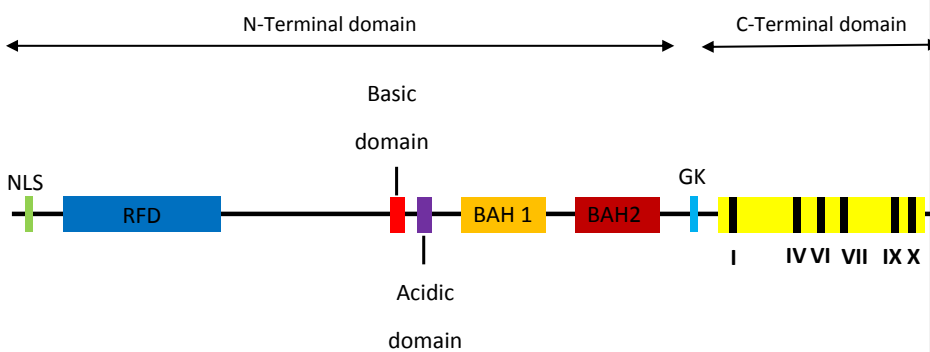


Figure 1.5: The structure of *Arabidopsis* MET1. The positions of the major conserved catalytic motifs at the C-terminus are represented by Roman numerals.

In the literature, the function of MET1 is primarily discussed in the context of its maintenance of CG methylation marks. The role of MET1, however, is not strictly limited to maintenance of CG methylation. At some target loci, it was found that methylation lost from the body of an endogenous target gene in a *met1* mutant, can be partially restored at CG sites when functional MET1 was re-introduced. The target *also* did not require passage through the germline to be re-methylated, suggesting MET1 may have *de novo* activity at CG

sequence contexts (Zubko *et al.*, 2012). It has been observed that MET1 can also influence non-CG methylation. REPETITIVE PETUNIA SEQUENCE (RPS) is a repetitive hypermethylated DNA fragment from *Petunia hybrida*, that attracts DNA methylation in all sequence contexts when transferred into *Arabidopsis thaliana*. When the RPS was introduced into a *met1 Arabidopsis* mutant via a genetic cross, a reduction in both CG and non-CG methylation at the RPS was observed. Similarly, both CG and non-CG methylation were eliminated at the RPS when transferred into a *drm2/cmt3* mutant. This suggests that MET1, DRM2 and CMT3 may coordinate with each other to establish methylation at the RPS (Singh *et al.*, 2008).

The novel functions of MET1 further extends histone modification layer of epigenetic control. H3K9 methylation, which associates with transcriptionally repressed heterochromatin, is lost when CG methylation is completely removed in a *met1* mutant (Tariq *et al.*, 2003). Conversely, loss of non-CG methylation in a *cmt3* mutant does not affect H3K9 methylation. When H3K9 methylation is reduced in a *kyp suvh5 suvh6* mutant *Arabidopsis*, there was no significant change in CG methylation, indicating H3K9 methylation is not required for targeting CG methylation (Stroud *et al.*, 2013). Therefore, MET1 and CG methylation may act as a scaffold to directly interact with H3K9 and initiate methylation at the N-terminal tail. The N-terminal domain of MET1 has also been shown to interact directly with the C-terminal domain of HISTONE DEACETYLASE 6 (HDA6) to cooperatively silence TEs and maintain heterochromatic gene silencing (Liu *et al.*, 2012).

1.9 Thesis objective

MET1 does not exclusively act as a CG-specific maintenance methyltransferase; the literature has illustrated that at specific loci MET1 can interact with other methyltransferases to coordinate both CG and non-CG methylation. If MET1 does play a coordinating role, it should involve the direct interaction of MET1 with individual proteins or complexes. Any changes in MET1 concentration, reduction as well as increase, could affect the efficiency and stability of complex formation or interaction with different factors, and could potentially alter epigenetic states at dense methylation regions. Any effect that was induced by protein interaction of MET1 would not necessarily require an increase in MET1

proteins with a functional catalytic activity. To test this model, we over-expressed catalytically active and inactive versions of the *MET1* gene under the control of the 35S promoter. This was tested in both the model organism *Arabidopsis* and a commercially viable crop, *Solanum lycopersicum* (tomato). By over-expressing MET1 I hope to induce heritable epi-alleles at distinct loci with altered gene expression and epigenetic marks, to generate different phenotypes for commercial use.

2 Over-expression of DNA methyltransferase MET1 in *Arabidopsis thaliana* generates new epi-alleles with heritable expression states

2.1 Introduction

DNA methylation influences a number of important processes in plants, including DNA repair (Yao *et al.*, 2012) transcription (Huettel *et al.*, 2007), and recombination (Mirouze *et al.*, 2012), with further implications for genome structure (Kato *et al.*, 2003), plant development (Finnegan *et al.*, 1996) and evolution (Lopez-Maury *et al.*, 2008). The stable changes in expression created by DNA methylation has emerged as a significant factor in shaping phenotypic diversity (Becker *et al.*, 2011; O'Malley and Ecker, 2012). DNA methylation patterns also respond and transform in response to environmental stimuli (Finnegan, 2002), indicating that DNA methylation may act as a molecular switch for evolutionary adaptation of plants to environmental change (Kou *et al.*, 2011). Various biotic (Boyko *et al.*, 2007), and abiotic stress conditions (Kovarik *et al.*, 1997) have been shown to alter the DNA methylation profile, further supporting this model.

In *Arabidopsis*, maintenance of methylation at CG sequences is catalyzed by the maintenance methyltransferase MET1 (Kankel *et al.*, 2003). To further understand the complex roles of MET1, MET1 knockdowns (Finnegan *et al.*, 1996) and knockouts (Kankel *et al.*, 2003) have been created, resulting in global DNA hypomethylation and developmental abnormalities. However, the effects of increasing *MET1* levels and what effect that may have on the global DNA methylation profile have never been assessed in plants. The current dogma states that the sole role of MET1 is to maintain CG methylation if this was truly the case we would predict that over-expression of MET1 would result in continued maintenance of CG methylation. Nevertheless, recent evidence suggests that MET1 functions deviate from the classical CG maintenance model. In a *met1* mutant, it has been observed that at certain loci the methylated histone mark H3K9 is lost, which results in the loss of CHG and CHH methylation marks (Stroud *et al.*, 2013). A reduction in DNA methylation in both CHG and CHH sequences and the change in histone marks in the *met1* mutant, highlights that MET1 has a more complex and diverse function than initially believed. Raising the question, what further roles and functions are MET1 responsible for?

Previous work had confirmed that MET1 does not exclusively act as a CG-specific maintenance methyltransferase. At particular loci, MET1 can act together with other methyltransferases as a central coordinator for both CG and non-CG methylation or 'dense methylation'. Loss of a functional MET1 causes loss of cytosine methylation in all three sequence context at loci that are densely methylated (Singh *et al.*, 2008). This coordinating role of MET1 has been observed in a number of *Arabidopsis* genes with dense DNA, further supporting this model (Watson *et al.*, 2014). While CHH and CHG methylation at these loci are dependent on the chromomethylases CMT2 and CMT3, all methylation marks are lost in a *met1* mutant, highlighting the important coordinating role MET1 plays. This indicates that DNA methylation patterns at particular loci are determined by the joint activity of several DNA methyltransferases that are fundamentally directed by MET1. This may be mediated by epigenetic complexes involving methyltransferases, methylcytosine-binding proteins (Woo *et al.*, 2008), chromatin remodeling factors (Kakutani *et al.*, 1996), and/or histone modifiers (Kelly *et al.*, 2012). MET1 may interact directly and recruit these factors, while other factors are recruited indirectly via epigenetic marks which have been established by the MET1 complex, leading to a change in epigenetic state at some loci and even establishing novel dense methylation at others.

The role of MET1 co-ordinating dense methylation would involve direct interaction with individual proteins or complexes. Any changes in MET1 concentration, reduction as well as increase, could affect the efficiency and stability of complex formation or interaction with different factors, and could potentially alter epigenetic states at dense methylation regions. Any effect that was induced by protein interaction of MET1 would not necessarily require an increase in MET1 proteins with a functional catalytic activity. To test this model, we over-expressed catalytically active and inactive versions of the *MET1* gene under the control of the 35S promoter. We find that at certain loci, over-expression of the *MET1* transgene, can establish new epigenetic marks while removing/reducing the presence of previous marks and alter expression levels which are stably maintained over numerous generations. All of which is independent of the catalytic function of MET1 to methylate.

2.2 Results

2.2.1 Generating MET1 over-expression lines

To investigate the quantitative effects of increased MET1, it was first necessary to produce an over-expression construct. This was accomplished by inserting the *MET1* cDNA sequence into the polylinker region of the plant transformation vector pGreen 0179, that contains the strong constitutive 35S promoter (Fig 2.1A). To analyze methylation-independent effects of overexpressing *met1* in *Arabidopsis*, a second construct was created to over-express MET1 with a mutated active site loop, rendering the MET1 protein catalytically inactive (Fig 2.1B). To inhibit the catalytic function a point mutation in the catalytic region of MET1, GGPPCQGFSGMNRFN, introduced a Cystine/Serine replacement (Hsieh, 1999).

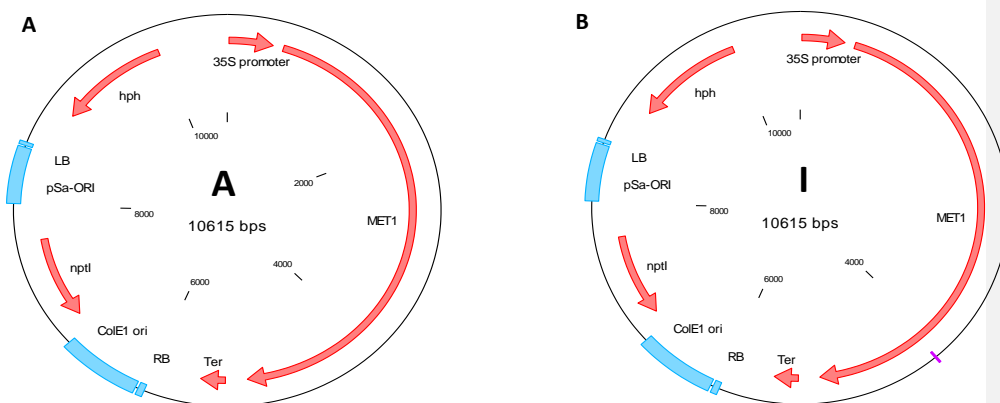


Figure 2.1: Maps of the Active MET1 and Inactive MET1 constructs. A) The MET1 wildtype cDNA sequence was inserted into the plant transformation vector 35S pGreen 0179, to produce the 35S MET1 over-expression construct. B) A mutation was introduced into the 35S MET1 construct to replace a cysteine with a serine codon within the active site. The position of the point mutation is highlighted by the purple marker.

The two transgenic constructs were transferred into *Arabidopsis*, and four transgenic lines were selected; A1 and A2 contained the catalytically active *MET1* cDNA, and I1 and I2 contained the catalytically inactive *MET1* cDNA. If a change in expression at particular loci was observed it was important to determine how stable these changes were if they were heritable over multiple generations or would revert to a wildtype expression state once the *MET1* over-expression (METo) transgene was lost. To investigate heritability, plants from the T2 generation of each line were selected which had retained the transgene (labeled '+') and plants that had lost the transgene (labeled '-') (Fig 2.2).

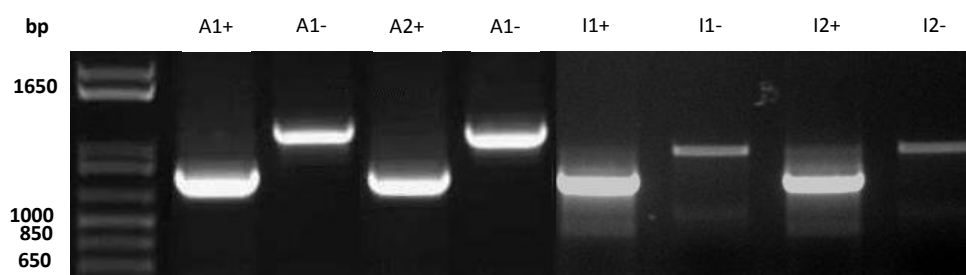


Figure 2.2: Genotyping *Arabidopsis* over-expressing *MET1*. Lines A1 and A2 express a catalytically active *MET1* transgene, lines I1 and I2 express a catalytically inactive *MET1* transgene. The larger bands at 1100 bp indicate the loss of the transgene; the primers were designed to span an intron generating a large band when amplifying wildtype *MET1*. The *Arabidopsis* plant that contains the transgene produces bands at 800 bp as the transgene contains a cDNA insert of *MET1* containing no introns and 1100 bp (WT gene). In plants that contained the transgene, the *MET1* cDNA was preferentially amplified producing a much brighter band than the WT band.

Before proceeding with any further analysis, the overall *MET1* expression levels were examined to ensure the transgene was not silenced (Fig 2.3). In the plants that had retained the transgene, *MET1* transcript levels were increased in all lines that possessed the METo

transgene, with the greatest increase in A2+ and I1+. In lines that had lost the transgene, *MET1* transcript levels had been restored to wildtype levels.

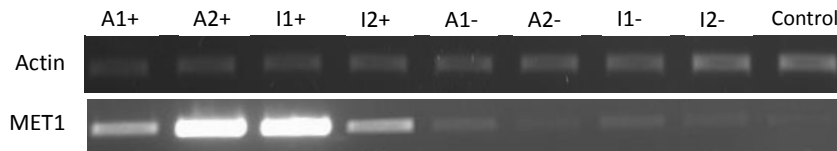
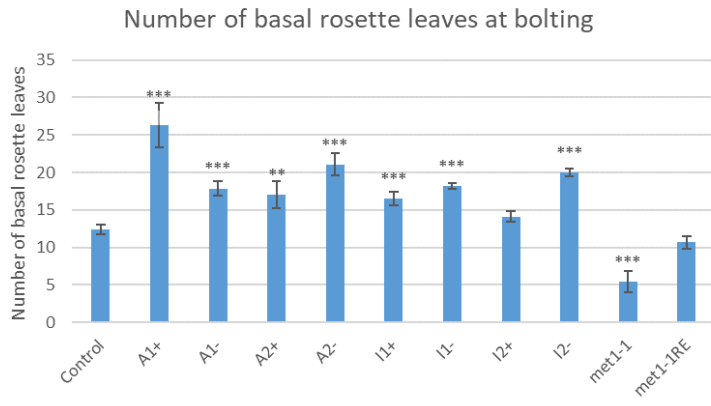


Figure 2.3: Semi-quantitative PCR analysis of the overall *MET1* transcript levels. cDNA was generated from seedlings 4 weeks after stratification. Lines A1 and A2 express a catalytically active *MET1* transgene, lines I1 and I2 express a catalytically inactive *MET* transgene. (+) indicates *MET1* transformants possessing the *MET*₀ transgene. Lines derived from *MET1* transformants, from which the transgene has been removed are labeled (-). Greater *MET1* transcript levels were detected at 24 cycles in lines containing the *MET*₀ transgene. Actin was used as a standardizing control to ensure equal concentration of input cDNA.

2.2.2 Phenotypic analysis of the *MET1* over-expression lines

Once it was established that eight stable *MET*₀ lines had been generated, four of which were homozygous for the *MET*₀ transgene, and four lines that had lost the transgene, it was important to evaluate plant growth. This would allow the rapid screening and evaluation of the different lines and provide information on the plant status, enabling an insight into the potential mechanism underlying the phenotypic differences. The *Arabidopsis met1* mutant has been previously well documented for its phenotypic differences, more specifically its delay in bolting (Ronemus *et al.*, 1996). It was decided to exploit this phenotype as an indication of vegetative development (Fig 2.4). Plants that bolt later should have a larger number of rosette leaves upon bolting, due to greater resources and developmental time in the vegetative state (Kankel *et al.*, 2003).

A



B

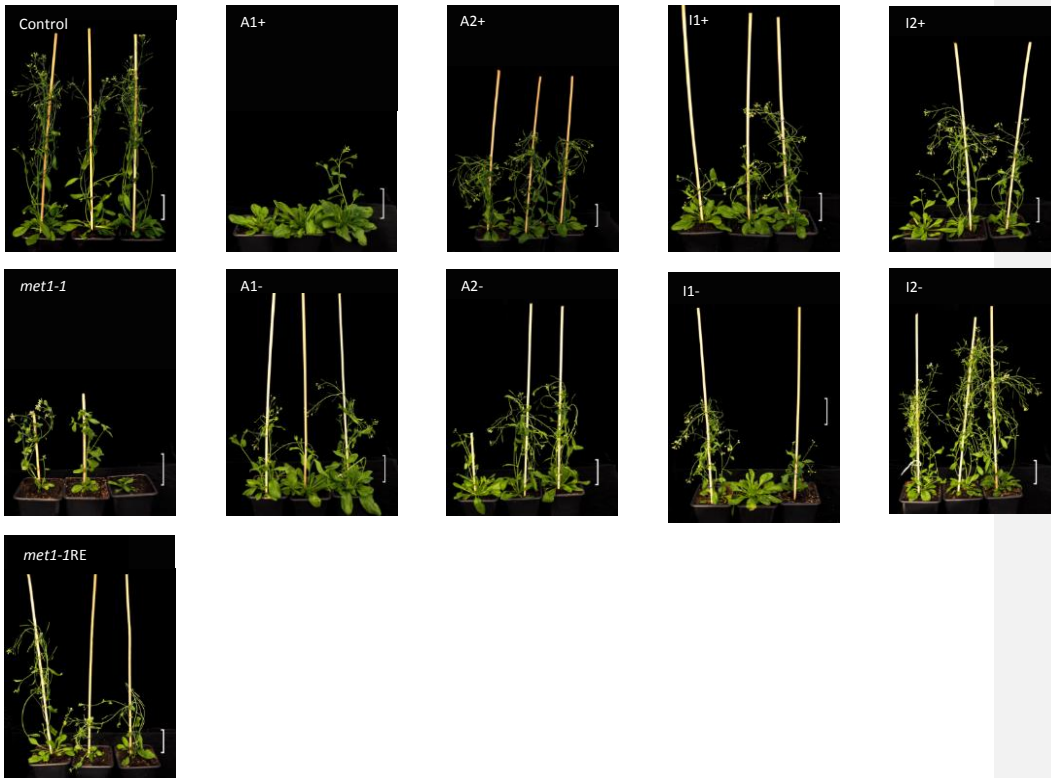
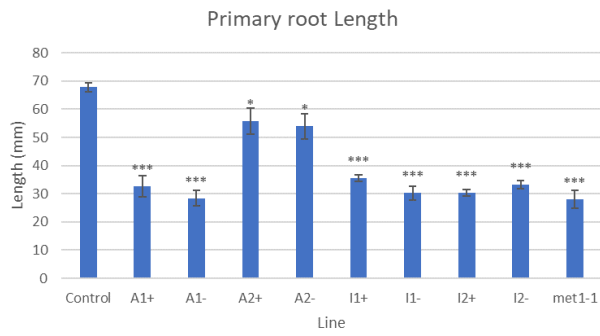
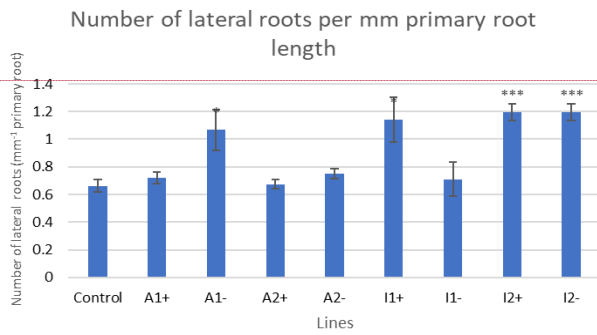


Figure 2.4: Phenotypic analysis of bolting and late-stage development. METo lines were compared with a wildtype control, a MET1 mutant, *met1-1*, and a derivative of *met1-1*, *met1-1* RE, with restored wildtype MET1 alleles. A) METo lines display a delay in bolting phenotype compared to both wildtype and mutated *met1 Arabidopsis*. Bolting time was analyzed by counting the number of basal rosette leaves upon bolting in long day conditions (Soppe *et al.*, 2002). The parameter used to determine when bolting had occurred was defined, as the stem reaching a minimum of 1 cm in vertical height, for a basal rosette leaf to be counted in the study the leaf had to be at least 1 cm in length and 0.5 cm in width. The significance of a change from wildtype is indicated by asterisks (if present): * = P<0.05, ** = P<0.01 ***=P<0.005, calculated by Student's two-tailed t-test. B) Image of wildtype, *met1* mutant and METo *Arabidopsis*, taken eight weeks after stratification. The scale bar indicates 5 cm.

Seven of the METo lines displayed a significant delay in bolting compared to wildtype *Arabidopsis*, including lines that have lost the METo transgene. This implies that there are common target loci in the METo lines involved in bolting and these loci are stably altered, not requiring the presence of the METo transgene. The delayed bolting phenotype was also present in lines that over-expressed the catalytically inactive version of MET1 indicating that MET1 does not need its catalytic function to induce a phenotypic change. The catalytically inactive line I2+ displayed no significant change in bolting time but still possessed the METo transgene. This suggests that the delayed bolting observed in the majority of METo lines is a stochastic event that requires the over-expression of MET1 but is not always sufficient to cause a change. In the later stages of development, a wide range of phenotypic differences can be observed for the eight different METo lines even within their own independent line, highlighting the broad effect over-expressing MET1 has on healthy plant development and its stochastic nature. There are similar phenotypes between the *met1-1* mutant and METo lines such as the irregular shoot structure that curls round, unable to support the entire plant. The root structure was also selected as a phenotypic marker (Fig 2.5). One study found that treating *Arabidopsis* seedlings with the DNA methylation inhibitor 5-azacytidine reduced the primary root length (Viridi *et al.*, 2015), suggesting the phenotype is associated with the disruption of methylation.

A**B**

Commented [CW3]: This axes is lateral roots per mm and so has units e.g. number of lateral roots (mm⁻¹ primary root)

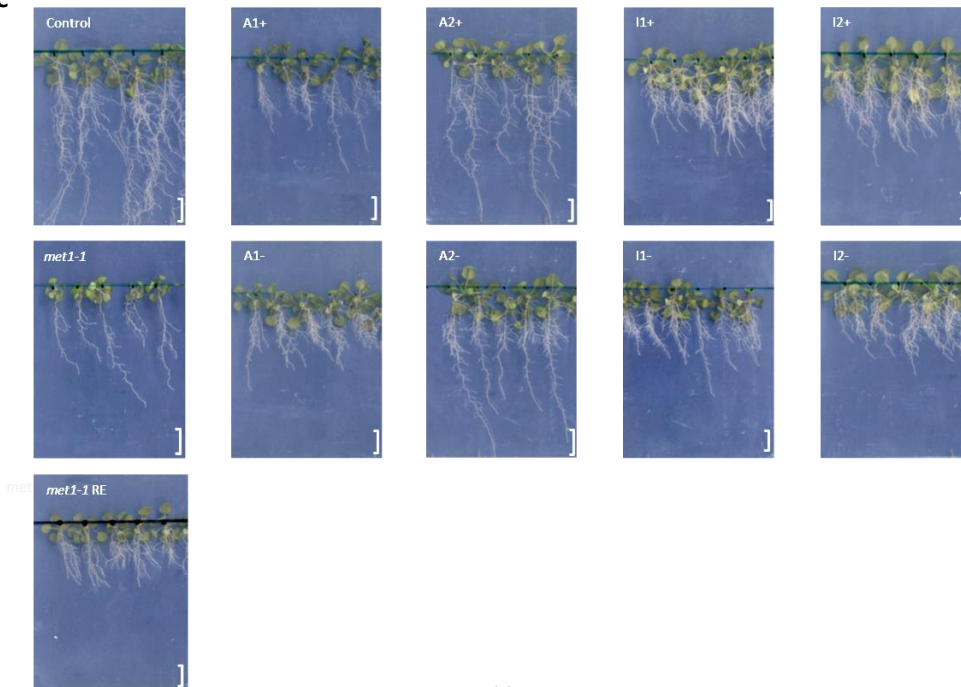
C

Figure 2.5: Root phenotype analysis of METo lines. METo lines were compared with a wildtype control a MET1 mutant, *met1-1*, and a derivative of *met1-1*, *met1-1* RE, with restored wildtype MET1 alleles. A) Primary root length at four weeks of development. All METo lines display significantly reduced root length, although the severity of the phenotype varies between lines. B) Number of lateral roots greater than 2 mm per mm of primary root length, at four weeks of development. The significance of a change from wildtype is indicated by asterisks (if present): * = $P < 0.05$, ** = $P < 0.01$ ***= $P < 0.005$, calculated by Student's two-tailed t-test. C) Image of wildtype, *met1-1* mutant and METo *Arabidopsis*, taken four weeks after stratification. The scale bar indicates 10mm

Primary root length was significantly reduced in all METo lines and the *met1-1* mutant compared to wildtype root length. The reduced primary root length is even maintained after the METo transgene has been lost. However, the severity of reduced primary root length varies between each line. The number of lateral root structures per mm of primary root length is increased in several METo lines, while a reduction in lateral roots is observed in the *met1-1* mutant. The joint appearance of distinct phenotypes among different METo lines, including lines that have lost the transgene, suggests that these are due to heritable changes induced at common target loci. The changes caused at these common target loci seem not to require the catalytic function of MET1. Many of the phenotypic differences observed in the METo lines appear to be novel and independent of a mutated *met1 Arabidopsis*. The randomness of the induction of phenotypes in different lines and the lack of a correlation between phenotypes and transgene expression, suggests that the induction of heritable changes is a chance event and that increased MET1 levels are required but not always sufficient to induce the individual phenotypes.

2.2.3 Transcript analysis of the MET1 over-expression lines

Once it was confirmed that a change in phenotype could be caused by over-expressing MET1, transcript profiling was carried out. Due to the stochastic phenotypes observed by over-expressing MET1, it was important to reduce variation specifically resulting from secondary effects, such as the plant's developmental stage (Ogneva *et al.*, 2016), circadian cycle (Lim *et al.*, 2014) and environmental stress (Secco *et al.*, 2015). It was established that all molecular analysis would be carried out at 4 weeks to minimise variation and allow easier comparison of the different lines. Pools of ten, four-week-old seedlings for lines A1+, A1-, A2+ and A2- were selected for transcript profiling. Due to the ubiquitous nature of MET1, there was extensive expression variation among the METo lines, including the lines that had lost the transgene. The RNA sequencing data was meticulously analyzed, identifying genes that had a greater than 2.5-fold change in expression, then organized into three major categories; transposable elements (S1 Table), genes expressing non-coding transcripts (S3 Table) and coding genes (S5 Table). Many small RNAs were found to have a significant change in expression this included; microRNAs, Natural antisense transcript (NAT), ncRNA, rRNA, snoRNA, snRNA, and tRNA. MicroRNA, NATs, ncRNA, and rRNA were primarily upregulated in METo lines with and without the transgene. Conversely, snoRNA, snRNA, and tRNA were mainly down-regulated, highlighting the possibility of a common pathway responsible for regulating expression which is maintained by methylation. A large number of transposable elements including gypsy and copia like retrotransposons were upregulated in lines with and without the transgene. This suggests that by over-expressing MET1 we are disrupting dense methylation which typically represses transposon expression. Interestingly the domesticated TE (DTE) *MUSTANG 8* (MUS8) was severely downregulated in the A1+ and A1- lines. In the *mus7/mus8* double mutants, multiple developmental abnormalities occur including shortened stem structure and reduced sterility (Joly-Lopez *et al.*, 2012), both phenotypes which are observed in multiple METo lines. Extensive expression changes were also found in protein-coding genes. Due to the large number of protein-coding genes that possessed greater than 2.5-fold change in expression, more stringent screening protocols were applied. Genes that maintained or increased in expression once the transgene was lost were selected. The shortened candidate list was then screened for the presence of MET1 dependent dense methylation, and six candidate genes were selected. The expression

levels of the six candidate genes and MET1 were tested further using qPCR for all eight METo lines along with a wildtype control, *met1-1* mutant and a derivative of *met1-1*, *met1-1* RE, with restored wildtype MET1 alleles (Fig 2.6).

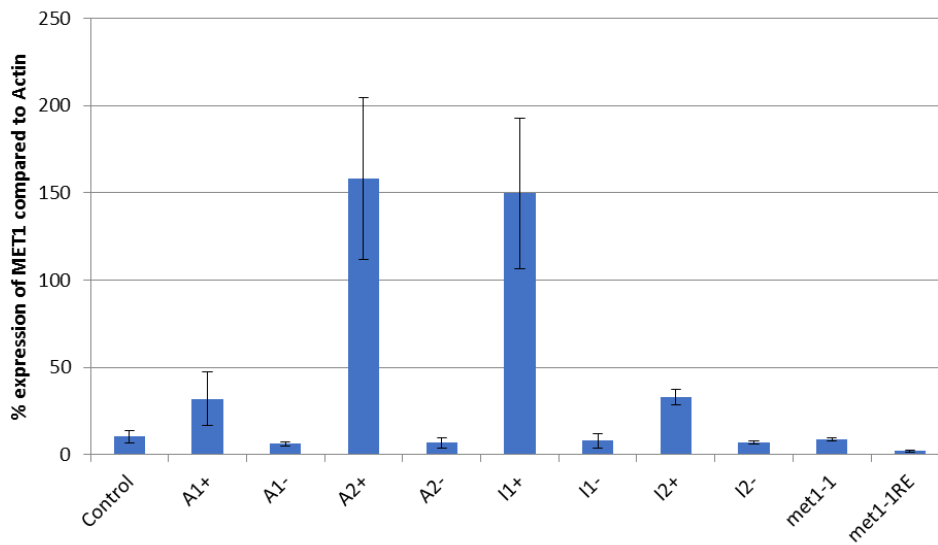
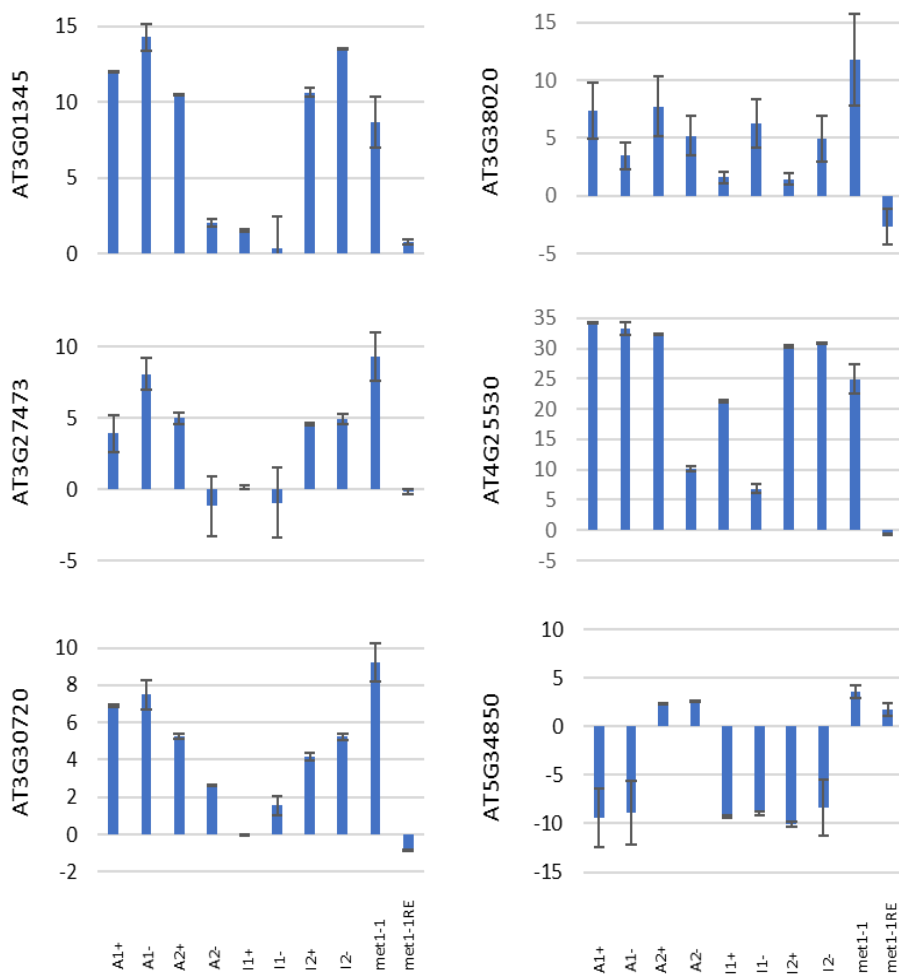


Figure 2.6: Comparison of *MET1* expression levels. The percentage of *MET1* transcripts compared to *Actin* transcription. The analysis was carried in METo transformants with (+) and without the transgene (-). Lines A1 and A2 express a catalytically active *MET1* transgene, lines I1 and I2 express a catalytically inactive *MET* transgene. Expression was also measured in the control line, *met1-1*, and *met1-1* RE. In A1+ and I2+, *MET1* expression is about 3-fold higher compared to the control. In A2+ and I1+, *MET1* levels increase are about 15-fold compared to the control line.

In plants that had retained the transgene, *MET1* transcript levels were ~3-fold greater in A1+ and I2+, and ~15-fold higher in A2+ and I1+. In lines that had lost the transgene, *MET1* transcript levels had been restored to wildtype levels. The level of *MET1* was also unaffected in a *met1-1* mutant. This expression data confirms that excess *MET1* is not required to maintain any of the phenotypes observed in the lines that have lost the METo transgene.

The difference in MET1 expression also verifies that the induction of phenotypes seen in the METo lines is a stochastic event that requires increased levels of MET1, but is not determined by the levels of MET1 transcript. QPCR was then used to confirm the change in expression levels for the six candidates identified in the transcript analysis (Fig 2.7)

A



B

Gene ID	Gene Name	Function
AT3G01345	N/A	Unknown expressed protein
AT3G27473	N/A	Cysteine/Histidine-rich C1 domain family protein
AT3G30720	QQS	Orphan gene that modulates carbon/nitrogen allocation
AT3G30820	ORF-1	RNA binding protein
AT4G25530	FWA	Homodomain-containing transcription factor for flowering
AT5G34850	PAP26	Purple acid phosphatase involved in phosphate scavenging

Figure 2.7: qPCR analysis of six genes with dense methylation. A) Analysis was carried in METo transformants with (+) and without the transgene (-). Lines A1 and A2 express a catalytically active MET1 transgene, lines I1 and I2 express a catalytically inactive MET transgene. Expression was also measured in the control line, *met1-1*, and *met1-RE*. The mean and the standard error are shown for three biological replicates each having three technical replicates for each line. Values on the y-axis represent the fold difference compared to the control line. B) Table of the six selected candidate genes containing gene ID, gene name and the function of the gene where possible.

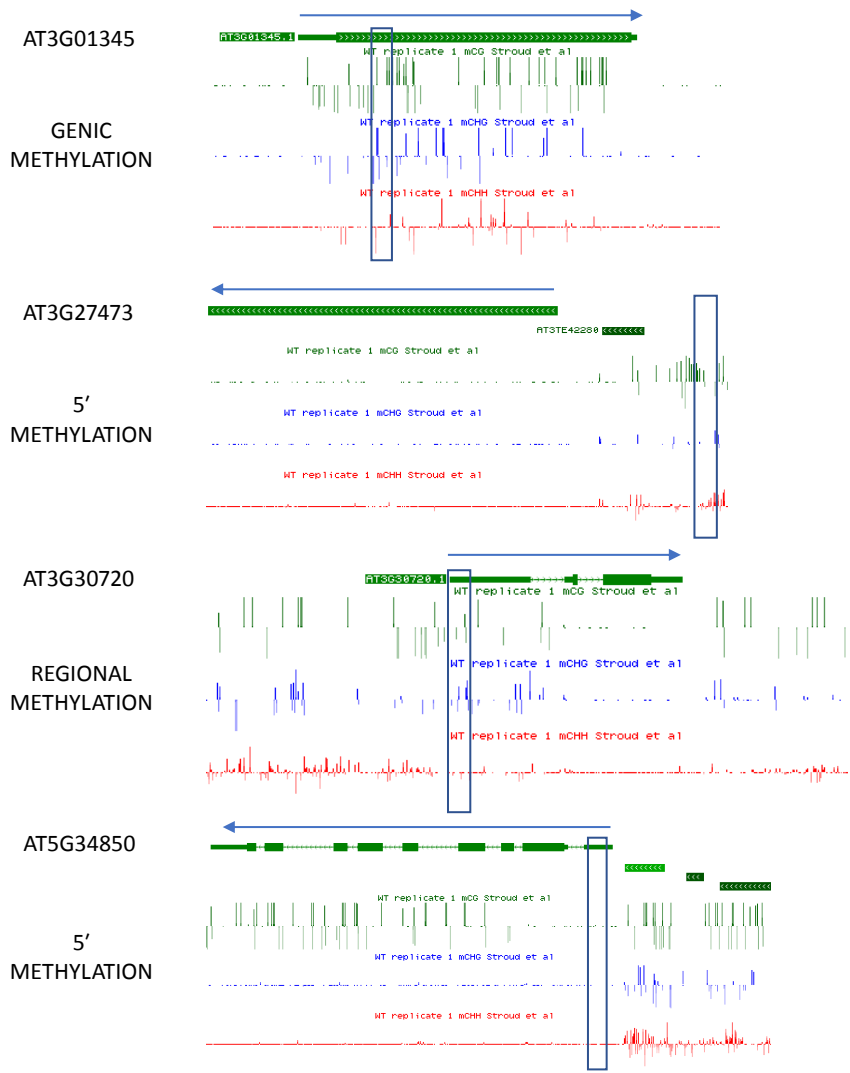
Q-PCR analysis of the six target genes confirmed that a change in expression had occurred at these loci, and the presence of the catalytic region is not required to cause a change in expression. As already observed in the phenotype analysis, we detect common expression changes for individual genes in all or some METo lines. For most genes, similar changes in METo lines are also detected in the *met1-1* mutant, while expression changes of AT4G35770 and AT5G34850 only occur in METo lines. In most METo lines that have lost the transgene, expression changes are conserved. In some cases; AT3G01345, A1, and AT3G38020, I2 an increase in expression are observed once the transgene is lost. Expression levels are predominantly increased in METo lines, but decreased expression can also occur. This is most evident for the gene AT5G34850, which is unchanged in the A2 lines but significantly reduced in all other METo lines.

2.2.4 Bisulphite analysis of MET1 over-expression lines

All the candidate genes selected for expression analysis contain MET1 dependent dense methylation located within or adjacent to its loci. To investigate if the change in expression corresponds to a change in dense methylation changes, bisulphite analysis was carried out for four of the target genes. The four candidate genes could be categorized into one of three distinct dense methylation categories (Fig 2.8A): Genic methylation, dense methylation present throughout the entire body of the gene, 5' methylation, dense methylation that is located within the promoter region of the gene, but not present in the gene body. Regional methylation is dense methylation that is localized at a particular exon or intron. The four genes selected possessed one of these distinct methylation pattern; AT3G01345 (genic), AT3G27473 and AT5G34850 (5'), and AT3G30720 (regional) (Fig 2.8B). AT5G34850 was selected due to it being the only candidate gene down-regulated when MET1 is over-expressed (Fig 2.7). Due to highly repetitive nature of transposons and the low efficiency of bisulphite primers, a genomic region of AT5G34850 close to the dense methylation was selected. It was believed that AT5G34850 was silenced due to dense methylation spreading from the transposon upstream into the gene itself.

Commented [CW4]: Check formatting here

A



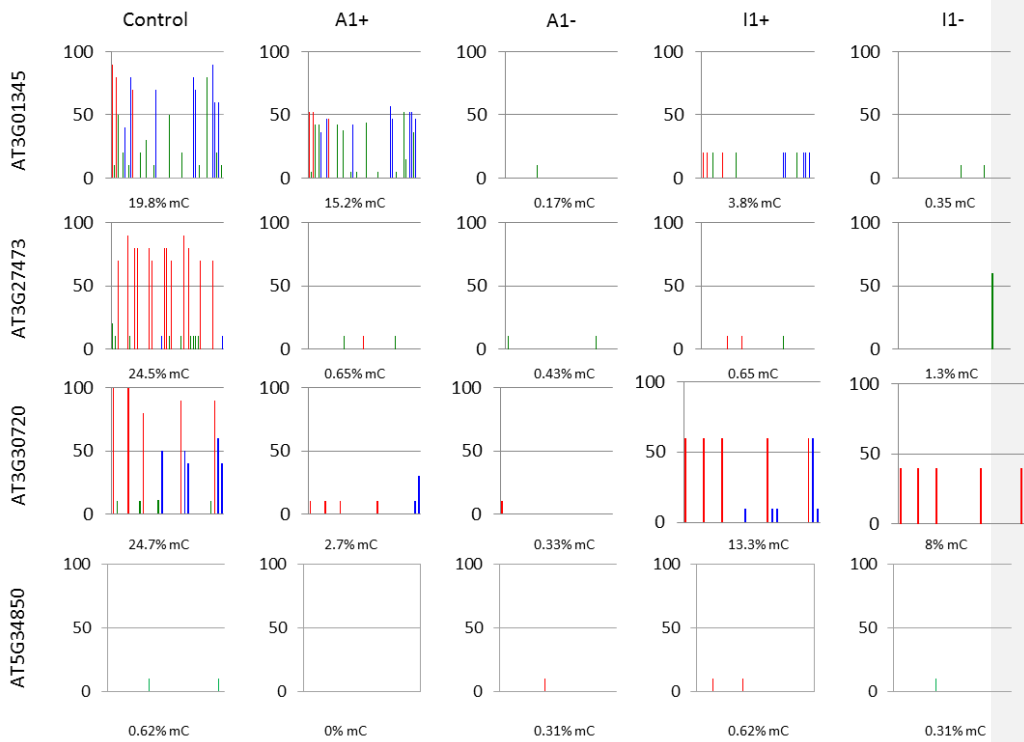
B

Figure 2.8: Bisulphite analysis of the METo lines. A) Genes with dense DNA methylation patterns in the genic region (AT3G01345), in the 5' region (AT3G27473), in the gene region (AT3G30720) and the down-regulated gene (AT5G34850). Boxes label sections that were analyzed by bisulphite sequencing (Figure 2.8B). DNA methylation patterns in the four genes with MET1-dependent dense methylation were extracted from <http://genomes.mcdb.ucla.edu>. B) DNA methylation analysis of AT3G01345, AT3G27473, AT3G30720, AT5G34850 regions in METo transformants (+) and in lines derived from METo transformants, from which the transgene has been removed (-). Line A expresses a catalytically active METo transgene; line I1 expresses a catalytically inactive METo transgene. Red denotes CG methylation, blue is CHG methylation, and green is CHH methylation.

Bisulphite sequencing analysis of the three candidate genes that were upregulated shows a reduction in methylation for all lines analyzed. In lines that have lost the METo transgene a decrease in methylation is maintained or even more severe, indicating that the METo transgene is not required to keep the hypomethylated state. For the A1 lines, a reduction in methylation correlates with an increase in expression. However, the I1 lines that also show a decline in methylation don't show a significant change in expression, highlighting a more complex mechanism determining the change in expression. Bisulphite analysis of AT5G34850 displayed no change in methylation for the region analyzed.

2.2.5 Histone analysis of the MET1 over-expression lines

As there was no direct correlation between a reduction in methylation and an increase in expression, other factors were also involved in determining expression change. The most likely candidate is histone modifications. There are numerous histone modifications that can alter the chromatin structure and regulate gene expression. Five histone marks were selected for further analysis, the repressive marks H3K9me2 and H3K27me3 and the active marks H3K4me3, H3K27ac and H4 acetylation (Fig 2.9).

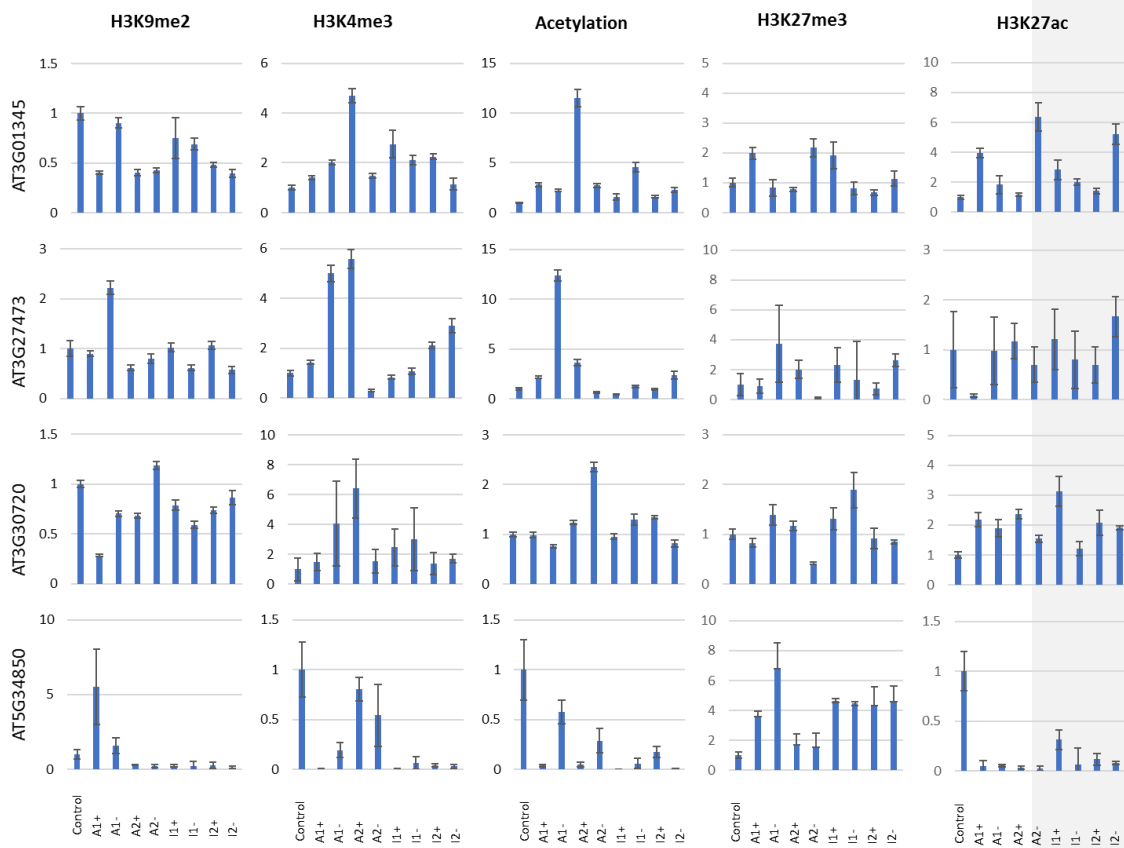


Figure 2.9: Histone analysis of the METo lines. ChIP analysis of H3K9me2, H3K4me3, H4ac, H3K27me3 and H3K27ac for *AT3G27473*, *AT3G01345*, *AT3G30720*, and *AT5G34850*. The relative H3K9me2, H3K4me3, H4ac, H3K27me3 and H3K27ac levels were determined by ChIP assays and normalized via the input DNA. The mean and the standard error are shown for three biological replicates each having three technical replicates for each line. Values on the y-axis represent the relative fold enrichment of histone modification compared to the control line.

Analysis of AT3G01345, AT3G27473, AT3G30720, and AT5G34850 suggests some conclusions about the significance of different histone marks for expression changes. In AT5G34850 a reduction of H3K9me2 does not directly lead to a decrease in gene expression, observed in A2+ and A2-. A decrease in H3K4me3 and an increase in H3K27me3 correlates with a reduction in AT5G34850 expression in all lines. At AT5G34850 deacetylation of H3K27 is required before H3K27 methylation but is not sufficient to reduce expression, seen in line A2+ and A2-. Levels of H3K4me3 need to be maintained or increased to enhance gene expression, a reduction in H3K4me3 directly leads to silencing which is seen in line A1- for gene AT3G27473. Significant increases of H3K4me3 can cause increased levels of acetylation, but the increase does not proportionately correlate. While METo expression may induce H4 acetylation and H3K9me2 changes, changes in expression appear to depend on changes in H3K4me3 levels. Over-expressing MET1 allows the disruption of dense methylation and alter multiple histone marks at particular loci, leading to complete restructuring of the chromatin environment. Studies have shown that a change to the chromatic structure can become stably maintained over multiple generations (Silveira *et al.*, 2013).

2.2.6 Heritability of epigenetic changes

Once it was established that an epigenetic change could be induced by over-expressing MET1, and change was still maintained without the presence of the METo transgene, it was important to determine if the epigenetic changes observed spanned multiple generations. We proceeded to self-fertilize the initial eight METo lines already analyzed, and carried out both phenotypic and molecular analysis. The easiest phenotypic marker used for determining heritability was primary root length and density of lateral root growth (Fig 2.10).

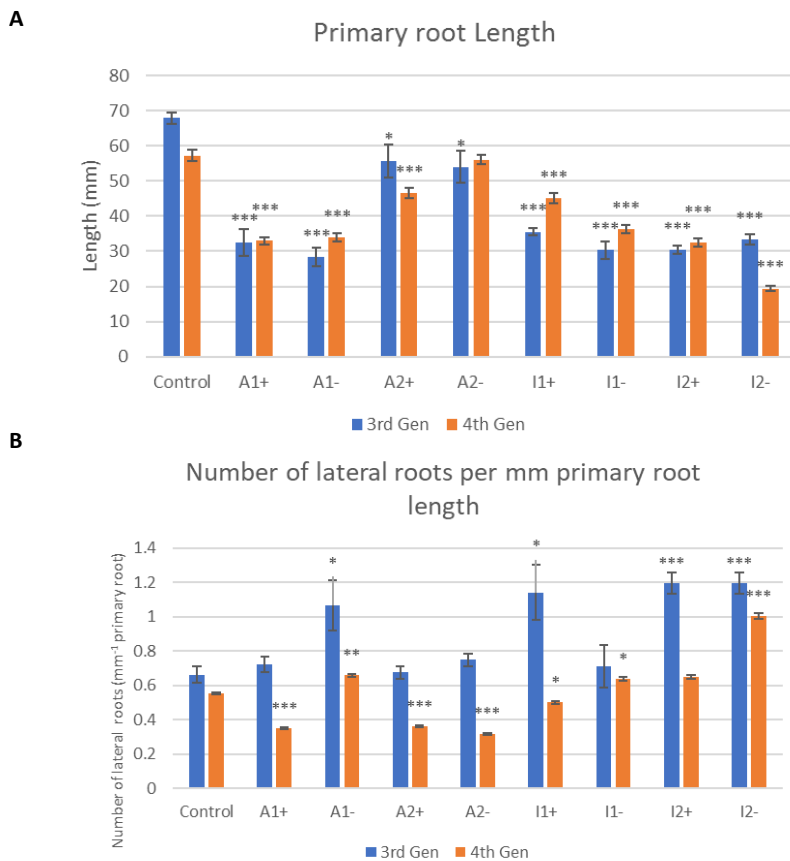


Figure 2.10: Transgenerational phenotypic analysis of METo lines. A) Primary root length at four weeks of development for both the 3rd and 4th generation of METo *Arabidopsis*. B) Number of lateral roots greater than 2mm per mm of primary root length, at four weeks of development for both the 3rd and 4th generation of METo *Arabidopsis*. The significance of a change from wildtype is indicated by asterisks (if present): * = P<0.05, ** = P<0.01 ***=P<0.005, calculated by Student's two-tailed t-test.

Commented [CW5]: Check y axis label as before

Seven of the eight, next-generation METo lines still possessed significantly shorter root length, regardless of METo transgene presence. However, the primary root length of A2- returned to a wildtype length after only one generation. This could be due to the lack of excess MET1 and reduced phenotypic severity in the third generation, allowing the A2- lines to immediately recover after one generation. Though the reduction in primary root length is still significant in the fourth generation, it is not as severe as the third generation of METo lines. Compared to the third generation which shows a significant increase in lateral root density in some lines, the fourth generation appears more sporadic. Lines A1+, A2+, A2- and I1+ show a significant reduction in lateral root density in the fourth generation, compared to the previous generation which has no significant change or an increase in lateral root density. The substantial increase in lateral root density observed in I2+ in the third generation is restored to a wildtype density in the next generation. Only A1- and I2- have maintained their increased lateral root density after one generation. Lateral root density appears to be more irregular, varying from one generation to the next, making it a poor phenotypic marker. However, primary root length is stably maintained after one generation without the presence of the METo transgene. This makes primary root length a good hereditary marker. Once it was confirmed that a change in phenotype is heritable over a generation, it was critical to determine if changes in gene expression are still maintained in the next generation. Expression analysis of MET1 and the six candidate genes were carried out in the fourth generation of METo lines (Fig 2.11).

Commented [CW6]: 2.11

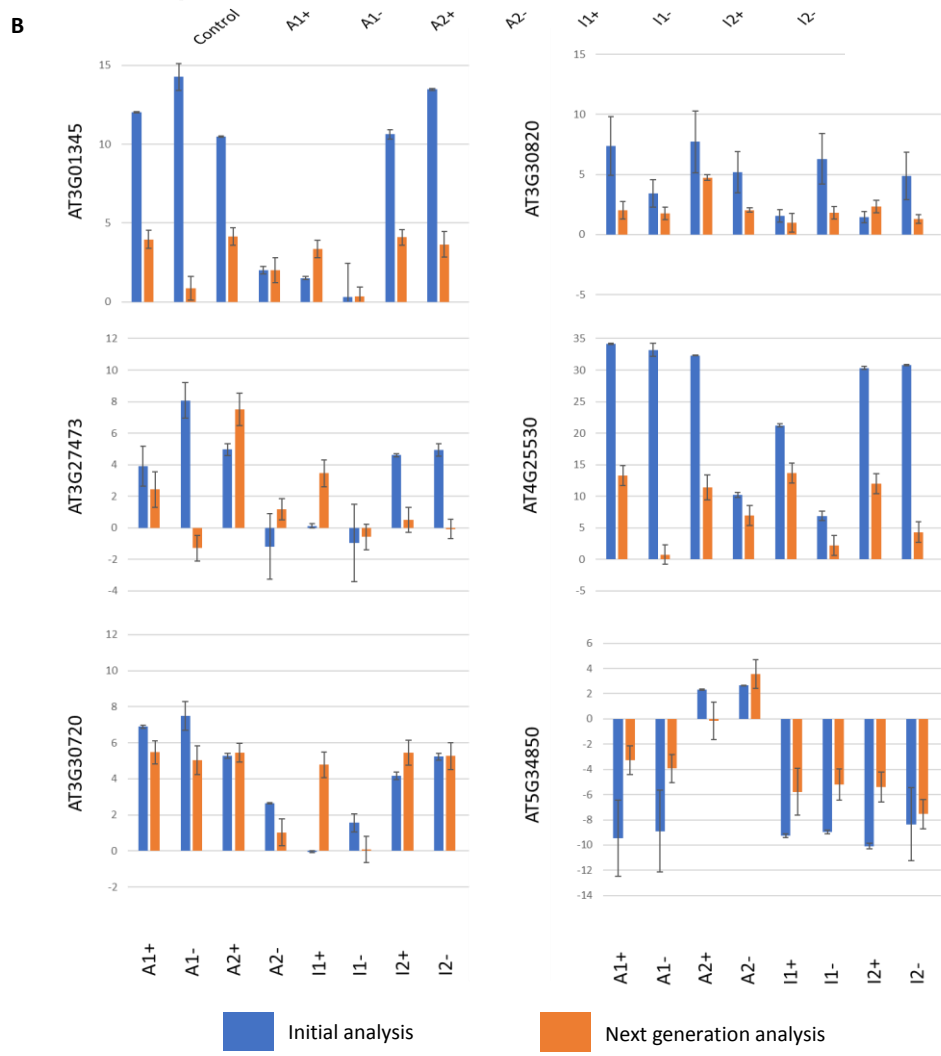
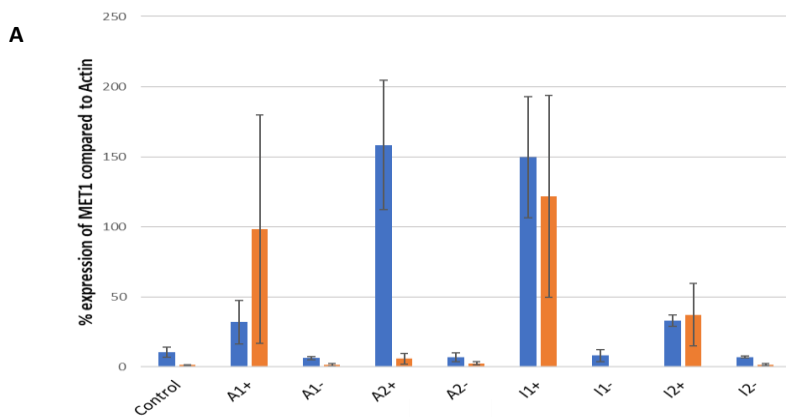


Figure 2.11: qRT-PCR analysis of *MET1* and the six different candidate genes for the 3rd and 4th generation. A) *MET1* expression levels as a percentage compared to actin expression for both 3rd and 4th generation METo *Arabidopsis*. B) Expression analysis of the six candidate genes compared to the wildtype control for both 3rd and 4th generation METo *Arabidopsis*. The mean and the standard error are shown for three biological replicates each having three technical replicates for each line. Values on the y-axis represent the fold difference compared to the control line.

In lines that still retained the METo transgene in the 4th generation, the levels of *MET1* transcript was maintained in A1+, I1+, and I2+ lines compared to the 3rd generation, though at greater variation. This could be due to silencing of the METo transgene in some of the plants within the line. This observation is supported by the complete restoration of native *MET1* transcript levels in the fourth generation of A2+, which had the strongest *MET1* expression in the previous generation. Lines that didn't possess the METo transgene in the 3rd generation still maintained innate *MET1* transcript levels in the next generation. There appears to be no correlation between the level of *MET1* and the increase or reduction of lateral root density. The heritability of expression in the six candidate genes can be categorized into three distinct groups. Genes that have been restored to wildtype in some lines and reduced in expression for others after one generation, AT3G01345, AT3G27473, and AT4G25530. Genes that show a reduction in expression change for all lines in the fourth generation, AT3G38020, and AT5G34850. And finally, genes that have retained or reduced expression change after one generation, AT3G30720. When the level of *MET1* transcript is compared to the heritability of each gene, there appears to be no definite correlation. Line A2+ which possessed high *MET1* transcript levels in the third generation but native *MET1* concentration in the fourth generation, displays varying expression heritability for each gene, demonstrating how over-expressing *MET1* is a stochastic event.

2.2.7 Protein analysis of over-expressing MET1

Some genes with altered expression in MET1 over-expression lines have also been reported to be affected in *met1* mutants. This implies that increased levels of MET1 transcript may generate co-suppression or protein degradation effects that would resemble a *met1* mutant. To confirm this is not the case, and increased MET1 transcripts lead to an increase in MET1 protein, Western blot was carried out. Unfortunately, there was no MET1 *Arabidopsis* antibody available at the time. To overcome this problem, a FLAG-tagged MET1 over-expression construct was created (S2 Fig) which would allow the analysis of the MET1 protein using an anti-FLAG antibody(Fig 2.12).

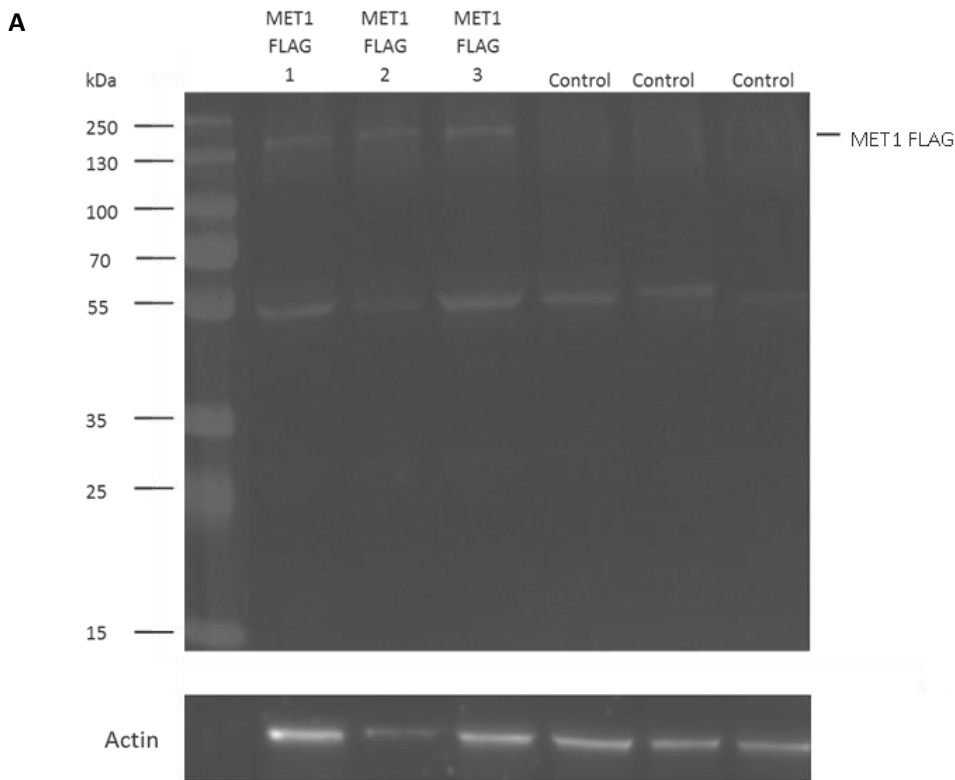




Figure 2.12: Protein analysis of over-expressed FLAG-tagged MET1. A) Western blot was carried out for FLAG-tagged MET1 transformants and wildtype control. The expected protein size of the FLAG-tagged MET1 is 176 kDa. Actin (40 kDa) was used as an internal control to determine the concentration of protein extract. B) Semi-quantitative PCR of control line and three biologically different over-expressing MET1 FLAG-tagged lines. Primers were used that only amplified MET1 cDNA with a FLAG tag. Three technical replicates were carried out for each line at 26 cycles. Actin was used as an internal reference to ensure the cDNA analyzed was of the same concentration.

Western blot identified that the MET1 FLAG-tagged protein was present only in the over-expression lines, with an expected protein band of 170 kDa. Secondary bands were observed in all lines at approximately 50 kDa indicating non-specific binding of the FLAG tag antibody. Semi-quantitative PCR of the control line and MET1 FLAG-tagged over-expression lines confirms that increased MET1 transcripts are translated, and doesn't cause co-suppression or protein degradation. Although changes in expression of individual genes are similar to that of a *met1* mutant, the mechanism behind the epigenetic change is distinctly different and doesn't involve the loss or reduction of the MET1 protein.

2.2.8 Genetic analysis of AT5G34850

Bisulphite analysis of the silenced gene AT5G34850 (Fig 2.8B), did not demonstrate any change in DNA methylation. However, dense methylation was present in a transposable region upstream of the gene (Fig 2.8A). Analysis of this region turned out to be more complicated than initially expected and PCR analysis of this locus was performed (Fig 2.13).

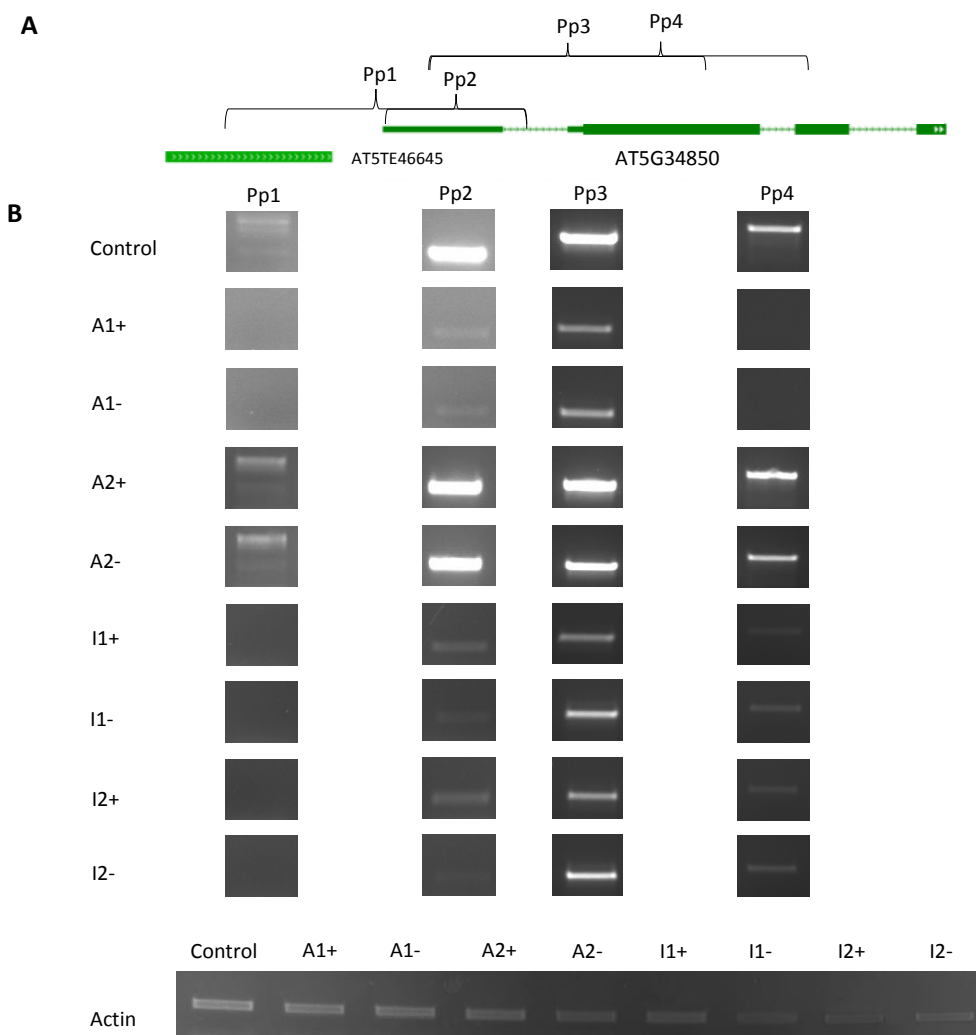


Figure 2.13: Mapping AT5G34850. A) The region of AT5G34850 mapped using four different primer pairs (Pp1-Pp4). B) PCR Mapping analysis of AT5G34850 region using the four different primer pairs. PCR analysis was carried out in MET1 transformants (+) and in lines derived from MET1 transformants, from which the transgene has been removed (-). Lines A expresses a catalytically active MET1 transgene; line I1 expresses a catalytically inactive MET transgene. Actin was used as an internal reference to confirm the DNA analyzed was of similar concentration.

PCR-analysis of the locus revealed that the upstream region of the gene, which contains multiple repetitive elements, had been deleted or rearranged in all six lines, in which the gene had been silenced. Moreover, a central region of AT5G34850 could not be amplified, in lines A1+ and A1- suggesting an extensive rearrangement of the locus. Highlighting the possibility of disrupted dense methylation at repetitive regions leading to transposition and gene disruption.

2.2.9 Investigating the phenotypic effects of over-expressing MET1.

Over-expression of MET1 caused distinct changes in both phenotype and gene expression. Although we have identified many different phenotypic changes, few have been directly correlated with a change in gene expression. One gene that has been identified is AT3G30820 (FWA) which is well documented to cause a delay in bolting when it is expressed (Koornneef *et al.*, 1991). In the METO lines, up-regulation of FWA directly correlates with late bolting. METo lines also display reduced primary root length which appears to correlate with the reduction of AT5G34850. However, line A2 that possess increased AT5G34850 levels, still have shorter root length, though not as severe as the remaining METo lines. Indicating that a reduction in AT5G34850 maybe partially responsible for the reduced primary root length, but other factors are involved. Although two genes have been identified to cause a change in phenotype, the remaining candidate genes have not been linked to a change in phenotype. To determine if the up-regulated candidate genes contribute to the observed METo phenotypes, constructs were created that either over-

expressed AT3G01345, AT3G27473, or AT3G30720 (S1 Fig). AT5G34850 was also further examined. AT5G34850 encoded a *PURPLE ACID PHOSPHATASE 26* (PAP26) which cleaves inorganic phosphate and transports it to the vacuole. As phosphate is involved in many important plant processes (Bolan *et al.*, 2003), silencing of PAP26 may be responsible for other phenotypic abnormalities. Phenotypic analysis was then carried out for each of the over-expression transformants, along with a pap26 mutant (Fig 2.14).

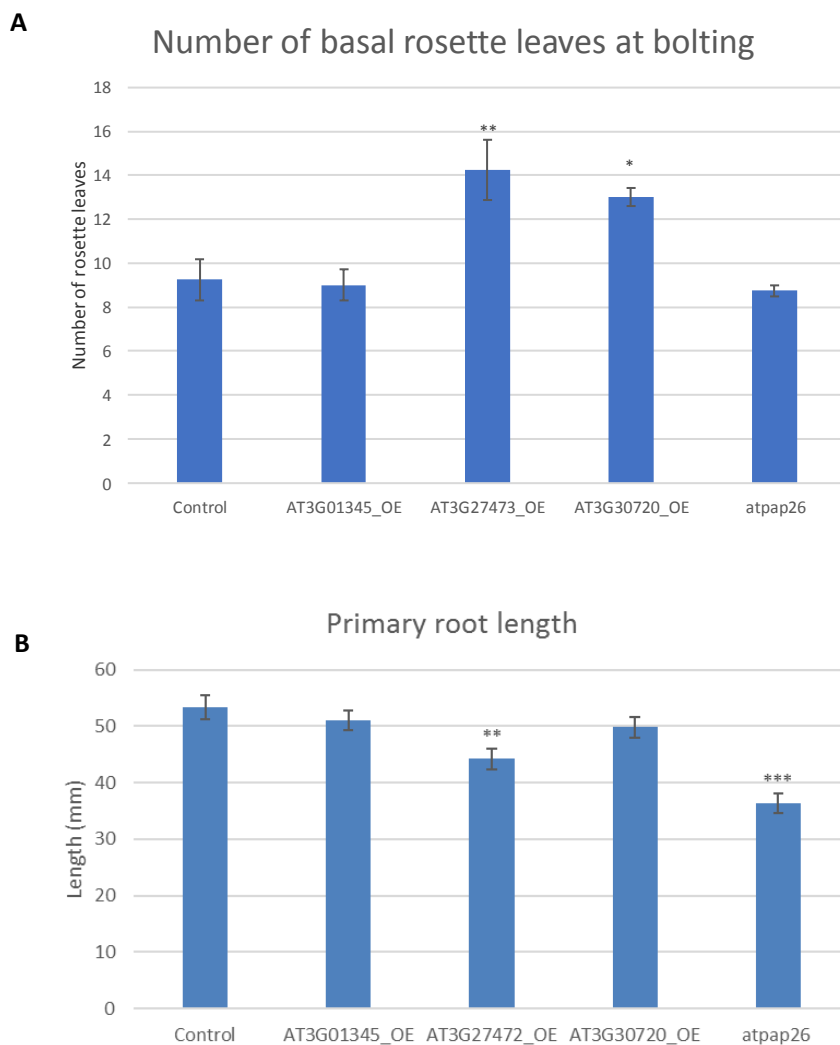


Figure 2.14: Phenotypic analysis of the candidate genes. A) Bolting analysis of the over-expressed AT3G01345, AT3G27473, and AT3G30720 lines compared to wildtype control and *pap26* mutant line. Bolting time was analyzed by counting the number of basal rosette leaves upon bolting in long day conditions (Soppe *et al.*, 2002). The parameter used to determine when bolting had occurred was defined, as the stem reaching a minimum of 1 cm in vertical height, for a basal rosette leaf to be counted in the study the leaf had to be at least 1 cm in length and 0.5 cm in width. B) Root phenotype analysis of over-expressed AT3G01345, AT3G27473 and AT3G30720 lines compared to wildtype control and *pap26* mutant line, at four weeks of development. The significance of a change from wildtype is indicated by asterisks (if present): * = $P < 0.05$, ** = $P < 0.01$, *** = $P < 0.005$, calculated by Student's two-tailed t-test.

Over-expression of AT3G01345 and AT3G307020 caused no significant change in primary root length compared to the control line. However, there was a significant reduction in lines that over-expressed AT3G27473. Although there was a significant decrease in the primary root length, it was not as significant as that observed in the METo lines (Fig 2.5A), indicating that an increase in AT3G27473 could contribute to shorter primary root length. A reduction in primary root length was even greater in the *pap26* mutant which had an average primary root length comparable to that of the METo lines (Fig 2.5A), suggesting that a reduction of PAP26 is likely to play a role in reducing the primary root length for METo lines. No substantial change in bolting was observed in either of the AT3G01345 over-expression lines or the *pap26* mutant. Lines that over-expressed AT3G27473 or AT3G30720 did take longer to bolt, but the severity of the delay was not as significant as that observed in the METo lines (Fig 2.4A). Furthermore, METo lines that don't have increased AT3G27473 or AT3G30720 expression (Fig 2.7) still take longer to bolt. This illustrates the complexity of over-expressing MET1 and the numerous effects it has on gene expression. Although genes have been identified in the METo lines to cause a primary phenotypic change, such as FWA, many genes that change in expression may enhance or diminish this phenotypic change. Along with the stochastic nature of increased MET1 and gene expression, directly correlating a change in gene expression with a phenotypic change becomes increasingly challenging.

2.3 Discussion

It has been extensively documented (Vongs *et al.*, 1993) (Finnegan *et al.*, 1996) that MET1 is exclusively responsible for the maintenance of cytosine methylation in a CG-specific context. Recently an alternative function of MET1 has been identified affecting specific loci with dense methylation in CG and non-CG contexts. At these loci, elimination of MET1 activity does not only cause loss of CG methylation but the loss of methylation marks in all sequence contexts. For some loci, this can result in heritable loss of dense methylation patterns creating novel epi-alleles and states of expression (Watson *et al.*, 2014). MET1 dependent dense methylation at many loci is independent of *de novo* methylation and other components of the RdDM pathway. Instead, dense methylation at these loci requires the nucleosome remodeler DDM1, with CHH methylation being controlled by CMT2 and CHG methylation by CMT3 (Watson *et al.*, 2014).

The coordinating role of MET1 for dense methylation, illustrated by the loss of CG and non-CG marks in *met1* mutants, could be based on the MET1 protein facilitating the access of CMT2 and CMT3 to dense methylation targets if MET1 is an essential component of a multi-protein complex that also contains CMT2 and/or CMT3. Alternatively, dense methylation could be mediated by MET1-controlled CG-methylation or by other epigenetic marks established by CG-methylation, which may be required to recruit CMT2 and CMT3. This could involve interaction of MET1 with histone regulators like HDA6, for which direct binding to MET1 has been demonstrated (Liu *et al.*, 2012) and which has been proposed to recruit MET1 to particular target loci as the initial step in establishing subsequent non-CG methylation (To *et al.*, 2011). As MET1 may interact with other epigenetic factors to form a stable complex, it may be sensitive to changes in MET1 concentration, leading to a disruption in complex formation. To test this, high levels of catalytically active and inactive MET1 proteins were introduced to the plant system.

Over-expression of MET1 led to numerous phenotypic variations, some of which were common in multiple METo lines. One example is the delayed bolting phenotype observed in seven of the eight METo lines. FWA is the gene primarily responsible for this delayed bolting and is commonly silenced in wildtype *Arabidopsis*. Although DNA methylation of FWA has been thoroughly examined, little is understood about the molecular basis of the late-

flowering phenotype (Ikeda *et al.*, 2007). In the METo lines increased expression of FWA correlates with a delay in bolting. Silencing of FWA is mediated by transposable-element-derived tandem repeats in the promoter region which are densely methylated (Lippman *et al.*, 2004). In lines that have lost the METo transgene, FWA activation is still retained, which suggests MET1 over-expression can induce heritable activation. In contrast, FWA allele activated in a *met1-1* mutant was efficiently remethylated and re-silenced upon restoration of the MET1 function (Kankel *et al.*, 2003). As the *met1-1* allele encodes a MET1 protein with a single amino acid substitution, it is possible that some of the induced phenotypes in the *met1-1* mutants are generated by changes in protein structure and interaction, which may produce similar effects as an increase in MET1 concentration.

Reduced primary root length which is present in the METo lines, is also observed in *Arabidopsis* seedlings treated with the DNA methylation inhibitor 5-azacytidine (Virdi *et al.*, 2015) suggesting the phenotype is associated with cytosine hypomethylation. Among the METo lines, leaf shape, flower structure, and floral organ identity were not significantly altered. Many of these phenotypes, however, have been reported in either the *ddm1* mutant (Kakutani *et al.*, 1996) or *MET1* antisense lines (Finnegan *et al.*, 1996), but the delay in bolting resembles phenotypes observed in some mutants associated with DNA methylation pathways. Both the *HDA6* mutant *axe1-5* and *HDA6* RNAi lines display late-flowering phenotypes (Wu *et al.*, 2008). Plants with altered MET1 functions show a range of flowering time effects. In both *met1-1* and *met1-3* mutants, a consistent delay in flowering is observed (Kankel *et al.*, 2003)(Saze *et al.*, 2003). Demethylation of DNA via 5-azacytidine (5-azaC) treatment or via expression of a *MET1* antisense gene causes early flowering, with the promotion of flowering being directly proportional to the decrease in methylation in *MET1* antisense lines (Finnegan *et al.*, 1998).

Delayed bolting phenotype and reduced primary root length are common phenotypes present in multiple METo lines, highlighting the possibility of common target loci. Though there are common targets, there was no direct correlation between the increased levels of MET1 and the severity of the phenotypes. The randomness of these induced phenotypes in different lines and the lack of a correlation between phenotypic severity and transgene expression levels suggests that the induction of heritable changes is a chance event and that

increased MET1 levels are required but not always sufficient to induce the individual phenotypes.

To identify potential target loci, transcript profiling was carried out for the catalytically active MET1 over-expression lines. In each line, the majority of genes with altered expression show an increase. Applying a cut-off of a log₂-fold change of 2.5, increased expression levels were observed in 644 genes in A1+, 565 genes in A1-, 22 in A2+ and 37 in A2-. Reduced expression was found in 240 genes in A1+, 77 genes in A1-, 0 genes in A2+ and 85 genes A2-. Genes with altered expression were organised into three categories; transposable elements (S2 Table), genes expressing non-coding transcripts (S4 Table) and coding genes (S6 Table).

The majority of genes encoding transposable elements are up-regulated (S1 Table). Silencing of the TE populations depends highly on methylation and small RNAs. Most TEs contain and are silenced via the presence of both CG and non-CG methylation (Cokus *et al.*, 2008). Indeed, a TE in the gypsy family, ATGP3, remains silent in single mutants of *met1* or *cmt3* but activates in a *met1 cmt3* double mutant (Tsukahara *et al.*, 2009). This suggests a redundant function of CG and non-CG methylation in the transcriptional silencing of TEs. Within the METo lines, numerous TEs are upregulated, implying a loss of methylation in all three sequence contexts. Among the many TEs upregulated a large subset of these are CACTA-like transposable elements. All CACTA elements carry short sequence motif repeats called subterminal repeats (STRs) in their subterminal regions. It is believed that methylation at these repeat motifs may prevent binding, impairing efficient excision/transposition (Miura *et al.*, 2001). In *met1* mutants increased transposition and transcription of CAC1 a CACTA element is observed (Vicent, 2010; Park *et al.*, 2014). This observation correlates with increased CACTA-like transcripts present in the METo lines. It is uncertain if transposition occurs in the METo lines, but given the increase in transcription, it is more than likely.

A number of retrotransposons are also upregulated in the METo lines, which are categorized into either Copia-like or gypsy-like elements. The gypsy-like elements can be further split into those that possess the Athila element and those that are unspecified. Research into Athelia elements identified they contain transcriptional silencing information (TSI) that are released in *met1* mutants (Kanno *et al.*, 2005). These TSI or a similar element may also be

present in other TEs, allowing targeted methylation at specific loci. This may explain why we observed common upregulation for TEs that contain TSI-like elements in the METo lines. Some TEs activated in MET1 over-expression lines also deviate in their heritability levels. While, for example, Athila elements that are activated in *met1* mutants are efficiently silenced again after re-introduction of a *MET1* transgene copy (Caton *et al.*, 2017), two-thirds of all Athila elements activated in MET1 over-expression lines, retain this status after removal of the *MET1* transgene.

Small RNAs have emerged as key regulators of gene expression, genome stability, and defense against foreign genetic elements (D'Ario *et al.*, 2017). When MET1 is over-expressed a number of these small RNAs change in expression (S3 Table), these changes appear to have a common underlying regulator for each class of small RNA. A group of micro RNAs that all code for precursors for miR854 are up-regulated in response to increased levels of MET1, which is heritably maintained once the METo transgene is lost. These precursors are all equally up-regulated in both lines indicating a mutual regulator for these miRNAs. Interestingly all miR854 precursors are located within the ATHILA retrotransposon family (Arteag-Vazquez *et al.*, 2006) which may explain the common response to increased levels of MET1. Transposable elements are frequently methylated at all sequence context which has been shown to be heritably disrupted when MET1 levels are significantly increased. With the removal of dense methylation, transcription at these loci can occur leading to increased miR854 expression. Interestingly these miR854 precursors are not located within the same retrotransposons indicating a common regulator of dense methylation at particular loci.

snoRNAs are an ancient class of small non-coding RNAs present in all eukaryotes and a subset of archaea that carry out a fundamental role in the modification and processing of ribosomal RNA. Within the METo lines a large number of these snoRNAs are heritably downregulated. Unfortunately little is known about the role of snoRNAs in plants. There are two main classes of snoRNAs those that direct 2'-O-methylation of the ribose (KissLaszlo *et al.*, 1996) and a group that guides pseudouridination of rRNAs, snRNAs and other RNA targets (Ganot *et al.*, 1997). Many of the snoRNAs identified by the transcript analysis are not annotated. However, two snoRNAs were identified. One of the snoRNAs, SNO30 belongs to the class that methylates ribose, while SNO111 carries out pseudouridylation. Little else is

known about these snoRNAs, but there appears to be no dense methylation present at these loci. The large number of snoRNAs that are heritably upregulated indicates a common epigenetic mechanism that controls expression.

Due to the large number of coding genes with altered expression, it was important to differentiate between potential primary and secondary targets of MET1-based epigenetic modifications. Using a methylome genome browser 31 primary target candidate genes with heritable dense methylation were identified (S6 Table). These genes were grouped into three categories, based on the presence of dense methylation in the promoter or 5' region (upstream), in the gene region (genic) or in the genomic region into which the gene is embedded (region). Several of the genes listed have been shown to be sensitive to DNA methylation changes. The gene responsible for delayed flowering, *FWA*, is up-regulated in METo lines and under the control of MET1 (Kinoshita *et al.*, 2004). The up-regulated gene AT4G03950, which encodes a nucleotide/sugar transporter family protein, is activated in a *ddm1-2* mutant (Lippman *et al.*, 2004). AT3G30720, Qua-Quine Starch (QQS), which is up-regulated in METo lines, is embedded within a TE-rich region and its expression levels are increased in *met1*, *ddc* (*ddm1/ddm2/cmt3*), *ddm1* and in the RNA-DEPENDENT RNA POLYMERASE 2 mutant *rdr2*. QQS expression levels correlate negatively with the DNA methylation level of repeated sequences located within the 5' end of the gene and can be inherited for several generations (Silveira *et al.*, 2013). Two genes are directly regulated by DNA methylation. The up-regulated gene AT3G50770, calmodulin-like 41 (CML41,) contains transposon promoter insertions (Baev *et al.*, 2010). Its increased expression, in response to elevated temperature, correlates with reduced promoter DNA methylation (Naydenov *et al.*, 2015). The down-regulated gene AT3G18610, nucleolin like 2 (NOR2), is involved in epigenetic regulation, as its disruption induces rDNA hypermethylation (Durut *et al.*, 2014).

Six genes were selected for further analysis for both expression changes and epigenetic features. Similar to the observed phenotypes, expression changes of the six analyzed genes occur independently of expression levels, catalytic activity or conservation of the MET1 transgene. Within individual lines, expression changes occur stochastically and with different intensity, inducing an increase in expression for all genes except AT5G34850, which displays a significant reduction in expression in six out of eight MET1-overexpression lines. In most MET1- overexpression lines that have lost the transgene, expression changes

were conserved. Bisulphite sequencing analysis was carried out for four of the target genes, and a reduction or loss of dense methylation marks for three of these genes was identified, independent of the expression levels of the three activated genes in different lines. This suggests that MET1 overexpression induced heritable hypomethylation at these loci, which in some cases was not sufficient to increase gene expression. The analysis of the silenced gene AT5G34850 revealed that the upstream region of the gene may have been deleted or rearranged in the lines that had been silenced. This along with the large number of transposable elements upregulated in the METo lines suggests transposition activity maybe occurring on a genome-wide scale.

Analysis of the five different histone marks (H3K9me2, H3K4me3, H4ac, H3K27me3, and H3K27ac), for the four target genes, revealed the complex nature of histone modifications. Among the histone marks tested, Acetylation and H3K4me3 levels show the most significant changes. While there was no consistent correlation between expression changes and individual H3K4me3 marks, some locus-specific correlations were detectable. Increased H3K4me3 levels correlated in all MET1 overexpression lines with enhanced AT3G27473 expression, and in seven out of eight MET1 overexpression lines with enhanced expression of AT3G01345. In the six lines with reduced expression of AT5G34850 H3K4me3 levels are also significantly reduced. However, it is unclear if silencing of AT5G34850 is the consequence of H3K4me3 reduction or of the loss of upstream regions that are required for gene expression. It is also unclear if H3K4me3 reduction is linked to DNA rearrangements or expression changes. Acetylation of either H4 or H3K27 positively correlates with H3K4me3 similar to what is seen in transposable elements in *met1* and *hda6* mutants (Liu *et al.*, 2012).

Expression analysis identified loci for which the presence of the MET1 transgene was not required to maintain expression changes. This suggests that for individual loci, altered gene expression can be inherited without the continuous presence of increased MET1 levels. Conversely, lines that have maintained the MET1 transgene and enhanced MET1 levels may continuously induce new novel epigenetic changes. To investigate this hypothesis and to test the long-term stability of MET1-induced expression changes, the expression profiles of six genes in the T3 and T4 generation were compared. In most lines, expression change in genes observed in the T3 generation, were also detectable in the T4 generation, although at lower levels. A comparison of the four lines that had lost the MET1 transgene suggests

locus-specific differences in the efficiency of maintaining expression levels, with altered states being preserved for AT3G30720 but reduced for AT5G34850. This corresponds to previous reports about locus-specific differences in the maintenance of epigenetic changes (Mirouze *et al.*, 2012). The stable epigenetic state of AT3G30720 confirms reports about a *ddm1*-derived hypomethylated epiallele of AT3G30720 that was inherited for at least eight generations (Silveira *et al.*, 2013). In some lines, enhanced expression levels are higher in T4 lines that have retained the MET1 transgene, supporting the hypothesis that epigenetic changes can be continuously induced in lines that have maintained increased MET1 expression.

The phenotypic investigation into the upregulated genes AT3G01345, AT3G27473, and AT3G30720, along with silenced gene AT5G34859, demonstrated the complex nature of phenotypic change and genetic cause. Increased expression of AT3G27473 induced both a delay in bolting and reduced primary root length. The severity of these phenotypes was not comparable to that seen in the METo lines. However, with the increase of FWA, which also causes late bolting, the phenotype may become compounded explaining the severe bolting delay observed in some METo lines. Similarly, the reduced root length seen in the *pap26* mutant may also be enhanced by the increased expression of AT3G27473. Little is known about AT3G27473 except that it is a Cysteine/Histidine-rich C1 domain family protein and that it is upregulated in an *ibm1* mutant, which displays no significant phenotypic abnormalities (Duque & Chua, 2003), although a number of genes have been identified to cause a phenotypic difference many remain uncharacterized.

Our data shows that MET1 over-expression can induce epigenetic changes, with enhanced MET1 expression levels being required but not always sufficient to cause epigenetic change. There is no direct correlation between the level of increased MET1 expression and the efficiency of the induction of epigenetic changes. This implies that MET1 proteins do not act as a transcription factor or like any other concentration-dependent gene regulator. MET1 over-expression behaves stochastically but not randomly as it induces similar changes in epigenetic and expression states at specific target loci in different MET1-overexpression lines. While the mechanisms involved in MET1 over-expression remain unclear, our data show that MET1 over-expression offers a new strategy to induce variants with novel combinations of epi-alleles.

3 Investigating the application of over-expressing MET1 in tomato

3.1 Introduction

Mankind has been improving crops for thousands of years (Doebley *et al.*, 2006), but recent developments in breeding strategies have given rise to many different crop varieties with greater yield and survivability. Varieties with desirable phenotypes must be self-fertilized multiple times to produce a pure line, which can then be crossed and used for breeding (Rommens *et al.*, 2007). With the advancement of technologies such as marker-assisted selection (MAS), plant breeders can identify single nucleotide polymorphisms (SNPs) associated with a trait (Tester & Langridge, 2010). This is particularly useful for traits that don't display a visible phenotype or when multiple genes are required for the desired characteristic. However, traditional crop breeding does have its limitations. The crossing of traits can only be carried out between plants that can sexually mate with each other, and even if they are successfully crossed unwanted traits may be introduced. Classical breeding strategies also rely on changes in the genome, though there is growing evidence that stable changes in gene expression can occur without altering the DNA sequence (Watson *et al.*, 2014). The molecular mechanisms that contribute to this epigenetic phenomenon are DNA methylation and histone modifications.

DNA methylation is the most frequent modification in plants, commonly acting as a transcriptional repressor, either by directly obstructing transcriptional proteins or by serving as a target for specific proteins which signal chromatin condensation (Klose & Bird, 2006). Changes in DNA methylation at individual loci can cause heritable changes in gene expression (epi-mutant), leading to epigenetic variation. These epigenetic changes are present throughout the plant kingdom. One example is the late flowering phenotype seen in *Arabidopsis*, which is caused by an epi-mutant, *fwa*, due to hypomethylation at direct repeats within the 5' region of the gene (Soppe *et al.*, 2000). The rice epi-mutant, Epi-d1, has shortened vegetative branch shoots, caused by hypermethylation at the gene promoter of *dwarf1* (Miura *et al.*, 2009). In tomato, hypermethylation of the colourless non-ripening locus (*Cnr*) inhibits fruit ripening (Fraser *et al.*, 2001). Histone modifications also play a fundamental role in epigenetic variation by altering the chromatin structure, allowing or

preventing transcriptional activators or repressors access to loci. A mutation in HDA6, a histone deacetylase, causes a delay in flowering in *Arabidopsis*. HDA6 prevents the chromatin forming an open structure, preventing transcription factors access to FLC, a gene which inhibits flowering (Yu *et al.*, 2011). In tomatoes, the histone deacetylase, SIHDA1, plays a significant role in fruit ripening by negatively regulating carotenoids, the chemical responsible for the red pigmentation (Guo *et al.*, 2017).

All studied plants use DNA methylation (Lane *et al.*, 2014), but not necessarily in the same way (Gent *et al.*, 2013)(Takuno & Gaut, 2013). Even the distribution of methylation varies among different plant species. In *Arabidopsis*, 22-30% of cytosines are methylated in a CG context, in comparison to 6-9% for CHG and 1.5-4% for CHH sites, giving an overall methylation level of 5% (Cokus *et al.*, 2008). Other important crop species contain higher levels of methylation, for example, rice, which has 14-18% of its genome methylated (Zemach *et al.*, 2010), and tomato, which has 22-24% of its genome methylated (Du *et al.*, 2012). This increase occurs across all contexts, with 73-85% of CG sites, 52-56% of CHG sites and 8-14% of CHH sites being methylated in tomato (Zhong *et al.*, 2013). Even the way the plant responds to a disruption in the epigenetic machinery varies among plant species. A loss of function for *met1* in *Arabidopsis* causes developmental abnormalities such as delayed bolting and abnormal floral development (Kankel *et al.*, 2003)(Finnegan *et al.*, 1996). There is also no phenotypic change to *Arabidopsis* in either a *cmt3* mutant (Lindroth *et al.*, 2001) or a *drm2* mutant (Cao & Jacobsen, 2002). However, a mutation in *met1* is lethal in rice at the seedling stage (Hu *et al.*, 2014), *cmt3* mutants have reduced fertility and dwarf phenotypes (Cheng *et al.*, 2015) and *drm2* mutants are sterile and have developmental abnormalities (Moritoh *et al.*, 2012). In tomato, an RNA Polymerase V mutation, one of the components of the RdDM pathway, causes lethality (Gouil & Baulcombe, 2016) and transformants containing a MET1 RNAi construct directed against the tomato MET1 gene could not be produced, suggesting seedling lethality (Watson, 2013). In tomato plants, it appears that accurate epigenetic regulation is essential for plant development. This makes understanding how different epigenetic mechanisms function in tomato, challenging to uncover.

Little is known about the role methylation plays in tomato development, except for its importance in fruit ripening. 5-azacytidine which removes methylation, induces early fruit ripening in the tomato, via the demethylation of the *CNR* gene promoter. This allows the binding of the transcription factor RIN (Ripening Inhibitor) and subsequent gene expression of *CNR* and other fruit ripening genes (Zhong *et al*, 2013). Although investigation into tomato methylation has been limited it still possesses many of the methyltransferase homologues found in *Arabidopsis* (Cao *et al.*, 2014). MET1 is structurally conserved but its precise function and its role in DNA methylation in tomato is still not clearly understood. It has been suggested that MET1 is essential for tomato development (Watson, M. R., 2013) making studying a *met1* mutant difficult. In the previous chapter, it has been demonstrated that over-expressing MET1 in *Arabidopsis* can disrupt dense methylation and cause epigenetic change. By applying the same strategy to tomato, we will be able to determine if MET1 functions in a similar manner in tomato as it does in *Arabidopsis*. If dense methylation is disrupted, we can investigate if it plays a larger role in gene regulation and stability and, if this disruption or alteration generates novel epi-alleles, whether they are heritably maintained in the next generation.

3.2 Results

3.2.1 Determining the structure of tomato MET1

Silencing of the tomato MET1 (SIMET) appears to be detrimental to the development of the plant (Watson, 2013). To investigate the function of MET1, the strategy to over-express the protein was chosen. Analysis of the SIMET protein was carried out, revealing that the structure and feature of the methyltransferase in tomato was essentially the same in *Arabidopsis*, consistent with both factors having similar functions in methylating DNA (Fig 3.1).

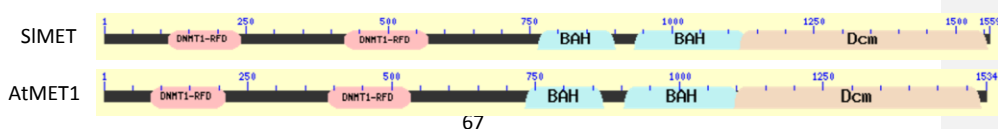


Figure 3.1: Predicted domains of Methyltransferases in *Solanum lycopersicum* and *Arabidopsis thaliana*. Both proteins are almost structurally identical possessing two DNMT1-RFD domains and BAH domain, and a single DNA methylase domain. Structural analysis was carried out using NCBI Conserved Domain Search (<https://www.ncbi.nlm.nih.gov/Structure/cdd/wrpsb.cgi>).

As both methyltransferases are fundamentally identical, the MET1 over-expression constructs (Fig 1.1) used in the *Arabidopsis* study were used to study tomato as well. The previous study confirmed that by altering the concentration of MET1 in *Arabidopsis*, the coordination of dense methylation was disrupted. As the structure of the methyltransferases is the same, it would be safe to assume they carry out the same function in tomato, including the coordination of dense methylation. If this is correct, by over-expressing either the catalytic active or inactive version of the *Arabidopsis* MET1 the epigenetic state could be altered in tomato. The two transgenic constructs were transferred into tomato, and six transgenic lines were selected; tA1+, tA2+, tA3+ and tA4+ containing the catalytically active *Arabidopsis* MET1 cDNA (*ArMET1*), and tI1+ and tI2+ contained the catalytically inactive *ArMET1*. Due to the long developmental time of tomato, only lines that possessed the transgene were analysed. Positive transformants were selected using the same primers designed for genotyping the *Arabidopsis* METo lines. The positive transformants were then allowed to self-fertilize, and their offspring were analysed.

3.2.2 Phenotypic analysis of the tomato ArMET1 over-expression lines

Over-expression of MET1 in *Arabidopsis* caused numerous phenotypes such as delayed bolting and shorter root growth. To determine if increased levels of *ArMET1* caused similar developmental abnormalities in tomato, extensive phenotypic analysis was carried out. Disrupting the epigenetic machinery has been shown to be detrimental to tomato (Gouil & Baulcombe, 2016; Watson, 2013). However, original tomato transformants containing the METo transgene fully developed and produced fruit. This indicates that over-expression of

Commented [CW7]: Remove initials

ArMET1 may not critically disrupt the epigenome. Although offspring were produced, increased levels of MET1 may still cause adverse developmental effects in the following generation. To ascertain if this was the case, germination for each METo line was assessed (Fig 3.2).

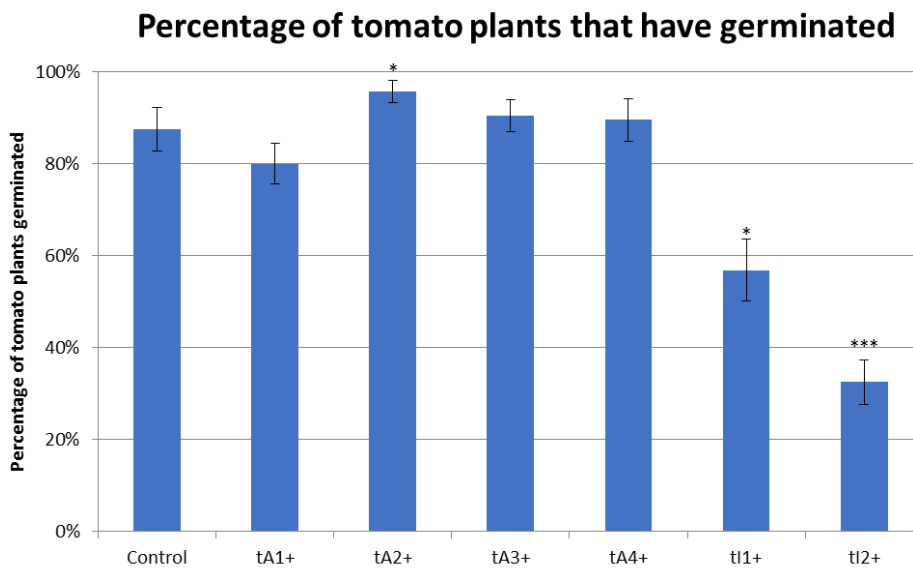
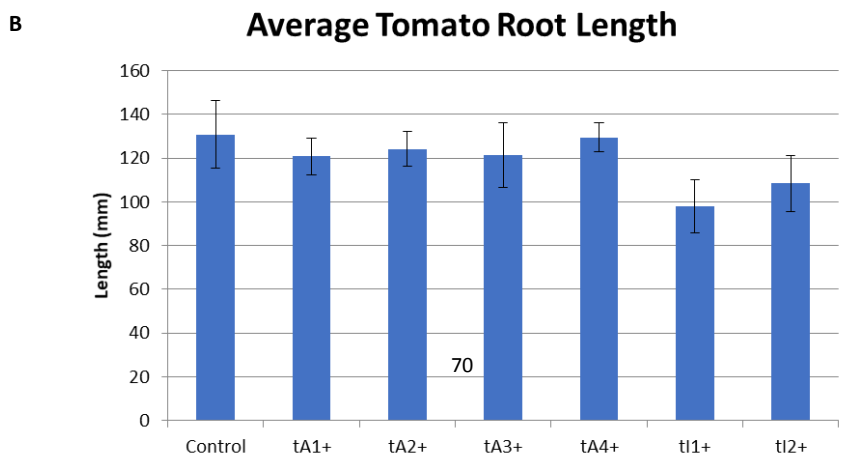
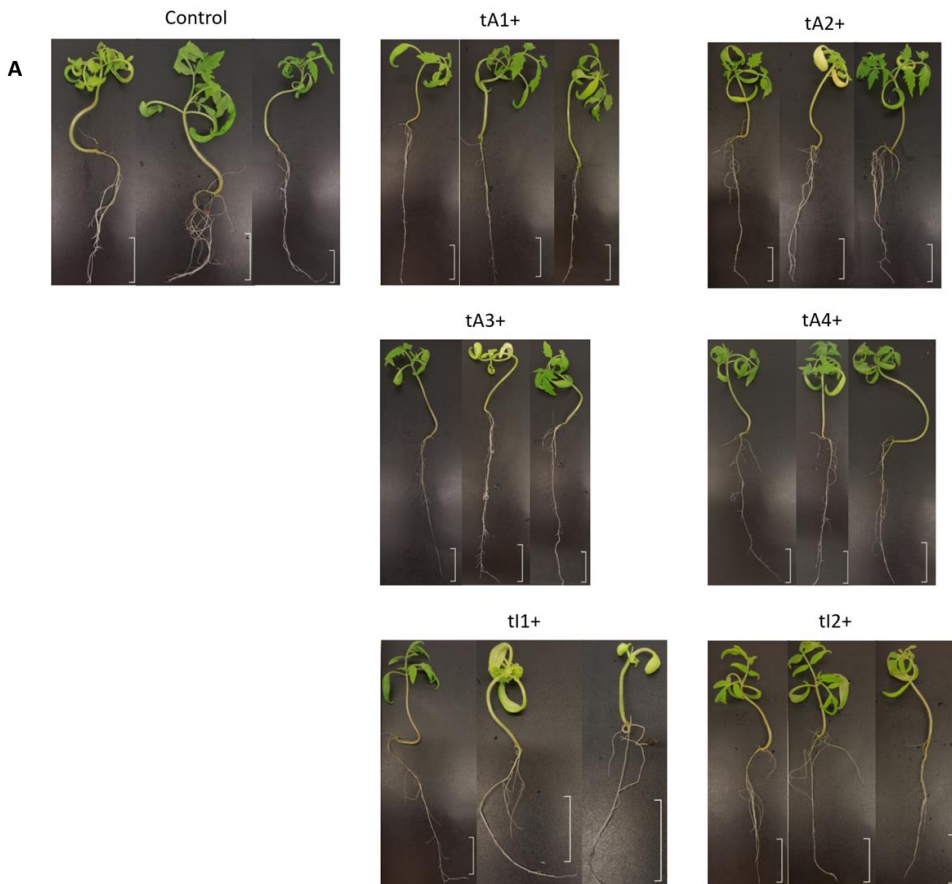


Figure 3.2: The germination of METo tomato lines. Line tA expresses a catalytically active METo transgene; line tI expresses a catalytically inactive METo transgene. Germination was determined by the emergence of the radicle after four weeks of development. The significance of a change from wildtype is indicated by asterisks (if present): * = $P < 0.05$, ** = $P < 0.01$ ***= $P < 0.005$, calculated by Student's two-tailed t-test.

Germination for three of the catalytically active METo lines was not significantly changed compared to the control lines, with the exception of line tA2+ which displayed increased germination. In comparison, both catalytically inactive METo lines have severely reduced germination with only 33% of seedlings germinating in line tI2+. Interestingly, germination was only severely affected in the catalytically inactive lines suggesting that that the mutated *ArMET1* may have a more dramatic effect on tomato development. To confirm if this is correct, further phenotypic analysis was carried out. Previous study of METo *Arabidopsis*

found that root length was reduced in all METo lines. To determine if similar phenotypes were observed in tomato, analysis of the root length and stem was carried out at four weeks of development (Fig3.3).



c

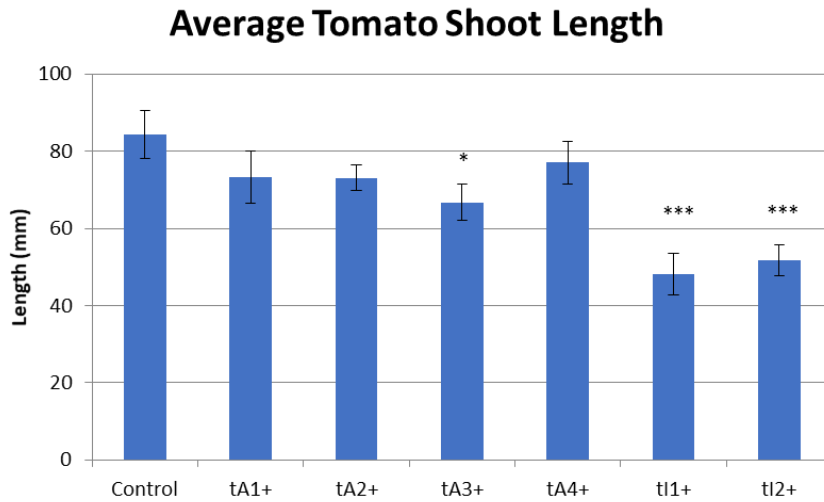


Figure 3.3: Phenotype analysis of tomato METo lines. A) Images of METo lines and wildtype control taken four weeks after stratification. The scale bar for shoot images indicates 3cm. B) The average primary root length at four weeks of development, comparing wildtype control and tMETo lines. B) The average shoot length at four weeks of development comparing wildtype control and tMETo lines. The significance of a change from wildtype is indicated by asterisks (if present): * = $P < 0.05$, ** = $P < 0.01$, *** = $P < 0.005$, calculated by Student's two-tailed t-test.

Compared to the control tomato line there was no significant change in the primary root length for all METo lines analysed, indicating that over-expression of ArMET1 responds differently in tomato root tissue than *Arabidopsis* root tissue. There was also no significant change in stem length for the tA lines. However, there is a significant reduction in the stem length for the catalytically inactive METo lines. Curiously the reduced stem length phenotype and reduction in germination are only present for the tI lines. This further supports the hypothesis that the catalytically inactive version of *ArMET1* has a much more significant effect on tomato development. During the phenotypic analysis, a number of

developmental abnormalities were observed (Fig 3.4); such as the degradation of chlorophyll and the acute curling of cotyledons and true leaves (Fig 3.4A). In one *tl* tomato, roots developed on the stem (Fig 3.4B). Unfortunately, these phenotypic abnormalities seldom appeared making it impossible to draw any significant conclusions. One phenotype that did appear a number of times in all METo lines was the abnormal development of the shoot apical meristem (SaM) or “blind” phenotype (Fig 3.4C-D). To determine if this was a significant phenotypic event, the number of blind tomatoes were determined for each METo line along with the control line and a line that had undergone plant transformation containing a GUS expression construct (Fig 3.4E).

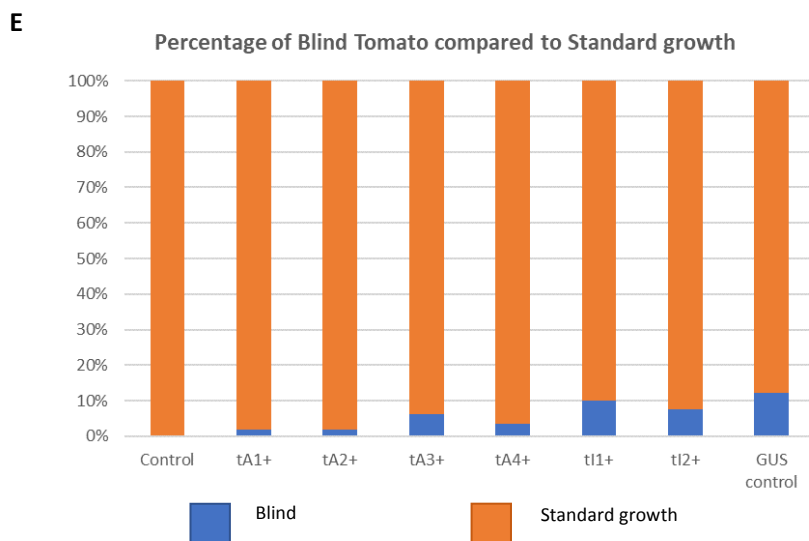


Figure 3.4: Phenotypic analysis of abnormal tomato development present in tMETo lines.

A) Image of diminished chlorophyll and acute leaf curling taken at four weeks of development for a catalytically active METo line. B) Image of abberant root growth on the stem of a catalytically inactive METo tomato. C) Image was taken of blind phenotype present in a catalytically active METo tomato D) Image was taken of blind phenotype found in a catalytically inactive METo tomato. E) The percentage of tomato plants that possess the blind phenotype at four weeks of development.

The blind phenotype was not present in any of the wildtype control plants. However, a number of blind plants were observed for each of the METo lines, independent of the catalytic activity of MET1. The percentage of blind plants was greater in the catalytically inactive METo lines which occurred in up to 10% of the plants analysed. The GUS transformant line also produced a similar number of plants possessing the blind phenotype, compared to the METo lines. This indicates the blind phenotype observed in the METo lines is, in fact, an artefact of plant transformation and not a causal effect of over-expressing MET1. Further investigation into the later stages of METo tomato development found no significant phenotypic abnormalities. Though numerous phenotypic analyses had been carried out, a characteristic phenotype that occurred across all METo lines could not be detected.

3.2.3 Transcript analysis of MET1 over-expression in tomato

The detection of no common phenotype in the METo lines implies that either the over-expression of MET1 causes no phenotypic difference due to its inability to disrupt dense methylation in tomato, or the METo transgene is silenced in tomato lines and over-expression of MET1 does not occur. To investigate if the METo transgene is silenced in tomato, qRT-PCR was used to measure the level of *MET1* transcripts (Fig 3.5). As the METo transgene over-expresses the *Arabidopsis* homologue of MET1, both ArMET1 and SIMET1 were analysed. Previous analysis identified that the blind phenotype observed in the METo lines might be linked to plants that have undergone a transformation. Plant transformation

has been shown to cause significant changes in the expression of many genes (Veena *et al.*, 2003) and is likely to be associated with many epigenetic changes. As the blind phenotype appears in the next generation of METo lines and occurs stochastically, it strongly suggests the phenotype is epigenetically linked. To study this possibility, MET1 transcripts were also examined in blind plants for both tA and tI plants (Fig 3.5)

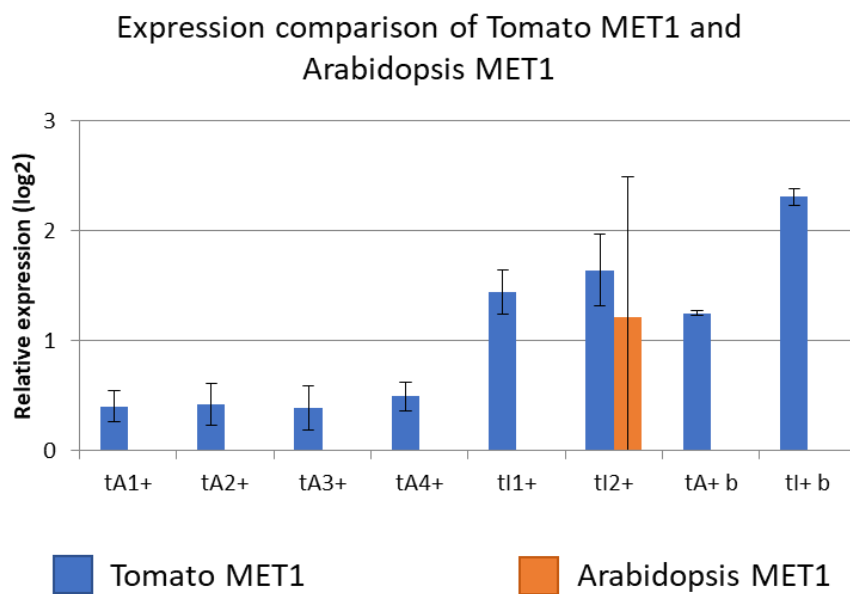


Figure 3.5: qRT-PCR analysis of ArMET1 and SIMET1. Transcription was measured for *ArMET1* and *SIMET1* in lines tA expressing a catalytically active *MET1* transgene, lines tI expressing a catalytically inactive MET transgene. Tomato lines possessing the blind phenotype were also analysed and denoted with a “b”. The analysis was carried out at 4 weeks after stratification. *ArMET1* expression was only detected in tI2+, Increased *SIMET1* expression was observed in tI1+, tI2+, tA+b and tI+b lines. The mean and the standard error are shown for three biological replicates each having three technical replicates for each line.

For both *SIMET1* and *ArMET1* the values on the y-axis represent the log₂ fold difference compared to the wildtype *SIMET1*.

qRT-PCR determined that *ArMET1* was not expressed in any of the catalytically active METo lines which resolves why no phenotypic abnormalities were observed. Conversely, *ArMET1* expression is detected in one of the catalytically inactive lines albeit with significant variation. This extreme difference in *ArMET1* expression is likely caused by the silencing of *ArMET1* in some of the plants analysed. No increase in *ArMET1* was detected for either of the blind tomatoes analysed. Interestingly an increase of *SIMET1* is detected for both the ti lines and plants that are blind. It may be possible that an increase in *SIMET1* is observed in response to a disruption of the epigenome, the blind phenotype has been linked to epigenetic change, and increased levels of MET1 have also been shown to alter the epigenome. No increase in *SIMET1* was detected in the tA lines, but they still possess the METo transgene, suggesting the transgene had been directly silenced. As no significant phenotypic marker was identified for the METo lines, and the blind phenotype is likely linked to an epigenetic change. It was decided to investigate if there were any genes with altered expression in the blind lines that are epigenetically regulated and have dense methylation. Three genes were identified that may play a role in causing the blind phenotype; *SELF-PRUNING 9D (SP9D)* which causes abnormal SaM development when silenced (Thouet *et al.*, 2008), a homologue of the *Arabidopsis* floral repressor (*CEN1.1*) (Cao *et al.*, 2016), over-expression causes delayed flowering and floral defects (Yoo *et al.*, 2010), and *WUSCHEL (WUS)* required for shoot and floral meristem integrity (Xu *et al.*, 2015). All three genes selected are involved in regulating correct SaM development and possess dense methylation within or adjacent to the gene (S3 Fig), *CLE3*, *CLE9* and *Blind* were also selected as they play a role in correct SaM development but didn't possess any dense methylation (Fig 3.6).

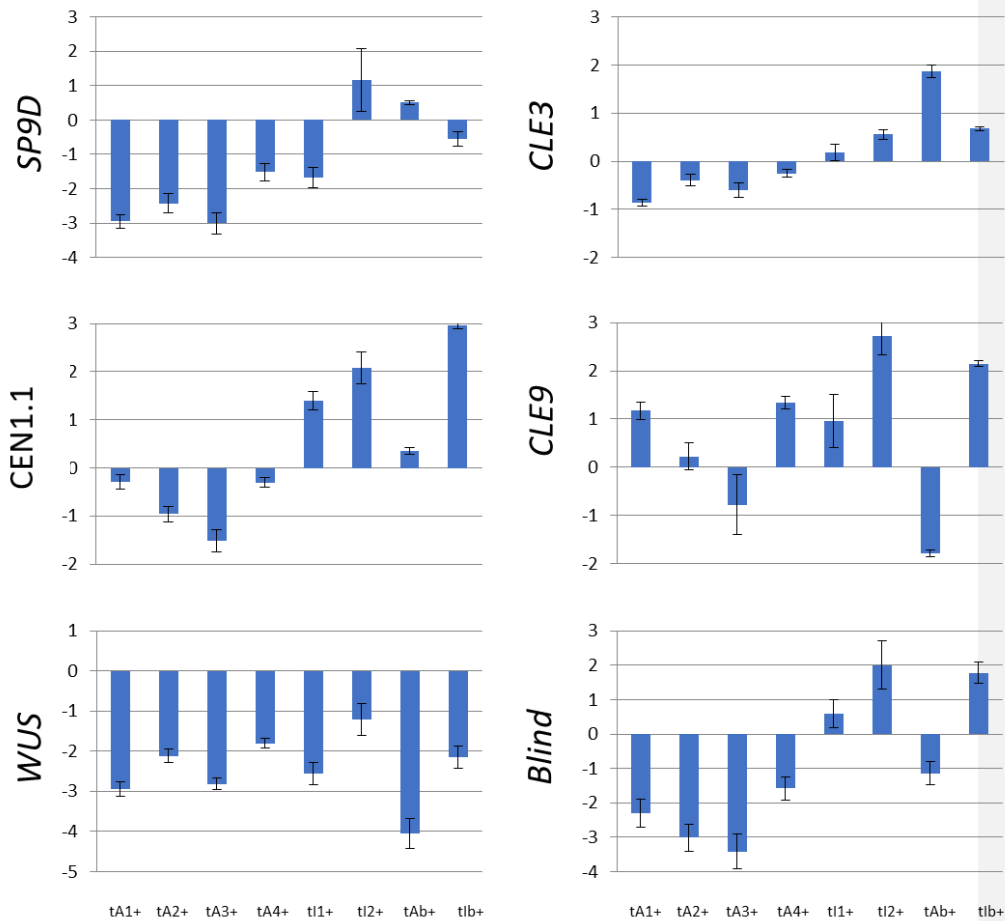


Figure 3.6: qRT-PCR analysis of the six genes selected for further analysis. Transcription was measured for six genes believed to play a role in the blind phenotype. Both increases and decreases in gene expression can be seen across different lines, with the exception of WUS, whose expression is reduced in all lines. Lines tA expressing a catalytically active MET1 transgene, lines tI expressing a catalytically inactive MET transgene. Tomato lines possessing the blind phenotype are denoted with a “b”. The analysis was carried out at 4 weeks after stratification and compared to the wildtype control. The mean and the standard

error are shown for three biological replicates each having three technical replicates for each line. Values on the y-axis represent the log₂ fold difference compared to the control line.

Analysis of all six genes found no significant correlation between increased *SIMET1* and gene expression. *WUS* was downregulated in all the METo lines including those that were blind which may imply that it is a common target in plants that have undergone transformation but that it is not responsible for the blind phenotype. Expression of *CEN1.1* was upregulated in all three of the tI lines which had increased SIMET1 levels, but not in tAb+. The *Blind* gene was down-regulated in the tA+ and tAb+ lines but cannot be directly linked to the blind phenotype as the gene is downregulated in lines that are not blind as well. The remaining genes displayed no common expression pattern and were highly variable across multiple lines.

3.3 Discussion

In the previous chapter, it was discovered that over-expression of MET1 could be used as a strategy to induce new epigenetic variants with novel epi-alleles. MET1 is structurally and functionally similar in many important crops species including; wheat (Thomas *et al.*, 2014), maize (Steward *et al.*, 2000), rice (Teerawanichpan *et al.*, 2004) and tomato (Cao *et al.*, 2014), making over-expression of MET1 in crops ideal. It was decided first to test this strategy in tomato plants, as the tomato MET1 is structurally and functionally similar to *Arabidopsis* MET1. Both the catalytically active and inactive METo construct was introduced in tomato and tested. Unfortunately, no significant phenotypic difference was observed in any of the over-expression lines except for a severe reduction in germination for lines that over-expressed the catalytically inactive form of MET1. Transcript analysis of MET1 revealed that *ArMET1* was completely silenced in all the catalytically active METo lines. Expression of the catalytically inactive *ArMET1* was detected, but due to the significant variation in transcription, stable expression of *ArMET1* could not be confirmed. As no significant expression of *ArMET1* could be detected, and germination in the catalytically inactive lines were significantly lower than both the wildtype control and the catalytically active lines, suggests excess catalytically inactive MET1 could be detrimental to tomato development. Over-expression of the catalytically active may also be detrimental but due to transgene silencing in the previous generation expression of *ArMET1* was silenced, preventing any developmental abnormalities in further generations. Disruption of the epigenome and MET1 has been shown to be detrimental to tomato development (Watson, 2013) supporting our observation that increased levels of MET1 causes tomato termination. Interfering with MET1 in tomato may cause such a severe response due to only possessing one copy of MET1. In comparison, *Arabidopsis* has three additional homologs of MET1 (MET2a, MET2b and MET3) which are structurally similar (Cao *et al.*, 2014), allowing for redundancy. Although over-expression of MET1 appears to be difficult in tomato, many other crop species have multiple copies of MET1 such as maize (Qian *et al.*, 2014) and wheat (Thomas *et al.*, 2014), making them prime candidates for over-expression of MET1.

Although *ArMET1* is silenced in tomato, it was identified that *SIMET1* levels increased in lines that possess the catalytically inactive METo transgene and those with the blind phenotype. The stochastic nature of the blind phenotype which appears in less than 10% of tomato plants, spanning at least two generations, implies an epigenetic disturbance possibly brought about by plant transformation. As increased levels of *MET1* were observed in lines that were epigenetically compromised, there may be a link between *MET1* levels and the disruption of the epigenome. To determine if this was the case, six genes were selected all of which play a role in SaM development. Three of the selected genes were also densely methylated, as increased levels of *MET1* have been shown to disrupt dense methylation. Analysis of the six genes could not confirm any direct link between the increased levels of *MET1* and abnormal development of the SaM causing the blind phenotype. One of the target genes, *WUS*, which causes abnormal SaM development in *Arabidopsis* when downregulated (Laux *et al.*, 1996), is also downregulated in all METo lines. However, downregulation of the *WUS* gene was observed in tomatoes that didn't possess the blind phenotype, indicating downregulation of *WUS* does not directly cause abnormal SaM development.

Despite not being able to over-express *MET1* in tomato we have identified that the stress of plant transformation disrupts the epigenome generating a stochastic phenotype. Further investigation into the epigenetic differences in plant transformants will be critical to determine common loci that are altered in response. We have also shown that *MET1* is upregulated in response to possible epigenetic disruption (Fig 3.5) making it an attractive candidate to follow in lines that have undergone transformation stress. Over-expressing *MET1* in tomato has also highlighted the importance of different expression strategies, such as targeted over-expression in certain tissue types or at distinct *MET1* target loci. Spatial and temporal over-expression of *MET1* will also offer the opportunity to test if *MET1* target loci alter their susceptibility to *MET1* over-expression in different tissues and identify developmental stages that are particularly sensitive to the induction of epigenetic switches.

4 General discussion

Variation in gene expression and phenotypes in plants can be induced by different epigenetic states. Our study has shown that by temporarily increasing the level of DNA methyltransferase MET1 we can cause heritable epigenetic changes at specific loci. This provides a new strategy to generate novel epi-alleles, and identify common epigenetic target loci and phenotypes. MET1 over-expression serves as a proof-of-concept study that should stimulate a wider application of over-expressing epigenetic regulator genes to examine the significance and targets of epigenetic regulation in different species.

4.1 Over-expression of MET1 induces heritable epigenetic diversity

The coordinating role of MET1 for dense methylation, illustrated by the loss of CG and non-CG marks in *met1* mutants (Singh *et al.*, 2008), may be facilitated by a MET1 multi-protein complex which guides CMT2 and CMT3 to dense methylation targets. Alternatively, MET1 could interact with histone regulators like HDA6, for which direct binding to MET1 has been demonstrated (Liu *et al.*, 2012) and which has been proposed to recruit MET1 to particular target loci as the initial step in establishing subsequent non-CG methylation (To *et al.*, 2011)

As the MET1 complex may involve direct interaction with other epigenetic factors, it should be sensitive to changes in MET1 concentration. To test this, high levels of catalytically active and inactive MET1 protein were introduced. The observation that both approaches can cause expression changes and hypomethylation of dense methylation loci resembles disruption caused by the imbalance of multi-protein complexes induced by over-expression of individual complex partners (Sopko *et al.*, 2006). Stoichiometric imbalances can sequester complex partners and disrupt the multiprotein complex. One of the earliest examples demonstrating this effect is the over-expression of either histone H2A-H2B or histone H3-H4 gene pairs in yeast, which causes aberrant chromosome segregation (Meeks-Wagner and Hartwell, 1986) and alters transcription due to disturbance of the histone octamer (Clarkadams *et al.*, 1988).

We observe that increased MET1 expression is required but not always sufficient to induce novel epi-alleles. The efficiency of which these epigenetic changes are caused is not directly correlated with the level of MET1. This implies that the epigenetic changes occur in a stochastic manner but with defined probability for individual loci, similar to the effects of position-effect-variegation (Elgin and Reuter, 2013). This explains why not all transformants display the same phenotypic changes and why particular phenotypes occur more frequently than others. This provides us with a pool of new epi-variants that can be used to link phenotypes to ectopically expressed epi-alleles.

The changes in histone marks that accompany expression changes in METo lines suggest a possible involvement of HDA6 or a related histone modifier. Similar effects are observed in transposable elements activated in *met1* and *hda6* mutants, which also show increased H4 acetylation and H3K4 methylation levels (Liu *et al.*, 2012). So, at some loci, increased levels of MET1 may interfere with the targeting functions of HDA6, causing the observed histone acetylation increases, stimulating hypomethylation and H3K4 methylation, leading to increased expression.

MET1 over-expression does not just copy the effects induced in a *met1* mutant. Some, but not all, phenotypes and genes whose expression are altered in METo lines, are not observed in a *met1* mutant. Expression changes of common target genes are also reversed when the *met1* mutant is restored to a wildtype background, but retained if the METo transgene is out crossed. Although expression change is preserved over multiple generations when the METo transgene is out crossed, the efficiency with which it is maintained varies between target loci. Further enhancement of gene expression is also observed in lines that have retained the METo transgene, suggesting epigenetic changes can be continuously induced in lines that have maintained increased MET1 expression.

4.2 Investigating the tomato epigenome

As tomato MET1 is structurally and functionally similar to *Arabidopsis* MET1 possessing the same conserved domains (Fig3.1), both the catalytically active and inactive METo constructs were introduced in tomato. However, unlike *Arabidopsis* which displayed a number of different phenotypic variants, tomato METo lines did not. Transcript analysis confirmed that *ArMET1* was silenced in all the METo lines. As only tomatoes with silenced *ArMET1* are observed, increased levels of MET1 may be detrimental to plant development. However, unlike the attempted silencing of MET1 which couldn't produce tomato lines transformed with a MET1 inverted repeat, tomatoes can be created containing the METo transgene. This suggests that enhanced MET1 levels may only be detrimental at a specific stage of development, allowing silencing of the transgene.

Although *ArMET1* is silenced in the METo lines, enhanced levels of *SIMET1* are observed in catalytically inactive METo lines. The increased levels of *SIMET1* in the METo lines could imply that MET1 is involved in transgene silencing, and increased levels of MET1 are required to establish this state. Enhanced levels of *SIMET1* are also observed in plants that are blind, but transcript analysis of six candidate genes involved in correct SaM development could not determine a correlation. Nevertheless, transcript analysis identified that *WUS*, a gene which possesses dense methylation, is down-regulated in every METo line, highlighting it as a possible epi-allele that is targeted during plant transformation.

4.3 Outlook and open questions

4.3.1 Linking phenotypic change to alternatively expressed epi-alleles

Over-expression of MET1 has identified a number of novel epi-alleles that induce distinct phenotypes. FWA is upregulated in METo lines and causes delayed bolting. PAP26 is downregulated and plays a significant role in reducing primary root length, and AT3G27473 contributes to both delayed bolting and reduced primary root length when upregulated. Although we have determined three epi-alleles that induce phenotypic change, transcript analysis has identified 31 protein-coding genes and many more small RNAs that may play a role in phenotypic development. Altering these genes may also increase or reduce certain stress tolerance. AT3G30775 (ERD5) for example is involved in pathogen response (Fabro *et al.*, 2016). Increased expression of ERD5 is observed in A1 lines, which may enhance their responsiveness to infections. We ascertained that a reduction of PAP26 correlates with shorter primary root length. PAP26 does not appear to cause root shortening directly, but a recent study found that Pi-deprived plants accelerate the degradation of AUX/IAA proteins (Perez-Torres *et al.*, 2008), which may disrupt root development. To see if this is the case, fluorescent auxin reporters can be transformed into METo lines, to visualize the transportation and distribution of auxin in the roots.

4.3.2 Using an inducible system to over-express MET1

The inability to over-express MET1 in tomato led to the speculation that increased levels of MET1 are lethal to tomato. To test this theory, the METo construct could be modified with an inducible system allowing over-expression of MET1 at different stages of development. The ability to generate tomatoes containing the METo transgene suggests that increased levels of MET1 can be tolerated at later stages of development and lethality occurs during the earlier stages of development. One stage that may be especially sensitive to altered levels of MET1 is embryogenesis. Genes that specify embryo cell identity are incorrectly

expressed, and auxin hormone gradients are not properly formed in abnormal *met1* embryos (Xiao *et al.*, 2006), leading to abnormal development and reduced seed viability. Different tissue types may also be more susceptible to epigenetic change. A reduction in root length is observed in all METo lines, yet the development of the flower appeared unaffected. Using a tissue-specific promoter, such as the root-specific promoter HPX1 (Park *et al.*, 2013), will allow us to test this susceptibility, and if the phenotypic changes observed are caused by an epigenetic disruption during embryogenesis or occur during root growth. We may also be able to induce epigenetic changes at distinct MET1 targets via CRISPR dCas9-MET1 fusions construct allowing precise induction of epi-alleles.

4.3.3 Investigating the protein interactions of MET1

Our findings support the idea that MET1 is part of a multiple protein complex that regulates dense methylation. However, we have yet to determine what proteins MET1 directly interacts with. Candidates include CMT2 and CMT3, which have been proposed to play a role in establishing dense methylation (Singh *et al.*, 2008), and HDA6 which has been shown to directly bind to MET1 (Liu *et al.*, 2012) and recruit it to particular target loci as the initial step in establishing subsequent non-CG methylation (To *et al.*, 2011). Using a FLAG-tagged MET1 and tandem affinity purification (TAP), proteins and complexes can be isolated that directly interact with MET1. This can also be used to investigate if the mutation in the catalytically inactive MET1 causes a novel conformational change preventing interaction with individual proteins or allows new interactions. Chromatin tandem affinity purification Sequencing (chTAP-seq) can also be implemented to map the genome-wide binding of the MET1 complex (Soleimani *et al.*, 2013), this may identify other target regions that don't have altered expression levels when grown in normal conditions, but change in response to environmental stress.

4.3.4 The function of the MET1 homologs

Over-expressing MET1 in *Arabidopsis* causes numerous phenotypic abnormalities, yet in tomato it appears to be lethal. This variation in susceptibility to epigenetic disruption may be due to the different homologs of MET1 found in *Arabidopsis* (Cao *et al.*, 2014). The structural similarity of both MET2a and MET2b compared to MET1 may imply some redundancy in function. Very little is known about the roles of the MET1 homologs except that MET2a and MET2b are expressed in the mature ovules (Jullien *et al.*, 2012). To determine if there is any redundancy in function a knockout line of all four METs (MET2, MET2a, MET2b, MET3) could be generated to see if the loss of all four METs are lethal. Investigation of the individual MET knockouts should also be studied to determine if the MET1 homologs are active at different stages of development or different tissue types and if they are part of a mechanism that can offset the loss of MET1.

4.3.5 Epigenetic changes induced by transformation

The investigation into the recurrence of the tomato blind phenotype implied it was likely an epigenetic event caused by the stress of plant transformation. It has been documented that plant transformation causes significant expression changes in many genes (Veena *et al.*, 2003), but little is known about the epigenetic effect. Whole transcript and methylome analysis should be carried out for plants that have undergone transformation to determine common target loci along with phenotypic analysis to determine the frequency at which abnormal phenotypes occur. We believe to have identified one common epi-allele, WUS, which is downregulated in all transformed lines and has dense methylation adjacent to the gene. The epigenetic effect of transforming crops will become more important as GM crops increase in popularity.

5 Materials and Methods

5.1 Materials

5.1.1 Arabidopsis material

All *Arabidopsis* analyzed possessed a *Columbia* background. Control *Arabidopsis* plants were derived from non-transgenic seeds raised from a transformation experiment where seeds were cultured on selection-free media. The *Arabidopsis* met1-1 mutant was provided by Dr. Ortrun Mittelsten Scheid (GMI, Vienna, Austria) and genotyped according to (Singh *et al.*, 2008). MET1 levels were restored (Met1-RE), by self-pollinating a plant derived from a cross between the met1-1 mutant and a wildtype line, and selected a line homozygous for the wildtype MET1 alleles. Homozygous *atpap26* T-DNA insertion mutants (Salk_152821) were obtained from the Nottingham Arabidopsis Stock Centre (<http://arabidopsis.info>) and genotyped using the T-DNA left-border and gene-specific primers.

T1 METo transformants A1, A2, I1, and I2, were selected on hygromycin medium and self-pollinated. T2 progeny plants of each line were grown without selections and were genotyped. To differentiate between transformants that had retained or lost the MET1 transgene, respectively, primers were designed annealing either side of an intron of the MET1 gene. These primers amplify part of the endogenous MET1 gene yielding a 1161bp fragment, while amplification of a part of the MET1 cDNA transgene without the intron produces a 786bp fragment. Plant with (+) and without (-) the transgene was isolated and selfed. T3 seeds of these plant were placed on hygromycin selection to confirm that the transgene had been lost in (-) plants and to identify (+) lines that were homozygous for the transgene. One (-) plant and one (+) plant, homozygous for the transgene, were selected for each line. The T1 AT3G01345, AT3G27473, and AT3G30720 over-expression lines were selected on hygromycin medium and genotyped using the corresponding primers.

5.1.2 *Solanum Lycopersicum* material

All *Solanum Lycopersicum* analyzed possessed the Moneyberg background. All tomato analysis was carried out in T1 METo transformants. A1, A2, A3, A4, I1, and I2 were genotyped using the *Arabidopsis* MET1 primers to generate one band at 786bp.

5.1.3 Bacterial strains

Plasmid cloning was carried out using *Escherichia coli* Dh5 α (New England Biolabs). Plant transformations were performed using *Agrobacterium tumefaciens* GV3101::pMP90 (Hellens *et al.*, 2000).

5.2 Primer list

	Forward Primer	Reverse Primer
Cloning		
AT3G01345	TGTCCCGGGCCAATTTGACATTTTTAA	TGTACTAGTTTTTTTTGTCAAACAAAGATC
AT3G27473	TGTCCCGGGATGACTTTTAGGCTAGAAG	TGTACTAGTCAAATTGCCCATGGAGGGCA
AT3G30720	TGTCCCGGGCTCAGAAGAAGCCTCCTTTC	TGTACTAGTTCTAGTTGTAATGGGCATTA
Genotyping		
METo	TCCAATCACCGTGAGAGACAC	TCATAGTCTATAGACATCATTGCTTG
met1-1	CTCTTTAGTAGAAGTTGGCATG	GTTAAGCTCATTATAGCCTTGC
Atpap-26	ATTGCTGAAAACCTTAAGCGGG	ATTTTGCCGATTTTCGGAAC
AT3G01345	TGCTTTGAAGACGTGGTTGGAACG	CAGCATTAGGTTTAGCCGCCA
AT3G27473	TGCTTTGAAGACGTGGTTGGAACG	GGAGCTCCATTGGTGATAAGC
AT3G30720	TGCTTTGAAGACGTGGTTGGAACG	CTAAGAACCAAACCAACTGG
MET1 FLAG	TCCAATCACCGTGAGAGACAC	TCTCGAGTTACTTGTATCGTC
Semi-qPCR analysis		
AT5G49160 (MET1)	GGGCTCGAGCTTCCATTATCATCAGTCAC	GGGGGTACCGCTGGTTGGATGAGACAGC

AT3G01345	GCGGCTAACCTAATGCTGC	CAGACCTGGCCTTAGAGGA
AT3G27473	CCCAAAGTGTATTACCCCAAACC	GATCGATCGCAAGCATCACA
AT3G30720	TTTCTCCACAGATGAAGACCAA	ATTTTGAGCCTTGCACACC
AT1G07920 (EF1 α)	GCGTGTCAATTGAGAGGTTCCG	GTCAAGAGCCTCAAGGAGAG
qPCR analysis Arabidopsis		
AT3G01345	TTGCTGCCACACCAAGTATCG	ACCAGCCCAAACAGAGGTAGAG
AT3G27473	GCCTCTGGATCTTAGCCTCCAATG	TGACGACAAGCTCGACATCTCC
AT3G30720	AAACCTCCTTTGATCTGTACAGC	ATGGCTGACCGTGTGAGTCTTG
AT3G30820	CAGAGCATCTTCGCTGTACCTG	TTCGTCGCGGAGAGAAATGAGG
AT4G25530	TCCCATGACTTGCGTGACTCTG	CACGTTGACCCATTTGCCTGTG
AT5G34850	TCACAGTTGGAGACGGAGGAAATC	TGGCTGTGTTCCGTAAACCTTC
AT5G49160 (MET1)	AGACCTCCGAAGAAGAAACAGA	CTCACGGTGATTGGACGGAA
AT3G18780 (ACT2)	CGGTATGGTGAAGGCTGGAT	ACAAACGAGGGCTGGAACAA
qPCR analysis Tomato		
WUS	CCAGCAACTTACCCTTTTCTTG	TAAAGCAGAGTTACCCCTTTGG
CLE9	CAATGCAAGCACAAATCCTCT	CCTGCATCCTGGCTTATTCT
CLE3	CTGCTGAGATTTTAGTAAAGCCTG	GAATGCCTTTCTGTTCTATTATCC
CEN1.1	GACCTGATGCTCCAAGTCC	TGGCTGCAGTTTCTCTCTGG
SP9D	GGTGAGCTATGAGACCCCAAG	CAGCGGTTTACGTTGTGC
<i>Blind</i>	TTCCAGCAGCCCAACAAAAC	GAACAACCTGCAACTTCCCAA
SIMET1	CGGCTTGCCTTGAAGTTTAT	GATGACAAAGTCCCTGATGG
eIF3-E	GAGCGATGGATGGTGAATCT	TTGTACGTGCGTCCAGAAAG
Bisulphite Sequencing		
AT3G01345	GTTGGTGAYAAAGAGAAGATG	ATAACAACATCAAAAAATTT
AT3G27473	ATAAAATATTAGGTTAAGTG	ATCTCRAATCAATATTTCCARCT
AT3G30720	GAGATATTGGYTTTGATTTGTYTGTTT	TCITRTTTCTTCTRATCTTCAAT
AT5G34850	GAATGTTGATTTAAAATYAGAATGAAG	CAAACCTTTTCTTRACACCAAATTTTC
ChIP analysis		
AT3G01345	CGAGGCCAAAGCTTCCAAC	GAGAGCGACAAGGGAACGAT
AT3G27473	ATCCACAACCGCATGACTT	GAGAACCCATCACCAGACGA
AT3G30720	AGGTTCAATTTGCCTCACACT	GCCCGACCCATGATATGACC
AT5G34850	TGGGTTACACCTGATGAACCTG	TGGTAAGTCCCTTGAGCAACA

AT5G34850 mapping		
Pp1	CTCACTCGCATAGTCCGACA	ATACAATCTGAGAAATTCGTTGTGA
Pp2	CAAACTTTTCTTGACACCAAATTTTC	ATACAATCTGAGAAATTCGTTGTGA
Pp3	AAGACCCAATCCATTTCCCTCA	TGGTAAGTCCCTTGAGCAACA
Pp4	AAGACCCAATCCATTTCCCTCA	CAATCTGTAATAGTATTTGTATC

5.3 Construction of plasmids and plant transformation

5.3.1 Over-expression Constructs

The METo and MET1 FLAG-tagged plasmids were constructed by Michael Watson (Watson, 2013). To create the AT3G01345, AT3G27473 and AT3G30720 over-expression constructs the MET1 gene was excised from the METo construct using SpeI and XmaI. The target genes were then amplified with primers containing the corresponding site and inserted into the over-expression construct.

5.3.2 *Arabidopsis* transformation by floral dip

Arabidopsis transformation was carried out by floral dip (Clough and Bent, 1998). 500 ml of LB media (10 g/l bacto-tryptone; 5 g/l bacto-yeast extract; 10 g/l NaCl) containing the appropriate antibiotics and bacteria were grown at 28°C until OD600 1.0 was reached. Cells were pelleted using centrifugation and re-suspended to an OD600 0.8 in 5% sucrose; 0.05% Silwet-L77. Wildtype plants were grown at 25°C, under long day conditions till they had appropriately matured at which point clipping of the primary bolt was carried out to induce lateral bolt formation. The plants were inverted into the re-suspended culture for 1 minute and placed into sealed bags for 24 hours to encourage infiltration. This process was repeated one week after the original floral dip. Seeds were harvested by bagging the matured plants. Positive transformants were identified by growing seeds on MS20 medium (4.405 g/l Murashige and Skoog plus vitamins; 20 g/l Sucrose; 0.55% agar; pH 5.8) containing the appropriate antibiotics, at 25°C, 16/8 hour day/light conditions for 2 weeks. Seeds were

sterilized by washing in 70% ethanol for 2 minutes, soaking in 30% bleach (4.8% active hypochlorite) for 10 minutes and washing 5 times with sterilized water.

5.3.3 Leaf disc transformation of *Solanum lycopersicum*

Leaf disc transformation of *Solanum lycopersicum* was carried out at the premises of ENZA ZADEN, Enkhuizen, The Netherlands (supervised by Iris Heidmann). Seeds of Moneyberg were sown onto MSB530 medium (Murashige and Skoog salts, B5 vitamins, Duchefa M0231; 30g/l Sucrose; 0.8% agar; pH 5.8) and germinated at 25°C, 16/8 hour day/light conditions for 10 days (until cotyledons expanded). Cotyledons were cut into 0.5cm pieces, placed onto solid co-cultivation medium (4.405g/l MSB5; 3% glucose; 0.8% agar; 200mg/l KH₂PO₄; 0.2mg/l 2; 4D, 0.1mg/l Kinetin; 0.1mg/l indole-3-acetic acid; 46.8 mM Acetosyringone; pH 5.8) and pre-cultured overnight. During this time *Agrobacterium* containing the required clone was grown in YEB media (5g/l Yeast extract; 5g/l Beef extract; 20g/l Sucrose; pH 7.2; 2.5mM MgSO₄, with the appropriate antibiotics. The *Agrobacterium* was washed with liquid co-cultivation medium (4.405g/l MSB5; 3% glucose; 200mg/l KH₂PO₄; 0.2mg/l 2; 4D, 0.1mg/l Kinetin; 0.1mg/l indole-3-acetic acid; 46.8 mM Acetosyringone; pH 5.8), diluted to a density of OD₆₀₀ 0.4 and poured over the explants. After one hour the explants were briefly dried, transferred onto fresh co-cultivation medium and incubated at 25°C for 76 hours under dim light conditions. The explants were transferred to selective medium (4.405g/l MSB5; 3% glucose; 0.8% agar; 2mg/l Zeatin; 500mg/l Cefotaxime; selective antibiotic; pH 5.8) for regeneration.

5.4 Agrobacterium protocols

5.4.1 *Agrobacterium tumefaciens* GV3101::pMP90 electro-competent cells

Agrobacterium was grown in 500 ml of liquid lysogeny broth (LB) (10 g/l bacto-tryptone; 5 g/l bacto-yeast extract; 10 g/l NaCl) and the appropriate antibiotics at 28°C, gently agitated. When an OD600 of 0.8 was reached the cells were pelleted and re-suspended in ice cold, sterile water. This procedure was repeated 3 times with a final re-suspension in 10% glycerol. The final re-suspension was made into stock aliquots, then frozen using liquid nitrogen and stored at -80°C.

5.4.2 Binary plasmid electroporation *Agrobacterium*

The plasmid construct pGreenII0029 were co-transferred with pSoup into *Agrobacterium*. pSoup is a helper plasmid that provides the replicase function for the pSa replication origin of pGreen. A pre-chilled 1 mm cuvette was loaded with 10–50 ng of plasmid construct, 10 ng of pSoup and 50 µl of electrocompetent cells of *Agrobacterium*. The cuvette was transferred onto a BioRAD Gene Pulser cell-porator using the following parameters: C = 25 µF, R = 400 Ω, 5 ms delay, and pulsed at V = 1.8 kV. Immediately after electroporation the cells were mixed with 950 µl LB in a 15 ml tube and incubated at 28°C for 4 hours with gentle agitation. The transformation mix was spread on LB plates containing 50 µg/ml Kanamycin, 50 µg/ml Gentamycin, and 12 µg/ml Tetracycline prior to incubation at 29°C for 3-4 days.

5.4.3 Isolation of plasmid DNA from *Agrobacterium tumefaciens* GV3101::pMP90

Mini-prep isolation of plasmid DNA from *Agrobacterium* was carried out using a modified alkaline lysis method (Wang, 2006). Individual colonies were grown in 10ml of liquid lysogeny broth (LB) (10 g/l bacto-tryptone; 5 g/l bacto-yeast extract; 10 g/l NaCl) supplemented with the required antibiotics for 48 hours at 28°C, and cultures were gently

shaken. The culture was pelleted by centrifugation, and the supernatant was discarded. The cells were re-suspended in 100µl of solution 1 (50mM glucose; 25mM Tris-HCl, pH8.0; 10mM EDTA, pH8.0; 4mg/ml lysozyme) and incubated at room temperature for 30mins, 200 µl of solution 2 (0.2M NaOH; 1%SDS) was added and mixed. Finally, 150 µl of solution 3 (3M KAc, pH 5.5) was added and mixed thoroughly. The solution was then centrifuged at 12,000 x g for 5 min at 4°C, and the supernatant was transferred to a new tube containing phenol:chloroform:IAA. The suspension was centrifuged at 12,000 x g for 1 minute, and the upper layer was transferred to a new tube. The isolated DNA was precipitated with an equal volume of Isopropanol and centrifuged at 12,000 x g for 10 min at 4°C to pellet the DNA. The pellet was washed with 70% ethanol and allowed to air dry. The DNA was dissolved in 30-50 µl of sterile ddH₂O.

5.5 E. coli protocols

5.5.1 Preparation of chemically competent E. coli cell

E.coli competent cells were made according to (Sambrook *et al.*, 1989). A glycerol stock of the E. coli strain DH5α was plated on LB (10g/l bacto-tryptone; 5g/l bacto-yeast extract; 10g/l NaCl 0.8% agar) and incubated overnight at 37°C. A single colony was selected and inoculated in 2 ml of LB broth and incubated overnight at 37°C with agitation. 1ml of the overnight culture was added to 500 ml of LB broth in a 2000 ml Erlenmeyer flask, followed by incubation at 37°C with agitation until the OD₆₀₀ reached 0.3–0.4. The culture was cooled on ice for 10 min and divided into two sterile round-bottom centrifuge tubes. The cells were collected by centrifugation at 5,000 x g for 10 min at 4°C and the supernatant discarded. The pelleted cells were kept on ice and gently resuspended in 100 ml of 100 mM ice cold, sterile MgCl₂. The cells were collected again by centrifugation. The supernatant was discarded, followed by cells re-suspension in 20 ml of ice-cold 100 mM CaCl₂. An additional 180 ml of ice-cold 100 mM CaCl₂ was added. This suspension was kept on ice for 20 min, and the cells were collected via centrifugation. The supernatant was discarded, and the cells were re-suspended in the 4ml volume of ice cold, sterile 85 mM CaCl₂ and 15% of glycerol

(w/v). The suspension was aliquoted into 1.5 ml tubes and frozen in liquid nitrogen prior to storage in -80°C freezer.

5.5.2 Heat-shock transformation

10–50 ng of plasmid DNA or 10 µl of ligation reaction were added to 100 µl of thawed competent cells on ice and gently mixed. The suspension was incubated for 30 minutes on ice prior to heat shock treatment at 42°C for 90 seconds and transferred immediately back on ice for 2 min. Then, 900 µl of LB was added and incubated at 37°C with agitation for 1 hour. Next, 100 µl of the culture was spread on warmed LB plates containing the appropriate antibiotic for correct transformation selection, followed by overnight incubation at 37°C.

5.5.3 Mini-prep isolation of plasmid DNA from E.coli

Mini-prep isolation of plasmid DNA from E.coli was carried out using a modified alkaline lysis method (Sambrook *et al.*, 1989). Individual colonies were grown in 2ml of liquid LB with the required antibiotics for 17 hours at 37°C. 1 ml of the overnight culture was transferred to a 1.5 ml tube and centrifuged for 5 min at max speed to pellet the cells. The supernatant was removed and resuspended in 100 µl of solution I (50 mM glucose; 25 mM Tris-HCl, pH 8; and 10 mM EDTA, pH 8) and thoroughly mixed. 200 µl of solution II (0.2 M NaOH and 1% SDS) and 150 µl of solution III (5 M Potassium Acetate; pH 5.5, adjusted with Glacial Acetic Acid) was added and placed on ice for 10mins. The tubes were then centrifuged at 12,000 x g for 5 min at 4°C. The supernatants were transferred into new tubes with an equal volume of ice-cold Isopropanol. The suspension was centrifuged at 12,000 x g for 10 min at 4°C to pellet the precipitated plasmid DNA. The supernatant was discarded, and the pellet was washed with 200 µl of 70% Ethanol and allowed to air-dry. The DNA was re-suspended using sterile distilled H₂O and RNase A (20mg/l).

5.6 Phenotypic analysis

5.6.1 *Arabidopsis* phenotyping

Seeds were sterilized by washing in 70% ethanol for 2 minutes, then soaked in 30% bleach (4.8% active hypochlorite) for 10 minutes and washed 3 times with sterilized water. Sterilised seeds were sown on MS15 medium (4.405g/l Murashige and Skoog plus vitamins; 15g/l Sucrose; 1% agar; pH 5.8) and germinated under long day conditions (25°C, 16/8 hour day/light). For the bolting analysis, 24 seedlings for each line were transferred to soil after two weeks and grown under long day conditions. Once the primary bolt reached 1cm in height from the base of the plant, leaves above 1cm in length were counted. Therefore, flowering time is measured as the total number of leaves before flowering, described by (Soppe *et al.*, 2000). For the root analysis, 30 seedlings for each line were transferred to 120mm square Petri-dishes containing MS15 (1% agar). Each plate contained 10 seedlings and was grown in a vertical position under long day conditions (25°C, 16/8 hour day/light). After four weeks of development, root images were captured using a flat-bed scanner at 800ppi (HP Scanjet G3110) and analyzed using ImageJ (Schneider *et al.*, 2012). Lateral roots were only counted if they were bigger than 2mm. The ratio was calculated by dividing the length of the primary root (mm) by the number of lateral roots.

5.6.2 Tomato phenotyping

Seeds were washed with 99% ethanol, soaked in 25% bleach (4% active hypochlorite) for 20 min and rinsed three times with sterilized water. Seeds were then sewn onto MSB530 medium (Murashige and Skoog salts, B5 vitamins, Duchefa M0231; 30 g/l Sucrose; 0.8% agar; pH 5.8) and grown under long day conditions (25°C, 16/8 hour day/light). For the phenotypic analysis, 100 seeds were sown for each line with each line was analyzed at 4 weeks of development. Germination was calculated by counting the number of seedlings that had emerged from the seed. The stem and root length was measured by removing each tomato plant from the media and using a ruler to measure their lengths. Blind plants were determined via abnormal growth at the shoot apical meristem.

5.7 DNA Protocol

5.7.1 Isolation of genomic DNA from *Arabidopsis*

Isolation of plant genomic DNA was carried out using a modified Vejlupkova and Fowler protocol (Vejlupkova & Fowler, 2003). Plant tissue was frozen in liquid nitrogen and ground, 560 µl of extraction buffer (200 mM NaCl; 18 mM NaHSO₃; 200 mM Tris-HCl, pH 8.0; 0.07 mM EDTA) and 50 µl of 5% sarkosyl was added and mixed. The suspension was mixed and incubated at 65° for 1 hour. An equal volume of phenol:chloroform:Isoamyl alcohol (IAA) (12:12:1) was added then centrifuged at 12,000 x g for 10 min at 4°C. The upper phase was transferred to a new Eppendorf tube and the phenol:chloroform:IAA extraction was repeated. The DNA was precipitated using 300µl of isopropanol and pelleted by centrifugation at 12,000 x g for 10 min at 4°C. The supernatant was discarded and washed with 70% ethanol. The DNA was re-pelleted and the supernatant removed and allowed to air-dry. The DNA was re-suspended using sterile distilled H₂O and RNase A (20 mg/l).

5.7.2 Restriction digest

Digestion reactions were made to a final volume of 50µl. A standard digestion reaction consisted of approximately 1µg of DNA, the 1x concentration of appropriate digestion buffer, 5-10 units of restriction endonuclease enzyme and 0.1mg/ml Bovine Serum Albumin (BSA) when required. The reaction was incubated at the optimum temperature for 2 hours.

5.7.3 Ligation reaction

Ligation reactions consisted of 1 x ligase buffer, 1 U/µl of T4 DNA Ligase (Promega M180A) and a 3:1 ratio of insert to vector. The final reaction was incubated at 16°C overnight.

5.7.4 Polymerase chain reaction (PCR)

PCR for genotyping was carried out using MyTaq DNA polymerase (Bioline). The reaction was made according to manufacturer's instructions which consisted of 0.3µl of MyTaq DNA polymerase, the 1x concentration of red buffer, 10µM of both forward and reverse primers, 250 ng of DNA template and H₂O to make the final volume to 50µl. The reaction was placed into a thermocycler with the following settings: initial denaturation at 95°C for 5 min, 25–29 cycles of denaturation at 15°C for 30 sec, annealing temperature (T_a, according to the primer annealing temperature) for 15 sec and extension at 72°C for 10 sec/kb and followed by final extension at 72°C for 5 min.

PCR for plasmid construction was carried out using the high fidelity polymerase Phusion (Finnzymes). The reaction was made according to manufacturer's instructions which consisted of 0.5 µl of Phusion High-Fidelity DNA Polymerase at 1 U/µl, 10 µl of 5× Phusion HF Buffer, 10mM dNTPs, 10 µM of both forward and reverse primer, and 250 ng of template DNA was added with H₂O to a final volume of 50 µl. The reaction was placed into a thermocycler with the following setting: initial denaturation at 98°C for 5 min, 25–29 cycles of denaturation at 98°C for 30 sec, annealing (T_a, according to the primer annealing temperature) for 30 sec and extension at 72°C for 30 sec/kb and followed by final extension at 72°C for 5 min. A negative control was run together with the DNA template replaced with H₂O.

5.7.5 Bisulphite analysis

Genomic DNA was isolated from, three replica samples, each contained ten pooled four-week-old seedlings of the T3 generation and subjected to bisulfite treatment using an EZ DNA Methylation-lightning kit (Zymo Research) according to the manufacturer's instructions. Regions containing dense methylation for AT3G01345 (Chr3: 129684..129860 - 177 bp), AT3G27473 (Chr3: 10171884..10172090 - 207 bp), AT3G30720 (Chr3: 12348994..12349109 - 116 bp) and AT5G34850 (Chr5: 13111304..13111574 – 271bp) were amplified by primers listed **S8 Table**. For each line, 10 clones were sequenced, and sequences were exported into

the BioEdit program (Hall, T. A., 1999). Aligned sequences were saved in FASTA format and analyzed by the CyMATE program (Hetzl *et al.*, 2007).

5.7.6 DNA sequencing

Approximately 100 ng/μl isolated plasmid DNA was sent to Beckman Genomics for sequencing using the appropriate primers. Sequencing reads were aligned using the Clustal function in Bioedit 7.0.9.0 (Higo *et al.*, 1999).

5.7.7 Data analysis

The ThaleMine platform <https://apps.araport.org/thalemine/begin.do> was used to extract the annotation for extracted genes. DNA methylation patterns for *Arabidopsis* were extracted from the Neomorph platform <http://neomorph.salk.edu/epigenome/epigenome.html> to identify genes with dense DNA methylation patterns. The tomato DNA methylation patterns were extracted using the tomato epigenome database <http://ted.bti.cornell.edu/cgi-bin/epigenome/home.cgi> to determine genes with dense DNA methylation patterns.

5.8 RNA analysis

5.8.1 Isolation of RNA from plants

Total plant RNA was isolated from each line, with for each line having replica samples, each contained ten pooled four-week-old seedlings of the T3 generation, and performed as described by (Stam *et al.*, 2000). 750µl of RNA extraction buffer (100mM Tris-HCL, pH8.5; 100mM NaCl; 20mM EDTA; 1% sarcosyl) was added to 0.5g of plant tissue ground in liquid nitrogen. The suspension was mixed and equal volume of phenol:chloroform:IAA (12:12:1) was added then centrifuged at 12,000 x g for 10 min at 4°C. The top phase was transferred to a new Eppendorf and phenol:chloroform:IAA extraction was repeated. Precipitation of the RNA was performed using Isopropanol, 4M LiCl, and 3M, pH7.0 NaAc. Extractions were quantified using the nano-drop spectrophotometer ND-1000 (Thermo Scientific). DNA was removed using the TURBO DNase kit (Ambion Applied Biosystems) according to the manufacturer's instructions.

5.8.2 Semi-quantitative PCR

cDNA was generated using SuperScript™ II. The reaction was made according to manufacturer's instructions which consisted of 10µg of isolated RNA, 50 µM oligo(dT)20 and 10 mM dNTP mix. The reaction was incubated at 65°C for 5 min and then placed on ice for at least 1 min. The 1x concentration of First stand buffer, 0.2M of DTT and 40 units/µl of RNaseOUT was added to each reaction. The mix was incubated at 25°C for 2 minutes at which point 200 units of SuperScript™ II was added to a final volume of 20 µl. The mix was incubated for a further 10 min, then 42°C for 50 min then final 70°C for 15 min. The solution was diluted with 20 µl of ddH₂O. Random primers were used as non-coding RNA would be analyzed in the expression analysis. 1µl of the diluted cDNA solution was added to a standard MyTaq reaction. The reaction was placed into a thermocycler with the following settings: initial denaturation at 95°C for 5 min, 25–29 cycles of denaturation at 15°C for 30 sec, annealing temperature (Ta, according to the primer annealing temperature) for 15 sec

and extension at 72°C for 10 sec/kb, when the thermocycler had performed 20 cycles the reaction was held at 72°C while 6 µl was removed from the total reaction, this was repeated twice more every three cycles then ran on a Agarose gel. Using Elongation Factor 1α which is ubiquitously expressed the reactions exponential phase could be determined and used to standardize each reaction for expression analysis.

5.8.3 Quantitative RT-PCR assay

Gene expression was analyzed using SsoFast EvaGreen Supermix (BioRad) on the Fluidigm Biomark 96.96 Dynamic Array according to the manufacturer's protocol. Data analysis was carried out utilizing the Fluidigm Gene Expression Analysis software using ACTIN 2 (AT3G18780) as the reference gene.

5.8.4 Sequencing and data analysis

Next-generation sequencing libraries were created from RNA using the TruSeq Stranded total RNA kit (Illumina) which removes rRNA and cleaves the remaining RNA allowing the ligation of random hexamers, and synthesis of cDNA for further analysis https://support.illumina.com/content/dam/illumina-support/documents/documentation/chemistry_documentation/samplepreps_truseq/truseqstrandedtotalrna/truseq-stranded-total-rna-sample-prep-guide-15031048-e.pdf.

Sequencing was carried out on a HiSeq 2500 to generate 50 bp single-end sequence data. Data analysis was carried out Dr. Ian M Carr (Leeds University, Leeds, England). The data were aligned to the *Arabidopsis* genome (TAIR website [<https://www.arabidopsis.org>]) using the STAR aligner (Dobin *et al.*, 2013). Reads mapping to each transcript were determined using the R package rsubRead (Liao *et al.*, 2013) and pairwise comparisons between the wildtype sample and each of the modified samples were performed using the R package DeSeq2 (Love *et al.*, 2014) to identify transcripts whose expression varied markedly between the control and experimental sample for each condition. Reads were used to calculate the mean value of read mapping to a transcript in all sample in the analysis (base Mean), the

change in expression between the control sample and the test sample given as a Log to the base 2 value ($\log_2\text{FoldChange}$), the standard error of variation for the $\log_2\text{FoldChange}$ values in the analysis ($\text{lfcSE} = \text{log fold change Standard Error}$), the Wald statistic; the $\log_2\text{FoldChange}$ divided by lfcSE , the probability the result is real; the $\log_2\text{FoldChange}$ divided by lfcSE , compared to a standard Normal distribution to generate a two-tailed p-value (pvalue) and the pvalue adjusted for multiple testing using the Benjamini-Hochberg test (Padj).

Raw data were submitted to the short-read archive of NCBI BioProject database under SubmissionID SUB2885208, BioProject ID PRJNA395995 for the following Datasets:

Accession	Sample Name	Organism	Tax ID	BioProject
SAMN07419160	WT_1	Arabidopsis thaliana	3702	PRJNA395995
SAMN07419161	WT_2	Arabidopsis thaliana	3702	PRJNA395995
SAMN07419162	WT_3	Arabidopsis thaliana	3702	PRJNA395995
SAMN07419163	A1+_1	Arabidopsis thaliana	3702	PRJNA395995
SAMN07419164	A1+_2	Arabidopsis thaliana	3702	PRJNA395995
SAMN07419165	A1+_3	Arabidopsis thaliana	3702	PRJNA395995
SAMN07419166	A1-_1	Arabidopsis thaliana	3702	PRJNA395995
SAMN07419167	A1-_2	Arabidopsis thaliana	3702	PRJNA395995
SAMN07419168	A1-_3	Arabidopsis thaliana	3702	PRJNA395995
SAMN07419169	A2+_1	Arabidopsis thaliana	3702	PRJNA395995
SAMN07419170	A2+_2	Arabidopsis thaliana	3702	PRJNA395995
SAMN07419171	A2+_3	Arabidopsis thaliana	3702	PRJNA395995
SAMN07419172	A2-_1	Arabidopsis thaliana	3702	PRJNA395995
SAMN07419173	A2-_2	Arabidopsis thaliana	3702	PRJNA395995
SAMN07419174	A2-_3	Arabidopsis thaliana	3702	PRJNA395995

5.9 Protein analysis

5.9.1 ChIP assay

28-day-old seedlings were harvested and cross-linked with 1% formaldehyde. Chromatin was extracted using the ChromaFlash Plant Chromatin Extraction Kit (Epigentek) and sheared to 200-500bp fragments using a Bioruptor (Diagenode). ChIP was carried out using the EpiQuik Plant ChIP Kit (Epigentek). Input samples and immunoprecipitated samples were analyzed using SsoFast EvaGreen Supermix (BioRad) on the Fluidigm Biomark 96.96 Dynamic Array according to the manufacturer's protocol. ChIP-qPCR results were first normalized with input sample. Relative enrichment was then calculated via the enrichment of the signal (the antibody of interest) compared to the enrichment of the noise (negative control). Antibodies used for ChIP: anti-acetyl-histone H4K5K8K12K16 (06-866; Millipore), H3K4me3 (07-473, Millipore), H3K9me3 (07-442, Millipore), normal rabbit IgG (12-370, Millipore).

5.9.2 Western blot assay

Protein was isolated from 28-day-old seedlings using the P-PER plant protein extraction kit (Pierce) in accordance with the manufacturer's instructions. Protein was then denatured by suspending the extract in equal volume laemmli buffer (Bio-Rad) and heated at 95°C for 5 minutes. The samples were resolved on 12% Mini-PROTEAN TGX Stain-Free Protein Gels (Bio-Rad) and transferred to Trans-Blot Turbo Mini Nitrocellulose Transfer Packs using the Trans-Blot Turbo Transfer (Bio-Rad). The nitrocellulose membranes were blocked with 5% (w/v) nonfat dry milk in Tris-buffered saline (TBS; 20 mM Tris and 137 mM NaCl, pH 7.7) with 0.1% (v/v) Tween-20. The Anti-FLAG (ab197345, Abcam) and Anti-Actin (ab197345, Abcam) were diluted 1/1000 in TBS-Tween/5% milk solution and incubated overnight at 4°C. Blots were washed with TBS-Tween 6 times for 10 min each. Blots were further incubated with horseradish peroxidase-conjugated anti-rabbit IgG (ab6721, abcam) at 1/2000 dilution and then washed as above. Blots were covered with SuperSignal™ West Pico PLUS Chemiluminescent Substrate (Thermo Scientific) for 20 minutes; bound antibodies were visualized on a G:BOX Chemi XX6 (Syngene).

6 References

- Agius, F., Kapoor, A. & Zhu, J.-K. (2006) Role of the Arabidopsis DNA Glycosylase/lyase ROS1 in Active DNA Demethylation. *PROCEEDINGS OF THE NATIONAL ACADEMY OF SCIENCES OF THE UNITED STATES OF AMERICA*, 103 (31) August, pp. 11796–11801.
- Agorio, A. & Vera, P. (2007) ARGONAUTE4 Is Required for Resistance to *Pseudomonas Syringae* in Arabidopsis. *PLANT CELL*, 19 (11) November, pp. 3778–3790.
- Antequera, F. & Bird, A. (1999) CpG Islands as Genomic Footprints of Promoters That Are Associated with Replication Origins. *CURRENT BIOLOGY*, 9 (17) September, pp. R661–R667.
- Baev, V., Naydenov, M., Apostolova, E., Ivanova, D., Doncheva, S., Minkov, I. & Yahubyan, G. (2010) Identification of RNA-Dependent DNA-Methylation Regulated Promoters in Arabidopsis. *PLANT PHYSIOLOGY AND BIOCHEMISTRY*, 48 (6) June, pp. 393–400.
- Baumbusch, L. O., Thorstensen, T., Krauss, V., Fischer, A., Naumann, K., Assalkhou, R., Schulz, I., Reuter, G. & Aalen, R. B. (2001) The Arabidopsis Thaliana Genome Contains at Least 29 Active Genes Encoding SET Domain Proteins That Can Be Assigned to Four Evolutionarily Conserved Classes. *NUCLEIC ACIDS RESEARCH*, 29 (21) November, pp. 4319–4333.
- Becker, C., Hagmann, J., Mueller, J., Koenig, D., Stegle, O., Borgwardt, K. & Weigel, D. (2011) Spontaneous Epigenetic Variation in the Arabidopsis Thaliana Methylome. *NATURE*, 480 (7376) December, pp. 245–U127.
- Berger, S. L. (2007) The Complex Language of Chromatin Regulation during Transcription. *NATURE*, 447 (7143) May, pp. 407–412.
- Bernatavichute, Y. V., Zhang, X., Cokus, S., Pellegrini, M. & Jacobsen, S. E. (2008) Genome-Wide Association of Histone H3 Lysine Nine Methylation with CHG DNA Methylation in Arabidopsis Thaliana. *PLOS ONE*, 3 (9) September.
- Bolan, N. S., Adriano, D. C. & Naidu, R. (2003) Role of Phosphorus in (Im)mobilization and Bioavailability of Heavy Metals in the Soil-Plant System. In: *REVIEWS OF*

ENVIRONMENTAL CONTAMINATION AND TOXICOLOGY, VOL 177. vol. 177. 175 FIFTH AVE, NEW YORK, NY 10010 USA: SPRINGER-VERLAG, pp. 1–44.

- Boyko, A., Kathiria, P., Zemp, F. J., Yao, Y., Pogribny, I. & Kovalchuk, I. (2007) Transgenerational Changes in the Genome Stability and Methylation in Pathogen-Infected Plants (Virus-Induced Plant Genome Instability). *NUCLEIC ACIDS RESEARCH*, 35 (5), pp. 1714–1725.
- BRINK, R. A. (1959) PARAMUTATION AT THE R-LOCUS IN MAIZE PLANTS TRISOMIC FOR CHROMOSOME-10. *PROCEEDINGS OF THE NATIONAL ACADEMY OF SCIENCES OF THE UNITED STATES OF AMERICA*, 45 (6), pp. 819–827.
- Bruner, S. D., Norman, D. P. G. & Verdine, G. L. (2000) Structural Basis for Recognition and Repair of the Endogenous Mutagen 8-Oxoguanine in DNA. *NATURE*, 403 (6772) February, pp. 859–866.
- Cao, D., Ju, Z., Gao, C., Mei, X., Fu, D., Zhu, H., Luo, Y. & Zhu, B. (2014) Genome-Wide Identification of Cytosine-5 DNA Methyltransferases and Demethylases in *Solanum Lycopersicum*. *GENE*, 550 (2) October, pp. 230–237.
- Cao, K., Cui, L., Zhou, X., Ye, L., Zou, Z. & Deng, S. (2016) Four Tomato FLOWERING LOCUS T-Like Proteins Act Antagonistically to Regulate Floral Initiation. *FRONTIERS IN PLANT SCIENCE*, 6 January.
- Cao, X., Aufsatz, W., Zilberman, D., Mette, M. F., Huang, M. S., Matzke, M. & Jacobsen, S. E. (2003) Role of the DRM and CMT3 Methyltransferases in RNA-Directed DNA Methylation. *Current Biology*, 13 (24) December, pp. 2212–2217.
- Cao, X. F., Aufsatz, W., Zilberman, D., Mette, M. F., Huang, M. S., Matzke, M. & Jacobsen, S. E. (2003) Role of the DRM and CMT3 Methyltransferases in RNA-Directed DNA Methylation. *CURRENT BIOLOGY*, 13 (24) December, pp. 2212–2217.
- Cao, X. F. & Jacobsen, S. E. (2002) Role of the Arabidopsis DRM Methyltransferases in de Novo DNA Methylation and Gene Silencing. *CURRENT BIOLOGY*, 12 (13) July, pp. 1138–1144.
- Casadesus, J. & Low, D. (2006) Epigenetic Gene Regulation in the Bacterial World.

MICROBIOLOGY AND MOLECULAR BIOLOGY REVIEWS, 70 (3) September, p. 830+.

- Catoni, M., Griffiths, J., Becker, C., Zabet, N. R., Bayon, C., Dapp, M., Lieberman-Lazarovich, M., Weigel, D. & Paszkowski, J. (2017) DNA Sequence Properties That Predict Susceptibility to Epiallelic Switching. *EMBO JOURNAL*, 36 (5) March, pp. 617–628.
- Chan, S. W.-L., Zhang, X., Bernatavichute, Y. V & Jacobsen, S. E. (2006) Two-Step Recruitment of RNA-Directed DNA Methylation to Tandem Repeats. *PLOS BIOLOGY*, 4 (11) November, pp. 1923–1933.
- Chen, T. P., Ueda, Y., Dodge, J. E., Wang, Z. J. & Li, E. (2003) Establishment and Maintenance of Genomic Methylation Patterns in Mouse Embryonic Stem Cells by Dnmt3a and Dnmt3b. *MOLECULAR AND CELLULAR BIOLOGY*, 23 (16) August, pp. 5594–5605.
- Cheng, C., Tarutani, Y., Miyao, A., Ito, T., Yamazaki, M., Sakai, H., Fukai, E. & Hirochika, H. (2015) Loss of Function Mutations in the Rice Chromomethylase OsCMT3a Cause a Burst of Transposition. *PLANT JOURNAL*, 83 (6) September, pp. 1069–1081.
- Choi, Y. H., Gehring, M., Johnson, L., Hannon, M., Harada, J. J., Goldberg, R. B., Jacobsen, S. E. & Fischer, R. L. (2002) DEMETER, a DNA Glycosylase Domain Protein, Is Required for Endosperm Gene Imprinting and Seed Viability in Arabidopsis. *CELL*, 110 (1) July, pp. 33–42.
- Clarkadams, C. D., Norris, D., Osley, M. A., Fassler, J. S. & Winston, F. (1988) Changes in Histone Gene Dosage Alter Transcription in Yeast. *GENES & DEVELOPMENT*, 2 (2) February, pp. 150–159.
- Cokus, S. J., Feng, S., Zhang, X., Chen, Z., Merriman, B., Haudenschild, C. D., Pradhan, S., Nelson, S. F., Pellegrini, M. & Jacobsen, S. E. (2008) Shotgun Bisulphite Sequencing of the Arabidopsis Genome Reveals DNA Methylation Patterning. *NATURE*, 452 (7184) March, pp. 215–219.
- Cooper, D. N., Taggart, M. H. & Bird, A. P. (1983) Unmethylated Domains in Vertebrate DNA. *NUCLEIC ACIDS RESEARCH*, 11 (3), pp. 647–658.
- D'Ario, M., Griffiths-Jones, S. & Kim, M. (2017) Small RNAs: Big Impact on Plant Development. *TRENDS IN PLANT SCIENCE*, 22 (12) December, pp. 1056–1068.

- Dahm, R. (2005) Friedrich Miescher and the Discovery of DNA. *Developmental Biology* [Online], 278 (2) February, pp. 274–288. Available from: <<http://linkinghub.elsevier.com/retrieve/pii/S0012160604008231>> [Accessed 8 June 2017].
- Dechiara, T. M., Robertson, E. J. & Efstratiadis, A. (1991) Parental Imprinting of the Mouse Insulin-Like Growth Factor-II Gene. *CELL*, 64 (4) February, pp. 849–859.
- Deleris, A., Halter, T. & Navarro, L. (2016) DNA Methylation and Demethylation in Plant Immunity. In: Leach, JE and Lindow, S ed., *ANNUAL REVIEW OF PHYTOPATHOLOGY, VOL 54*. vol. 54. 4139 EL CAMINO WAY, PO BOX 10139, PALO ALTO, CA 94303-0897 USA: ANNUAL REVIEWS, pp. 579–603.
- Dobin, A., Davis, C. A., Schlesinger, F., Drenkow, J., Zaleski, C., Jha, S., Batut, P., Chaisson, M. & Gingeras, T. R. (2013) STAR: Ultrafast Universal RNA-Seq Aligner. *BIOINFORMATICS*, 29 (1) January, pp. 15–21.
- Doebley, J. F., Gaut, B. S. & Smith, B. D. (2006) The Molecular Genetics of Crop Domestication. *CELL*, 127 (7) December, pp. 1309–1321.
- Du, J., Zhong, X., Bernatavichute, Y. V., Stroud, H., Feng, S., Caro, E., Vashisht, A. A., Terragni, J., Chin, H. G., Tu, A., Hetzel, J., Wohlschlegel, J. A., Pradhan, S., Patel, D. J. & Jacobsen, S. E. (2012) Dual Binding of Chromomethylase Domains to H3K9me2-Containing Nucleosomes Directs DNA Methylation in Plants. *CELL*, 151 (1) September, pp. 167–180.
- Dupont, C., Armant, D. R. & Brenner, C. A. (2009) Epigenetics: Definition, Mechanisms and Clinical Perspective. *SEMINARS IN REPRODUCTIVE MEDICINE*, 27 (5) September, pp. 351–357.
- Duque, P. & Chua, N. H. (2003) IMB1, a Bromodomain Protein Induced during Seed Imbibition, Regulates ABA- and phyA-Mediated Responses of Germination in Arabidopsis. *PLANT JOURNAL*, 35 (6) September, pp. 787–799.
- Durut, N., Abou-Ellail, M., Pontvianne, F., Das, S., Kojima, H., Ukai, S., Bures, A. de, Comella, P., Nidelet, S., Rialle, S., Merret, R., Echeverria, M., Bouvet, P., Nakamura, K. & Saez-Vasquez, J. (2014) A Duplicated NUCLEOLIN Gene with Antagonistic Activity Is Required for Chromatin Organization of Silent 45S rDNA in Arabidopsis. *PLANT CELL*, 26 (3)

March, pp. 1330–1344.

- Fabro, G., Soledad Rizzi, Y. & Elena Alvarez, M. (2016) Arabidopsis Proline Dehydrogenase Contributes to Flagellin-Mediated PAMP-Triggered Immunity by Affecting RBOHD. *MOLECULAR PLANT-MICROBE INTERACTIONS*, 29 (8) August, pp. 620–628.
- Finnegan, E. J. (2002) Epialleles - a Source of Random Variation in Times of Stress. *CURRENT OPINION IN PLANT BIOLOGY*, 5 (2) April, pp. 101–106.
- Finnegan, E. J. & Dennis, E. S. (1993) Isolation and Identification by Sequence Homology of a Putative Cytosine Methyltransferase from Arabidopsis-Thaliana. *NUCLEIC ACIDS RESEARCH*, 21 (10) May, pp. 2383–2388.
- Finnegan, E. J., Genger, R. K., Peacock, W. J. & Dennis, E. S. (1998) DNA Methylation in Plants. *ANNUAL REVIEW OF PLANT PHYSIOLOGY AND PLANT MOLECULAR BIOLOGY*, 49, pp. 223–247.
- Finnegan, E. J., Peacock, W. J. & Dennis, E. S. (1996) Reduced DNA Methylation in Arabidopsis Thaliana Results in Abnormal Plant Development. *PROCEEDINGS OF THE NATIONAL ACADEMY OF SCIENCES OF THE UNITED STATES OF AMERICA*, 93 (16) August, pp. 8449–8454.
- Fraser, P. D., Bramley, P. & Seymour, G. B. (2001) Effect of the Cnr Mutation on Carotenoid Formation during Tomato Fruit Ripening. *PHYTOCHEMISTRY*, 58 (1) September, pp. 75–79.
- Gehring, M., Huh, J. H., Hsieh, T. F., Penterman, J., Choi, Y., Harada, J. J., Goldberg, R. B. & Fischer, R. L. (2006) DEMETER DNA Glycosylase Establishes MEDEA Polycomb Gene Self-Imprinting by Allele-Specific Demethylation. *CELL*, 124 (3) February, pp. 495–506.
- Gent, J. I., Ellis, N. A., Guo, L., Harkess, A. E., Yao, Y., Zhang, X. & Dawe, R. K. (2013) CHH Islands: De Novo DNA Methylation in near-Gene Chromatin Regulation in Maize. *GENOME RESEARCH*, 23 (4) April, pp. 628–637.
- Gohlke, J., Scholz, C.-J., Kneitz, S., Weber, D., Fuchs, J., Hedrich, R. & Deeken, R. (2013) DNA Methylation Mediated Control of Gene Expression Is Critical for Development of Crown Gall Tumors. *PLOS GENETICS*, 9 (2) February.

- Goto, T. & Monk, M. (1998) Regulation of X-Chromosome Inactivation in Development in Mice and Humans. *MICROBIOLOGY AND MOLECULAR BIOLOGY REVIEWS*, 62 (2) June, p. 362+.
- Gouil, Q. & Baulcombe, D. C. (2016) DNA Methylation Signatures of the Plant Chromomethyltransferases. *PLOS GENETICS*, 12 (12) December.
- Guo, J.-E., Hu, Z., Zhu, M., Li, F., Zhu, Z., Lu, Y. & Chen, G. (2017) The Tomato Histone Deacetylase SIHDA1 Contributes to the Repression of Fruit Ripening and Carotenoid Accumulation. *Scientific Reports* [Online], 7 (1), p. 7930. Available from: <<https://doi.org/10.1038/s41598-017-08512-x>>.
- Hall, T. A. (1999) BioEdit: A User-Friendly Biological Sequence Alignment Editor and Analysis Program for Windows 95/98/NT. *Nucleic Acids Symposium Series*, 41, pp. 95–98.
- Havecker, E. R., Wallbridge, L. M., Hardcastle, T. J., Bush, M. S., Kelly, K. A., Dunn, R. M., Schwach, F., Doonan, J. H. & Baulcombe, D. C. (2010) The Arabidopsis RNA-Directed DNA Methylation Argonautes Functionally Diverge Based on Their Expression and Interaction with Target Loci. *PLANT CELL*, 22 (2) February, pp. 321–334.
- Hellens, R., Mullineaux, P. & Klee, H. (2000) A Guide to Agrobacterium Binary Ti Vectors. *TRENDS IN PLANT SCIENCE*, 5 (10) October, pp. 446–451.
- Henderson, I. R., Zhang, X., Lu, C., Johnson, L., Meyers, B. C., Green, P. J. & Jacobsen, S. E. (2006) Dissecting Arabidopsis Thaliana DICER Function in Small RNA Processing, Gene Silencing and DNA Methylation Patterning. *NATURE GENETICS*, 38 (6) June, pp. 721–725.
- Hermann, A., Gowher, H. & Jeltsch, A. (2004) Biochemistry and Biology of Mammalian DNA Methyltransferases. *CELLULAR AND MOLECULAR LIFE SCIENCES*, 61 (19–20) October, pp. 2571–2587.
- Hetzl, J., Foerster, A. M., Raidl, G. & Scheid, O. M. (2007) CyMATE: A New Tool for Methylation Analysis of Plant Genomic DNA after Bisulphite Sequencing. *PLANT JOURNAL*, 51 (3) August, pp. 526–536.
- Hsieh, C. L. (1999) In Vivo Activity of Murine de Novo Methyltransferases, Dnmt3a and

- Dnmt3b. *MOLECULAR AND CELLULAR BIOLOGY*, 19 (12) December, pp. 8211–8218.
- Hsieh, T.-F., Ibarra, C. A., Silva, P., Zemach, A., Eshed-Williams, L., Fischer, R. L. & Zilberman, D. (2009) Genome-Wide Demethylation of Arabidopsis Endosperm. *SCIENCE*, 324 (5933) June, pp. 1451–1454.
- Hu, L., Li, N., Xu, C., Zhong, S., Lin, X., Yang, J., Zhou, T., Yuliang, A., Wu, Y., Chen, Y.-R., Cao, X., Zemach, A., Rustgi, S., Wettstein, D. von & Liu, B. (2014) Mutation of a Major CG Methylase in Rice Causes Genome-Wide Hypomethylation, Dysregulated Genome Expression, and Seedling Lethality. *PROCEEDINGS OF THE NATIONAL ACADEMY OF SCIENCES OF THE UNITED STATES OF AMERICA*, 111 (29) July, pp. 10642–10647.
- Huettel, B., Kanno, T., Daxinger, L., Bucher, E., Winden, J. van der, Matzke, A. J. M. & Matzke, M. (2007) RNA-Directed DNA Methylation Mediated by DRD1 and Pol IVb: A Versatile Pathway for Transcriptional Gene Silencing in Plants. *BIOCHIMICA ET BIOPHYSICA ACTA-GENE STRUCTURE AND EXPRESSION*, 1769 (5–6), pp. 358–374.
- Ikeda, Y., Kobayashi, Y., Yamaguchi, A., Abe, M. & Araki, T. (2007) Molecular Basis of Late-Flowering Phenotype Caused by Dominant Epi-Alleles of the FWA Locus in Arabidopsis. *PLANT AND CELL PHYSIOLOGY*, 48 (2) February, pp. 205–220.
- Jackson, J. P., Lindroth, A. M., Cao, X. F. & Jacobsen, S. E. (2002) Control of CpNpG DNA Methylation by the KRYPTONITE Histone H3 Methyltransferase. *NATURE*, 416 (6880) April, pp. 556–560.
- Jahnke, S. & Scholten, S. (2009) Epigenetic Resetting of a Gene Imprinted in Plant Embryos. *CURRENT BIOLOGY*, 19 (19) October, pp. 1677–1681.
- Jeltsch, A. (2006) Molecular Enzymology of Mammalian DNA Methyltransferases. In: Doerfler, W and Bohm, P ed., *DNA METHYLATION: BASIC MECHANISMS*. vol. 301. HEIDELBERGER PLATZ 3, D-14197 BERLIN, GERMANY: SPRINGER-VERLAG BERLIN, pp. 203–225.
- Jiricny, J. (2002) DNA Repair - An APE That Proofreads. *NATURE*, 415 (6872) February, pp. 593–594.
- Johnson, L. M., Cao, X. F. & Jacobsen, S. E. (2002) Interplay between Two Epigenetic Marks:

DNA Methylation and Histone H3 Lysine 9 Methylation. *CURRENT BIOLOGY*, 12 (16) August, pp. 1360–1367.

Joly-Lopez, Z., Forczek, E., Hoen, D. R., Juretic, N. & Bureau, T. E. (2012) A Gene Family Derived from Transposable Elements during Early Angiosperm Evolution Has Reproductive Fitness Benefits in *Arabidopsis Thaliana*. *PLoS Genetics* [Online], 8 (9) September, p. e1002931. Available from: <<http://dx.plos.org/10.1371/journal.pgen.1002931>> [Accessed 26 July 2017].

Jones, L., Ratcliff, F. & Baulcombe, D. F. (2001) RNA-Directed Transcriptional Gene Silencing in Plants Can Be Inherited Independently of the RNA Trigger and Requires Met1 for Maintenance. *CURRENT BIOLOGY*, 11 (10) May, pp. 747–757.

Jullien, P. E., Mosquna, A., Ingouff, M., Sakata, T., Ohad, N. & Berger, F. (2008) Retinoblastoma and Its Binding Partner MSI1 Control Imprinting in *Arabidopsis*. *PLOS BIOLOGY*, 6 (8) August, pp. 1693–1705.

Jullien, P. E., Susaki, D., Yelagandula, R., Higashiyama, T. & Berger, F. (2012) DNA Methylation Dynamics during Sexual Reproduction in *Arabidopsis Thaliana*. *CURRENT BIOLOGY*, 22 (19) October, pp. 1825–1830.

Kakutani, T., Jeddelloh, J. A., Flowers, S. K., Munakata, K. & Richards, E. J. (1996) Developmental Abnormalities and Epimutations Associated with DNA Hypomethylation Mutations. *PROCEEDINGS OF THE NATIONAL ACADEMY OF SCIENCES OF THE UNITED STATES OF AMERICA*, 93 (22) October, pp. 12406–12411.

Kankel, M. W., Ramsey, D. E., Stokes, T. L., Flowers, S. K., Haag, J. R., Jeddelloh, J. A., Riddle, N. C., Verbsky, M. L. & Richards, E. J. (2003) *Arabidopsis* MET1 Cytosine Methyltransferase Mutants. *GENETICS*, 163 (3) March, pp. 1109–1122.

Kato, M., Miura, A., Bender, J., Jacobsen, S. E. & Kakutani, T. (2003) Role of CG and Non-CG Methylation in Immobilization of Transposons in *Arabidopsis*. *CURRENT BIOLOGY*, 13 (5) March, pp. 421–426.

Kelly, T. K., Liu, Y., Lay, F. D., Liang, G., Berman, B. P. & Jones, P. A. (2012) Genome-Wide Mapping of Nucleosome Positioning and DNA Methylation within Individual DNA Molecules. *GENOME RESEARCH*, 22 (12) December, pp. 2497–2506.

- Kim, J. K., Samaranyake, M. & Pradhan, S. (2009) Epigenetic Mechanisms in Mammals. *CELLULAR AND MOLECULAR LIFE SCIENCES*, 66 (4) February, pp. 596–612.
- Kinoshita, T., Miura, A., Choi, Y. H., Kinoshita, Y., Cao, X. F., Jacobsen, S. E., Fischer, R. L. & Kakutani, T. (2004) One-Way Control of FWA Imprinting in Arabidopsis Endosperm by DNA Methylation. *SCIENCE*, 303 (5657) January, pp. 521–523.
- Klose, R. J. & Bird, A. P. (2006) Genomic DNA Methylation: The Mark and Its Mediators. *TRENDS IN BIOCHEMICAL SCIENCES*, 31 (2) February, pp. 89–97.
- Koornneef, M., Hanhart, C. J. & Vanderveen, J. H. (1991) A Genetic and Physiological Analysis of Late Flowering Mutants in Arabidopsis-Thaliana. *MOLECULAR & GENERAL GENETICS*, 229 (1) September, pp. 57–66.
- Kornberg, R. D. (1974) Chromatin Structure - Repeating Unit of Histones and DNA. *SCIENCE*, 184 (4139), pp. 868–871.
- Kou, H. P., Li, Y., Song, X. X., Ou, X. F., Xing, S. C., Ma, J., Wettstein, D. Von & Liu, B. (2011) Heritable Alteration in DNA Methylation Induced by Nitrogen-Deficiency Stress Accompanies Enhanced Tolerance by Progenies to the Stress in Rice (*Oryza Sativa* L.). *JOURNAL OF PLANT PHYSIOLOGY*, 168 (14) September, pp. 1685–1693.
- Kovarik, A., Koukalova, B., Bezdek, M. & Opatrný, Z. (1997) Hypermethylation of Tobacco Heterochromatic Loci in Response to Osmotic Stress. *THEORETICAL AND APPLIED GENETICS*, 95 (1–2) July, pp. 301–306.
- Lane, A. K., Niederhuth, C. E., Ji, L. & Schmitz, R. J. (2014) pENCODE: A Plant Encyclopedia of DNA Elements. vol. 48. pp. 49–70.
- Lanouette, S., Mongeon, V., Figeys, D. & Couture, J.-F. (2014) The Functional Diversity of Protein Lysine Methylation. *MOLECULAR SYSTEMS BIOLOGY*, 10 (4) April.
- Larsen, F., Gundersen, G., Lopez, R. & Prydz, H. (1992) CPG Islands as Gene Markers in the Human Genome. *GENOMICS*, 13 (4) August, pp. 1095–1107.
- Laux, T., Mayer, K. F. X., Berger, J. & Jürgens, G. (1996) The WUSCHEL Gene Is Required for Shoot and Floral Meristem Integrity in Arabidopsis. *DEVELOPMENT*, 122 (1) January, pp. 87–96.

- Lee, Y. F., Tawfik, D. S. & Griffiths, A. D. (2002) Investigating the Target Recognition of DNA Cytosine-5 Methyltransferase HhaI by Library Selection Using in Vitro Compartmentalisation. *NUCLEIC ACIDS RESEARCH*, 30 (22) November, pp. 4937–4944.
- Liao, Y., Smyth, G. K. & Shi, W. (2013) The Subread Aligner: Fast, Accurate and Scalable Read Mapping by Seed-and-Vote. *NUCLEIC ACIDS RESEARCH*, 41 (10) May.
- Lim, A. S. P., Srivastava, G. P., Yu, L., Chibnik, L. B., Xu, J., Buchman, A. S., Schneider, J. A., Myers, A. J., Bennett, D. A. & Jager, P. L. De (2014) 24-Hour Rhythms of DNA Methylation and Their Relation with Rhythms of RNA Expression in the Human Dorsolateral Prefrontal Cortex. *PLOS GENETICS*, 10 (11) November.
- Lindroth, A. M., Cao, X. F., Jackson, J. P., Zilberman, D., McCallum, C. M., Henikoff, S. & Jacobsen, S. E. (2001) Requirement of CHROMOMETHYLASE3 for Maintenance of CpXpG Methylation. *SCIENCE*, 292 (5524) June, pp. 2077–2080.
- Lippman, Z., Gendrel, A. V., Black, M., Vaughn, M. W., Dedhia, N., McCombie, W. R., Lavine, K., Mittal, V., May, B., Kasschau, K. D., Carrington, J. C., Doerge, R. W., Colot, V. & Martienssen, R. (2004) Role of Transposable Elements in Heterochromatin and Epigenetic Control. *NATURE*, 430 (6998) July, pp. 471–476.
- Liu, X., Yu, C.-W., Duan, J., Luo, M., Wang, K., Tian, G., Cui, Y. & Wu, K. (2012) HDA6 Directly Interacts with DNA Methyltransferase MET1 and Maintains Transposable Element Silencing in Arabidopsis. *PLANT PHYSIOLOGY*, 158 (1) January, pp. 119–129.
- Lopez-Maury, L., Marguerat, S. & Baehler, J. (2008) Tuning Gene Expression to Changing Environments: From Rapid Responses to Evolutionary Adaptation. *NATURE REVIEWS GENETICS*, 9 (8) August, pp. 583–593.
- Love, M. I., Huber, W. & Anders, S. (2014) Moderated Estimation of Fold Change and Dispersion for RNA-Seq Data with DESeq2. *GENOME BIOLOGY*, 15 (12).
- Luo, M., Bilodeau, P., Dennis, E. S., Peacock, W. J. & Chaudhury, A. (2000) Expression and Parent-of-Origin Effects for FIS2, MEA, and FIE in the Endosperm and Embryo of Developing Arabidopsis Seeds. *PROCEEDINGS OF THE NATIONAL ACADEMY OF SCIENCES OF THE UNITED STATES OF AMERICA*, 97 (19) September, pp. 10637–10642.

- Mathieu, O., Reinders, J., Caikovski, M., Smathajitt, C. & Paszkowski, J. (2007) Transgenerational Stability of the Arabidopsis Epigenome Is Coordinated by CG Methylation. *CELL*, 130 (5) September, pp. 851–862.
- Melamed-Bessudo, C. & Levy, A. A. (2012) Deficiency in DNA Methylation Increases Meiotic Crossover Rates in Euchromatic but Not in Heterochromatic Regions in Arabidopsis. *PROCEEDINGS OF THE NATIONAL ACADEMY OF SCIENCES OF THE UNITED STATES OF AMERICA*, 109 (16) April, pp. E981–E988.
- Meyer, P., Linn, F., Heidmann, I., Meyer, H., Niedenhof, I. & Saedler, H. (1992) Endogenous and Environmental-Factors Influence 35S Promoter Methylation of a Maize A1 Gene Construct in Transgenic Petunia and its Color Phenotype. *MOLECULAR & GENERAL GENETICS*, 231 (3) February, pp. 345–352.
- Mi, S., Cai, T., Hu, Y., Chen, Y., Hodges, E., Ni, F., Wu, L., Li, S., Zhou, H., Long, C., Chen, S., Hannon, G. J. & Qi, Y. (2008) Sorting of Small RNAs into Arabidopsis Argonaute Complexes Is Directed by the 5' Terminal Nucleotide. *CELL*, 133 (1) April, pp. 116–127.
- Mirouze, M., Lieberman-Lazarovich, M., Aversano, R., Bucher, E., Nicolet, J., Reinders, J. & Paszkowski, J. (2012) Loss of DNA Methylation Affects the Recombination Landscape in Arabidopsis. *PROCEEDINGS OF THE NATIONAL ACADEMY OF SCIENCES OF THE UNITED STATES OF AMERICA*, 109 (15) April, pp. 5880–5885.
- Miura, A., Nakamura, M., Inagaki, S., Kobayashi, A., Saze, H. & Kakutani, T. (2009) An Arabidopsis jmjC Domain Protein Protects Transcribed Genes from DNA Methylation at CHG Sites. *EMBO JOURNAL*, 28 (8) April, pp. 1078–1086.
- Miura, K., Agetsuma, M., Kitano, H., Yoshimura, A., Matsuoka, M., Jacobsen, S. E. & Ashikari, M. (2009) A Metastable DWARF1 Epigenetic Mutant Affecting Plant Stature in Rice. *PROCEEDINGS OF THE NATIONAL ACADEMY OF SCIENCES OF THE UNITED STATES OF AMERICA*, 106 (27) July, pp. 11218–11223.
- Morales-Ruiz, T., Ortega-Galisteo, A. P., Ponferrada-Marin, M. I., Martinez-Macias, M. I., Ariza, R. R. & Roldan-Arjona, T. (2006) DEMETER and REPRESSOR OF SILENCING 1 Encode 5-Methylcytosine DNA Glycosylases. *PROCEEDINGS OF THE NATIONAL ACADEMY OF SCIENCES OF THE UNITED STATES OF AMERICA*, 103 (18) May, pp. 6853–

6858.

- Moritoh, S., Eun, C.-H., Ono, A., Asao, H., Okano, Y., Yamaguchi, K., Shimatani, Z., Koizumi, A. & Terada, R. (2012) Targeted Disruption of an Orthologue of DOMAINS REARRANGED METHYLASE 2, OsDRM2, Impairs the Growth of Rice Plants by Abnormal DNA Methylation. *PLANT JOURNAL*, 71 (1) July, pp. 85–98.
- Muller, H. J. (1930) Types of Visible Variations Induced by X-Rays in *Drosophila*. *JOURNAL OF GENETICS*, 22 (3) July, pp. 299-U7.
- NAPOLI, C., LEMIEUX, C. & JORGENSEN, R. (1990) INTRODUCTION OF A CHIMERIC CHALCONE SYNTHASE GENE INTO PETUNIA RESULTS IN REVERSIBLE CO-SUPPRESSION OF HOMOLOGOUS GENES IN TRANS. *PLANT CELL*, 2 (4) April, pp. 279–289.
- Naydenov, M., Baev, V., Apostolova, E., Gospodinova, N., Sablok, G., Gozmanova, M. & Yahubyan, G. (2015) High-Temperature Effect on Genes Engaged in DNA Methylation and Affected by DNA Methylation in *Arabidopsis*. *PLANT PHYSIOLOGY AND BIOCHEMISTRY*, 87 February, pp. 102–108.
- O'Malley, R. C. & Ecker, J. R. (2012) Epiallelic Variation in *Arabidopsis Thaliana*. *Cold Spring Harbor symposia on quantitative biology* [Online], 77 January, pp. 135–145. Available from: <<http://www.ncbi.nlm.nih.gov/pubmed/23223383>> [Accessed 11 July 2017].
- Ogneva, Z. V., Dubrovina, A. S. & Kiselev, K. V (2016) Age-Associated Alterations in DNA Methylation and Expression of Methyltransferase and Demethylase Genes in *Arabidopsis Thaliana*. *BIOLOGIA PLANTARUM* [Online], 60 (4), pp. 628–634. Available from: <<https://link.springer.com/content/pdf/10.1007%2Fs10535-016-0638-y.pdf>> [Accessed 26 July 2017].
- Park, S.-H., Jeong, J. S., Han, E. H., Redillas, M. C. F. R., Bang, S. W., Jung, H., Kim, Y. S. & Kim, J.-K. (2013) Characterization of the Root-Predominant Gene Promoter HPX1 in Transgenic Rice Plants. *PLANT BIOTECHNOLOGY REPORTS*, 7 (3) July, pp. 339–344.
- Penterman, J., Zilberman, D., Huh, J. H., Ballinger, T., Henikoff, S. & Fischer, R. L. (2007) DNA Demethylation in the *Arabidopsis* Genome. *PROCEEDINGS OF THE NATIONAL ACADEMY OF SCIENCES OF THE UNITED STATES OF AMERICA*, 104 (16) April, pp. 6752–6757.

- Perez-Torres, C.-A., Lopez-Bucio, J., Cruz-Ramirez, A., Ibarra-Laclette, E., Dharmasiri, S., Estelle, M. & Herrera-Estrella, L. (2008) Phosphate Availability Alters Lateral Root Development in Arabidopsis by Modulating Auxin Sensitivity via a Mechanism Involving the TIR1 Auxin Receptor. *PLANT CELL*, 20 (12) December, pp. 3258–3272.
- Posfai, J., Bhagwat, A. S., Posfai, G. & Roberts, R. J. (1989) Predictive Motifs Derived from Cytosine Methyltransferases. *NUCLEIC ACIDS RESEARCH*, 17 (7) April, pp. 2421–2435.
- Qian, W., Miki, D., Zhang, H., Liu, Y., Zhang, X., Tang, K., Kan, Y., La, H., Li, X., Li, S., Zhu, X., Shi, X., Zhang, K., Pontes, O., Chen, X., Liu, R., Gong, Z. & Zhu, J.-K. (2012) A Histone Acetyltransferase Regulates Active DNA Demethylation in Arabidopsis. *SCIENCE*, 336 (6087) June, pp. 1445–1448.
- Qian, Y., Xi, Y., Cheng, B. & Zhu, S. (2014) Genome-Wide Identification and Expression Profiling of DNA Methyltransferase Gene Family in Maize. *PLANT CELL REPORTS*, 33 (10) October, pp. 1661–1672.
- Ramsahoye, B. H., Biniszkiwicz, D., Lyko, F., Clark, V., Bird, A. P. & Jaenisch, R. (2000) Non-CpG Methylation Is Prevalent in Embryonic Stem Cells and May Be Mediated by DNA Methyltransferase 3a. *PROCEEDINGS OF THE NATIONAL ACADEMY OF SCIENCES OF THE UNITED STATES OF AMERICA*, 97 (10) May, pp. 5237–5242.
- Reik, W., Dean, W. & Walter, J. (2001) Epigenetic Reprogramming in Mammalian Development. *SCIENCE*, 293 (5532) August, pp. 1089–1093.
- Richmond, T. J. (1999) Hot Papers - Crystal Structure - Crystal Structure of the Nucleosome Core Particle at 2.8 Angstrom Resolution by K. Luger, A.W. Mader, R.K. Richmond, D.F. Sargent, T.J. Richmond - Comments. *SCIENTIST*, 13 (23) November, p. 15.
- Rommens, C. M., Haring, M. A., Swords, K., Davies, H. V & Belknap, W. R. (2007) The Intragenic Approach as a New Extension to Traditional Plant Breeding. *TRENDS IN PLANT SCIENCE*, 12 (9) September, pp. 397–403.
- Ronemus, M. J., Galbiati, M., Ticknor, C., Chen, J. C. & Dellaporta, S. L. (1996) Demethylation-Induced Developmental Pleiotropy in Arabidopsis. *SCIENCE*, 273 (5275) August, pp. 654–657.

- Saze, H., Scheid, O. M. & Paszkowski, J. (2003) Maintenance of CpG Methylation Is Essential for Epigenetic Inheritance during Plant Gametogenesis. *NATURE GENETICS*, 34 (1) May, pp. 65–69.
- Saze, H., Shiraiishi, A., Miura, A. & Kakutani, T. (2008) Control of Genic DNA Methylation by a *jmjC* Domain - Containing Protein in *Arabidopsis Thaliana*. *SCIENCE*, 319 (5862) January, pp. 462–465.
- Schneider, C. A., Rasband, W. S. & Eliceiri, K. W. (2012) NIH Image to ImageJ: 25 Years of Image Analysis. *NATURE METHODS*, 9 (7) July, pp. 671–675.
- Secco, D., Wang, C., Shou, H., Schultz, M. D., Chiarenza, S., Nussaume, L., Ecker, J. R., Whelan, J. & Lister, R. (2015) Stress Induced Gene Expression Drives Transient DNA Methylation Changes at Adjacent Repetitive Elements. *ELIFE*, 4 July.
- Silveira, A. B., Trontin, C., Cortijo, S., Barau, J., Vieira Del Bem, L. E., Loudet, O., Colot, V. & Vincentz, M. (2013) Extensive Natural Epigenetic Variation at a De Novo Originated Gene. *PLOS GENETICS*, 9 (4) April.
- Singh, A., Zubko, E. & Meyer, P. (2008) Cooperative Activity of DNA Methyltransferases for Maintenance of Symmetrical and Non-Symmetrical Cytosine Methylation in *Arabidopsis Thaliana*. *PLANT JOURNAL*, 56 (5) December, pp. 814–823.
- Soleimani, V. D., Palidwor, G. A., Ramachandran, P., Perkins, T. J. & Rudnicki, M. A. (2013) Chromatin Tandem Affinity Purification Sequencing. *NATURE PROTOCOLS*, 8 (8) August, pp. 1525–1534.
- Sopko, R., Huang, D. Q., Preston, N., Chua, G., Papp, B., Kafadar, K., Snyder, M., Oliver, S. G., Cyert, M., Hughes, T. R., Boone, C. & Andrews, B. (2006) Mapping Pathways and Phenotypes by Systematic Gene Overexpression. *MOLECULAR CELL*, 21 (3) February, pp. 319–330.
- Soppe, W. J. J., Jacobsen, S. E., Alonso-Blanco, C., Jackson, J. P., Kakutani, T., Koornneef, M. & Peeters, A. J. M. (2000) The Late Flowering Phenotype of *Fwa* Mutants Is Caused by Gain-of-Function Epigenetic Alleles of a Homeodomain Gene. *MOLECULAR CELL*, 6 (4) October, pp. 791–802.

- Soppe, W. J. J., Jasencakova, Z., Houben, A., Kakutani, T., Meister, A., Huang, M. S., Jacobsen, S. E., Schubert, I. & Fransz, P. F. (2002) DNA Methylation Controls Histone H3 Lysine 9 Methylation and Heterochromatin Assembly in Arabidopsis. *EMBO JOURNAL*, 21 (23) December, pp. 6549–6559.
- Steward, N., Kusano, T. & Sano, H. (2000) Expression of ZmMET1, a Gene Encoding a DNA Methyltransferase from Maize, Is Associated Not Only with DNA Replication in Actively Proliferating Cells, but Also with Altered DNA Methylation Status in Cold-Stressed Quiescent Cells. *Nucleic Acids Research* [Online], 28 (17) September, pp. 3250–3259. Available from: <<http://www.ncbi.nlm.nih.gov/pmc/articles/PMC110715/>>.
- Stroud, H., Greenberg, M. V. C., Feng, S., Bernatavichute, Y. V & Jacobsen, S. E. (2013) Comprehensive Analysis of Silencing Mutants Reveals Complex Regulation of the Arabidopsis Methylome. *CELL*, 152 (1–2) January, pp. 352–364.
- Takuno, S. & Gaut, B. S. (2012) Body-Methylated Genes in Arabidopsis Thaliana Are Functionally Important and Evolve Slowly. *MOLECULAR BIOLOGY AND EVOLUTION*, 29 (1) January, pp. 219–227.
- Takuno, S. & Gaut, B. S. (2013) Gene Body Methylation Is Conserved between Plant Orthologs and Is of Evolutionary Consequence. *PROCEEDINGS OF THE NATIONAL ACADEMY OF SCIENCES OF THE UNITED STATES OF AMERICA*, 110 (5) January, pp. 1797–1802.
- Tariq, M., Saze, H., Probst, A. V, Lichota, J., Habu, Y. & Paszkowski, J. (2003) Erasure of CpG Methylation in Arabidopsis Alters Patterns of Histone H3 Methylation in Heterochromatin. *PROCEEDINGS OF THE NATIONAL ACADEMY OF SCIENCES OF THE UNITED STATES OF AMERICA*, 100 (15) July, pp. 8823–8827.
- Taverna, S. D., Li, H., Ruthenburg, A. J., Allis, C. D. & Patel, D. J. (2007) How Chromatin-Binding Modules Interpret Histone Modifications: Lessons from Professional Pocket Pickers. *NATURE STRUCTURAL & MOLECULAR BIOLOGY*, 14 (11) November, pp. 1025–1040.
- Teerawanichpan, P., Chandrasekharan, M. B., Jiang, Y. M., Narangajavana, J. & Hall, T. C. (2004) Characterization of Two Rice DNA Methyltransferase Genes and RNAi-Mediated

- Reactivation of a Silenced Transgene in Rice Callus. *PLANTA*, 218 (3) January, pp. 337–349.
- Tester, M. & Langridge, P. (2010) Breeding Technologies to Increase Crop Production in a Changing World. *SCIENCE*, 327 (5967) February, pp. 818–822.
- Thomas, M., Pingault, L., Poulet, A., Duarte, J., Throude, M., Faure, S., Pichon, J.-P., Paux, E., Probst, A. V. & Tatout, C. (2014) Evolutionary History of Methyltransferase 1 Genes in Hexaploid Wheat. *BMC GENOMICS*, (15) October.
- Thouet, J., Quinet, M., Ormenese, S., Kinet, J.-M. & Perilleux, C. (2008) Revisiting the Involvement of SELF-PRUNING in the Sympodial Growth of Tomato. *PLANT PHYSIOLOGY*, 148 (1) September, pp. 61–64.
- To, T. K., Kim, J.-M., Matsui, A., Kurihara, Y., Morosawa, T., Ishida, J., Tanaka, M., Endo, T., Kakutani, T., Toyoda, T., Kimura, H., Yokoyama, S., Shinozaki, K. & Seki, M. (2011) Arabidopsis HDA6 Regulates Locus-Directed Heterochromatin Silencing in Cooperation with MET1. *PLOS GENETICS*, 7 (4) April.
- Tran, R. K., Zilberman, D., Bustos, C. de, Ditt, R. F., Henikoff, J. G., Lindroth, A. M., Delrow, J., Boyle, T., Kwong, S., Bryson, T. D., Jacobsen, S. E. & Henikoff, S. (2005) Chromatin and siRNA Pathways Cooperate to Maintain DNA Methylation of Small Transposable Elements in Arabidopsis. *GENOME BIOLOGY*, 6 (11).
- Tsukahara, S., Kobayashi, A., Kawabe, A., Mathieu, O., Miura, A. & Kakutani, T. (2009) Bursts of Retrotransposition Reproduced in Arabidopsis. *NATURE*, 461 (7262) September, pp. 423-U125.
- Vanderkrol, A. R. & Chua, N. H. (1991) The Basic Domain Of Plant B-Zip Proteins Facilitates Import of a Reporter Protein into Plant Nuclei. *PLANT CELL*, 3 (7) July, pp. 667–675.
- Veena, Jiang, H. M., Doerge, R. W. & Gelvin, S. B. (2003) Transfer of T-DNA and Vir Proteins to Plant Cells by Agrobacterium Tumefaciens Induces Expression of Host Genes Involved in Mediating Transformation and Suppresses Host Defense Gene Expression. *PLANT JOURNAL*, 35 (2) July, pp. 219–236.
- Virdi, K. S., Laurie, J. D., Xu, Y.-Z., Yu, J., Shao, M.-R., Sanchez, R., Kundariya, H., Wang, D.,

- Riethoven, J.-J. M., Wamboldt, Y., Arrieta-Montiel, M. P., Shedge, V. & Mackenzie, S. A. (2015) Arabidopsis MSH1 Mutation Alters the Epigenome and Produces Heritable Changes in Plant Growth. *NATURE COMMUNICATIONS*, (6) February.
- Waddington, C. H. (1942) The Epigenotype. *Endeavour*, 1 (1) February, pp. 18–20.
- Waddington, C. H. (1957) The Strategy of the Genes. *Allen & Unwin*, London.
- Wassenegger, M., Heimes, S., Riedel, L. & Sanger, H. L. (1994) RNA-Directed de Novo Methylation of Genomic Sequences in Plants. *Cell*, 76 (3) February, pp. 567–576.
- Watson, J. D. & Crick, F. H. C. (1953) GENETICAL IMPLICATIONS OF THE STRUCTURE OF DEOXYRIBONUCLEIC ACID. *NATURE*, 171 (4361), pp. 964–967.
- Watson, M., Hawkes, E. & Meyer, P. (2014) Transmission of Epi-Alleles with MET1-Dependent Dense Methylation in Arabidopsis Thaliana. *PLOS ONE*, 9 (8) August.
- Watson, M. R. (2013) 'Heritable Epigenetic Variation of DNA Methylation Targets in Plants', PhD thesis, University of Leeds, Leeds.
- Wierzbicki, A. T., Ream, T. S., Haag, J. R. & Pikaard, C. S. (2009) RNA Polymerase V Transcription Guides ARGONAUTE4 to Chromatin. *NATURE GENETICS*, 41 (5) May, pp. 630–634.
- Williams, B. P., Pignatta, D., Henikoff, S., Gehring, M., Winter, C. & Brooks, M. (2015) Methylation-Sensitive Expression of a DNA Demethylase Gene Serves As an Epigenetic Rheostat. *PLOS Genetics* [Online], 11 (3) March, p. e1005142. Available from: <<http://dx.plos.org/10.1371/journal.pgen.1005142>> [Accessed 19 June 2017].
- Wolffe, A. P. & Guschin, D. (2000) Chromatin Structural Features and Targets That Regulate Transcription. *JOURNAL OF STRUCTURAL BIOLOGY*, 129 (2–3) April, pp. 102–122.
- Woo, H. R., Dittmer, T. A. m & Richards, E. J. (2008) Three SRA-Domain Methylcytosine-Binding Proteins Cooperate to Maintain Global CpG Methylation and Epigenetic Silencing in Arabidopsis. *PLOS GENETICS*, 4 (8) August.
- Wu, K., Zhang, L., Zhou, C., Yu, C.-W. & Chaikam, V. (2008) HDA6 Is Required for Jasmonate Response, Senescence and Flowering in Arabidopsis. *JOURNAL OF EXPERIMENTAL BOTANY*, 59 (2) February, pp. 225–234.

- Xiao, W. Y., Custard, K. D., Brown, R. C., Lemmon, B. E., Harada, J. J., Goldberg, R. B. & Fischer, R. L. (2006) DNA Methylation Is Critical for Arabidopsis Embryogenesis and Seed Viability. *PLANT CELL*, 18 (4) April, pp. 805–814.
- Xu, C., Liberatore, K. L., MacAlister, C. A., Huang, Z., Chu, Y.-H., Jiang, K., Brooks, C., Ogawa-Ohnishi, M., Xiong, G., Pauly, M., Eck, J. Van, Matsubayashi, Y., Knaap, E. van der & Lippman, Z. B. (2015) A Cascade of Arabinosyltransferases Controls Shoot Meristem Size in Tomato. *NATURE GENETICS*, 47 (7) July, p. 784+.
- Yao, Y., Bilichak, A., Golubov, A. & Kovalchuk, I. (2012) ddm1 Plants Are Sensitive to Methyl Methane Sulfonate and NaCl Stresses and Are Deficient in DNA Repair. *PLANT CELL REPORTS*, 31 (9) September, pp. 1549–1561.
- Yoo, S. J., Chung, K. S., Jung, S. H., Yoo, S. Y., Lee, J. S. & Ahn, J. H. (2010) BROTHER OF FT AND TFL1 (BFT) Has TFL1-like Activity and Functions Redundantly with TFL1 in Inflorescence Meristem Development in Arabidopsis. *PLANT JOURNAL*, 63 (2) July, pp. 241–253.
- Yu, A., Lepere, G., Jay, F., Wang, J., Bapaume, L., Wang, Y., Abraham, A.-L., Penterman, J., Fischer, R. L., Voinnet, O. & Navarro, L. (2013) Dynamics and Biological Relevance of DNA Demethylation in Arabidopsis Antibacterial Defense. *PROCEEDINGS OF THE NATIONAL ACADEMY OF SCIENCES OF THE UNITED STATES OF AMERICA*, 110 (6) February, pp. 2389–2394.
- Yu, B., Yang, Z. Y., Li, J. J., Minakhina, S., Yang, M. C., Padgett, R. W., Steward, R. & Chen, X. M. (2005) Methylation as a Crucial Step in Plant microRNA Biogenesis. *SCIENCE*, 307 (5711) February, pp. 932–935.
- Yu, C.-W., Liu, X., Luo, M., Chen, C., Lin, X., Tian, G., Lu, Q., Cui, Y. & Wu, K. (2011) HISTONE DEACETYLASE6 Interacts with FLOWERING LOCUS D and Regulates Flowering in Arabidopsis. *PLANT PHYSIOLOGY*, 156 (1) May, pp. 173–184.
- Zemach, A., McDaniel, I. E., Silva, P. & Zilberman, D. (2010) Genome-Wide Evolutionary Analysis of Eukaryotic DNA Methylation. *SCIENCE*, 328 (5980) May, pp. 916–919.
- Zheng, X., Pontes, O., Zhu, J., Miki, D., Zhang, F., Li, W.-X., Iida, K., Kapoor, A., Pikaard, C. S. & Zhu, J.-K. (2008) ROS3 Is an RNA-Binding Protein Required for DNA Demethylation in

Arabidopsis. *NATURE*, 455 (7217) October, pp. 1259-U70.

Zhu, J.-K. (2009) Active DNA Demethylation Mediated by DNA Glycosylases. *ANNUAL REVIEW OF GENETICS*, 43, pp. 143–166.

Zhu, J., Kapoor, A., Sridhar, V. V, Agius, F. & Zhu, J.-K. (2007) The DNA Glycosylase/lyase ROS1 Functions in Pruning DNA Methylation Patterns in Arabidopsis. *CURRENT BIOLOGY*, 17 (1) January, pp. 54–59.

Zilberman, D., Gehring, M., Tran, R. K., Ballinger, T. & Henikoff, S. (2007) Genome-Wide Analysis of Arabidopsis Thaliana DNA Methylation Uncovers an Interdependence between Methylation and Transcription. *NATURE GENETICS*, 39 (1) January, pp. 61–69.

7 Supplementary data

	baseMean	log2Fold	lfcSE	stat	pvalue	padj	1	2	3	4	5	6	Line	Description
AT3G30765	14.684143	-4.181766371	0.555460021	-7.528474078	5.13E-14	1.57E-12	0	0	0	4.16453883	5.310931324	5.065040979	A1+	CACTA-like transposase family (En/Spm)
AT3G30765	40.230815	-1.876447169	0.179034379	-10.4809321	1.06E-25	4.93E-23	0	0	0	6.479588225	5.5779349	5.897561509	A2+	CACTA-like transposase family (En/Spm)
AT3G32230	24.951584	-4.372631122	0.545465225	-8.016633432	1.09E-15	3.88E-14	0.640148721	0	0	6.476563218	5.396254736	4.391288416	A1+	CACTA-like transposase family (En/Spm)
AT3G32230	120.16903	-2.809610952	0.179264518	-15.67298974	2.31E-55	3.62E-52	0.954186367	0	0	7.437782895	8.331808521	7.829757627	A2+	CACTA-like transposase family (En/Spm)
AT5G28927	10.498964	-3.653404815	0.573042287	-6.37545133	1.82E-10	3.78E-09	0	0	0	3.480233365	4.786788781	4.767143513	A1+	CACTA-like transposase family (En/Spm)
AT5G28927	26.040792	-1.525089694	0.175505661	-8.689689465	3.63E-18	1.18E-15	0	0	0	5.708773051	5.959583079	5.482576886	A2+	CACTA-like transposase family (En/Spm)
AT1G33130	4.0486113	-1.945298709	0.512918761	-3.792605881	0.000149075	0.00134277	0	0	0.588988589	2.797162804	3.546623725	3.027056186	A1-	CACTA-like transposase family (Ptta/En/Spm)
AT1G33130	206.7877	-7.139678165	0.47208837	-15.12360528	1.13E-51	3.16E-49	0	0	0.626414477	7.353641488	9.270813213	8.851451371	A1+	CACTA-like transposase family (Ptta/En/Spm)
AT1G33130	152.60219	-2.398624313	0.180176955	-13.31260323	1.96E-40	1.86E-37	0	0	0.940325156	7.275227783	8.847923629	8.238471098	A2+	CACTA-like transposase family (Ptta/En/Spm)
AT1G36460	7.3340864	-2.854420102	0.513380945	-5.560042949	2.70E-08	4.67E-07	0	0	0	3.222033331	4.483532941	3.935732613	A1-	CACTA-like transposase family (Ptta/En/Spm)
AT1G36460	171.74301	-4.044193077	0.582499238	-6.942829821	3.84E-12	9.79E-11	0	0	0	6.448866468	8.728738155	9.02751837	A1+	CACTA-like transposase family (Ptta/En/Spm)
AT1G36460	21.274829	-1.274520171	0.17025739	-7.485843472	7.11E-14	1.63E-11	0	0	0	5.245529421	5.856362086	5.120067235	A2+	CACTA-like transposase family (Ptta/En/Spm)
AT1G39110	24.922991	-4.44739519	0.465643996	-9.551063099	1.28E-21	6.68E-20	0	0	0.588988589	4.94268382	6.024848039	5.811684378	A1-	CACTA-like transposase family (Ptta/En/Spm)
AT1G39110	288.18671	-7.655498912	0.457105457	-16.74777404	5.88E-63	2.56E-60	0	0	0.626414477	7.97502982	9.475822275	9.58482238	A1+	CACTA-like transposase family (Ptta/En/Spm)
AT1G39110	34.174178	-1.697925204	0.177899091	-9.544316359	1.37E-21	5.21E-19	0	0	0.940325156	5.843766725	6.477159848	5.92140565	A2+	CACTA-like transposase family (Ptta/En/Spm)
AT1G40118	4.4192272	-2.148026849	0.511409912	-4.200205745	2.67E-05	0.000283432	0	0	0	2.192330878	3.546623725	3.728967903	A1-	CACTA-like transposase family (Ptta/En/Spm)
AT1G40118	38.543363	-5.537633727	0.50935096	-10.87194128	1.57E-27	1.29E-25	0	0	0	5.646896475	6.379024116	6.657141708	A1+	CACTA-like transposase family (Ptta/En/Spm)
AT1G40124	10.600207	-3.827523708	0.565320878	-6.770533086	1.28E-11	3.06E-10	0	0	0	4.16453883	4.654502272	4.553554369	A1+	CACTA-like transposase family (Ptta/En/Spm)
AT1G42500	20.868839	-4.444168111	0.531475983	-8.361935918	6.17E-17	2.44E-15	0	0	0.694589061	5.74125297	5.625572377	4.628319815	A1+	CACTA-like transposase family (Ptta/En/Spm)
AT1G42500	60.316593	-2.054377194	0.179785146	-11.42684609	3.07E-30	1.82E-27	0	0	1.024858076	6.340382871	7.397307751	6.836085095	A2+	CACTA-like transposase family (Ptta/En/Spm)
AT1G43840	47.590252	-5.715878568	0.482165993	-11.8545867	2.04E-32	2.27E-30	0	0	0.694589061	6.301797049	6.95819704	6.40407374	A1+	CACTA-like transposase family (Ptta/En/Spm)
AT1G43840	81.150941	-2.066787907	0.179500696	-11.51409414	1.12E-30	7.10E-28	0	0	1.024858076	6.376463566	7.680228928	7.648770878	A2+	CACTA-like transposase family (Ptta/En/Spm)
AT1G49080	3.2273194	-1.759047298	0.499803614	-3.519476946	0.000432399	0.00344651	0	0	0	2.192330878	3.546623725	2.610741738	A1-	CACTA-like transposase family (Ptta/En/Spm)
AT1G49080	103.51033	-4.649504435	0.569143991	-8.169293722	3.10E-16	1.16E-14	0	0	0	6.066915882	8.185975431	8.054206022	A1+	CACTA-like transposase family (Ptta/En/Spm)
AT1G49080	9.3591187	-0.690790182	0.14532984	-4.753257692	2.00E-06	1.94E-04	0	0	0	4.034776506	4.799921877	3.898037328	A2+	CACTA-like transposase family (Ptta/En/Spm)
AT1G49090	15.050042	-3.284303293	0.487867228	-6.731961284	1.67E-11	4.11E-10	1.026048597	0.588988589	0	3.816762292	5.617177427	4.837143627	A1-	CACTA-like transposase family (Ptta/En/Spm)
AT1G49090	299.58635	-7.539912221	0.436738134	-17.26414901	8.76E-67	4.79E-64	1.082007379	0.626414477	0	8.148628238	9.542844371	9.58716708	A1+	CACTA-like transposase family (Ptta/En/Spm)
AT1G49090	29.688565	-1.468636906	0.175803476	-8.353855901	6.61E-17	1.97E-14	1.523548554	0.940325156	0	5.59831633	6.330810854	5.663124249	A2+	CACTA-like transposase family (Ptta/En/Spm)
AT1G50850	5.3377543	-2.374480474	0.514522979	-4.614916281	3.93E-06	4.88E-05	0	0	0	2.526213436	4.089833736	3.613294506	A1-	CACTA-like transposase family (Ptta/En/Spm)
AT1G50850	159.34958	-7.160355178	0.473568079	-15.12001231	1.20E-51	3.30E-49	0	0	0	7.308122313	8.516472182	8.762964227	A1+	CACTA-like transposase family (Ptta/En/Spm)
AT1G50850	22.442535	-1.330827884	0.171633354	-7.753900119	8.91E-15	2.22E-12	0	0	0	5.708773051	5.715995759	5.035194817	A2+	CACTA-like transposase family (Ptta/En/Spm)
AT2G06250	62.278677	-5.849703939	0.433988581	-13.47893514	2.08E-41	2.83E-39	0	0	0	6.691428291	7.470110277	6.585144057	A1+	CACTA-like transposase family (Ptta/En/Spm)
AT2G06250	43.420057	-5.338637405	0.527085868	-10.12859142	1.43E-24	2.87E-22	0	0	0	7.292624406	5.476812514	5.958938819	A1+	CACTA-like transposase family (Ptta/En/Spm)
AT2G06490	43.207362	-5.237175356	0.429643353	-12.18958776	3.53E-34	3.42E-32	0.602380384	0.588988589	0	6.863492531	6.024848039	6.315890736	A1-	CACTA-like transposase family (Ptta/En/Spm)
AT2G06490	42.742307	-5.281807795	0.48889813	-10.80349355	3.31E-27	2.66E-25	0.640148721	0.626414477	0	6.476563218	6.871459168	5.706299342	A1+	CACTA-like transposase family (Ptta/En/Spm)
AT2G06590	278.71646	-7.908651285	0.384255004	-20.58177825	4.00E-94	3.31E-91	0	0	0	8.91945513	9.396977901	9.013813458	A1-	CACTA-like transposase family (Ptta/En/Spm)
AT2G06590	66.175387	-6.007148626	0.503854655	-11.92238389	9.05E-33	1.02E-30	0	0	0	7.743857191	8.610594236	6.198606574	A1+	CACTA-like transposase family (Ptta/En/Spm)
AT2G06590	15.244722	-0.956274072	0.159438784	-5.997750665	2.00E-09	2.72E-07	0	0	0	4.427639234	5.527266304	4.745752287	A2+	CACTA-like transposase family (Ptta/En/Spm)
AT2G06670	204.54662	-7.571446207	0.388488261	-19.48951095	1.35E-84	8.24E-82	0	0	0	8.57684784	8.830120753	8.619515542	A1-	CACTA-like transposase family (Ptta/En/Spm)
AT2G06670	65.27555	-5.929783281	0.508142524	-11.66952774	1.82E-31	1.91E-29	0	0	0	7.788737976	6.680573214	6.148681867	A1+	CACTA-like transposase family (Ptta/En/Spm)
AT2G06670	11.367729	-0.855903059	0.155248554	-5.51311452	3.53E-08	4.22E-06	0	0	0	4.357162671	4.799921877	4.514488038	A2+	CACTA-like transposase family (Ptta/En/Spm)
AT2G06720	59.971085	-5.508782656	0.438623618	-12.55924769	3.54E-36	3.82E-34	0	0	0.653468127	6.054369667	7.470110277	6.888597855	A1-	CACTA-like transposase family (Ptta/En/Spm)
AT2G06720	158.17241	-7.211839279	0.447918757	-16.10077533	2.52E-58	9.25E-56	0	0	0.694589061	6.69405066	8.33388287	7.745438878	A1+	CACTA-like transposase family (Ptta/En/Spm)
AT2G06720	55.144391	-2.297664455	0.180209781	-12.74994311	3.12E-37	2.59E-34	0	0	1.024858076	6.750962371	6.99730186	6.605319246	A2+	CACTA-like transposase family (Ptta/En/Spm)
AT2G06800	40.166409	-4.995732237	0.464140198	-10.76341212	5.12E-27	3.63E-25	0	0	0	5.672031041	7.128344859	5.730732322	A1-	CACTA-like transposase family (Ptta/En/Spm)
AT2G06800	45.421027	-5.508323982	0.518532795	-10.62290376	2.33E-26	1.80E-24	0	0	0	5.319969209	6.841347652	6.917791694	A1+	CACTA-like transposase family (Ptta/En/Spm)
AT2G06800	22.160542	-1.38577305	0.173066185	-8.007185529	1.17E-15	3.22E-13	0	0	0	5.245529421	5.624714968	5.605416368	A2+	CACTA-like transposase family (Ptta/En/Spm)
AT2G10000	50.611623	-5.472569969	0.431500094	-12.68266228	7.38E-37	8.21E-35	0	0	0.653468127	6.417856728	7.128344859	6.334274225	A1-	CACTA-like transposase family (Ptta/En/Spm)
AT2G10000	6.3574225	-2.793155777	0.583964961	-4.783087965	1.73E-06	1.98E-05	0	0	0.694589061	3.684038477	4.164272639	3.284432598	A1+	CACTA-like transposase family (Ptta/En/Spm)
AT2G10640	73.369323	-5.802083302	0.486319369	-11.93060296	8.20E-33	9.28E-31	0.626414477	0.694589061	5.992129826	7.472095394	7.649976592	A1+	CACTA-like transposase family (Ptta/En/Spm)	
AT2G12300	10.471056	-2.857509562	0.51416595	-5.557555804	2.74E-08	4.73E-07	0	0	0	2.526213436	4.545092181	4.028969492	A1-	CACTA-like transposase family (Ptta/En/Spm)
AT2G12300	113.42747	-3.811981822	0.585169473	-6.514321066	7.30E-11	1.60E-09	0	0	0	5.786213592	8.161811847	8.417829413	A1+	CACTA-like transposase family (Ptta/En/Spm)
AT2G12300	21.315229	-1.227944798	0.168847983	-7.27487202	3.53E-13	7.17E-11	0	0	0	5.245529421	5.934461902	4.99080971	A2+	CACTA-like transposase family (Ptta/En/Spm)
AT2G13160	10.095763	-3.389372496	0.503777481	-6.727915843	1.72E-11	4.22E-10	0	0	0	4.041933031	4.792504907	4.277198875	A1-	CACTA-like transposase family (Ptta/En/Spm)
AT2G13160	101.99372	-6.786868229	0.473587122	-14.33077023	1.41E-46	2.94E-44	0	0	0	7.984706492	7.850243522	7.032350776	A1+	CACTA-like transposase family (Ptta/En/Spm)
AT2G13160	188.72581	-3.015593931	0.179119694	-16.83564697	1.34E-63	2.96E-60	0	0	0	5.888656024	9.012919444	8.564184444	A2+	CACTA-like transposase family (Ptta/En/Spm)
AT2G13175	33.597119	-4.83780432	0.437895005	-11.04786392	2.24E-28	1.70E-26	0.588988589	0.653468127	5.7000812964	6.434335581	5.937261568	A1-	CACTA-like transposase family (Ptta/En/Spm)	
AT2G13175	17.324107	-4.180599895	0.51966921	-8.044732721	8.64E-16	3.10E-14	0.626414477	0.694589061	5.319969209	5.123468832	4.953150701	A1+	CACTA-like transposase family (Ptta/En/Spm)	
AT2G13310	27.125723	-4.537443433	0.462591348	-9.808751186	1.03E-22	5.75E-21	0.602380384	0	0	5.800812964	6.244071671	5.074348265	A1-	CACTA-like transposase family (Ptta/En/Spm)

AT2G13310	179.21853	-6.925891881	0.478086337	-14.48669695	1.47E-47	3.47E-45	0.640148721	0	0	0	7.037640449	8.942393828	8.827851728	A1+	CACTA-like transposase family (Ptta/En/Sp/m)
AT2G13310	51.11748	-1.839123188	0.178512353	-10.30249814	6.87E-25	3.15E-22	0.954186367	0	0	0	5.967202726	1.686667132	6.677105214	A2+	CACTA-like transposase family (Ptta/En/Sp/m)
AT2G13870	20.295202	-3.895571054	0.495855092	-7.856269128	3.96E-15	1.33E-13	0	0	0	0	3.937326911	6.244071671	5.074348265	A1-	CACTA-like transposase family (Ptta/En/Sp/m)
AT2G13870	178.89096	-4.013723005	0.583007705	-6.884511075	5.80E-12	1.45E-10	0	0	0	0	6.476563218	8.854670971	9.034408035	A1+	CACTA-like transposase family (Ptta/En/Sp/m)
AT2G13870	55.869896	-1.988732408	0.179339147	-11.0892264	1.42E-28	7.53E-26	0	0	0	0	6.24602418	7.3128121408	6.677105214	A2+	CACTA-like transposase family (Ptta/En/Sp/m)
AT2G14230	230.52403	-6.580635482	0.333787318	-19.71505546	1.60E-86	1.96E-83	2.121326742	1.894766578	1.796470461	9.175955433	8.678527207	8.605327509	A1+	CACTA-like transposase family (Ptta/En/Sp/m)	
AT2G14230	76.952873	-2.139727759	0.179910656	-11.89327973	1.28E-32	8.98E-30	2.727903006	2.484087445	2.36149799	6.723210612	7.634164624	7.190249371	A2+	CACTA-like transposase family (Ptta/En/Sp/m)	
AT2G14970	15.2081	-4.154419067	0.557761933	-7.448373254	9.45E-14	2.83E-12	0	0	0	0	4.021446993	5.476812514	5.065040979	A1+	CACTA-like transposase family (Ptta/En/Sp/m)
AT3G29634	31.457695	-4.756759299	0.514064222	-9.253239365	2.18E-20	1.13E-18	0.640148721	0.626414477	0	5.051918249	5.883728226	6.620982316	A1+	CACTA-like transposase family (Ptta/En/Sp/m)	
AT3G29650	38.296938	-4.802009354	0.472312498	-10.16701734	2.78E-24	1.69E-22	0	0	0	0	5.197878395	7.128344859	5.811684378	A1-	CACTA-like transposase family (Ptta/En/Sp/m)
AT3G29730	7.9405242	-2.539987006	0.505151386	-5.028169921	4.95E-07	7.15E-06	0.602380384	0.588988589	0.653468127	3.222033331	4.483532941	4.116544802	A1-	CACTA-like transposase family (Ptta/En/Sp/m)	
AT3G29730	124.66054	-6.462805545	0.453906903	-14.23817417	5.31E-46	1.08E-43	0.640148721	0.626414477	0.694589061	6.961280029	8.161811847	8.40193474	A1+	CACTA-like transposase family (Ptta/En/Sp/m)	
AT3G29730	21.211755	-1.233208217	0.171952347	-7.171802188	7.40E-13	1.45E-10	0.954186367	0.940325156	1.024858076	5.4624789	5.686205962	4.99080971	A2+	CACTA-like transposase family (Ptta/En/Sp/m)	
AT3G29734	85.490999	-4.716689998	0.325619928	-14.48526209	1.50E-47	2.61E-45	1.619590486	2.710637931	2.324984772	7.030399376	7.672572658	7.405735635	A1-	CACTA-like transposase family (Ptta/En/Sp/m)	
AT3G29734	149.00303	-5.567399774	0.328744058	-16.93536243	2.47E-64	1.17E-61	1.693301494	2.803425391	2.413854982	8.558079749	7.894906359	8.07440268	A1+	CACTA-like transposase family (Ptta/En/Sp/m)	
AT3G29736	66.079903	-4.687293692	0.346655247	-13.52148489	1.17E-41	1.60E-39	1.353130444	2.469293851	1.718867729	6.740426363	7.182410679	7.11811844	A1-	CACTA-like transposase family (Ptta/En/Sp/m)	
AT3G29736	125.20746	-5.665701496	0.34771476	-16.29410696	1.09E-59	4.23E-57	1.419792043	2.559127732	1.796470461	8.240343172	7.603487774	7.956029515	A1-	CACTA-like transposase family (Ptta/En/Sp/m)	
AT3G29739	57.848371	-4.78961221	0.390424692	-12.26769798	1.35E-34	1.36E-32	1.353130444	1.329165983	1.442988428	6.417856728	7.425970407	6.456789178	A1-	CACTA-like transposase family (Ptta/En/Sp/m)	
AT3G29739	86.720343	-5.641600726	0.392402562	-14.37707415	7.21E-47	1.56E-44	1.419792043	1.395704924	1.513627237	7.777647993	7.040014478	7.384788387	A1+	CACTA-like transposase family (Ptta/En/Sp/m)	
AT3G30218	69.922816	-5.8868097	0.453647891	-12.97660546	1.66E-38	2.54E-36	0	0	1.061739724	0.694589061	6.503738247	7.370331015	7.363060739	A1+	CACTA-like transposase family (Ptta/En/Sp/m)
AT3G30396	5.5641966	-2.505083764	0.515124086	-4.863068593	1.16E-06	1.58E-05	0	0	0	3.025182302	4.089833736	3.487531741	A1-	CACTA-like transposase family (Ptta/En/Sp/m)	
AT3G30396	95.634488	-4.206484277	0.578269798	-7.274258986	3.48E-13	9.78E-12	0	0	0	5.786213592	7.835043274	8.196139899	A1+	CACTA-like transposase family (Ptta/En/Sp/m)	
AT3G30396	20.103713	-1.325076647	0.171871458	-7.709695715	1.26E-14	3.08E-12	0	0	0	5.321529027	5.422755442	5.348296429	A2+	CACTA-like transposase family (Ptta/En/Sp/m)	
AT3G30663	132.31262	-6.802671775	0.486891335	-13.97164271	2.32E-44	4.45E-42	0	0	0	6.795247521	8.344656357	8.494777544	A1+	CACTA-like transposase family (Ptta/En/Sp/m)	
AT3G30663	15.226259	-1.01468414	0.162105356	-6.259415149	3.86E-10	5.59E-08	0	0	0	0.653468127	6.942973576	5.348623431	4.514488038	A2+	CACTA-like transposase family (Ptta/En/Sp/m)
AT3G30744	8.6825539	-2.476283574	0.514696549	-4.811152469	1.50E-06	2.00E-05	0	0	0.653468127	2.797162804	5.26298084	3.197406586	A1-	CACTA-like transposase family (Ptta/En/Sp/m)	
AT3G30744	83.661791	-6.561245225	0.453448588	-14.46965632	1.88E-47	4.36E-45	0	0	0.694589061	2.941510623	7.349087498	7.566881295	A1+	CACTA-like transposase family (Ptta/En/Sp/m)	
AT3G30746	16.305106	-3.883095245	0.492299358	-7.887670745	3.08E-15	1.05E-13	0	0	0	4.700053001	5.766238278	4.351279944	A1-	CACTA-like transposase family (Ptta/En/Sp/m)	
AT3G30746	24.237105	-5.029104576	0.521771641	-9.638516503	5.50E-22	3.20E-20	0	0	0	5.437371235	5.823389642	5.598854652	A1+	CACTA-like transposase family (Ptta/En/Sp/m)	
AT3G30767	2.7055071	-1.699639415	0.496778375	-3.421323272	0.000623172	0.004765903	0	0	0	2.562213436	2.665086523	2.833863982	A1-	CACTA-like transposase family (Ptta/En/Sp/m)	
AT3G30767	47.173085	-5.451382856	0.523606829	-10.4112142	2.20E-25	1.63E-23	0	0	0	5.192160237	6.779170955	7.125631731	A1-	CACTA-like transposase family (Ptta/En/Sp/m)	
AT3G30767	18.399534	-1.23598202	0.16962344	-7.28662276	3.18E-13	6.55E-11	0	0	0	5.358078375	5.270474873	5.078255057	A2+	CACTA-like transposase family (Ptta/En/Sp/m)	
AT3G30780	7.4933643	-2.962891523	0.512288797	-5.78363521	7.31E-09	1.35E-07	0	0	0	3.395221171	4.089833736	4.351279944	A1-	CACTA-like transposase family (Ptta/En/Sp/m)	
AT3G30780	42.552797	-5.59615046	0.509534354	-10.98287175	4.62E-28	3.92E-26	0	0	0	6.838581092	6.57366301	5.671366059	A1+	CACTA-like transposase family (Ptta/En/Sp/m)	
AT3G30780	86.928524	-2.438085277	0.180249009	-13.52620631	1.10E-41	1.12E-38	0	0	0	6.831151563	7.851051244	7.490410749	A2+	CACTA-like transposase family (Ptta/En/Sp/m)	
AT3G31920	24.562812	-4.448211334	0.556243224	-7.996881841	1.28E-15	4.52E-14	0	0	0	4.021446993	5.553108971	6.446015138	A1+	CACTA-like transposase family (Ptta/En/Sp/m)	
AT3G32226	14.081242	-3.757195693	0.573342328	-6.553145495	5.63E-11	1.25E-09	0	0	0	4.626795005	5.694569514	3.458449401	A1+	CACTA-like transposase family (Ptta/En/Sp/m)	
AT3G32226	107.55951	-2.346893305	0.180181647	-13.02515181	8.80E-39	7.81E-36	0	0	0	6.831151563	8.051285726	8.072696438	A2+	CACTA-like transposase family (Ptta/En/Sp/m)	
AT3G32240	163.90936	-7.191516929	0.3999233	-17.98224041	2.68E-72	1.13E-69	0	0	0	8.024870774	8.687845658	8.292875588	A1-	CACTA-like transposase family (Ptta/En/Sp/m)	
AT3G32240	142.49938	-6.975919031	0.479714134	-14.54182509	6.58E-48	1.63E-45	0	0	0	8.887002983	7.491614392	7.676644444	A1+	CACTA-like transposase family (Ptta/En/Sp/m)	
AT3G32240	49.746173	-2.012901497	0.179645535	-11.20485126	3.86E-29	2.14E-26	0	0	0	6.226388597	7.068308623	6.529773434	A2+	CACTA-like transposase family (Ptta/En/Sp/m)	
AT3G32677	71.723497	-5.8473802	0.499871218	-11.69777332	1.31E-31	1.39E-29	0.640148721	0	0	5.829815291	7.472095394	7.631920166	A1+	CACTA-like transposase family (Ptta/En/Sp/m)	
AT3G33166	69.008133	-2.525308695	0.512247691	-4.92985862	8.23E-07	1.15E-05	2.210244364	2.817685107	1.442988428	6.154180496	8.17743592	5.48961735	A1-	CACTA-like transposase family (Ptta/En/Sp/m)	
AT3G33166	97.522775	-4.547974891	0.436860864	-10.41057981	2.22E-25	1.63E-23	2.29555514	2.911630873	1.513627237	8.013353068	7.938227945	6.173860166	A1+	CACTA-like transposase family (Ptta/En/Sp/m)	
AT3G33166	18.252487	-0.662643997	0.170879602	-3.877844119	0.000105387	0.00735803	2.918845404	3.588268282	2.03712832	4.843112829	5.100202951	8.488821471	A2+	CACTA-like transposase family (Ptta/En/Sp/m)	
AT3G42720	190.4478	-7.028891146	0.391552285	-17.95134754	4.68E-72	1.94E-69	0.602380384	0.588988589	0	7.950467731	8.959615924	8.641826921	A1-	CACTA-like transposase family (Ptta/En/Sp/m)	
AT3G42720	333.08907	-7.654669261	0.451440225	-16.95561081	1.73E-64	8.41E-62	0.640148721	0.626414477	0	10.18942734	8.695459103	8.708005919	A1+	CACTA-like transposase family (Ptta/En/Sp/m)	
AT3G42720	44.578165	-1.698542994	0.17757352	-9.565294403	1.12E-21	4.38E-19	0.954186367	0.940325156	0	6.226388597	7.056714212	5.92140565	A2+	CACTA-like transposase family (Ptta/En/Sp/m)	
AT3G46487	43.008742	-4.22406203	0.461251937	-9.154229747	5.47E-20	2.56E-18	1.353130444	0	0	1.101575979	4.934746195	7.284819017	6.138961869	A1-	CACTA-like transposase family (Ptta/En/Sp/m)
AT3G46487	439.5033	-8.217801045	0.375058759	-21.91070294	2.05E-106	3.52E-103	1.419792043	0	0	1.161466416	9.434343195	9.904984574	9.946192271	A1+	CACTA-like transposase family (Ptta/En/Sp/m)
AT3G46487	35.871132	-1.603098849	0.17815491	-8.998342234	2.29E-19	8.13E-17	1.930722108	0	0	1.618012324	5.791275092	6.54511919	6.013026524	A2+	CACTA-like transposase family (Ptta/En/Sp/m)
AT4G03775	17.084336	-3.817532925	0.563008201	-6.780599141	1.20E-11	2.86E-10	0.640148721	0	0	5.913254063	5.019733684	3.6137176	A1+	CACTA-like transposase family (Ptta/En/Sp/m)	
AT4G03910	5.7002888	-2.004248577	0.507909253	-3.946076128	7.94E-05	0.000768661	0	0	0	1.757146478	4.792504907	2.610741738	A1-	CACTA-like transposase family (Ptta/En/Sp/m)	
AT4G03910	237.40606	-7.71361368	0.45909815	-16.80166577	2.37E-63	1.05E-60	0	0	0	5.90792982	9.177482928	9.221112472	A1+	CACTA-like transposase family (Ptta/En/Sp/m)	
AT4G03910	22.880766	-1.261555376	0.169630316	-7.437086758	1.03E-13	2.28E-11	0	0	0	2.295973566	6.079018602	5.160701666	A2+	CACTA-like transposase family (Ptta/En/Sp/m)	
AT4G04170	1209.6751	-5.434912969	0.41821587	-12.9954728	1.30E-38	1.57E-36	4.572990162	4.655421041	3.173323909	10.57513732	11.2446996	11.66794833	A1-	CACTA-like transposase family (Ptta/En/Sp/m)	
AT4G04170	528.83917	-3.169233812	0.167847682	-18.88166008	1.62E-79	5.37E-76	5.400859372	5.495378993	3.952951229	9.973666002	10.22217364	9.77515791	A2+	CACTA-like transposase family (Ptta/En/Sp/m)	
AT4G04430	94.569738	-6.300144286	0.441509129	-14.26956741	3.39E-46	9.66E-44	1.082007379	0.626414477	0	7.625138353	7.909491907	7.032350776	A1+	CACTA-like transposase family (Ptta/En/Sp/m)	
AT4G04430	198.9275	-3.15													

AT4G07518	9.1272643	-0.683690108	0.147247454	-4.64313703	3.43E-06	3.19E-04	0	0.940325156	0	4.034776506	4.558214482	4.078534946	A2+	CACTA-like transposase family (Ptta/En/Spm)
AT4G08091	39.669101	-4.837240091	0.447793077	-10.80240228	3.35E-27	2.40E-25	0	1.006034927	0	5.454346907	6.889210391	6.27840572	A1-	CACTA-like transposase family (Ptta/En/Spm)
AT4G08091	385.48988	-8.405287875	0.400963157	-20.96274367	1.44E-97	2.05E-94	0	1.061739724	0	9.718646435	9.326220191	6.697625491	A1+	CACTA-like transposase family (Ptta/En/Spm)
AT4G08091	31.026126	-1.482909377	0.175320627	-8.458271017	2.71E-17	8.49E-15	0	1.504834619	0	6.303376628	6.079018602	5.348296429	A2+	CACTA-like transposase family (Ptta/En/Spm)
AT4G08598	45.567449	-5.468095977	0.447418769	-12.22142735	2.39E-34	2.33E-32	0	0	0	6.105138068	6.244071671	7.041870662	A1-	CACTA-like transposase family (Ptta/En/Spm)
AT4G08598	30.398894	-5.09407699	0.528033429	-9.647262292	5.05E-22	2.96E-20	0	0	0	6.582320762	5.123468832	5.773726325	A1+	CACTA-like transposase family (Ptta/En/Spm)
AT4G32340	451.6961	-1.671618206	0.173295373	-9.646063717	5.11E-22	2.98E-20	7.740014238	7.49093163	7.927315529	9.163229078	9.646610833	9.45988882	A1+	CACTA-like transposase family (Ptta/En/Spm)
AT5G19015	13.758436	-4.104313733	0.557344361	-7.364053578	1.78E-13	5.17E-12	0	0	0	4.896561069	5.220242777	4.208431314	A1+	CACTA-like transposase family (Ptta/En/Spm)
AT5G19015	37.707028	-1.298298791	0.169278724	-7.669592241	1.73E-14	4.17E-12	0	0	0	4.942735706	6.870591504	6.348180357	A2+	CACTA-like transposase family (Ptta/En/Spm)
AT5G28923	137.97609	-6.423606911	0.496719024	-12.93207346	2.97E-38	4.38E-36	0	0.626414477	0	6.1332434805	8.477846986	8.619142096	A1+	CACTA-like transposase family (Ptta/En/Spm)
AT5G28923	14.16914	-0.937100426	0.160311403	-5.845500745	5.05E-09	6.62E-07	0	0.940325156	0	4.843112829	5.2297536	4.383282909	A2+	CACTA-like transposase family (Ptta/En/Spm)
AT5G29408	44.617635	-1.730668814	0.177278128	-9.76244972	1.63E-22	6.58E-20	0	0	0	5.680189541	6.883775214	6.663030935	A2+	CACTA-like transposase family (Ptta/En/Spm)
AT5G29568	5.5922814	-2.52671883	0.5151406	-4.902878713	9.44E-07	1.31E-05	0	0	0	3.222033331	4.089833736	3.349749908	A1-	CACTA-like transposase family (Ptta/En/Spm)
AT5G29568	62.894222	-1.979836961	0.58218025	-3.400728487	6.72E-04	4.30E-03	0	0	0	3.480233365	7.260839943	7.75381203	A1+	CACTA-like transposase family (Ptta/En/Spm)
AT5G30450	63.36628	-5.832860914	0.423380071	-13.77689058	3.51E-43	5.18E-41	0.602380384	0	0	6.605874948	6.952811471	7.334467632	A1-	CACTA-like transposase family (Ptta/En/Spm)
AT5G30450	8.0965071	-0.61934977	0.142898944	-4.334180179	1.46E-05	1.20E-03	0	0	0	4.034776506	4.345992327	3.798546962	A2+	CACTA-like transposase family (Ptta/En/Spm)
AT5G30480	23.95814	-4.273007881	0.487077138	-8.77275394	1.74E-18	7.42E-17	0	0	0	4.324976877	5.617177427	6.27840572	A1-	CACTA-like transposase family (Ptta/En/Spm)
AT5G30480	8.867826	-0.627890677	0.14070358	-4.462506773	8.10E-06	0.000708832	0	0	0	4.122374089	4.799921877	3.450808994	A2+	CACTA-like transposase family (Ptta/En/Spm)
AT5G32563	26.679603	-4.355785642	0.561718607	-7.75439088	8.88E-15	2.90E-13	0	0	0	3.480233365	6.247434088	6.246861259	A1+	CACTA-like transposase family (Ptta/En/Spm)
AT5G32566	17.127012	-3.891844404	0.495342709	-7.856872281	3.94E-15	1.32E-13	0	0	0	3.933736191	5.26298084	5.702706421	A1-	CACTA-like transposase family (Ptta/En/Spm)
AT5G32566	217.37425	-2.812918788	0.592362208	-4.748646608	2.05E-06	2.33E-05	0	0	0	6.030007392	9.363776641	9.187510222	A1+	CACTA-like transposase family (Ptta/En/Spm)
AT5G32566	24.19211	-1.400160113	0.173112417	-8.08815532	6.06E-16	1.70E-13	0	0	0	5.393724612	6.008550051	5.38305632	A2+	CACTA-like transposase family (Ptta/En/Spm)
AT5G34790	103.37912	-2.528163688	0.287765071	-8.78512702	1.56E-18	6.99E-17	4.768132494	4.816916094	4.880072038	7.525286068	7.923931472	6.841279286	A1+	CACTA-like transposase family (Ptta/En/Spm)
AT5G34790	104.55986	-1.248198868	0.166883691	-7.4661372	7.46E-14	1.70E-11	5.493835355	5.55299258	5.602852452	7.552565265	7.433619666	7.045866277	A2+	CACTA-like transposase family (Ptta/En/Spm)
AT5G36655	8.651573	-5.58827164	0.505798017	-9.05899106	4.21E-07	6.15E-06	1.026048597	0.588988589	0	3.222033331	4.792504907	4.028969492	A1-	CACTA-like transposase family (Ptta/En/Spm)
AT5G36655	320.78694	-6.928219905	0.48666463	-14.23612788	5.47E-46	1.11E-43	1.082007379	0.626414477	0	7.074356635	9.919469095	9.684545676	A1+	CACTA-like transposase family (Ptta/En/Spm)
AT5G36655	125.54573	-2.524350709	0.180179549	-14.01019552	1.35E-44	1.80E-41	1.523548554	0.940325156	0	7.226639302	8.464962907	7.967829969	A2+	CACTA-like transposase family (Ptta/En/Spm)
AT1G42410	3.4990828	-1.67117003	0.506920138	-3.296712645	0.000978235	0.007045104	0	0	0.653468127	2.192330878	3.546623725	2.833863982	A1-	CACTA-like transposase family (Tnp1/En/Spm)
AT1G33570	97.239371	-2.771920546	0.592327666	-6.197070805	2.87E-06	3.19E-05	0	0	0	4.896561069	8.047769012	8.189982436	A1+	CACTA-like transposase family (Tnp1/En/Spm)
AT1G34530	29.121055	-4.920650526	0.514521671	-9.563455749	1.14E-21	6.47E-20	0.640148721	0	0	5.694845984	6.420348952	5.31182967	A1+	CACTA-like transposase family (Tnp1/En/Spm)
AT1G34530	62.39218	-2.00574266	0.179470125	-11.17597853	5.35E-29	2.90E-26	0.954186367	0	0	6.284511346	7.477760881	6.909454177	A2+	CACTA-like transposase family (Tnp1/En/Spm)
AT1G35600	293.66203	-5.63438844	0.552721048	-10.19383804	2.11E-24	1.49E-22	0	0	0	7.732415395	9.556809943	9.642326152	A1+	CACTA-like transposase family (Tnp1/En/Spm)
AT1G35600	29.920608	-1.572905872	0.175943326	-8.939843925	3.90E-19	1.36E-16	0	0	0	5.817759631	6.311427547	5.545303641	A2+	CACTA-like transposase family (Tnp1/En/Spm)
AT1G36630	1211.5243	-4.924761673	0.560229973	-8.790607275	1.49E-18	6.72E-17	1.923129797	3.634383687	1.161466416	5.56813662	11.77537587	11.12481774	A1+	CACTA-like transposase family (Tnp1/En/Spm)
AT1G39190	6.0752071	-2.720491937	0.5856355	-4.645367192	3.39E-06	3.71E-05	0	0	0.694589061	3.480233365	4.164272639	3.284432598	A1+	CACTA-like transposase family (Tnp1/En/Spm)
AT1G39190	11.572768	-0.808730753	0.154491609	-5.234787542	1.65E-07	1.87E-05	0	0	1.024858076	7.36096999	4.799921877	4.078534946	A2+	CACTA-like transposase family (Tnp1/En/Spm)
AT1G42410	56.587698	-5.902700771	0.478972938	-12.32366237	6.76E-35	8.43E-33	0	0	0.694589061	6.961280029	7.117439888	6.293554041	A1+	CACTA-like transposase family (Tnp1/En/Spm)
AT1G42410	130.64656	-2.707270193	0.179853623	-15.05263082	3.32E-51	4.90E-48	0	0	1.024858076	7.488067396	8.550119731	7.85473927	A2+	CACTA-like transposase family (Tnp1/En/Spm)
AT1G52850	7.2330936	-2.472240442	0.51441568	-4.80591968	1.54E-06	2.05E-05	0.602380384	0	0	2.797162804	4.792504907	3.487531741	A1-	CACTA-like transposase family (Tnp1/En/Spm)
AT1G52850	350.50317	-3.432665812	0.58981978	-5.819855366	5.89E-09	9.83E-08	0.640148721	0	0	7.037640449	9.841749487	10.04502139	A1+	CACTA-like transposase family (Tnp1/En/Spm)
AT1G52850	96.303447	-2.32593616	0.180224766	-12.90575215	4.18E-38	3.58E-35	0.954186367	0	0	8.869634388	8.119745491	7.52972226	A2+	CACTA-like transposase family (Tnp1/En/Spm)
AT3G30836	229.96415	-7.606872633	0.392471801	-19.38195972	1.10E-83	6.48E-81	0	0	0	8.831735225	9.161544904	8.469584068	A1-	CACTA-like transposase family (Tnp1/En/Spm)
AT3G30836	252.46866	-8.026060757	0.441515052	-18.17845329	7.65E-74	4.79E-71	0	0	0	9.052569459	8.506912398	9.283167007	A1+	CACTA-like transposase family (Tnp1/En/Spm)
AT3G30836	8.4934548	-0.637906993	0.14160628	-4.504793088	6.64E-06	0.000591073	0	0	0	3.841804147	4.684124191	3.798546962	A2+	CACTA-like transposase family (Tnp1/En/Spm)
AT3G32950	15.490315	-4.218748586	0.554886221	-7.602907454	2.90E-14	9.05E-13	0	0	0	4.16453883	5.476812514	5.065040979	A1+	CACTA-like transposase family (Tnp1/En/Spm)
AT3G42650	4.2318645	-1.822551011	0.501897842	-3.631318682	0.000281977	0.002357208	0	0	0	1.131025967	4.089833736	3.197406586	A1-	CACTA-like transposase family (Tnp1/En/Spm)
AT3G42650	12.288477	-3.440434667	0.582305333	-5.908300119	3.46E-09	5.96E-08	0	0	0	5.545934233	4.508850015	2.857049598	A1+	CACTA-like transposase family (Tnp1/En/Spm)
AT3G42650	103.40095	-2.292793985	0.180088248	-12.73150253	3.95E-37	3.19E-34	0	0	0	6.764640597	7.903774937	8.104288802	A2+	CACTA-like transposase family (Tnp1/En/Spm)
AT5G28524	8.8468137	-3.462843375	0.577523605	-5.996020499	2.02E-09	3.65E-08	0	0	0	3.480233365	4.654502272	4.302754999	A1+	CACTA-like transposase family (Tnp1/En/Spm)
AT2G04770	3.5397797	-1.829871083	0.502459676	-3.641826741	0.00027071	0.002274869	0	0	0	1.757146478	3.546623725	3.197406586	A1-	CACTA-like transposase family (Tnp2/En/Spm)
AT1G35590	5.9050085	-2.923907162	0.58913953	-4.963013031	6.94E-07	8.54E-06	0	0	0	4.16453883	3.04536424	6.1371716	A1+	CACTA-like transposase family (Tnp2/En/Spm)
AT1G35590	33.347057	-1.822651038	0.178930744	-10.1863492	2.28E-24	1.03E-21	0	0	0	6.123990007	6.124155242	5.990660999	A2+	CACTA-like transposase family (Tnp2/En/Spm)
AT1G36200	10.453467	-3.602817924	0.574528961	-6.270907415	3.59E-10	7.12E-09	0	0	0	4.626795005	4.907957693	3.458449401	A1+	CACTA-like transposase family (Tnp2/En/Spm)
AT1G36200	69.313769	-2.057128667	0.179481312	-11.46152011	2.06E-30	1.27E-27	0	0	0	6.265396101	7.341066495	7.490414799	A2+	CACTA-like transposase family (Tnp2/En/Spm)
AT1G36470	7.6375554	-3.311198603	0.581098212	-6.98173792	1.21E-08	1.93E-07	0	0	0	3.480233365	4.164272639	4.302754999	A1+	CACTA-like transposase family (Tnp2/En/Spm)
AT1G36470	23.558115	-1.462888044	0.174597088	-8.37865088	5.35E-17	1.62E-14	0	0	0	5.4624789	5.715995759	5.575673072	A2+	CACTA-like transposase family (Tnp2/En/Spm)
AT1G49070	66.000713	-3.73890785	0.585140249	-6.389763575	1.66E-10	3.46E-09	0	0	0	5.051918249	7.491614392	7.538084162	A1+	CACTA-like transposase family (Tnp2/En/Spm)
AT1G49070	16.844641	-1.156916239	0.167333666	-6.9138283	4.72E-12	8.42E-10	0	0	0	5.284029613	5.100202951	4.945015614	A2+	CACTA-like transposase family (Tnp2/En/Spm)
AT1G50860	6.5491679	-3.063565776	0.586847602	-5.220385098	1.79E-07	2.42E-06	0	0	0	3.242825236	3.710677785	4.302754999	A1+	CACTA-like transposase family (Tnp2/En/Spm)
AT1G50860	18.24178	-1.228419184	0.169420087	-7.250729279	4.15E-13	8.29E-11	0	0	0	5.123451569	5.386165538	5.160701666	A2+	CACTA-like transposase family (Tnp2/En/Spm)
AT2G04770	526.65975	-3.990396274	0.584242153	-6.830038282	8.49E-12	2.08E-10	0	0	0	7				

AT2G12210	10.686503	-3.168434945	0.509569723	-6.217863424	5.04E-10	1.06E-08	0	0	0	3.222033331	5.26298084	4.277198875	A1-	CTACTA-like transposase family (Tnp2/En/Spm)
AT2G12260	8.2152549	-3.447059269	0.577419481	-5.969766147	2.38E-09	4.23E-08	0	0	0	3.862584211	3.955228997	4.474701533	A1+	CTACTA-like transposase family (Tnp2/En/Spm)
AT2G12260	25.46327	-1.540410341	0.175857278	-8.759434688	1.96E-18	6.61E-16	0	0	0	8.708773051	5.801843191	5.575673072	A2+	CTACTA-like transposase family (Tnp2/En/Spm)
AT2G12980	13.261685	-4.006133564	0.561661424	-7.132648594	9.85E-13	2.68E-11	0	0	0	5.192160237	4.907957693	3.998987077	A1+	CTACTA-like transposase family (Tnp2/En/Spm)
AT2G12980	30.121872	-1.557190015	0.175646514	-8.865476322	7.62E-19	2.60E-16	0	0	0	5.393724612	6.231180129	6.05674353	A2+	CTACTA-like transposase family (Tnp2/En/Spm)
AT2G13000	11.791175	-3.270020969	0.586068705	-5.579586391	2.41E-08	3.69E-07	0	0	0	5.192160237	5.019733684	2.247074573	A1+	CTACTA-like transposase family (Tnp2/En/Spm)
AT2G13000	26.070618	-1.240433856	0.168584301	-7.357944059	1.87E-13	4.01E-11	0	0	0	4.736096999	5.959583079	6.140393456	A2+	CTACTA-like transposase family (Tnp2/En/Spm)
AT3G29648	20.271226	-4.012294423	0.480776707	-8.345442627	7.09E-17	2.74E-15	0	0	0.588988589	4.408199229	6.024848039	5.239507661	A1-	CTACTA-like transposase family (Tnp2/En/Spm)
AT3G29648	128.17169	-6.769604743	0.468571617	-14.44732139	2.61E-47	5.87E-45	0	0	0.626414477	8.676251419	7.411902045	7.585764934	A1+	CTACTA-like transposase family (Tnp2/En/Spm)
AT3G29732	8.6586059	-2.743504569	0.573080947	-4.787289798	1.69E-06	1.94E-05	0	0	0	1.513627237	3.684038477	3.955228997	A1+	CTACTA-like transposase family (Tnp2/En/Spm)
AT3G29732	25.480887	-1.391868646	0.175051369	-7.951201135	1.85E-15	4.96E-13	0	0	0	2.03712832	5.4624789	5.88267912	A2+	CTACTA-like transposase family (Tnp2/En/Spm)
AT3G30393	57.626377	-5.531672528	0.492443844	-11.23310323	2.80E-29	2.54E-27	0.640148721	0.626414477	0	6.102903647	6.460522959	7.576354011	A1+	CTACTA-like transposase family (Tnp2/En/Spm)
AT3G30393	91.687573	-2.893087563	0.177483067	-16.30063987	9.77E-60	1.86E-56	0.954186367	0.940325156	0	7.599114199	7.610568916	7.339298824	A2+	CTACTA-like transposase family (Tnp2/En/Spm)
AT3G30837	152.96397	-6.874620299	0.386512414	-17.78628589	9.03E-71	3.51E-68	0	0	0	8.089333495	8.611075358	8.002302092	A1-	CTACTA-like transposase family (Tnp2/En/Spm)
AT3G30837	164.35786	-7.263472645	0.425415704	-17.07382352	2.32E-65	1.17E-62	0	0	0	8.47126108	7.994037884	8.563071869	A1+	CTACTA-like transposase family (Tnp2/En/Spm)
AT3G30837	9.2967141	-0.640539405	0.146230477	-4.380341354	1.18E-05	1.00E-03	0	0	0	3.862584211	4.558214482	3.798546962	A2+	CTACTA-like transposase family (Tnp2/En/Spm)
AT3G33151	19.11477	-3.253420275	0.495879456	-6.560909583	5.35E-11	1.26E-09	1.026048597	0.588988589	0	4.142578534	6.342337877	4.116544802	A1-	CTACTA-like transposase family (Tnp2/En/Spm)
AT3G33151	39.068335	-4.878310784	0.499530848	-9.765784843	1.58E-22	9.75E-21	1.082007379	0.626414477	0	6.921528684	6.200761211	5.356497891	A1+	CTACTA-like transposase family (Tnp2/En/Spm)
AT3G33151	7.9448211	-1.95267571	0.454605832	-4.29531601	1.74E-05	0.00257285	0.976967723	0.557947347	0	5.098259903	2.575486135	3.171895689	A2-	CTACTA-like transposase family (Tnp2/En/Spm)
AT3G42721	7.1876367	-3.271409496	0.581807801	-5.622835398	1.88E-08	2.92E-07	0	0	0	3.862584211	3.710677785	4.208433134	A1+	CTACTA-like transposase family (Tnp2/En/Spm)
AT3G42721	15.30039	-1.086407338	0.165067139	-6.581608836	4.65E-11	7.64E-09	0	0	0	5.080350208	5.006885355	4.848821471	A2+	CTACTA-like transposase family (Tnp2/En/Spm)
AT3G43128	15.403669	-3.966917784	0.488407911	-8.122124076	4.58E-16	1.66E-14	0	0	0	4.764642118	5.45092181	4.614569198	A1-	CTACTA-like transposase family (Tnp2/En/Spm)
AT3G43128	16.285657	-3.995756942	0.567041222	-7.046678064	1.83E-12	4.83E-11	0	0	0	5.953230919	4.508850015	3.998987077	A1+	CTACTA-like transposase family (Tnp2/En/Spm)
AT3G43128	62.563307	-1.726891457	0.176564437	-9.780516864	1.37E-22	5.67E-20	0	0	0	5.791275092	7.331476042	7.339298824	A2+	CTACTA-like transposase family (Tnp2/En/Spm)
AT4G03900	1.743681	-3.28011116	0.58131377	-5.642582941	1.68E-08	2.62E-07	0	0	0	3.862584211	3.955228997	3.998987077	A1+	CTACTA-like transposase family (Tnp2/En/Spm)
AT4G03900	22.350659	-1.421169185	0.173866903	-8.173891421	2.99E-16	8.73E-14	0	0	0	5.495665116	5.592957866	5.450160215	A2+	CTACTA-like transposase family (Tnp2/En/Spm)
AT4G04270	15.113198	-3.602476795	0.501248032	-7.187014348	6.62E-13	1.84E-11	0	0	0	4.700053001	5.766238278	3.728967903	A1-	CTACTA-like transposase family (Tnp2/En/Spm)
AT4G06588	9.3981764	-2.919275487	0.50075703	-5.829724426	5.55E-09	1.04E-07	0.602380384	0.653468127	0	3.933736191	4.792504907	3.935732613	A1-	CTACTA-like transposase family (Tnp2/En/Spm)
AT4G06650	9.5049098	-3.378279529	0.58136571	-5.810937025	6.21E-09	1.03E-07	0	0	0	2.958502988	4.907957693	4.474701533	A1+	CTACTA-like transposase family (Tnp2/En/Spm)
AT4G08016	88.191431	-3.679891125	0.585287394	-6.287323391	3.23E-10	6.44E-09	0	0	0.694589061	5.545934233	7.411902045	2.96985525	A1+	CTACTA-like transposase family (Tnp2/En/Spm)
AT4G08016	14.012222	-0.91272927	0.159267496	-5.730794833	1.00E-08	1.28E-06	0	0	1.024858076	4.990080801	5.144691693	4.238940698	A2+	CTACTA-like transposase family (Tnp2/En/Spm)
AT4G08092	5.6899211	-2.844170036	0.590101718	-4.819796228	1.44E-06	1.67E-05	0	0	0	3.242825326	4.164272639	3.284432598	A1+	CTACTA-like transposase family (Tnp2/En/Spm)
AT4G08092	7.2269196	-0.581925538	0.137384869	-4.235732391	2.28E-05	0.001792876	0	0	0	4.283065666	3.903537434	3.576267804	A2+	CTACTA-like transposase family (Tnp2/En/Spm)
AT5G28165	9.3588743	-2.822871836	0.498420189	-5.665363632	1.48E-08	2.64E-07	0.602380384	0.588988589	0.653468127	3.549829232	4.483532941	4.553113256	A1-	CTACTA-like transposase family (Tnp2/En/Spm)
AT5G28165	345.54808	-6.624176079	0.506477022	-13.07892717	4.35E-39	6.81E-37	0.640148721	0.626414477	0.694589061	6.448866468	9.982907884	9.929657968	A1+	CTACTA-like transposase family (Tnp2/En/Spm)
AT5G28165	50.188723	-2.092500831	0.180244527	-11.60923369	3.70E-31	2.40E-28	0.954186367	0.940325156	1.024858076	6.651401798	6.909786619	6.330479789	A2+	CTACTA-like transposase family (Tnp2/En/Spm)
AT5G28926	5.326641	-2.770383105	0.591131274	-4.686578474	2.78E-06	3.10E-05	0	0	0	3.242825326	3.04536424	4.107506639	A1+	CTACTA-like transposase family (Tnp2/En/Spm)
AT5G28926	22.188125	-1.374081989	0.172777199	-7.95291277	1.82E-15	4.94E-13	0	0	0	7.36801232	5.493263672	5.238690264	A2+	CTACTA-like transposase family (Tnp2/En/Spm)
AT5G32825	22.489426	-2.887557775	0.589965609	-4.894451019	9.86E-07	1.18E-05	0.640148721	0.694589061	0	6.200761211	5.958938819	A1+	CTACTA-like transposase family (Tnp2/En/Spm)	
AT5G45085	5.7702011	-2.832287813	0.590626951	-4.795392101	1.62E-06	1.87E-05	0	0	0	3.862584211	2.545235219	4.107506639	A1+	CTACTA-like transposase family (Tnp2/En/Spm)
AT5G45085	17.929745	-1.180824765	0.167928345	-7.031717995	2.04E-12	3.82E-10	0	0	0	5.358078375	5.348623431	4.848821471	A2+	CTACTA-like transposase family (Tnp2/En/Spm)
AT1G40075	19.843255	-3.393708314	0.576466999	-5.887081687	3.93E-09	6.72E-08	0.640148721	0.626414477	0	2.133098153	5.625572377	6.070397959	A1+	CTACTA-like transposase family, putative
AT2G06790	8.0943842	-3.42089319	0.578277347	-5.915661765	3.31E-09	5.73E-08	0	0	0	4.021446993	3.710677785	4.474701533	A1+	CTACTA-like transposase family, putative
AT2G06790	21.797464	-1.397860822	0.173413399	-8.060582	7.58E-16	2.10E-13	0	0	0	5.559831633	5.422755442	5.450160215	A2+	CTACTA-like transposase family, putative
AT2G10480	6.7244493	-3.155970598	0.584605189	-5.398464908	6.72E-08	9.68E-07	0	0	0	4.16453883	3.416037926	3.881635851	A1+	CTACTA-like transposase family, putative
AT2G10480	21.546898	-1.359020996	0.172507351	-7.878046887	3.33E-15	8.76E-13	0	0	0	5.393724612	5.686205962	5.276158547	A2+	CTACTA-like transposase family, putative
AT5G30470	14.705658	-2.999256133	0.511971436	-5.858248967	4.68E-09	8.94E-08	0	0	0.588988589	2.192330878	5.046836798	5.730732322	A1-	CTACTA-like transposase family, putative
AT5G32103	17.644358	-3.099206531	0.583577188	-5.310705413	1.09E-07	1.53E-06	0.626414477	0.694589061	1.429370861	5.883728226	5.522504977	A1+	CTACTA-like transposase family, putative	
AT5G32103	8.7951814	-0.603842885	0.143833593	-4.198204818	2.69E-05	2.10E-03	0	0.940325156	1.024858076	4.49483273	4.345992327	3.450808994	A2+	CTACTA-like transposase family, putative
AT1G30180	10.707436	2.950244534	0.575387679	5.12740304	2.94E-07	3.84E-06	4.056385374	4.898080211	4.377786483	0	0	A1+	copia-like retrotransposon family (Ty1_Copia-element)	
AT1G34967	12.688541	-3.393419248	0.574526263	-5.906464973	3.50E-09	6.02E-08	0.640148721	0	0	3.242825326	5.625572377	4.302754999	A1+	copia-like retrotransposon family (Ty1_Copia-element)
AT1G47650	26.054403	-3.983552009	0.5745362	-6.93350917	4.11E-12	1.04E-10	0	0	0	2.600442178	6.200761211	6.316345691	A1+	copia-like retrotransposon family (Ty1_Copia-element)
AT2G06930	15.459839	-3.956776392	0.488990688	-8.091721353	5.88E-16	2.11E-14	0	0	0	4.88574345	5.45092181	4.488922482	A1-	copia-like retrotransposon family (Ty1_Copia-element)
AT2G07400	106.37065	-6.720861493	0.407200101	-16.50505851	3.37E-61	8.58E-59	0	0	0	7.633460012	7.915397839	7.652776989	A1-	copia-like retrotransposon family (Ty1_Copia-element)
AT2G07400	10.943769	-0.745359222	0.148646259	-5.014315394	5.32E-07	5.73E-05	0	0	0	4.427639234	5.054298527	3.798546962	A2+	copia-like retrotransposon family (Ty1_Copia-element)
AT2G07550	16.459169	-3.182614602	0.471510581	-6.749826471	1.48E-11	3.67E-10	1.026048597	0.588988589	1.718867729	5.050236022	3.546623725	5.730732322	A1-	copia-like retrotransposon family (Ty1_Copia-element)
AT2G09830	38.188946	-5.158340814	0.439752208	-11.7310782	8.93E-32	7.91E-30	0	0	0.588988589	6.313781463	6.520816798	5.913005388	A1-	copia-like retrotransposon family (Ty1_Copia-element)
AT2G11950	12.15926	-3.541845688	0.50052889	-7.076206304	1.48E-12	4.01E-11	0	0	0	4.408199229	5.26298084	4.028969492	A1-	copia-like retrotransposon family (Ty1_Copia-element)
AT2G11950	12.421397	-3.93103733	0.563445371	-6.978465206	3.02E-12	7.75E-11	0	0	0	4.524364692	5.220242777	4.107506639	A1+	copia-like retrotransposon family (Ty1_Copia-element)
AT2G13930	7.1135987	-3.234881943	0.582892949	-5.549701615	2.86E-08	4.34E-07	0	0	0	3.684038477	3.710677785	4.302754999	A1+	copia-like retrotransposon family (Ty1_Copia-element)
AT2G16000	8.3866167	-2.996237966	0.507965279	-5.898509389	3.67E-09	7.10E-08	0	0	0.653468127	4.700053				

AT4G05510	17.338996	-2.961154516	0.58669667	-5.047164351	4.48E-07	5.68E-06	0	0	1.161466416	6.391824885	2.545235219	3.998987077	A1+	hAT-like transposase family (hobo/Ac/Tam3)
AT5G35608	14.992602	-3.709583606	0.491722639	-7.544056981	4.56E-14	1.40E-12	0	0.588988589	0	4.324976877	4.483532941	5.644966461	A1-	hAT-like transposase family (hobo/Ac/Tam3)
AT5G35608	9.675927	-2.335743457	0.592094168	-3.945184935	7.97E-05	6.50E-04	0	0.626414477	0	0	5.220242777	4.474701533	A1+	hAT-like transposase family (hobo/Ac/Tam3)
AT5G34853	153.53888	5.968867259	0.437787363	13.63416984	2.51E-42	4.57E-40	8.264962839	8.322675221	8.197286765	1.429370861	0	1.169324837	A1+	MUG8 MUSTANG 8 Encodes a member of a domesticated transposable element gene family MUSTANG. Members of this family are derived from transposable elements genes but gained function in plant fitness and flower development.
AT5G34853	142.97172	5.682772746	0.395418489	14.3715403	7.81E-47	1.31E-44	8.15735959	8.214127808	8.087478402	0	2.665086523	1.015522753	A1-	MUG8 MUSTANG 8 Encodes a member of a domesticated transposable element gene family MUSTANG. Members of this family are derived from transposable elements genes but gained function in plant fitness and flower development.
AT1G35995	91.851902	-4.959512262	0.548113449	-9.048331642	1.45E-19	7.16E-18	0.640148721	0.626414477	0	4.021446993	7.804153723	8.291244604	A1+	Mutator-like transposase family
AT1G36085	49.625928	-5.646815497	0.439173117	-12.85783504	7.77E-38	8.95E-36	0	0	0	6.976880928	6.602405842	6.27840572	A1-	Mutator-like transposase family
AT1G36085	34.007737	-4.661094974	0.553914113	-8.414833395	3.93E-17	1.58E-15	0	0	0	3.862584211	6.574739482	6.602556983	A1+	Mutator-like transposase family
AT1G36085	8.1353733	-0.629098155	0.141020618	-4.461036734	8.16E-06	7.09E-04	0	0	0	3.841804147	4.558214482	3.798546962	A2+	Mutator-like transposase family
AT1G67240	31.615309	-4.602968984	0.451819474	-10.18762857	2.25E-24	1.38E-22	0	0.588988589	0.653468127	5.197878395	6.434335581	6.096513381	A1-	Mutator-like transposase family
AT1G67240	107.03716	-6.768719782	0.430596338	-15.7194086	1.11E-55	3.72E-53	0	0.626414477	0.694589061	7.766472101	7.656330959	7.811101638	A1+	Mutator-like transposase family
AT1G78350	12.29228	-3.47916684	0.581207105	-5.986105141	2.15E-09	3.86E-08	0	0	0	2.604042178	5.310931324	4.953150701	A1+	Mutator-like transposase family
AT2G04310	3.4131603	-1.739923964	0.506683336	-3.443947475	0.000594859	0.004577994	0	0.653468127	3.549829232	0	3.349749908	0	A1-	Mutator-like transposase family
AT2G04310	7.7077301	-3.12666905	0.574639721	-5.441094546	5.30E-08	7.73E-07	0	0.694589061	4.29471016	3.955228997	3.753887089	0	A1+	Mutator-like transposase family
AT2G10955	8.0244078	-2.849751817	0.513567718	-5.548930977	2.87E-08	4.95E-07	0	0	0.933736191	4.792504907	3.027056186	0	A1-	Mutator-like transposase family
AT2G12066	5.6093716	-2.646170685	0.514931481	-5.13887922	2.76E-07	4.15E-06	0	0	0	3.549829232	3.546623725	3.728967903	A1-	Mutator-like transposase family
AT2G12066	11.951183	-3.985727034	0.560199794	-7.114831312	1.12E-12	3.04E-11	0	0	0	4.896561069	4.654502272	4.302754999	A1+	Mutator-like transposase family
AT2G14570	14.413079	-3.967855322	0.490756604	-8.085179671	6.21E-16	2.23E-14	0	0	0	4.88574345	4.089833736	5.422470072	A1-	Mutator-like transposase family
AT2G15810	235.69625	-3.593904352	0.460319443	-7.807413763	5.84E-15	1.93E-13	3.632364657	4.596507354	2.622111348	8.41524017	9.408365814	8.477875946	A1-	Mutator-like transposase family
AT2G15810	195.45686	-2.037843098	0.178820971	-11.39599614	4.38E-30	2.53E-27	4.434608628	5.435368285	3.366368779	8.508637534	8.779035457	8.228948531	A2+	Mutator-like transposase family
AT2G23500	8.4635139	-3.030670364	0.507439309	-5.972478496	2.34E-09	4.65E-08	0.602380384	0	0	4.486881573	2.665086523	4.614569198	A1-	Mutator-like transposase family
AT2G23500	17.546855	-4.220446014	0.539899999	-7.81708839	5.41E-15	1.82E-13	0.640148721	0	0	5.694845984	5.019733684	4.553554369	A1+	Mutator-like transposase family
AT2G23720	57.503249	-5.861067596	0.43287616	-13.53982532	9.10E-42	1.28E-39	0	0	0	7.191775937	6.752923424	6.554110094	A1-	Mutator-like transposase family
AT2G23720	42.350222	-4.916868193	0.547707692	-8.977175714	2.78E-19	1.35E-17	0	0	0	4.16453883	6.900955033	6.902810395	A1+	Mutator-like transposase family
AT2G23720	10.593724	-0.732977749	0.147916142	-4.955360098	7.22E-07	7.62E-05	0	0	0	4.357162671	5.006885535	3.798546962	A2+	Mutator-like transposase family
AT3G29695	7.7527356	-3.283500097	0.582044031	-5.641325954	1.69E-08	2.64E-07	0	0	0	4.524364692	3.955228997	3.458449401	A1+	Mutator-like transposase family
AT3G30170	63.288777	-5.83354758	0.407020908	-14.33183075	1.38E-46	2.26E-44	0.602380384	0	0.653468127	7.094620947	6.822675636	7.041870662	A1-	Mutator-like transposase family
AT3G30170	266.52839	-7.923117705	0.409314352	-19.35704836	1.78E-83	1.83E-80	0.640148721	0	0.694589061	9.293513457	8.862188413	8.989025613	A1+	Mutator-like transposase family
AT3G30170	10.99374	-0.789868942	0.15563994	-5.07497587	3.88E-07	4.26E-05	0.954186367	0	0	1.024858076	4.357162671	4.622542481	A2+	Mutator-like transposase family
AT3G30585	9.0123459	-2.523056502	0.512671502	-4.921390195	8.59E-07	1.20E-05	0	0	1.101575979	2.526213436	4.792504907	4.488922482	A1-	Mutator-like transposase family
AT3G31450	9.6752956	-3.440287115	0.503022467	-6.839231522	7.96E-12	2.01E-10	0	0	0	4.56149373	4.089833736	4.351279944	A1-	Mutator-like transposase family
AT3G31450	11.353188	-3.918886544	0.562588601	-6.968122004	3.27E-12	8.36E-11	0	0	0	4.896561069	4.346824447	4.391288416	A1+	Mutator-like transposase family
AT3G31909	4.2081117	-2.276156301	0.513492359	-4.432697506	9.31E-06	0.000108125	0	0	0	3.549829232	2.665086523	3.349749908	A1-	Mutator-like transposase family
AT3G31909	9.8212406	-3.737566177	0.568165378	-6.57830681	4.76E-11	1.07E-09	0	0	0	4.524364692	4.164272639	4.391288416	A1+	Mutator-like transposase family
AT3G33160	16.8562	-4.239368177	0.480029045	-8.831482632	1.03E-18	4.46E-17	0	0	0	5.101147555	5.046836798	5.199956346	A1-	Mutator-like transposase family
AT3G33160	14.970133	-2.962665316	0.5914331	-5.009316919	5.46E-07	6.83E-06	0	0	0	6.205775127	3.955228997	1.806583236	A1+	Mutator-like transposase family
AT3G33377	13.009203	-2.586841509	0.514964739	-5.023337161	5.08E-07	7.32E-06	0	0.588988589	0	3.222033331	6.024848039	2.610741738	A1+	Mutator-like transposase family
AT3G33377	7.3865274	-2.949480582	0.581485841	-5.072317109	3.93E-07	5.02E-06	0	0.626414477	0	4.16453883	4.346824447	3.086509522	A1+	Mutator-like transposase family
AT3G33377	12.293117	-2.612679333	0.454984527	-5.742347656	9.34E-09	2.75E-07	0	0.557947347	0	5.669115043	4.132225326	2.975939682	A2-	Mutator-like transposase family
AT3G34299	11.948489	-2.484710571	0.515138235	-4.823386036	1.41E-06	1.90E-05	0	0.588988589	0	3.222033331	5.901330042	2.346684959	A1-	Mutator-like transposase family
AT3G34299	7.3865274	-2.949480582	0.581485841	-5.072317109	3.93E-07	5.02E-06	0	0.626414477	0	4.16453883	4.346824447	3.086509522	A1+	Mutator-like transposase family
AT3G34299	11.600292	-2.608031273	0.454931814	-5.732795974	9.88E-09	2.90E-07	0	0.557947347	0	5.46159418	4.132225326	2.975939682	A2-	Mutator-like transposase family
AT3G42353	7.5913909	-3.282026226	0.58173424	-5.641796549	1.68E-08	2.63E-07	0	0	0	4.29471016	4.164272639	3.458449401	A1+	Mutator-like transposase pseudogene
AT3G42535	13.408283	-3.356230711	0.480371276	-6.98674313	2.81E-12	7.44E-11	1.026048597	0	0.653468127	4.826463083	5.046836798	4.351279944	A1-	Mutator-like transposase family
AT3G42712	8.2910246	-2.612577323	0.511429145	-5.10838568	3.25E-07	4.83E-06	1.026048597	0	0	3.025182302	4.089833736	4.730144422	A1-	Mutator-like transposase family
AT3G42712	9.9485221	-2.397130215	0.592111981	-4.048440654	5.16E-05	0.000438124	1.082007379	0	0	5.597298362	1.773370384	3.284432598	A1+	Mutator-like transposase family
AT4G08720	19.037686	-4.120162341	0.463580406	-8.887697342	6.24E-19	2.73E-17	0	1.006034927	0	5.331804227	5.046836798	5.422470072	A1+	Mutator-like transposase family
AT4G08720	27.145615	-4.801278484	0.497132701	-9.657941383	4.55E-22	2.68E-20	0	1.061739724	0	5.492673666	6.050935773	5.740406713	A1+	Mutator-like transposase family
AT4G09380	56.794203	-5.579024584	0.419305522	-13.3053926	2.15E-40	2.79E-38	0.602380384	0.588988589	0	7.179983389	6.752923424	6.489964658	A1+	Mutator-like transposase family
AT4G09380	44.099436	-4.776702752	0.531430563	-8.988385465	2.51E-19	1.22E-17	0.640148721	0.626414477	0	4.14102287	6.985988276	6.887671894	A1+	Mutator-like transposase family
AT4G09380	12.8135	-0.795447079	0.154833346	-5.137440355	2.79E-07	3.10E-05	0.954186367	0.940325156	0	4.620502376	5.2297536	3.991107087	A2+	Mutator-like transposase family
AT4G28970	226.58394	-7.665271537	0.389249245	-19.69245064	2.50E-86	1.69E-83	0	0	0	9.061194775	8.778397788	8.60444726	A1-	Mutator-like transposase family
AT4G28970	118.31291	-2.889032433	0.592383427	-4.876963634	1.08E-06	1.28E-05	0	0	0	5.257479592	8.497288844	8.291244604	A1+	Mutator-like transposase family
AT4G28970	26.527676	-1.357364529	0.171771549	-7.902149906	2.74E-15	7.29E-13	0	0	0	5.358078375	6.311427547	5.38305632	A2+	Mutator-like transposase family

AT2G12910	28.40033	-4.326288441	0.479987987	-9.013326491	2.00E-19	8.99E-18	0	0.588988589	0	4.700053001	5.45092181	6.688789219	A1-	transposable element gene.
AT2G12910	11.512156	-3.32404621	0.576139035	-5.769969437	7.93E-09	1.30E-07	0	0.626414477	0	5.492673666	3.955228997	3.458449401	A1+	transposable element gene.
AT2G13040	40.948059	-5.31259129	0.525965801	-10.10064016	5.49E-24	3.76E-22	0	0	0	5.051918249	6.871459168	6.620982316	A1+	transposable element gene.
AT2G13040	12.308112	-0.587477064	0.136775743	-4.295184606	1.75E-05	1.41E-03	0	0	0	2.61591609	5.422755442	4.798207118	A2+	transposable element gene.
AT2G13050	123.0577	-6.871474786	0.47835284	-14.36486671	8.60E-47	1.84E-44	0	0	0	7.110161548	8.525969037	7.873905475	A1+	transposable element gene.
AT2G13050	36.009216	-1.188526447	0.166164911	-7.152692088	8.51E-13	1.64E-10	0	0	0	4.620502376	6.687245722	6.514177692	A2+	transposable element gene.
AT2G13070	5.4545384	-2.574391168	0.592372442	-4.345899617	1.39E-05	1.34E-04	0	0	0	2.133098153	4.346824447	3.458449401	A1+	transposable element gene.
AT2G13320	7.4012508	-2.72383927	0.514524097	-5.293900298	1.20E-07	1.90E-06	0	0	0	3.395221171	4.792504907	3.197406586	A1-	transposable element gene.
AT2G13320	23.025959	-4.94214413	0.552041589	-8.141079411	3.92E-16	1.45E-14	0	0	0	4.021446993	5.941644221	5.987621232	A1+	transposable element gene.
AT2G13400	55.764733	-5.809485694	0.432258619	-13.43983774	3.53E-41	4.75E-39	0	0	0	6.51492659	7.128344859	6.731026182	A1-	transposable element gene.
AT2G13400	99.295915	-6.80844549	0.470753584	-14.46286492	2.08E-47	4.77E-45	0	0	0	7.074356635	7.865285288	7.850673244	A1+	transposable element gene.
AT2G13431	54.83296	-4.290799772	0.350276573	-12.24974806	1.69E-34	1.67E-32	2.744250341	1.329166983	1.950365559	6.907064143	6.434335581	6.850788829	A1-	transposable element gene.
AT2G13431	45.382614	-3.992261146	0.383999102	-10.39653771	2.57E-25	1.89E-23	2.836608464	1.395704924	2.032847348	6.503738247	6.610886935	6.246861259	A1+	transposable element gene.
AT2G14240	37.946883	-5.34899425	0.498177694	-10.73893811	6.68E-27	5.35E-25	0	0.626414477	0	6.704468582	6.152527787	5.773726325	A1+	transposable element gene.
AT2G14240	9.599877	-0.733097528	0.150475996	-4.871858107	1.11E-06	0.000114429	0	0.940325156	0	4.283065666	4.345992327	4.312916238	A2+	transposable element gene.
AT2G14730	112.49597	-6.804677446	0.405644055	-16.77499609	3.72E-63	1.06E-60	0	0	0	7.936517773	7.850087419	7.660082573	A1-	transposable element gene.
AT2G14730	75.108723	-6.296267267	0.491240499	-12.81707692	1.32E-37	1.87E-35	0	0	0	7.864068852	6.810594236	6.760480718	A1+	transposable element gene.
AT2G14730	10.756258	-0.697484795	0.145429707	-4.796026948	1.62E-06	1.61E-04	0	0	0	3.618975234	5.144691693	4.312916238	A2+	transposable element gene.
AT2G15550	10.091431	-2.90583615	0.513674112	-5.65669437	1.54E-08	2.74E-07	0	0	0	5.26213436	5.26298084	4.277198875	A1-	transposable element gene.
AT2G15800	58.321516	-3.217801576	0.41145667	-7.82051139	5.26E-15	1.74E-13	3.133118363	3.098095738	1.950365559	5.831289127	7.709866036	6.096513381	A1-	transposable element gene.
AT2G15800	58.533188	-3.470068077	0.415514291	-8.351260476	6.75E-17	2.65E-15	3.22917984	3.194694488	2.032847348	7.468440023	5.883728226	6.620982316	A1+	transposable element gene.
AT2G15815	7.4659887	-3.014141415	0.579289591	-5.203201306	1.96E-07	2.64E-06	0	0.694589061	4.524364692	3.416037926	3.753887089	A1+	transposable element gene.	
AT2G22710	22.225542	-2.757169608	0.393351051	-7.009437506	2.39E-12	6.36E-11	2.50181502	2.469293851	1.718867729	5.331804227	5.45092181	5.352044354	A1+	transposable element gene.
AT2G22710	25.257901	-2.599575319	0.509962821	-5.097578125	3.44E-07	4.43E-06	2.591298417	2.559127732	1.796470461	6.582320762	4.346824447	4.699400813	A1+	transposable element gene.
AT2G23480	10.992653	-3.44493078	0.494289296	-6.969335735	3.18E-12	8.36E-11	0.602380384	0	0	4.56149373	4.483532941	4.488922482	A0-	transposable element gene.
AT2G23480	15.000007	-4.043426221	0.543909359	-7.434004744	1.05E-13	3.14E-12	0.640148721	0	0	4.812122267	5.396254736	4.474701533	A1+	transposable element gene.
AT2G23710	6.0183011	-2.534992023	0.592357662	-4.279495626	1.87E-05	1.76E-04	0	0	0	1.429370861	4.164272639	4.208431314	A1+	transposable element gene.
AT3G15310	10.513018	2.708416882	0.505231993	5.36073906	8.29E-08	1.35E-06	4.048461583	4.470931021	4.773757176	0	0	0	A1-	transposable element gene.
AT3G15310	13.408933	1.852320008	0.507406939	3.650561052	2.62E-04	1.87E-03	4.150128613	4.575093957	4.880072038	2.604042178	2.545235219	1.806583236	A1+	transposable element gene.
AT3G15310	10.589572	1.866057273	0.443390218	4.2086111726	2.57E-05	0.000363659	3.956508363	4.380679	4.68533847	0	2.106732017	1.100718415	A2-	transposable element gene.
AT3G29610	4.8031839	-2.426966544	0.514764409	-4.714713179	2.42E-06	3.11E-05	0	0	0	3.933736191	2.665086523	3.349749908	A1-	transposable element gene.
AT3G29610	8.692379	-3.553974273	0.573922037	-6.19243389	9.92E-10	1.14E-08	0	0	0	4.021446993	4.164272639	4.391288416	A1+	transposable element gene.
AT3G29612	51.274592	-5.587478956	0.425829895	-13.12138724	2.48E-39	3.07E-37	0	0.588988589	0	6.605874948	6.952811471	6.473472544	A1-	transposable element gene.
AT3G29612	56.301741	-5.900255931	0.479992503	-12.29412004	9.74E-35	1.21E-32	0	0.626414477	0	6.238497703	7.117439888	6.976208025	A1+	transposable element gene.
AT3G29700	20.115936	-4.494001114	0.472834688	-9.504381184	2.01E-21	1.03E-19	0	0	0	5.637955601	5.046836798	5.352044354	A1-	transposable element gene.
AT3G29700	34.89875	-5.508519685	0.505533096	-10.89645709	1.20E-27	9.93E-26	0	0	0	6.066915882	6.420348952	5.899804421	A1+	transposable element gene.
AT3G29710	5.2433163	-2.505605853	0.589892049	-4.247566749	2.16E-05	0.000199965	0	0.626414477	0	3.480233365	3.955228997	2.857049598	A1+	transposable element gene.
AT3G29738	7.7461279	-3.011180944	0.511590391	-5.885921625	3.96E-09	7.63E-08	0	0	0	4.408199229	4.089833736	3.487531741	A1-	transposable element gene.
AT3G29738	12.642058	-3.941544236	0.564727092	-6.979555774	2.96E-12	7.61E-11	0	0	0	4.896561069	3.710677785	5.168874549	A1+	transposable element gene.
AT3G30360	7.9309221	-2.77319341	0.51455778	-5.397487807	6.76E-08	1.11E-06	0	0	0	2.526213436	4.483532941	4.488922482	A1-	transposable element gene.
AT3G30665	3.9645793	-2.098246477	0.510802781	-4.107742865	4.00E-05	0.000409246	0	0	0	2.797162804	3.546623725	3.027056186	A1-	transposable element gene.
AT3G30665	25.231159	-5.102905165	0.518769925	-9.836547797	7.84E-23	4.90E-21	0	0	0	5.545934233	5.760416915	5.740406713	A1+	transposable element gene.
AT3G30670	34.929758	-5.176798218	0.527826146	-9.807771478	1.04E-22	6.50E-21	0	0	0	4.976329861	6.646150789	6.38878277	A1+	transposable element gene.
AT3G30690	9.2895755	-3.318079765	0.505436017	-6.564786946	5.21E-11	1.23E-09	0	0	0	4.324976877	4.483532941	4.028969492	A1-	transposable element gene.
AT3G30690	8.9017759	-2.901552641	0.591048155	-4.909164536	9.15E-07	1.10E-05	0	0	0	5.257479592	1.773370384	3.881635851	A1+	transposable element gene.
AT3G30700	10.140938	-3.479510551	0.501681166	-6.935700975	4.04E-12	1.05E-10	0	0	0	4.324976877	4.483532941	4.42174209	A1-	transposable element gene.
AT3G30700	7.0882809	-2.506210132	0.592168505	-4.232258402	2.31E-05	2.13E-04	0	0	0	5.123742659	1.773370384	2.857049598	A1+	transposable element gene.
AT3G31310	36.359973	-5.326646946	0.445419046	-11.95873189	5.84E-33	5.44E-31	0	0	0	6.269953976	6.13861985	6.200380869	A1-	transposable element gene.
AT3G31440	4.0356306	-1.822876781	0.513454492	-3.550220731	0.000384908	0.003107451	0	1.006034927	0	3.549829232	2.665086523	3.027056186	A1-	transposable element gene.
AT3G31440	11.318674	-3.463667004	0.553352476	-6.259422623	3.86E-10	7.61E-09	0	0	0	4.021446993	4.786788781	4.699400813	A1+	transposable element gene.
AT3G31540	46.894253	-5.42176299	0.449146254	-12.07126397	1.50E-33	1.41E-31	0	0	0	5.800812964	6.822675636	6.850788829	A1-	transposable element gene.
AT3G31540	115.2923	-7.070074629	0.460817165	-15.34247237	3.98E-53	1.25E-50	0	0	0	8.191040906	7.673523812	7.631920166	A1+	transposable element gene.
AT3G31540	10.472742	-0.805245632	0.152565408	-5.278035443	1.31E-07	1.49E-05	0	0	0	4.679457118	4.345992327	4.312916238	A2+	transposable element gene.
AT3G31915	5.5012543	-2.588698221	0.592378764	-4.370005103	1.24E-05	1.21E-04	0	0	0	3.684038477	1.773370384	4.302754999	A1+	transposable element gene.
AT3G31955	7.3489814	-3.277026102	0.581979767	-5.630824795	1.79E-08	2.79E-07	0	0	0	4.16453883	3.416037926	4.208431314	A1+	transposable element gene.
AT3G32070	22.91236	-4.618160718	0.467867982	-9.870649189	5.58E-23	3.14E-21	0	0	0	5.530616574	5.766238278	5.315498883	A1-	transposable element gene.
AT3G32070	36.967923	-5.584574785	0.50305424	-11.10133728	1.24E-28	1.11E-26	0	0	0	6.172293093	6.499608502	5.958938819	A1+	transposable element gene.
AT3G32897	10.430213	-3.185607688	0.508740468	-6.261754055	3.81E-10	8.14E-09	0	0	0	3.689460601	5.26298084	3.83605124	A1-	transposable element gene.
AT3G32897	14.512702	-1.005376193	0.161867526	-6.21110495	5.26E-10	7.57E-08	0	0	0	4.843112829	5.2297536	4.575871343	A2+	transposable element gene.
AT3G32966	129.24947	-6.67245426	0.476103628	-14.01470997	1.27E-44	2.45E-42	0.640148721	0	0	6.838581092	8.323028526	8.423088959	A1+	transposable element gene.
AT3G32966	6.522717	-0.520915554	0.135207336	-3.852716634	1.17E-04	0.008029416	0.954186367	0	0	3.734687502	3.903537434	3.691684035	A2+	transposable element gene.
AT3G33072	406.86385	-6.748503357	0.452824486	-14.9031326	3.14E-50	5.85E-48	0	0	0	8.957944187	10.28907469	9.442346388	A1-	transposable element gene.

AT5G30852	20.374557	-4.255527317	0.481951325	-8.829786537	1.05E-18	4.52E-17	0	0	0	4.56149373	5.901330042	5.387686903	A1-	transposable element gene.
AT5G31302	14.217857	-3.93807026	0.489184408	-8.050148297	8.27E-16	2.95E-14	0	0	0	4.94268382	5.046836798	4.614569198	A1-	transposable element gene.
AT5G31302	6.154328	-2.555797231	0.592380694	-4.314450586	1.60E-05	0.000125499	0	0	0	4.812122267	2.545235219	2.58406216	A1+	transposable element gene.
AT5G32107	136.35825	-6.783069573	0.385305431	-17.60439649	2.28E-69	8.61E-67	0	0	0.588988589	0.653468127	7.857284392	8.328940593	A1-	transposable element gene.
AT5G32107	66.2424	-5.537367429	0.50027827	-11.06857476	1.78E-28	1.56E-26	0	0	0.626414477	0.694589061	6.175565832	6.420348952	A1+	transposable element gene.
AT5G32107	23.449132	-1.361568254	0.173942021	-7.827713204	4.97E-15	1.28E-12	0	0	0.940325156	1.024858076	5.590875464	5.801843191	A2+	transposable element gene.
AT5G32228	108.72814	-6.745192619	0.407087983	-16.56937298	1.16E-61	3.07E-59	0	0	0	7.571623371	7.915397839	7.80552781	A1-	transposable element gene.
AT5G32228	63.985227	-5.896961252	0.509395484	-11.57639091	5.43E-31	5.43E-29	0	0	0	7.799743361	6.420348952	6.293554041	A1+	transposable element gene.
AT5G32228	20.051301	-1.241839337	0.169490971	-7.32687604	2.36E-13	4.97E-11	0	0	0	5.358078375	5.686205962	4.945015614	A2+	transposable element gene.
AT5G32241	13.284003	-3.797216667	0.493645304	-7.692196474	1.45E-14	4.65E-13	0	0	0	4.324976877	5.046836798	4.887807353	A1-	transposable element gene.
AT5G32312	5.2578319	-2.571805006	0.515140281	-4.992436235	5.96E-07	8.52E-06	0	0	0	3.689460601	2.665086523	3.935732613	A1-	transposable element gene.
AT5G32312	2.5728345	-1.827535357	0.579444091	-3.153945974	1.61E-03	0.009108675	0	0	0	2.958502598	1.773370384	2.857049598	A1+	transposable element gene.
AT5G32405	6.5580989	-2.616643183	0.51271005	-5.103553525	3.33E-07	4.94E-06	0.602380384	0	0	3.395221171	4.089833736	3.83605124	A1-	transposable element gene.
AT5G32405	4.0497877	-2.207408884	0.592357433	-3.726481281	1.94E-04	0.001432921	0.640148721	0	0	3.480233365	2.545235219	3.284432598	A1+	transposable element gene.
AT5G32420	7.6337885	-3.06712195	0.510344292	-6.009907424	1.86E-09	3.73E-08	0	0	0	4.041933031	4.089833736	3.935732613	A1-	transposable element gene.
AT5G32420	8.2367697	-3.102718818	0.587534802	-5.280910688	1.29E-07	1.78E-06	0	0	0	5.051918249	3.04536424	3.458449401	A1+	transposable element gene.
AT5G32434	6.2325286	-2.790469563	0.514061604	-5.428278518	5.69E-08	9.45E-07	0	0	0	4.041933031	3.546623725	3.613294506	A1-	transposable element gene.
AT5G32434	6.4150285	-3.090381946	0.585948754	-5.274150558	1.33E-07	1.85E-06	0	0	0	3.480233365	3.710677785	4.107506639	A1+	transposable element gene.
AT5G32473	17.044129	-3.986981473	0.48918138	-8.150313226	3.63E-16	1.33E-14	0	0	0	4.408199239	5.766238278	4.887807353	A1-	transposable element gene.
AT5G32473	9.922484	-3.6599421	0.571870212	-6.399952332	1.55E-10	3.25E-09	0	0	0	4.896561069	3.955228997	4.107506639	A1+	transposable element gene.
AT5G32483	7.2370737	-2.978930468	0.511697308	-5.821665315	5.83E-09	1.09E-07	0	0	0	3.816762292	4.089833736	3.935732613	A1-	transposable element gene.
AT5G32483	3.003126	-1.877612338	0.581215089	-3.230494826	1.24E-03	0.007273047	0	0	0	3.684038477	1.773370384	2.247074573	A1+	transposable element gene.
AT5G32488	9.0069636	-3.264555399	0.506611187	-6.44390705	1.16E-10	2.61E-09	0	0	0	3.933736191	4.483532941	4.277198875	A1-	transposable element gene.
AT5G32490	13.771068	-3.959177993	0.489261679	-8.09214815	5.86E-16	2.11E-14	0	0	0	4.88574345	4.483532941	5.074348265	A1-	transposable element gene.
AT5G32490	7.3300222	-2.8496939	0.591063945	-4.821295434	1.43E-06	1.66E-05	0	0	0	4.872329861	3.04536424	2.857049598	A1+	transposable element gene.
AT5G32495	213.13654	-7.365784333	0.388659727	-18.95175604	4.27E-80	2.29E-77	0.602380384	0	0	8.531166023	9.13437142	8.448643443	A1-	transposable element gene.
AT5G32495	9.8117616	-0.727069548	0.149981239	-4.847736653	1.25E-06	0.000127275	0.954186367	0	0	4.49483273	4.49088377	3.991107087	A2+	transposable element gene.
AT5G32510	7.1918987	-2.844115206	0.513385328	-5.539923041	3.03E-08	5.18E-07	0	0	0	3.395221171	4.483532941	3.728967903	A1-	transposable element gene.
AT5G32511	105.49723	-6.476083907	0.420941086	-15.38477503	2.07E-53	4.22E-51	0	0	0	7.33690362	8.280185693	7.352617396	A1-	transposable element gene.
AT5G32511	87.297087	-6.742902359	0.468033481	-14.40688034	4.68E-47	1.03E-44	0	0	0	7.720882129	7.16684068	7.427285971	A1+	transposable element gene.
AT5G32511	14.336701	-0.945650013	0.159132987	-5.942514078	2.81E-09	3.75E-07	0	0	0	5.205973566	5.054298527	4.238940698	A2+	transposable element gene.
AT5G32515	26.220799	-4.86742007	0.460319589	-10.5740016	3.93E-26	2.65E-24	0	0	0	5.672031041	5.617177427	5.913005388	A1-	transposable element gene.
AT5G32515	101.44194	-4.081239332	0.580742123	-7.027627528	2.10E-12	5.49E-11	0	0	0	5.786213592	8.267496444	7.956025915	A1+	transposable element gene.
AT5G32516	12.634525	-3.24693402	0.50995316	-6.366595766	1.93E-10	4.23E-09	0	0	0	2.797162804	5.046836798	5.278003551	A1-	transposable element gene.
AT5G32516	14.7594	-4.252176722	0.552025347	-7.702864992	1.33E-14	4.29E-13	0	0	0	5.379864119	4.654502272	4.628319815	A1+	transposable element gene.
AT5G32516	7.9215794	-0.630099433	0.141169359	-4.463429156	8.07E-06	7.08E-04	0	0	0	4.357162671	4.097076912	3.691684035	A2+	transposable element gene.
AT5G32517	18.965438	-4.057506393	0.48796638	-8.315135147	9.16E-17	3.51E-15	0	0	0	4.764642118	6.024848039	4.614569198	A1-	transposable element gene.
AT5G32517	13.961474	-3.55599316	0.580449837	-6.12592975	9.03E-10	1.69E-08	0	0	0	5.913254063	3.955228997	3.458449401	A1+	transposable element gene.
AT5G32520	6.848218	-2.630366522	0.515140651	-5.106113284	3.29E-07	4.88E-06	0	0	0	3.025182302	2.665086523	4.887807353	A1-	transposable element gene.
AT5G32520	5.9309944	-2.106951447	0.586971466	-3.589529591	3.31E-04	2.31E-03	0	0	0	4.346824447	4.107506639	4.107506639	A1+	transposable element gene.
AT5G32591	7.5715233	-2.781592755	0.514067011	-5.410953623	6.27E-08	1.04E-06	0	0	0	3.395221171	4.792504907	3.349749908	A1-	transposable element gene.
AT5G32591	5.8784712	-2.847944912	0.590250971	-4.824972851	1.40E-06	1.63E-05	0	0	0	4.16453883	3.710677785	2.857049598	A1+	transposable element gene.
AT5G32623	62.218994	-2.881159269	0.592263874	-4.864654753	1.15E-06	1.36E-05	0	0	0.694589061	4.414102287	7.214605745	7.685425298	A1+	transposable element gene.
AT5G32623	28.684203	-1.410869885	0.173542835	-8.129807728	4.30E-16	1.22E-13	0	0	0	5.245529421	6.330810854	5.798037166	A2+	transposable element gene.
AT5G32630	4.7579157	-1.895588785	0.515001896	-3.680741369	0.000232557	0.001993377	0.602380384	1.006034927	0	3.025182302	3.546623725	3.349749908	A1-	transposable element gene.
AT5G32630	35.226609	-3.010235297	0.589207832	-5.108953303	3.24E-07	4.19E-06	0	0	0	6.336480569	7.032350776	6.11739724	A1+	transposable element gene.
AT5G32726	26.800544	-4.851990243	0.461536679	-10.51268612	7.55E-26	5.03E-24	0	0	0	5.492985692	5.766238278	6.007675152	A1-	transposable element gene.
AT5G32775	13.197985	-3.817627268	0.492496189	-7.751587433	9.08E-15	2.95E-13	0	0	0	4.56149373	5.046836798	4.673513852	A1-	transposable element gene.
AT5G33150	6.1201893	-2.763380308	0.514294475	-5.373147959	7.74E-08	1.26E-06	0	0	0	3.549829232	3.546623725	4.028969492	A1-	transposable element gene.
AT5G33150	6.2011606	-2.763144317	0.591532367	-4.671163357	2.99E-06	3.31E-05	0	0	0	4.626795005	3.04536424	2.857049598	A1+	transposable element gene.
AT5G33240	14.536413	-4.041305802	0.486935538	-8.299467772	1.05E-16	3.99E-15	0	0	0	5.050236022	4.483532941	5.117444234	A1-	transposable element gene.
AT5G33240	18.714887	-4.637454159	0.536915131	-8.6372201	5.76E-18	2.48E-16	0	0	0	4.896561069	5.476812514	5.356497891	A1+	transposable element gene.
AT5G33254	47.555531	-5.652721147	0.435555116	-12.97819941	1.63E-38	1.94E-36	0	0	0	6.533580725	6.752923424	6.456789718	A1-	transposable element gene.
AT5G33254	22.470994	-4.925930927	0.525750832	-9.36932597	7.30E-21	3.92E-19	0	0	0	5.74125297	5.396254736	5.399824542	A1+	transposable element gene.
AT5G33255	105.44682	-6.57970285	0.402274948	-16.35623318	3.93E-60	9.89E-58	0	0	0.588988589	0.626414477	7.470110277	8.025113884	A1-	transposable element gene.
AT5G33255	57.344516	-6.053831986	0.467921073	-12.93772034	2.76E-38	4.09E-36	0	0	0.626414477	6.680852378	6.985988276	8.72372855	A1+	transposable element gene.
AT5G33255	14.742384	-1.010648714	0.163507598	-6.18105045	6.37E-10	9.01E-08	0	0	0.940325156	4.620502376	5.006885355	5.078255057	A2+	transposable element gene.
AT5G33384	7.1605157	-2.971755705	0.580381526	-5.120348551	3.05E-07	3.96E-06	0.640148721	0	0	4.414102287	3.710677785	3.458449401	A1+	transposable element gene.
AT5G33387	7.549534	-3.029097404	0.511087721	-5.92676615	3.09E-09	6.02E-08	0	0	0	3.689460601	4.089833736	4.199106927	A1-	transposable element gene.
AT5G33387	5.8974304	-2.705263841	0.591919061	-4.570327293	4.87E-06	5.12E-05	0	0	0	2.133098153	3.955228997	4.208431314	A1+	transposable element gene.
AT5G33391	87.362994	-6.94207174	0.413586287	-15.70218206	1.46E-55	3.21E-53	0	0	0	7.409395174	7.284819017	7.652776989	A1-	transposable element gene.
AT5G33391	57.148643	-5.939408823	0.501625828	-11.84031701	2.42E-32	2.68E-30	0	0	0	6.030007392	6.841347652	7.373965466	A1+	transposable element gene.

AT5G33391	14.016196	-0.922296732	0.158059096	-5.835138591	5.37E-09	6.97E-07	0	0	0	5.080350208	5.146691693	4.16096601	A2+	transposable element gene.
AT5G33427	9.9768948	-3.345466481	0.583097526	-5.737404687	9.61E-09	1.55E-07	0	0	0	5.319969209	3.416037926	3.6137176	A1+	transposable element gene.
AT5G34623	5.1715913	-2.385348634	0.515006109	-4.631689979	3.63E-06	4.53E-05	0	0.588988589	0	6.689460601	2.665086523	3.83605124	A1-	transposable element gene.
AT5G34623	4.4784438	-2.719331581	0.587535942	-4.628366349	3.69E-06	3.99E-05	0	0.626414477	0	2.604042178	3.955228997	4.302754999	A1+	transposable element gene.
AT5G34835	3.4259184	-1.643064078	0.503864039	-3.260927454	0.00110484	0.007860908	0	0	0.653468127	1.757146478	2.665086523	3.728967903	A1-	transposable element gene.
AT5G34835	6.6124325	-2.818312103	0.583768388	-4.827791568	1.38E-06	1.61E-05	0	0	0.694589061	3.242825326	4.346824447	3.6137176	A1+	transposable element gene.
AT5G34843	5.5158592	-2.57841138	0.592382088	-4.35261537	1.35E-05	0.0013054	0	0	0	4.524364692	2.545235219	2.857049598	A1+	transposable element gene.
AT5G35048	17.167248	-4.054774777	0.47644378	-8.510499981	1.73E-17	7.01E-16	0.602380384	0	0	5.454346907	5.046836798	4.837143627	A1-	transposable element gene.
AT5G35048	6.1986894	-2.554255449	0.590536856	-4.32531081	1.52E-05	1.46E-04	0.640148721	0	0	2.133098153	3.955228997	4.302754999	A1+	transposable element gene.
AT5G35061	4.8660162	-1.957423842	0.506923916	-3.861375995	0.00011275	0.001049837	0	0	0	2.526213436	4.483532941	2.023221944	A1-	transposable element gene.
AT5G35061	6.3005165	-2.771599765	0.591480237	-4.685870454	2.79E-06	3.11E-05	0	0	0	2.133098153	4.164272639	4.208431314	A1+	transposable element gene.
AT5G35145	37.360186	-5.306860058	0.446362674	-11.88912149	1.35E-32	1.24E-30	0	0	0	6.00174936	6.434335581	6.259291536	A1-	transposable element gene.
AT5G35146	32.400293	-5.10264461	0.452691789	-11.27178522	1.81E-29	1.47E-27	0	0	0	6.054369667	6.244071671	5.785201876	A1-	transposable element gene.
AT5G35146	16.803256	-3.897551643	0.571521998	-6.819600396	9.13E-12	2.23E-10	0	0	0	6.102903647	4.346824447	3.881635851	A1+	transposable element gene.
AT5G35794	4.6456695	-2.314588745	0.514014015	-4.502968161	6.70E-06	8.00E-05	0	0	0	2.797162804	3.546623725	3.613294506	A1-	transposable element gene.
AT5G35794	5.2728983	-2.599693255	0.592313581	-4.389048876	1.14E-05	0.000111871	0	0	0	2.133098153	3.955228997	3.881635851	A1+	transposable element gene.
AT5G36650	55.601656	-2.914816715	0.592314033	-4.921066449	8.61E-07	1.04E-05	0	0	0	4.29471016	7.190920881	7.416778359	A1+	transposable element gene.
AT5G36650	20.533907	-1.165026506	0.166908584	-6.980027501	2.95E-12	5.45E-10	0	0	0	4.679457118	5.829360154	5.450160215	A2+	transposable element gene.
AT5G37385	49.966473	-5.666660556	0.438298081	-12.9287825	3.10E-38	3.67E-36	0	0	0	6.976880928	6.602405842	6.315890736	A1-	transposable element gene.
AT5G37385	33.846393	-4.490466078	0.560847636	-8.006570399	1.18E-15	4.19E-14	0	0	0	8.006233365	6.610886935	6.602556983	A1+	transposable element gene.
AT5G37385	8.5258178	-0.604588654	0.138908324	-4.352429259	1.35E-05	0.00112263	0	0	0	3.94151438	4.799921877	3.450808994	A2+	transposable element gene.
AT5G37390	2.9319493	-1.794993304	0.501114007	-3.58200585	0.000340966	0.002792183	0	0	0	3.025182302	2.665086523	2.610741738	A1-	transposable element gene.
AT5G37390	6.2264784	-2.562952023	0.592386544	-4.326485887	1.52E-05	0.00145393	0	0	0	1.429370861	4.164272639	4.302754999	A1+	transposable element gene.
AT5G38595	9.1613423	-2.971866038	0.513615409	-5.786169934	7.20E-09	1.34E-07	0	0	0	4.408199229	0	5.1592901	A1-	transposable element gene.
AT5G38595	13.366731	-3.144458412	0.589083525	-5.337882113	9.40E-08	1.32E-06	0	0	0	1.429370861	5.476812514	5.168874549	A1+	transposable element gene.
AT4G06474	9.7575109	-2.928834601	0.579396188	-5.054977339	4.30E-07	5.47E-06	0.640148721	0.626414477	0	5.319969209	3.04536424	3.6137176	A1+	transposable element gene; retroelement pol polyprotein
AT2G09910	21.12784	-3.717153931	0.485248075	-7.660316692	1.85E-14	5.92E-13	0.602380384	0.588988589	0	4.324976877	6.342337877	4.784635763	A1-	transposable element gene; similar to ASV2, DNA binding
AT1G54430	11.538683	-3.527397112	0.550330927	-6.409592736	1.46E-10	3.06E-09	1.082007379	0	0	4.626795005	4.164272639	4.831847463	A1+	transposable element gene; similar to AT hook motif-containing protein-related
AT3G42100	20.470802	-3.985051845	0.48686798	-8.185076869	2.72E-16	1.02E-14	0.640148721	0.626414477	1.513627237	5.123742659	5.476812514	5.441887867	A1+	transposable element gene; similar to AT hook motif-containing protein-related
AT3G42100	18.022249	-3.667337502	0.451208367	-8.127813599	4.37E-16	1.59E-14	0.602380384	0.588988589	1.442988428	5.150323533	5.046836798	5.315498883	A1-	transposable element gene; similar to AT hook motif-containing protein-related
AT3G42100	5.8280072	-1.718922919	0.455097361	-3.777044358	1.59E-04	1.80E-03	0.569648577	0.557947347	1.385594591	4.13977271	2.928709658	3.344390632	A2-	transposable element gene; similar to AT hook motif-containing protein-related
AT4G01980	21.716676	-3.183229072	0.50614161	-6.289206443	3.19E-10	6.38E-09	1.693301494	1.66670863	1.513627237	6.270494512	4.786788781	4.474701533	A1+	transposable element gene; similar to myb family protein
AT4G01980	26.786068	-3.700203649	0.403239963	-9.176182888	4.47E-20	2.11E-18	1.619590486	1.593003473	1.442988428	5.492985692	5.901330042	5.730732322	A1-	transposable element gene; similar to myb family protein
AT2G07510	6.0512614	-2.758010467	0.514509891	-5.360461511	8.30E-08	1.35E-06	0	0	0	4.142578534	2.665086523	3.935732613	A1-	transposable element gene; similar to Ulp1 protease family protein
AT1G08740	7.6717875	-3.213353548	0.583769548	-5.504489846	3.70E-08	5.52E-07	0	0	0	3.684038477	4.654502272	3.458449401	A1+	transposable element gene; similar to Ulp1 protease family protein
AT1G08740	19.046346	-1.070106948	0.163652952	-6.538879606	6.20E-11	9.82E-09	0	0	0	4.559035468	5.856362086	5.160701666	A2+	transposable element gene; similar to Ulp1 protease family protein
AT1G21020	7.1813948	-3.068866846	0.586959663	-5.228411834	1.71E-07	2.32E-06	0	0	0	3.480233365	4.654502272	3.284432598	A1+	transposable element gene; similar to Ulp1 protease family protein
AT1G21020	17.483416	-1.030708196	0.1623197	-6.349865098	2.16E-10	3.28E-08	0	0	0	4.49483273	5.715995759	5.035194817	A2+	transposable element gene; similar to Ulp1 protease family protein
AT1G34610	8.9063313	-3.35427951	0.56773693	-5.90815804	3.46E-09	5.96E-08	0.640148721	0	0	3.862584211	4.346824447	4.391288416	A1+	transposable element gene; similar to Ulp1 protease family protein
AT2G14010	4.0057742	-1.655556218	0.505801626	-3.273133441	0.001063623	0.007579306	0.602380384	0	0	1.757146478	4.089833736	2.610741738	A1-	transposable element gene; similar to Ulp1 protease family protein
AT2G14010	8.2273884	-2.823423178	0.587266581	-4.80773684	1.53E-06	1.77E-05	0.640148721	0	0	2.133098153	4.654502272	4.474701533	A1+	transposable element gene; similar to Ulp1 protease family protein
AT2G29240	7.3617831	-2.976907305	0.580130138	-5.131447428	2.88E-07	3.77E-06	0.640148721	0	0	3.684038477	4.508850015	3.458449401	A1+	transposable element gene; similar to Ulp1 protease family protein
AT2G29240	18.844512	-1.054560156	0.164241643	-6.420784275	1.36E-10	2.08E-08	0.954186367	0	0	4.559035468	5.801843191	5.160701666	A2+	transposable element gene; similar to Ulp1 protease family protein
AT3G09170	8.2077612	-3.218892902	0.572302279	-5.62446284	1.86E-08	2.89E-07	0.640148721	0	0	3.684038477	4.346824447	4.208431314	A1+	transposable element gene; similar to Ulp1 protease family protein
AT3G26530	7.6717875	-3.213353548	0.583769548	-5.504489846	3.70E-08	5.52E-07	0	0	0	3.684038477	4.654502272	3.458449401	A1+	transposable element gene; similar to Ulp1 protease family protein

AT3G26530	18.867305	-1.071386855	0.163733831	-6.543466614	6.01E-11	9.63E-09	0	0	0	4.559035468	5.829360154	5.160701666	A2+	transposable element gene; similar to Ulp1 protease family protein
AT4G04400	14.12851	-3.969424199	0.565396107	-7.020607591	2.21E-12	5.77E-11	0	0	0	5.646896475	4.164272639	4.302754999	A1+	transposable element gene; similar to Ulp1 protease family protein
AT4G04530	6.0191964	-2.466152951	0.514248615	-4.795643355	1.62E-06	2.14E-05	0.602380384	0	0	3.222033331	4.089833736	3.613294506	A1-	transposable element gene; similar to Ulp1 protease family protein
AT4G04530	7.1529376	-2.906265746	0.582749097	-4.987164738	6.13E-07	7.60E-06	0.640148721	0	0	2.958502988	4.346824447	4.107506639	A1+	transposable element gene; similar to Ulp1 protease family protein
AT4G04530	6.8753685	-0.539592529	0.136726358	-3.946514301	7.93E-05	5.66E-03	0.954186367	0	0	3.618975234	4.097076912	3.798546962	A2+	transposable element gene; similar to Ulp1 protease family protein
AT4G07580	6.0640196	-2.692817422	0.514821018	-5.230589517	1.69E-07	2.62E-06	0	0	0	3.222033331	3.546623725	4.199106927	A1-	transposable element gene; similar to Ulp1 protease family protein
AT4G07580	2.9290879	-1.917977401	0.582797775	-3.290982712	0.00099838	0.006033487	0	0	0	3.480233365	1.773370384	2.58406216	A1+	transposable element gene; similar to Ulp1 protease family protein
AT5G44890	7.6717875	-3.213353548	0.583769548	-5.504489846	3.70E-08	5.52E-07	0	0	0	3.684038477	4.654502272	3.458449401	A1+	transposable element gene; similar to Ulp1 protease family protein
AT5G44890	18.867305	-1.071386855	0.163733831	-6.543466614	6.01E-11	9.63E-09	0	0	0	4.559035468	5.829360154	5.160701666	A2+	transposable element gene; similar to Ulp1 protease family protein
AT1G17277	8.0652508	-2.706820418	0.514748032	-5.258534758	1.45E-07	2.28E-06	0	0	0	3.025182302	5.046836798	3.349749908	A1-	transposable element gene; similar to zinc finger protein
AT2G15520	13.558998	-3.596860713	0.48982748	-7.343117438	2.09E-13	6.06E-12	0	0	0.653468127	4.700053001	5.26298084	4.277198875	A1-	transposable element gene; similar to zinc finger protein
AT5G27500	12.963645	-3.126901056	0.589237179	-5.306693414	1.12E-07	1.56E-06	0	0	0	1.429370861	5.396254736	5.168874549	A1+	transposable element gene; similar to zinc finger protein
AT1G61510	6.5960005	-2.930731827	0.589573155	-4.970938388	6.66E-07	8.21E-06	0	0	0	2.604042178	3.955228997	4.391288416	A1+	transposable element gene; transposase IS4 family protein
AT1G61510	12.700731	-3.463534543	0.505070863	-6.857521983	7.01E-12	1.78E-10	0	0	0	5.331804227	4.792504907	3.487531741	A1-	transposable element gene; transposase IS4 family protein
AT3G30820	39.641246	-5.25048676	0.435705375	-12.05054393	1.93E-33	1.81E-31	0.602380384	0	0	6.105138068	6.520816798	6.315890736	A1-	retrotransposon ORF-1 protein
AT3G30820	44.402842	-5.681777104	0.481833834	-11.7919845	4.29E-32	4.70E-30	0.640148721	0	0	6.704468582	6.152527787	6.545825544	A1+	retrotransposon ORF-1 protein
AT4G02960	21.143653	-4.056091184	0.48217195	-8.412125974	4.03E-17	1.62E-15	0.640148721	1.061739724	1.161466416	5.192160237	5.531089971	5.441887867	A1+	RE2, retro element 2, a copia-type retrotransposon element containing LTRs and encoding a polyprotein. This retro element exists in two loci in Landsberg erecta but only once in Columbia
AT4G02960	14.949411	-3.313414293	0.466718157	-7.099390156	1.25E-12	3.41E-11	0.602380384	1.006034927	1.101575979	4.408199229	5.046836798	5.1592901	A1-	RE2, retro element 2, a copia-type retrotransposon element containing LTRs and encoding a polyprotein. This retro element exists in two loci in Landsberg erecta but only once in Columbia
AT1G50735	122.61481	-6.854758422	0.479254641	-14.30295678	2.10E-46	4.35E-44	0	0	0	7.110161548	8.544777235	7.827060764	A1+	SADHU NON-CODING RETROTRANSPON 8-1, SADHU8-1
AT1G50735	18.891848	-1.124512154	0.165755801	-6.784149606	1.17E-11	2.03E-09	0	0	0	4.942735706	5.801843191	4.897720133	A2+	SADHU NON-CODING RETROTRANSPON 8-1, SADHU8-1
AT3G02515	111.49392	-3.921817062	0.242097615	-16.19932134	5.10E-59	1.27E-56	3.632364657	3.534563286	3.825554911	7.725574522	7.74621963	7.717232473	A1-	SADHU NON-CODING RETROTRANSPON 6-1, SADHU6-1
AT3G02515	105.51688	-3.762202139	0.259473629	-14.49936223	1.22E-47	2.91E-45	3.731919154	3.634383687	3.928250694	7.755208958	7.756542763	7.373965466	A1+	SADHU NON-CODING RETROTRANSPON 6-1, SADHU6-1
AT3G31442	3.865358	-1.750651476	0.512320001	-3.417105465	0.000632908	0.004818839	0	0.006034927	0	3.549829232	2.665086523	2.833863982	A1-	SADHU NON-CODING RETROTRANSPON 7-2, SADHU7-2
AT3G31442	9.7133564	-3.178959466	0.565177063	-5.624714225	1.86E-08	2.89E-07	0	1.061739724	0	3.684038477	4.786788781	4.302754999	A1+	SADHU NON-CODING RETROTRANSPON 7-2, SADHU7-2
AT3G42658	56.470238	-4.666410974	0.352753048	-13.228549	6.00E-40	7.63E-38	2.038898622	1.593003473	1.718867729	6.990447813	6.520816798	6.850788829	A1-	SADHU NON-CODING RETROTRANSPON 3-2, SADHU3-2
AT3G42658	74.343944	-5.027691351	0.374933911	-13.4095402	5.32E-41	8.93E-39	2.121326742	1.66670863	1.796470461	7.426453731	7.327526492	6.760480718	A1+	SADHU NON-CODING RETROTRANSPON 3-2, SADHU3-2
AT2G10010	6.5637727	-2.967269897	0.588694122	-5.040427251	4.64E-07	5.87E-06	0	0	0	4.29471016	3.955228997	2.857049598	A1+	TNP2-like transposon protein, putative
AT2G10010	31.79599	-5.103404938	0.45245429	-11.27938237	1.66E-29	1.35E-27	0	0	0	5.831289127	6.13861985	6.052777968	A1-	TNP2-like transposon protein, putative

Supplementary Table 1: List of transposable elements with at least log₂-fold increases (negative log₂-fold change) or decreases (positive log₂-fold change) of 2.5 in at least one of the four lines A1+, A1-, A2+ or A2-.

	No of genes	Genes with heritable changes	Percentage heritable changes
Transposable elements			
CACTA-like transposase family (En/Spm)	3	0	0
CACTA-like transposase family (Ptta/En/Spm)	59	39	66.1
CACTA-like transposase family (Tnp1/En/Spm)	18	3	16.7
CACTA-like transposase family (Tnp2/En/Spm)	32	7	21.9
CACTA-like transposase family, putative	4	0	0
copia-like retrotransposon family (Ty1-Copia-element)	19	7	36.8
gypsy-like retrotransposon family (Athila)	59	39	66.1
gypsy-like retrotransposon pseudogene (Athila)	4	4	100
gypsy-like retrotransposon genes and pseudogenes (Athila)	63	43	68.3
gypsy-like retrotransposon family (Ty3-element)	26	16	61.5
hAT-like transposase family (hobo/Ac/Tam3)	12	9	75
Mutator-like transposase family	24	16	66.7
non-LTR retrotransposon family (LINE)	11	8	72.7
transposable element gene	64	37	57.8
transposable element gene; pseudogene, hypothetical protein	86	69	80.2

Supplementary Table 2: Summary of transposable elements with altered transcript levels and their heritability rates. Data were compiled for different categories of transposable elements (S1 table) that showed at least log₂-fold changes of +/- 2.5 in line A1+ compared to wildtype. For each gene, the values in A1+ and A1- were compared to score the heritability of expression changes.

	baseMean	log2Fold	lfcSE	stat	pvalue	padj	1	2	3	4	5	6	Line	Description
MIRNAs														
AT4G06130	48.823041	2.6616341	0.348037596	7.647547598	2.05E-14	6.52E-13	6.687749963	6.511758058	6.281227452	3.395221171	0	3.935732613	A1-	MIR3932b
AT4G06130	56.134961	2.3431358	0.331764122	7.062655706	1.63E-12	4.31E-11	6.794708176	6.619508776	6.39006114	4.16453883	3.416037926	4.391288416	A1+	MIR3932b
AT4G06130	60.809848	1.0775738	0.262319457	4.107868466	3.99E-05	5.35E-04	6.590660618	6.418172921	6.190579894	5.411740146	5.158863172	5.233721953	A2-	MIR3932b
AT5G04935	29.951077	-5.003175	0.455475867	-10.98450158	4.54E-28	3.38E-26	0	0	0	5.861134793	6.13861985	5.758224149	A1-	MIR854b
AT5G04935	18.476253	-3.819838	0.575639136	-6.635820583	3.23E-11	7.37E-10	0	0	0	6.36243543	3.710677785	4.208431314	A1+	MIR854b
AT5G04985	18.992956	-4.38776	0.475560101	-9.226510241	2.80E-20	1.34E-18	0	0	0	5.454346907	5.26298084	5.117444234	A1-	MIR854c
AT5G04985	8.6734198	-3.307702	0.582592139	-5.677560769	1.37E-08	2.16E-07	0	0	0	4.896561069	3.955228997	3.284432598	A1-	MIR854c
AT5G04995	16.571824	-4.208004	0.481002172	-8.748409344	2.16E-18	9.14E-17	0	0	0	5.197878395	5.046836798	5.029925195	A1-	MIR854a
AT5G04995	9.5193979	-3.570653	0.574916843	-6.210729652	5.27E-10	1.02E-08	0	0	0	4.896561069	3.710677785	4.107506639	A1+	MIR854a
NATs														
AT1G05147	55.602953	-3.988832	0.381352049	-10.45971049	1.32E-25	8.65E-24	2.628119155	2.331571897	1.101575979	6.623396307	7.333420192	6.052777968	A1-	Natural antisense transcript overlaps with AT1G15040
AT1G05147	36.593085	-3.503192	0.426228318	-8.219049683	2.05E-16	7.77E-15	2.719161113	2.419481965	1.161466416	5.913254063	6.646150789	5.671366059	A1+	Natural antisense transcript overlaps with AT1G15040
AT1G05147	50.075779	-1.829317	0.452272253	-4.044725079	5.24E-05	6.77E-04	2.546368521	2.256221163	1.053248618	3.751761308	7.194898619	7.063667894	A2-	Natural antisense transcript overlaps with AT1G15040
AT1G20515	36.490043	3.2198279	0.471245751	6.832587651	8.34E-12	2.05E-10	5.93821284	5.688356515	6.16070483	3.242825326	0	1.806583236	A1+	Natural antisense transcript overlaps with AT1G20520
AT2G05914	130.97942	-6.158549	0.352696197	-17.461342	2.82E-68	9.80E-66	1.619590486	1.329166983	0.653468127	7.864669958	8.352713783	7.812101098	A1-	Natural antisense transcript overlaps with AT2G05915
AT2G05914	86.917578	-5.305366	0.45978717	-11.53874334	8.41E-31	8.32E-29	1.693301494	1.395704924	0.694589061	8.240343172	7.013254259	6.466537287	A1+	Natural antisense transcript overlaps with AT2G05915
AT2G05914	17.889952	-1.00982	0.170991517	-5.905672939	3.51E-09	4.65E-07	2.24791129	1.909535826	1.024858076	5.035921409	5.054298527	5.200222885	A2+	Natural antisense transcript overlaps with AT2G05915
AT2G07213	61.604197	-2.712589	0.333356156	-8.137210545	4.04E-16	1.47E-14	3.748167935	3.403219343	4.091061435	5.974701535	7.128344859	7.041870662	A1-	Natural antisense transcript overlaps with AT2G07215
AT2G07335	204.71295	4.2594967	0.307963187	13.83118793	1.65E-43	3.10E-41	8.346436517	8.638298194	8.854750781	3.242825326	3.416037926	4.767143513	A1+	Natural antisense transcript overlaps with AT2G0720
AT2G09885	43.322048	1.8782984	0.365222821	5.142883563	2.71E-07	4.07E-06	6.270122728	5.819185431	6.15931073	3.025182302	5.26298084	3.83605124	A1-	Natural antisense transcript overlaps with AT2G47380
AT2G09885	42.045404	2.3501722	0.368886625	6.370987908	1.88E-10	3.88E-09	6.376741883	5.926227133	6.268024009	3.242825326	3.710677785	3.881635851	A1+	Natural antisense transcript overlaps with AT2G47380
AT2G09885	34.146669	2.5441704	0.369242779	6.890237295	5.57E-12	2.75E-10	6.173363621	5.726260252	6.068770621	0	3.44909067	2.749120822	A2-	Natural antisense transcript overlaps with AT2G47380
AT2G36792	982.81518	2.7691232	0.561632593	4.930488851	8.20E-07	9.97E-06	10.49933628	10.8479465	11.18839905	7.697535257	4.907957693	5.356497891	A1+	Natural antisense transcript overlaps with AT2G36790
AT2G36792	1241.0115	0.863097	0.243536863	3.544009519	3.94E-04	3.92E-03	10.29344818	10.64450757	10.98642687	9.999441728	9.963046814	9.0923252	A2-	Natural antisense transcript overlaps with AT2G36790
AT2G36792	2263.4614	0.7865937	0.170552202	4.612040642	3.99E-06	3.66E-04	11.24620047	11.60475651	11.93077862	9.651728572	10.69851526	10.70819435	A2+	Natural antisense transcript overlaps with AT2G36790
AT3G01055	54.390945	3.0220773	0.373896769	8.082651678	6.34E-16	2.31E-14	6.61731651	6.704698897	6.66084573	4.16453883	0	3.284432598	A1+	Natural antisense transcript overlaps with AT3G01830
AT4G08285	17.542525	2.9092223	0.523180879	5.560643358	2.69E-08	4.09E-07	4.935457856	4.84448128	5.46889724	2.133098153	0	1.169324837	A1+	Natural antisense transcript overlaps with AT4G30430
AT4G09715	20.361683	2.9701382	0.499284644	5.948787415	2.70E-09	4.75E-08	5.284562511	5.226103179	5.407161218	2.604042178	0	1.169324837	A1+	Natural antisense transcript overlaps with AT4G38560
AT5G03195	105.74101	2.7465586	0.287074818	9.567396353	1.10E-21	5.72E-20	7.494287162	7.240783438	7.889067639	4.700053001	4.483532941	4.553113256	A1-	Natural antisense transcript overlaps with AT5G20720
AT5G03195	118.87937	2.3741958	0.280577995	8.461803224	2.63E-17	1.07E-15	7.601677754	7.348990441	7.998818478	4.976329861	4.907957693	5.482759454	A1+	Natural antisense transcript overlaps with AT5G20720
AT5G03195	97.741857	2.7384995	0.294967689	9.284065879	1.63E-20	1.98E-18	7.396776466	7.146773257	7.797601071	3.751761308	4.689499909	4.354624822	A2-	Natural antisense transcript overlaps with AT5G20720
ncRNA														
AT1G05913	524.34374	3.7121625	0.264491909	14.03507019	9.51E-45	1.45E-42	9.808132885	10.23482958	9.703019224	5.530616574	6.952811471	5.553777891	A1-	ncRNA
AT1G05913	550.20548	4.3674999	0.23246395	18.78785905	9.49E-79	7.87E-76	9.9159845	10.3436432	9.813090394	5.597298362	5.883728226	5.1178917	A1+	ncRNA
AT1G05913	483.13673	3.9467849	0.230304717	17.13722999	7.83E-66	1.15E-62	9.710172648	10.14025391	9.611266371	6.077046792	5.512431154	5.437984731	A2-	ncRNA
AT1G06407	10.304055	-3.63271	0.573663237	-6.332477475	2.41E-10	4.92E-09	0	0	0	3.480233365	4.654502272	4.831847463	A1+	ncRNA
AT1G06963	14.603947	-3.802096	0.557930763	-6.814636956	9.45E-12	2.30E-10	0.640148721	0	0	4.626795005	5.625572377	3.998987077	A1+	ncRNA
AT1G07343	6.6693705	-2.548344	0.592338632	-4.302173569	1.69E-05	1.60E-04	0	0	0	1.429370861	3.710677785	4.767143513	A1+	ncRNA
AT1G07347	7.9805402	-3.408031	0.578027773	-5.895964619	3.72E-09	6.39E-08	0	0	0	3.862584211	4.346824447	3.998987077	A1+	ncRNA
AT1G08757	16.70058	3.3855569	0.564489274	5.997557514	2.00E-09	3.62E-08	5.061448268	4.362753915	5.621671634	0	0	0	A1+	ncRNA
AT1G08997	22.676064	-3.726693	0.58028439	-6.422183256	1.34E-10	2.84E-09	0	0	0	2.133098153	6.102625836	6.04333002	A1+	ncRNA

AT1G09937	1264.193	3.6086169	0.231180738	15.60950505	6.27E-55	1.33E-52	11.02423082	10.97890462	11.52787383	6.93539757	8.037766677	7.249843723	A1-	ncRNA	
AT1G09937	1353.5064	3.7615434	0.191267566	19.66639438	4.19E-86	4.89E-83	11.13214853	11.08775332	11.63803637	7.535810907	7.117439888	7.604404592	A1+	ncRNA	
AT1G09937	1141.7187	4.3273864	0.235347144	18.38724842	1.66E-75	9.17E-72	10.92620611	10.88429624	11.4360393	5.887451322	6.204711947	6.865499146	A2-	ncRNA	
AT1G16635	268.33312	2.6678037	0.306940563	8.6915972	3.57E-18	1.51E-16	8.384633266	9.344062651	8.729302177	5.492985692	6.889210391	5.45643433	A1-	ncRNA	
AT1G16635	271.51231	3.5185047	0.285428427	12.32709967	6.47E-35	8.15E-33	8.492289634	9.452801918	8.839250637	5.051918249	5.476812514	5.265734139	A1+	ncRNA	
AT1G16635	239.3398	3.1137092	0.280274411	11.10950231	1.13E-28	2.59E-26	8.286863447	9.24955632	8.637659007	5.546159418	5.346451484	5.143166376	A2-	ncRNA	
AT1G26558	28.610013	-1.358995	0.346714834	-3.91963291	8.87E-05	0.0008498	3.955140356	3.654941018	4.315217066	5.800812964	5.046836798	5.352044354	A1-	ncRNA	
AT1G26558	113.70484	-3.254951	0.384964573	-8.45519638	2.79E-17	1.13E-15	4.056385374	3.755490433	4.420076183	6.332434805	8.137236645	8.100899128	A1+	ncRNA	
AT1G67105	935.66206	-7.525751	0.282104937	-26.67713391	8.67E-157	3.71E-153	3.439113844	2.331571897	2.324987472	11.2768577	10.70843776	10.49642506	A1-	ncRNA	
AT1G67105	1941.5379	-8.81461	0.231995177	-37.99479832	0.00E+00	0.00E+00	3.537458392	2.419481965	2.413854982	11.97572236	11.88737174	11.89818231	A1+	ncRNA	
AT1G67105	103.72517	-2.339764	0.175022383	-13.36836973	9.25E-41	9.12E-38	4.233600219	3.062067384	3.043224528	7.771603214	7.626342189	7.46629918	A2+	ncRNA	
AT2G01422	3.1864764	-1.790105	0.5006145	-3.57581537	0.0003491	0.0028482	0	0	0	3.549829232	2.665086523	2.023221944	A1-	ncRNA	
AT2G01422	50.416064	-2.896084	0.59233579	-4.889260274	1.01E-06	1.20E-05	0	0	0	4.16453883	7.013254259	7.307265373	A1+	ncRNA	
AT2G01422	10.433363	-0.703839	0.14595901	-4.822167899	1.42E-06	0.0001442	0	0	0	4.034776506	5.100202951	3.898037328	A2+	ncRNA	
AT2G04365	7.7122616	-3.296247	0.581375449	-5.669738289	1.43E-08	2.26E-07	0	0	0	4.16453883	4.346824447	3.458449401	A1+	ncRNA	
AT2G04365	23.689369	-1.4108	0.173425807	-8.134888169	4.12E-16	1.18E-13	0	0	0	5.919088094	5.422755442	5.38305632	A2+	ncRNA	
AT2G04655	111.02298	-6.740296	0.407790576	-16.52881686	2.28E-61	5.85E-59	0	0	0	7.589563082	8.06680322	7.703155833	A1-	ncRNA	
AT2G04655	99.48946	-6.958769	0.459719043	-15.13700414	9.23E-52	2.61E-49	0	0	0	7.777647993	7.567152095	7.576354011	A1+	ncRNA	
AT2G04655	19.171737	-1.175363	0.167499656	-7.017108386	2.27E-12	4.21E-10	0	0	0	4.843112829	5.715995759	5.200222885	A2+	ncRNA	
AT2G04885	33.499762	-5.069979	0.442341174	-11.46169356	2.05E-30	1.72E-28	0	0	0.653468127	6.313781463	5.766238278	6.11789374	A1-	ncRNA	
AT2G04885	42.26849	-5.007706	0.528246327	-9.479869927	2.55E-21	1.41E-19	0	0	0	6.094589061	7.308122313	5.883728226	5.265734139	A1+	ncRNA
AT2G05015	13.052662	-3.770821	0.496611727	-7.593097522	3.12E-14	9.77E-13	0	0	0	4.486881573	4.089833736	5.387686903	A1-	ncRNA	
AT2G05015	15.914916	-4.340577	0.548734019	-7.910165327	2.57E-15	8.87E-14	0	0	0	5.192160237	5.310931324	4.474701533	A1+	ncRNA	
AT2G05695	18.104277	-4.34751	0.476926929	-9.115672451	7.82E-20	3.61E-18	0	0	0	5.197878395	5.046836798	5.387686903	A1-	ncRNA	
AT2G05695	16.963381	-4.361354	0.54997019	-7.930165023	2.19E-15	7.65E-14	0	0	0	5.646896475	5.019733684	4.474701533	A1-	ncRNA	
AT2G05705	8.1447355	-2.859586	0.502857583	-5.68667129	1.30E-08	2.32E-07	0.602380384	0.588988589	0	4.041933031	4.089833736	4.116544802	A1-	ncRNA	
AT2G05705	4.4561877	-2.192706	0.589424186	-3.720082212	1.99E-04	1.47E-03	0.640148721	0.626414477	0	3.242825326	3.416037926	3.086509522	A1+	ncRNA	
AT2G06002	66.051339	-3.922005	0.306529395	-12.7948751	1.75E-37	2.00E-35	2.95174695	3.010544612	2.622113348	7.144016123	6.520816798	7.200593083	A1-	ncRNA	
AT2G06002	148.67925	-5.092287	0.272129773	-18.71271489	3.90E-78	3.13E-75	3.046205971	3.106370194	2.714973081	8.113776852	8.086793566	8.347650993	A1+	ncRNA	
AT2G06002	43.383864	-1.375224	0.179652068	-7.654928498	1.93E-14	4.64E-12	3.721080197	3.793422494	3.366368779	6.206482075	6.349937186	6.200094267	A2+	ncRNA	
AT2G06562	10.248946	-3.300567	0.506001863	-6.522835338	6.90E-11	1.59E-09	0	0	0	3.816762292	5.046836798	4.116544802	A1-	ncRNA	
AT2G06562	15.875661	-4.055738	0.563704688	-7.194792108	6.26E-13	1.73E-11	0	0	0	5.74125297	4.907957693	3.881635851	A1+	ncRNA	
AT2G06562	16.463037	-0.993684	0.160909395	-6.175424797	6.60E-10	9.29E-08	0	0	0	4.49483273	5.655788051	4.848821471	A2+	ncRNA	
AT2G15555	176.0742	-6.87679	0.355386119	-19.35019433	2.03E-83	1.16E-80	1.353130444	1.006034927	0	8.316365464	8.591227044	8.461244257	A1-	ncRNA	
AT2G15555	159.39426	-6.451781	0.447143504	-14.42888176	3.41E-47	7.61E-45	1.419792043	1.061739724	0	9.084419273	7.673523812	7.711451677	A1+	ncRNA	
AT2G15555	21.865422	-1.171308	0.171669595	-6.823038999	8.91E-12	1.56E-09	1.930722178	1.504834619	0	5.205973566	5.829360154	5.160701666	A1+	ncRNA	
AT3G02832	182.61034	2.0278331	0.252553472	8.029321813	9.80E-16	3.46E-14	8.005626973	8.402177918	8.135299128	5.567290803	6.889210391	5.888334403	A1-	ncRNA	
AT3G02832	193.6654	1.9964918	0.22139417	9.017815701	1.92E-19	9.41E-18	8.113189803	8.510768507	8.245120211	5.953230919	6.050935773	6.564984969	A1+	ncRNA	
AT3G02832	151.39799	2.8101524	0.256099873	10.97287702	5.16E-28	1.15E-25	7.907948362	8.307810212	8.043769793	4.697193151	4.593952335	5.437984731	A2-	ncRNA	
AT3G03595	106.58741	3.1234482	0.273626116	11.41502212	3.52E-30	2.93E-28	7.582742463	7.596944741	7.613246262	4.486881573	4.792504907	3.83605124	A1-	ncRNA	
AT3G03595	120.60765	2.5208433	0.249700222	10.09547869	5.78E-24	3.94E-22	7.69016738	7.70530352	7.722902776	4.414102287	5.396254736	5.31182967	A1+	ncRNA	
AT3G03595	99.8122	3.0787937	0.282334566	10.90477082	1.09E-27	2.34E-25	7.485198306	7.502793118	7.521863972	5.098259903	3.212236784	4.089549378	A2-	ncRNA	
AT3G05595	12.678385	-3.459008	0.572410697	-6.042877979	1.51E-09	2.76E-08	0	0	0.626414477	2.958502988	5.220242777	5.065040979	A1-	ncRNA	
AT3G05595	11.120442	-2.322125	0.495863455	-4.682993634	2.83E-06	3.59E-05	0	0	1.329166983	1.718867729	3.933736191	3.613294506	A1+	ncRNA	
AT3G05595	10.895202	-2.69462	0.535406757	-5.032845862	4.83E-07	6.09E-06	0	0	1.395704924	1.796470461	4.524364692	4.508850015	A1+	ncRNA	
AT3G06095	37.398873	-3.762939	0.361773169	-10.40137784	2.44E-25	1.55E-23	2.038898622	2.179301789	1.950365559	6.178903081	6.342337877	6.007675152	A1-	ncRNA	
AT3G06095	14.189569	-2.315023	0.468687926	-4.939368904	7.84E-07	9.54E-06	2.121326742	2.264856247	2.032847348	4.976329861	4.164272639	4.831847463	A1+	ncRNA	
AT3G06115	6.4998139	-2.793598	0.513885457	-5.436227586	5.44E-08	9.05E-07	0	0	0	3.549829232	4.089833736	3.728967903	A1-	ncRNA	
AT3G06115	7.3432909	-2.85385	0.59104962	-4.828444506	1.38E-06	1.61E-05	0	0	0	4.976329861	2.545235219	3.284432598	A1+	ncRNA	
AT3G06355	28019.634	-2.522475	0.563271644	-4.478256843	7.53E-06	7.65E-05	11.46816674	10.47013768	12.52638238	15.5667125	16.54516271	13.7533635	A1+	ncRNA	
AT3G06465	1813.5336	-9.780498	0.318758301	-30.68311762	9.56E-207	1.23E-202	1.026048597	1.329166983	0.653468127	11.97387592	11.9453993	11.50913359	A1-	ncRNA	
AT3G06465	1978.6814	-9.439226	0.40928241	-23.06286683	1.09E-117	2.55E-114	1.082007379	1.395704924	0.694589061	12.76320516	11.49136942	10.99486382	A1+	ncRNA	
AT3G06465	397.15801	-3.40005	0.17758609	-19.14592453	1.05E-81	3.98E-78	1.523548554	1.909535826	1.024858076	9.433615891	10.19862811	9.004551154	A2+	ncRNA	
AT3G06495	4.7900837	-2.583776	0.592301127	-4.362267484	1.29E-05	0.0001251	0	0	0	4.021446993	3.04536424	2.857049598	A1+	ncRNA	

AT3G06715	11.579514	-3.430857	0.504104985	-6.805837512	1.00E-11	2.53E-10	0	0	0	4.764642118	5.046836798	3.613294506	A1-	ncRNA	
AT3G06715	16.702012	-4.091985	0.563400401	-7.263014112	3.79E-13	1.06E-11	0	0	0	5.953230919	4.508850015	4.208431314	A1+	ncRNA	
AT3G06955	62.637813	-5.238758	0.371641179	-14.09627842	4.00E-45	6.20E-43	1.353130444	1.329166983	1.101575979	6.963185251	6.752923424	7.149601521	A1-	ncRNA	
AT3G06955	83.225114	-5.712284	0.392543367	-14.551981	5.67E-48	1.42E-45	1.419792043	1.395704924	1.161466416	7.649676544	7.190920881	7.237331421	A1+	ncRNA	
AT3G09855	171.33762	2.6942834	0.213463584	12.62174711	1.60E-36	1.76E-34	8.165194244	8.31350289	8.220902579	5.454346907	5.45092181	5.422470072	A1-	ncRNA	
AT3G09855	181.83264	2.8871096	0.216317083	13.34665539	1.24E-40	2.05E-38	8.272799467	8.422073819	8.330745406	5.257479592	5.220242777	5.561184823	A1+	ncRNA	
AT3G09855	152.70772	3.2877278	0.245412151	13.3967606	6.32E-41	3.24E-38	8.067474297	8.219153513	8.129353813	4.911618862	4.381482195	4.645984426	A2-	ncRNA	
AT3G60176	15.341404	-3.73465	0.496710598	-7.518764252	5.53E-14	1.69E-12	0	0	0	4.408199229	5.766238278	4.277198875	A1-	ncRNA	
AT3G60176	10.843168	-3.680914	0.572614806	-6.428254954	1.29E-10	2.73E-09	0	0	0	5.192160237	3.955228997	3.998987077	A1+	ncRNA	
AT4G04195	36.417973	1.986113	0.37500583	5.296218969	1.18E-07	1.88E-06	5.832072401	5.67001866	6.193595463	2.526213436	4.483532941	3.935732613	A1-	ncRNA	
AT4G04195	36.282964	2.3952139	0.413396006	5.79399373	6.87E-09	1.14E-07	5.93821284	5.776857722	6.302343639	2.133098153	3.04536424	3.998987077	A1+	ncRNA	
AT4G04195	28.939961	2.7656996	0.402518134	6.870993716	6.38E-12	3.09E-10	5.735779293	5.577281985	6.103024215	0	0	2.975939682	A2-	ncRNA	
AT4G04223	157.56276	-2.520726	0.206976499	-12.17880468	4.03E-34	3.88E-32	5.751099165	5.161453918	5.439554059	8.083015303	8.203817522	7.979123798	A1-	ncRNA	
AT4G04223	150.45195	-2.369698	0.207847996	-11.4011278	4.13E-30	3.96E-28	5.857134047	5.267420785	5.547305751	8.07806267	7.865285288	8.033722608	A1+	ncRNA	
AT4G04223	153.26058	-1.116415	0.160082309	-6.974004024	3.08E-12	5.65E-10	6.594304266	6.009174426	6.277467465	7.771603214	8.015797778	7.711656574	A2+	ncRNA	
AT4G04945	7.7368967	-3.09772	0.510403724	-6.069155455	1.29E-09	2.62E-08	0	0	0	3.933736191	3.546623725	4.488922482	A1-	ncRNA	
AT4G04945	9.0157365	-3.487812	0.577061357	-6.044091269	1.50E-09	2.75E-08	0	0	0	4.812122267	3.955228997	3.753887089	A1-	ncRNA	
AT4G05025	14.491238	-4.023225	0.486810329	-8.26446136	1.40E-16	5.32E-15	0	0	0	4.88574345	4.792504907	5.029925195	A1-	ncRNA	
AT4G05025	14.31584	-4.252794	0.550896091	-7.719774592	1.17E-14	3.79E-13	0	0	0	5.192160237	4.786788781	4.628319815	A1+	ncRNA	
AT4G05205	29.717519	-4.819155	0.451258748	-10.67936007	1.27E-26	8.88E-25	0.602380384	0	0	5.530616574	6.024848039	6.11789374	A1-	ncRNA	
AT4G05275	31.925181	-4.565796	0.479211376	-9.527729032	1.61E-21	8.29E-20	0	0	0	4.56149373	6.679626697	6.096513381	A1-	ncRNA	
AT4G05275	95.997712	-6.83138	0.467271465	-14.61972342	2.10E-48	5.30E-46	0	0	0	7.935660723	7.28341303	7.478705843	A1+	ncRNA	
AT4G05275	8.8167831	-0.67484	0.144329398	-4.675694995	2.93E-06	0.0002756	0	0	0	4.357162671	4.49088377	3.691684035	A2+	ncRNA	
AT4G05715	53.420059	-5.785971	0.43636386	-13.259511	3.97E-40	5.11E-38	0	0	0	7.030399376	6.024848039	6.996420111	A1-	ncRNA	
AT4G05715	63.737038	-6.309307	0.481567844	-13.10159593	3.22E-39	5.08E-37	0	0	0	7.245106023	6.574739482	7.112669494	A1-	ncRNA	
AT4G06225	73.952946	2.3236194	0.296344236	7.840946877	4.47E-15	1.49E-13	6.702182107	7.216534536	7.089741713	4.486881573	3.546623725	4.730144422	A1-	ncRNA	
AT4G06225	77.890846	2.7032611	0.325856971	8.29585175	1.08E-16	4.17E-15	6.809150372	7.324729778	7.19916109	4.626795005	3.04536424	4.391288416	A1+	ncRNA	
AT4G06225	70.3751	2.3267078	0.303180652	7.674327995	1.66E-14	1.21E-12	6.605082971	7.122553314	6.998571252	4.697193151	4.593952335	3.764554301	A2-	ncRNA	
AT4G06835	42.172386	-5.375498	0.433468414	-12.40113051	2.58E-35	2.68E-33	0.602380384	0	0	6.691428291	6.13861985	6.352426407	A1-	ncRNA	
AT4G06835	36.603391	-5.452186	0.486957893	-11.19642241	4.25E-29	3.83E-27	0.640148721	0	0	6.205775127	6.200761211	6.222935658	A1+	ncRNA	
AT4G07250	4.9453716	-2.490548	0.515041314	-4.835627023	1.33E-06	1.79E-05	0	0	0	3.816762292	2.665086523	3.613294506	A1-	ncRNA	
AT4G07250	7.2616747	-3.294327	0.581130161	-5.668827486	1.44E-08	2.27E-07	0	0	0	4.021446993	3.710677785	4.107506639	A1-	ncRNA	
AT4G12917	28.754857	2.6664719	0.403785184	6.603689244	4.01E-11	9.54E-10	5.751099165	5.519575713	5.920918954	2.526213436	2.665086523	2.610741738	A1+	ncRNA	
AT4G12917	35.453267	1.7657682	0.359614275	4.910172616	9.10E-07	1.10E-05	5.857134047	5.626188002	6.029365218	3.862584211	3.955228997	3.998987077	A1+	ncRNA	
AT4G15242	40.076715	-5.198751	0.426891458	-12.17815555	4.06E-34	3.90E-32	0.602380384	0	0	6.633468127	6.397633656	6.024848039	6.538339128	A1-	ncRNA
AT4G15242	24.620587	-4.544712	0.512469698	-8.86825528	7.43E-19	3.45E-17	0.640148721	0	0	0.694589061	4.896561069	6.050935773	5.740406713	A1+	ncRNA
AT4G15242	9.1882805	-0.602987	0.143486897	-4.202386953	2.64E-05	2.07E-03	0.954186367	0	0	1.024858076	3.734687502	4.854512068	3.798546962	A2+	ncRNA
AT5G02055	86.772778	2.5558124	0.361255996	7.074795829	1.50E-12	4.05E-11	7.241112308	7.77354067	6.432438154	4.041933031	5.26298084	3.935732613	A1-	ncRNA	
AT5G02055	88.600286	3.0992307	0.391418267	7.917951205	2.41E-15	8.34E-14	7.348392176	7.881961892	6.541407703	4.16453883	4.164272639	3.284432598	A1+	ncRNA	
AT5G02055	78.698431	2.5048905	0.353510311	7.085763498	1.38E-12	7.59E-11	7.143709534	7.679330847	6.341669335	3.751761308	4.491625127	3.881211899	A2-	ncRNA	
AT5G02645	183.06143	2.6156896	0.210388554	12.4326611	1.74E-35	1.83E-33	8.251135012	8.427751358	8.240166489	5.530616574	5.901330042	5.553777891	A1-	ncRNA	
AT5G02645	190.29001	2.9288383	0.223982625	13.07618529	4.50E-39	7.02E-37	8.358761198	8.536347396	8.350014033	5.437371235	4.786788781	5.671366059	A1+	ncRNA	
AT5G02645	162.59499	3.1565002	0.23940612	13.18470972	1.07E-39	5.27E-37	8.153394626	8.333378573	8.148613507	5.263497762	4.491625127	4.88827397	A2-	ncRNA	
AT5G05005	21.767391	-4.572814	0.469111493	-9.747818705	1.88E-22	1.03E-20	0	0	0	5.414644739	5.617177427	5.387868903	A1-	ncRNA	
AT5G05005	11.253832	-3.26372	0.586088875	-5.568644308	2.57E-08	3.92E-07	0	0	0	5.646896475	3.416037926	3.284432598	A1+	ncRNA	
AT5G09505	94.107807	2.4192131	0.350666098	6.898907918	5.24E-12	1.34E-10	7.289703994	7.942732892	6.497922124	4.408199229	5.046836798	4.553113256	A1-	ncRNA	
AT5G09505	95.938344	3.0652989	0.389840635	7.862953727	3.75E-15	1.28E-13	7.397006648	8.051207178	6.606946228	3.684038477	4.508850015	3.881635851	A1+	ncRNA	
AT5G09505	83.328881	2.6718322	0.360704315	7.407264415	1.29E-13	8.28E-12	7.192279014	7.848473607	6.407104606	3.219377994	4.262230145	3.989138089	A2-	ncRNA	
AT5G38005	33.731313	-2.713038	0.367301321	-7.386410702	1.51E-13	4.45E-12	3.045280967	2.917335146	3.078658264	5.861134793	5.046836798	6.538339128	A1-	ncRNA	
AT5G38005	69.574642	-3.250172	0.473362337	-6.866139013	6.60E-12	1.64E-10	3.140591735	3.012283854	3.17624359	4.722432463	7.707306794	7.341000853	A1+	ncRNA	
rRNAs															
AT2G01010	3295391.4	-3.751054	0.507863981	-7.385941303	1.51E-13	4.44E-12	16.69229962	18.26786165	17.33721329	22.42885568	23.3182788	21.55438117	A1+	rRNA	
AT2G01010	3526008.2	-2.380492	0.454930768	-5.232646511	1.67E-07	3.95E-06	16.48626062	18.06430481	17.13514948	23.7354431	22.02422948	21.20335748	A2-	rRNA	
AT3G41768	3791353.1	-3.786996	0.509862872	-7.427479557	1.11E-13	3.28E-12	16.81472678	18.40595433	17.46228853	22.63101579	23.52562975	21.75266084	A1+	rRNA	

AT1G41768	4039253.4	-2.396709	0.454946145	-5.268115394	1.38E-07	3.32E-06	16.60868761	18.20239743	17.26022461	23.93081247	22.22995819	21.39951895	A2-	rRNA
snoRNAs														
AT1G04517	23.219139	3.2372332	0.451975708	7.162405194	7.93E-13	2.19E-11	5.459832183	5.503631239	5.635183114	1.131025967	0	1.60562261	A1-	snoRNA
AT1G04517	25.294096	3.2934347	0.491257017	6.704097012	2.03E-11	4.73E-10	5.565434319	5.610218077	5.743245306	0	0	2.58406216	A1+	snoRNA
AT1G04517	21.705127	2.9537402	0.419467162	7.041648299	1.90E-12	1.02E-10	5.364062716	5.411129121	5.545223732	0	1.407936067	1.100718415	A2-	snoRNA
AT1G04527	24.593383	3.3889002	0.463000314	7.319433928	2.49E-13	7.18E-12	5.89624286	5.201540617	5.700220394	1.131025967	0	1.015522753	A1-	snoRNA
AT1G04527	27.032315	3.3325395	0.493637547	6.750984627	1.47E-11	3.48E-10	6.00246284	5.30758796	5.808376819	1.429370861	0	2.247074573	A1+	snoRNA
AT1G04527	23.252455	2.8235328	0.420817487	6.709637413	1.95E-11	8.72E-10	5.799872345	5.10953994	5.610176994	0	0	2.148557953	A2-	snoRNA
AT1G05247	256.583	2.0676163	0.474633535	4.356237214	1.32E-05	0.0001491	8.313564819	9.316947419	8.681785153	4.94268382	6.889210391	4.887807353	A1-	snoRNA
AT1G05247	259.67917	3.8079054	0.305305198	12.47245528	1.06E-35	1.40E-33	8.421205468	9.425683623	8.791725241	4.626795005	5.310931324	4.699400813	A1+	snoRNA
AT1G05247	225.6679	3.5251882	0.300594841	11.72737431	9.23E-32	2.75E-29	8.21581033	9.222443943	8.590149466	4.697193151	5.018717888	4.43316397	A2-	snoRNA
AT1G05917	518.52924	3.1763787	0.411035928	7.727739765	1.09E-14	3.54E-13	9.798090474	10.23059788	9.694066052	5.454346907	6.889210391	5.117444234	A1-	snoRNA
AT1G05917	544.95368	4.5185175	0.243039194	18.59172343	3.75E-77	2.92E-74	9.905941279	10.33941125	9.804136429	5.379864119	5.823389642	4.831847463	A1+	snoRNA
AT1G05917	476.34405	4.1549269	0.234922559	17.68636829	5.34E-70	1.47E-66	9.700131027	10.13602245	9.602313907	5.669115043	5.403926096	5.189154551	A2-	snoRNA
AT1G06087	86.036178	1.5143162	0.282411756	5.362086286	8.23E-08	1.34E-06	6.958103052	7.274061416	6.78702067	4.764642118	5.766238278	5.674125282	A1-	snoRNA
AT1G06087	93.870613	1.4223606	0.253178836	5.618007336	1.93E-08	3.00E-07	7.065233812	7.38228424	6.896258094	5.646896475	5.476812514	5.773726325	A1+	snoRNA
AT1G06087	65.104585	2.6180028	0.374154983	6.997107983	2.61E-12	1.38E-10	6.86084559	7.180036492	6.6960127	1.407936067	4.578473362	4.578473362	A2-	snoRNA
AT1G06243	216.92693	2.1309216	0.283214472	7.524056209	5.31E-14	1.62E-12	8.241286045	8.891602497	8.187268232	5.530616574	6.952811471	6.096513381	A1-	snoRNA
AT1G06243	214.12524	2.9488991	0.271844816	10.84772978	2.04E-27	1.66E-25	8.34890989	9.000282301	8.297102669	5.545934233	5.823389642	5.1178917	A1+	snoRNA
AT1G06243	193.97859	2.4221971	0.27596083	8.77732207	1.67E-18	1.71E-16	8.143547939	8.797151611	8.095726963	6.394694577	5.403926096	5.399380504	A2-	snoRNA
AT1G06453	3433.6808	2.1856308	0.154458761	14.15025449	1.86E-45	2.90E-43	12.3674824	12.50025936	12.5213162	10.01905655	10.57332173	10.09019609	A1+	snoRNA
AT1G06453	3653.028	2.3134996	0.101479959	22.79760087	4.84E-115	8.89E-112	12.47543037	12.60914193	12.63149662	10.11868132	10.27528698	10.32759529	A1+	snoRNA
AT1G06453	2909.2632	3.0085106	0.264643285	11.36817266	6.02E-30	1.49E-27	12.26942817	12.40561939	12.42946568	8.759290069	8.329989586	9.692461628	A2-	snoRNA
AT1G07593	24.917296	3.2406977	0.458958956	7.060974863	1.65E-12	4.46E-11	5.372294687	5.421153397	6.02613228	0	0	2.023221944	A1+	snoRNA
AT1G07593	28.6164	2.7496809	0.453446839	6.063954292	1.33E-09	2.45E-08	5.477748719	5.527603984	6.13470185	2.604042178	1.773370384	2.857049598	A1-	snoRNA
AT1G07593	23.242549	2.944716	0.425129504	6.926632884	4.31E-12	2.16E-10	5.276669222	5.328777953	5.935720392	0	0	1.717749548	A2-	snoRNA
AT1G07897	537.78415	2.1107167	0.449423416	4.696499234	2.65E-06	3.37E-05	9.37009857	10.07475427	10.08881785	6.224753232	7.977879279	6.259291536	A1+	snoRNA
AT1G07897	586.64852	2.6238478	0.220816106	11.791929	4.30E-32	4.70E-30	9.477909016	10.18355768	10.19891889	7.037640449	7.54863521	7.284328671	A1+	snoRNA
AT1G07897	461.63003	3.9092054	0.272677219	14.3363843	1.30E-46	8.94E-44	9.272178488	9.980188119	9.997038292	5.098259903	4.943185652	5.919339118	A2-	snoRNA
AT1G08117	27.692177	2.5361253	0.399660246	6.345703294	2.21E-10	4.83E-09	5.509913585	5.698312318	5.792588979	2.526213436	2.665086523	2.833863982	A1+	snoRNA
AT1G08117	31.578144	2.232108	0.396424726	5.630597427	1.80E-08	2.80E-07	5.615596492	5.805191445	5.900872131	3.684038477	3.416037926	2.857049598	A1+	snoRNA
AT1G08117	26.947695	2.1191618	0.368850758	5.745309638	9.18E-09	2.71E-07	5.414065571	5.605538376	5.70243257	3.219377994	2.575486135	3.171895698	A2-	snoRNA
AT1G08353	29.366595	2.5008422	0.40266447	6.210734804	5.27E-10	1.11E-08	5.751099165	5.404076523	6.0387604	2.526213436	2.665086523	3.027056186	A1-	snoRNA
AT1G08353	31.729082	2.5815371	0.436945632	5.90814263	3.46E-09	5.96E-08	5.857134047	5.510497912	6.147344174	1.429370861	3.04536424	3.458449401	A1+	snoRNA
AT1G08353	25.274927	3.0651383	0.419639419	7.304219191	2.79E-13	1.71E-11	5.654908771	5.311728223	5.948335841	0	1.407936067	1.100718415	A2-	snoRNA
AT1G08937	129.85936	2.4537107	0.25065858	9.789055141	1.25E-22	6.95E-21	7.758751624	7.608172481	8.047421967	4.997461935	5.046836798	5.45643433	A1-	snoRNA
AT1G08937	141.78645	2.3906042	0.252566513	9.465246244	2.93E-21	1.61E-19	7.866238886	7.716535461	8.157219345	5.051918249	5.310931324	5.773726325	A1+	snoRNA
AT1G08937	112.92637	3.1246058	0.300584093	10.39511352	2.61E-25	4.76E-23	7.661146689	7.514016942	7.955913814	3.751761308	3.212236784	4.772209565	A2-	snoRNA
AT1G09087	37.315144	2.2043579	0.370147802	5.955345055	2.60E-09	5.12E-08	5.694476593	5.894484451	6.343626073	3.025182302	4.089833736	3.613294506	A1-	snoRNA
AT1G09087	39.585418	2.2504196	0.386602596	5.821015168	5.85E-09	9.77E-08	5.800434055	6.001620748	6.452517557	3.242825326	3.416037926	3.998987077	A1+	snoRNA
AT1G09087	31.983828	2.768443	0.395162055	7.005842275	2.46E-12	1.30E-10	5.598361522	5.801471258	6.252926932	3.219377994	2.575486135	1.100718415	A2-	snoRNA
AT1G09787	192.22253	2.6249574	0.298007517	8.808359607	1.27E-18	5.45E-17	8.10672694	8.574255406	8.462658347	4.324976877	6.13861985	5.888334403	A1+	snoRNA
AT1G09787	206.98519	2.7173653	0.237665646	11.4335637	2.84E-30	2.76E-28	8.214317172	8.682880863	8.572556049	5.829815291	5.997324674	5.265734139	A1+	snoRNA
AT1G09787	162.34738	3.9627019	0.304648524	13.0074549	1.11E-38	5.10E-36	8.009021612	8.479855192	8.371060541	2.366511377	2.928709658	4.43316397	A2-	snoRNA
AT1G12013	1167.3385	2.5666408	0.189721773	13.52844625	1.06E-41	1.47E-39	11.02674146	10.66801514	11.19813873	8.114333143	8.12317979	8.612001074	A1-	snoRNA, SNOR111 small nucleolar RNA111, Encodes a H/ACA-box snoRNA (snoR111)
AT1G12013	1278.1098	2.4518478	0.189447222	12.94211558	2.60E-38	3.89E-36	11.13465926	10.77685135	11.30829204	8.429358011	8.289966426	8.901296897	A1+	snoRNA, SNOR111 small nucleolar RNA111, Encodes a H/ACA-box snoRNA (snoR111)
AT1G12013	1018.2135	3.2581262	0.28328753	11.50112811	1.30E-30	3.46E-28	10.92871667	10.57341841	11.10631245	6.464267165	6.739154825	7.921922333	A2-	snoRNA, SNOR111 small nucleolar RNA111, Encodes a H/ACA-box snoRNA (snoR111)
AT1G74456	86.445678	2.1211635	0.26587131	7.978158606	1.49E-15	5.19E-14	7.175392869	7.156618187	7.183705966	4.408199229	5.046836798	5.239507661	A1-	snoRNA
AT1G74456	88.729407	2.623643	0.274137658	9.570531146	1.06E-21	6.09E-20	7.282640674	7.264783507	7.293174481	4.626795005	4.786788781	4.302754999	A1+	snoRNA
AT1G74456	76.980778	2.3537816	0.279585449	8.418827407	3.80E-17	3.53E-15	7.078021345	7.062646845	7.092491617	4.13977271	3.830719935	4.94298265	A2-	snoRNA
AT1G75163	49.197211	2.3974089	0.356426406	6.726238297	1.74E-11	4.26E-10	6.190466913	6.819292537	6.124191366	3.689466061	4.483532941	3.349749908	A1-	snoRNA

AT1G75163	51.05374	2.6543309	0.382690912	6.935965374	4.03E-12	1.02E-10	6.29700948	6.927264094	6.23286803	2.958502988	3.955228997	3.753887089	A1+	snoRNA
AT1G75163	43.990716	2.624445	0.367930168	7.13301395	9.82E-13	5.52E-11	6.093782378	6.725501714	6.03368393	4.13977271	2.575486135	2.749120822	A2-	snoRNA
AT2G06855	20.931565	1.8943863	0.436167985	4.343249229	1.40E-05	0.0001575	5.44274445	5.201540617	5.072871496	1.757146478	0	3.728967903	A1-	snoRNA
AT2G06855	20.909296	3.1433119	0.508188047	6.185332159	6.20E-10	1.19E-08	5.548318378	5.30758796	5.179914355	2.133098153	1.773370384	0	A1+	snoRNA
AT2G06855	19.233713	2.1417382	0.404786412	5.29103273	1.22E-07	2.97E-06	5.347002412	5.10953994	4.983820297	2.366511377	1.407936067	2.749120822	A2-	snoRNA
AT2G07605	338.45148	4.2670513	0.235084603	18.15113062	1.26E-73	5.39E-71	9.101388046	9.469408531	9.427383815	4.826463083	5.046836798	4.837143627	A1-	snoRNA
AT2G07605	366.17689	4.228809	0.231082292	18.30001318	8.27E-75	5.45E-72	9.209166304	9.57816123	9.537428184	4.812122267	5.396254736	5.065040979	A1+	snoRNA
AT2G07605	316.63301	4.1216597	0.240377596	17.14660519	6.66E-66	1.05E-62	9.003499358	9.374889674	9.335654918	4.697193151	4.689499909	4.94298265	A2-	snoRNA
AT2G08375	28.13785	2.0883649	0.403727541	5.172708424	2.31E-07	3.50E-06	5.620422581	6.000540497	5.299658902	3.816762292	0	2.833863982	A1-	snoRNA
AT2G08375	28.287035	3.108885	0.475206672	6.542174478	6.06E-11	1.33E-09	5.726274087	6.107801916	5.407161218	2.133098153	0	2.58406216	A1+	snoRNA
AT2G08375	24.468135	2.6531768	0.408632107	6.49282515	8.42E-11	3.43E-09	5.524410585	5.90741087	5.210198496	0	2.106732017	2.148557953	A2-	snoRNA
AT2G08725	69.048748	2.7961517	0.314816353	8.881850103	6.58E-19	2.87E-17	6.680479387	7.067236961	7.101827421	3.689460601	4.089833736	4.028969492	A1-	snoRNA
AT2G08725	75.553025	2.6977062	0.319619627	8.440364664	3.16E-17	1.28E-15	6.787432498	7.17535527	7.2112533	4.626795005	4.164272639	3.753887089	A1+	snoRNA
AT2G08725	63.951043	2.5973663	0.312177484	8.320159045	8.78E-17	7.85E-15	6.583395012	6.973309422	7.010651154	2.366511377	3.9893347	4.18342451	A2-	snoRNA
AT2G08900	32.911927	2.3287388	0.40690706	5.723023813	1.05E-08	1.90E-07	5.66530953	6.211553858	5.477153115	2.192330878	4.483532941	2.833863982	A1-	snoRNA
AT2G08900	31.514505	3.118112	0.467490304	6.66989667	2.56E-11	5.91E-10	5.771225908	6.31903844	5.584967802	2.133098153	0	2.857049598	A1+	snoRNA
AT2G08900	28.080058	2.475544	0.397461143	6.228392604	4.71E-10	1.78E-08	5.569234427	6.118216516	5.387414361	2.366511377	1.407936067	2.975939682	A2-	snoRNA
AT2G08910	91.126945	3.8056712	0.330686581	11.5083933	1.20E-30	1.01E-28	7.452214476	7.648609059	7.239470236	3.222033331	2.665086523	3.349749908	A1-	snoRNA
AT2G08910	99.539817	3.7654976	0.333439211	11.29290571	1.42E-29	1.32E-27	7.559587988	7.756986903	7.348966434	3.480233365	3.710677785	3.458449401	A1+	snoRNA
AT2G08910	85.157825	3.6501074	0.327773739	11.13605806	8.37E-29	1.97E-26	7.354720429	7.554439666	7.148231159	2.366511377	3.212236784	3.171895698	A2-	snoRNA
AT2G09705	292.24816	2.9193911	0.207336632	14.08044042	5.01E-45	7.71E-43	8.83451826	9.010611693	9.170517665	5.769679089	6.602405842	5.888334403	A1-	snoRNA
AT2G09705	327.91736	2.4077987	0.18287363	13.16646216	1.37E-39	2.20E-37	8.942258029	9.119309897	8.280532003	6.391824885	6.747047976	6.809500787	A1+	snoRNA
AT2G09705	260.59487	3.4138159	0.265239693	12.87068274	6.58E-38	2.79E-35	8.736667109	8.9161445	9.078815614	5.98536134	3.9893347	5.318927657	A2-	snoRNA
AT2G35387	83.816929	3.5957466	0.324662653	11.07533191	1.65E-28	1.27E-26	7.175392869	7.446603607	7.271922665	3.025182302	4.089833736	3.349749908	A1-	snoRNA
AT2G35387	89.671937	3.690752	0.335366536	11.00512904	3.61E-28	3.09E-26	7.282640674	7.554902855	7.381434488	3.242825326	3.710677785	3.458449401	A1+	snoRNA
AT2G35387	77.251891	3.3436159	0.319950934	10.450402	1.46E-25	2.68E-23	7.078021345	7.352507464	7.180669633	0	3.9893347	3.171895698	A2-	snoRNA
AT2G35744	384.23273	3.0917277	0.237957406	12.99277799	1.34E-38	1.61E-36	8.991111109	9.817775184	9.41532859	6.292034142	6.13861985	6.096513381	A1-	snoRNA
AT2G35744	413.44923	3.1971334	0.240743337	13.28025704	3.01E-40	4.93E-38	9.09887432	9.92659629	9.525371666	6.238497703	6.460522959	6.015744504	A1+	snoRNA
AT2G35744	366.27336	2.8017397	0.27096007	10.34004627	4.64E-25	8.40E-23	8.893237096	9.723226723	9.32360085	6.823201689	6.298620126	5.650144966	A2-	snoRNA
AT2G35747	317.21625	3.0215096	0.261648055	11.54799193	7.56E-31	6.47E-29	8.998438693	9.623976327	8.697798685	5.890375522	6.342337877	5.730732322	A1+	snoRNA
AT2G35747	335.38114	3.3012162	0.26304751	12.54988575	3.98E-36	5.41E-34	9.10620294	9.732744061	8.807741625	5.829815291	5.823389642	5.773726325	A1+	snoRNA
AT2G35747	303.2958	2.6678908	0.267934764	9.957240123	2.34E-23	3.60E-21	8.900563669	9.52944345	8.606160448	6.594090181	6.03318807	5.835067996	A2-	snoRNA
AT3G01155	92.579904	2.9495531	0.316892092	9.307752331	1.31E-20	6.41E-19	7.062469209	7.543361337	7.452655121	3.222033331	5.26298084	4.199106927	A1-	snoRNA
AT3G01155	102.55071	2.526211	0.278995223	9.054674613	1.37E-19	6.78E-18	7.16965839	7.651699606	7.56224781	4.722432463	5.123468832	4.699400813	A1+	snoRNA
AT3G01155	80.346875	3.5393768	0.333680474	10.60708379	2.76E-26	5.40E-24	6.965154819	7.449228828	7.361329851	2.366511377	3.44909067	2.975939682	A2-	snoRNA
AT3G02445	110.35528	3.2662663	0.341666794	9.559800331	1.18E-21	6.15E-20	7.447938931	8.226323448	7.149182564	4.041933031	4.483532941	3.728967903	A1-	snoRNA
AT3G02445	119.84433	3.1135297	0.354423421	8.784774243	1.57E-18	7.03E-17	7.555310678	8.334873834	7.258633396	3.862584211	4.164272639	4.831847463	A1+	snoRNA
AT3G02445	100.52375	3.3681893	0.35039291	9.612607012	7.07E-22	9.47E-20	7.350446602	8.131993222	7.057984008	3.219377994	3.212236784	3.764554301	A2-	snoRNA
AT3G03175	19.847794	2.5346772	0.445210937	5.69320526	1.25E-08	2.25E-07	4.932557833	5.31552177	5.361282085	1.131025967	2.665086523	2.346684959	A1-	snoRNA
AT3G03175	21.567552	2.5727862	0.471078613	5.461479424	4.72E-08	6.95E-07	5.037115057	5.421786065	5.46889724	2.604042178	2.545235219	1.806583236	A1+	snoRNA
AT3G03175	17.312618	2.6559317	0.430340674	6.171695614	6.76E-10	2.49E-08	4.837803717	5.223319487	5.271721142	0	0	1.717749548	A2-	snoRNA
AT3G05335	86.901842	2.4493686	0.284937522	8.596160218	8.24E-18	3.38E-16	7.133409862	7.324852229	7.113812726	4.142578534	5.617177427	4.42174209	A1-	snoRNA
AT3G05335	90.375789	2.5157954	0.273371296	9.202851428	3.49E-20	1.78E-18	7.240636406	7.433098507	7.223244998	4.626795005	4.346824447	4.893773618	A1+	snoRNA
AT3G05335	78.051182	2.601759	0.293807318	8.855320168	8.34E-19	8.86E-17	7.036059059	7.23080545	7.022630749	5.098259903	3.212236784	4.271562656	A2-	snoRNA
AT3G09865	169.13045	2.7740677	0.217325094	12.76459912	2.58E-37	2.94E-35	8.149482156	8.302025239	8.215351027	5.373818996	5.45092181	5.278003551	A1-	snoRNA
AT3G09865	179.78219	2.9465887	0.217895592	13.52293842	1.15E-41	2.00E-39	8.25708341	8.410593534	8.325192482	5.257479592	5.220242777	5.399824542	A1+	snoRNA
AT3G09865	149.71405	3.40665	0.253089591	13.46025343	2.68E-41	1.41E-38	8.05176608	8.207678317	8.123803486	4.445238744	4.132225326	4.645984426	A2-	snoRNA
AT3G13855	262.22886	3.8419861	0.219651489	17.49128189	1.67E-68	6.04E-66	8.961422831	8.912886428	9.000188337	4.94268382	4.483532941	5.074348265	A1+	snoRNA, U6 small nucleolar RNA26
AT3G13855	288.39783	3.4684014	0.226236345	15.33087633	4.76E-53	1.45E-50	9.069181791	9.021569467	9.110179598	5.257479592	4.654502272	5.987621232	A1+	snoRNA, U6 small nucleolar RNA26
AT3G13855	241.27046	4.3339458	0.252727098	17.14871809	6.43E-66	1.05E-62	8.863552963	8.818432526	8.908506911	4.445238744	3.9893347	4.18342451	A2-	snoRNA, U6 small nucleolar RNA26
AT3G14735	262.34318	3.8212114	0.218705487	17.47195014	2.34E-68	8.25E-66	8.961422831	8.911376517	9.000188337	4.997461935	4.483532941	5.074348265	A1-	snoRNA, U6 small nucleolar RNA1
AT3G14735	288.30721	3.4678828	0.226300079	15.32426704	5.26E-53	1.57E-50	9.069181791	9.020059328	9.110179598	5.257479592	4.654502272	5.987621232	A1+	snoRNA, U6 small nucleolar RNA1
AT3G21805	770.43056	2.4049657	0.475595051	5.05675099	4.26E-07	6.21E-06	9.976395522	10.86417755	10.43113328	5.70532018	7.946976782	6.27840572	A1-	snoRNA
AT3G21805	794.10692	4.3916438	0.271738529	16.16128503	9.46E-59	3.52E-56	10.08425991	10.97302195	10.5412549	6.503738247	5.625572377	5.482759454	A1+	snoRNA

AT3G21805	696.92475	3.9092219	0.247888576	15.77007705	5.00E-56	4.80E-53	9.878422823	10.76957318	10.33933533	5.782409601	6.328611903	6.122608045	A2-	snoRNA
AT3G47348	309.12112	2.378436	0.175457323	13.55563825	7.34E-42	1.04E-39	8.989641116	9.155406717	8.944233915	6.496028094	6.602405842	6.674430901	A1-	snoRNA
AT3G47348	326.14097	2.6319017	0.182889941	14.39063153	5.93E-47	1.29E-44	9.097404118	9.264123433	9.054216982	6.138015508	6.810594236	6.425196846	A1+	snoRNA
AT3G47348	282.78739	2.5754513	0.188109548	13.69123112	1.15E-42	6.84E-40	8.891767306	9.060921413	8.852559814	6.394694577	5.996292971	6.382187399	A2-	snoRNA
AT3G50825	141.44121	2.9017036	0.246214366	11.78527319	4.65E-32	4.18E-30	7.961317368	8.102113116	7.990056538	5.101147555	2.665086523	5.1592901	A1-	snoRNA
AT3G50825	157.04446	2.8440914	0.225931807	12.58827346	2.45E-36	3.35E-34	8.068867569	8.210632003	8.099837644	5.257479592	5.019733684	5.265734139	A1+	snoRNA
AT3G50825	129.73624	3.4073302	0.264566906	12.87889804	5.92E-38	2.56E-35	7.863651069	8.007812254	7.898562926	4.13977271	4.381482195	4.089549378	A2-	snoRNA
AT4G06010	164.24242	2.3556333	0.251026914	9.383986852	6.35E-21	3.16E-19	7.772493982	8.436176083	8.084436315	5.737858488	5.901330042	5.387686903	A1-	snoRNA
AT4G06010	172.48461	2.5945095	0.255770214	10.14390786	3.53E-24	2.46E-22	7.879985799	8.544773895	8.194243854	5.74125297	5.476812514	5.356497891	A1+	snoRNA
AT4G06010	156.62084	2.1727385	0.258115595	8.417695489	3.84E-17	3.55E-15	7.674884605	8.341801644	7.992919083	6.163252036	5.661270196	5.318927657	A2-	snoRNA
AT4G06240	68.348933	2.7541136	0.323725675	8.507553915	1.78E-17	7.16E-16	6.620956795	7.156618187	7.046626167	3.549829232	3.546623725	4.277198875	A1-	snoRNA
AT4G06240	72.397866	3.1158781	0.346394685	8.995167067	2.36E-19	1.15E-17	6.727867157	7.264783507	7.156021903	4.021446993	3.04536424	3.753887089	A1+	snoRNA
AT4G06240	65.406785	2.5425544	0.319151557	7.966605066	1.63E-15	1.34E-13	6.523914066	7.062646845	6.955476821	4.13977271	4.381482195	3.344390632	A2-	snoRNA
AT4G06250	78.882345	2.6986309	0.291248594	9.265730116	1.94E-20	9.99E-19	6.987859024	7.274061416	7.189380394	4.041933031	3.546623725	4.553113256	A1-	snoRNA
AT4G06250	83.811852	3.1554501	0.317512615	9.938030606	2.84E-23	1.85E-21	7.095006873	7.38228424	7.298851775	3.684038477	4.508850015	3.6137176	A1+	snoRNA
AT4G06250	72.385533	2.9572797	0.304229235	9.720563773	2.46E-22	3.47E-20	6.890584909	7.180036492	7.098163484	3.751761308	6.352487504	3.764554301	A2-	snoRNA
AT4G06310	78.543778	2.7242078	0.293688728	9.275833674	1.76E-20	8.61E-19	6.958103052	7.283430105	7.19503259	4.041933031	3.546623725	4.488922482	A1-	snoRNA
AT4G06310	84.48376	3.019074	0.326259146	9.253607241	2.17E-20	1.13E-18	7.065233812	7.391657317	7.304506815	3.242825326	4.907957693	3.753887089	A1+	snoRNA
AT4G06310	71.119009	3.0076698	0.310916001	9.673576654	3.90E-22	5.32E-20	6.86084559	7.189401091	7.10381314	2.366511377	3.830719935	3.764554301	A2-	snoRNA
AT4G07625	36.644043	3.5183175	0.430750803	8.167872145	3.14E-16	1.15E-14	5.818888546	6.324776786	6.193595463	1.757146478	3.546623725	0	A1-	snoRNA
AT4G07625	38.766109	3.5532625	0.44996692	7.896719478	2.86E-15	9.84E-14	5.9250122	6.432368802	6.302343639	2.133098153	1.773370384	2.247074573	A1+	snoRNA
AT4G07625	35.42415	2.6599551	0.376041457	7.073568645	1.51E-12	8.25E-11	5.722611772	6.23133989	6.103024215	3.219377994	3.212236784	1.717749548	A2-	snoRNA
AT4G07635	126.09933	3.2757592	0.263043985	12.45327529	1.34E-35	1.42E-33	7.849068745	7.974892644	7.757738543	4.408199229	4.483532941	4.351279944	A1-	snoRNA
AT4G07635	131.82729	3.9066605	0.318661701	12.2593975	1.50E-34	1.82E-32	7.956585164	8.08337633	7.867446715	4.626795005	3.710677785	2.58406216	A1+	snoRNA
AT4G07635	121.26384	3.0038614	0.268727927	11.1780766	5.22E-29	1.24E-26	7.751435384	7.880624596	7.666310099	5.411740146	4.381482195	3.989138089	A2-	snoRNA
AT4G15258	81.05739	2.605063	0.303435721	8.585221924	9.07E-18	3.86E-16	6.865515418	7.339335077	7.217261608	4.414102287	4.654502272	4.208431314	A1+	snoRNA, SNOR37-2 small nucleolar RNA37-2 Encodes a C/D box snoRNA (snoR37-2)
AT4G39361	264.39394	2.428293	0.211186864	11.4983146	1.35E-30	1.13E-28	8.519097462	9.044067528	8.839865209	6.154180496	6.434335581	6.352426407	A1-	snoRNA
AT4G39361	279.06718	2.6385369	0.209475591	12.59591559	2.22E-36	3.06E-34	8.626781536	9.152769484	8.949832114	6.238497703	6.102625836	6.270396543	A1+	snoRNA
AT4G39361	243.61429	2.5526745	0.244150511	10.45533126	1.39E-25	2.57E-23	8.421300627	8.949595987	8.748205552	6.464267165	6.104262848	5.437984731	A1-	snoRNA
AT4G39366	421.10016	2.211342	0.181079193	12.21201574	2.68E-34	2.61E-32	9.339266424	9.533628834	9.444093667	6.787814836	7.470110277	7.316086623	A1-	snoRNA
AT4G39366	441.5255	2.4136843	0.161724026	14.92471045	2.28E-50	6.09E-48	9.447703474	9.642387976	9.554139811	6.859769358	7.013254259	7.329843115	A1+	snoRNA
AT4G39366	370.44518	2.6535109	0.179005992	14.82358705	1.03E-49	8.43E-47	9.241349655	9.439103969	9.352363184	6.163252036	6.522722717	6.807710617	A2-	snoRNA
AT5G00750	332.76555	4.1072302	0.241031664	17.04021012	4.13E-65	1.25E-62	9.273137359	9.071366691	9.544914699	4.632436165	5.26298084	5.1592901	A1-	snoRNA
AT5G00750	367.93338	3.4839313	0.237047472	14.69718832	6.72E-49	1.71E-46	9.380936875	9.180072373	9.654971125	5.74125297	5.019733684	6.222935658	A1+	snoRNA
AT5G00750	307.15831	4.3345365	0.258187075	16.78835577	2.97E-63	3.64E-60	9.175227938	8.976891677	9.453175026	4.445238744	4.262230145	4.645984426	A2-	snoRNA
AT5G01785	273.40377	2.5348558	0.238785554	10.61561603	2.52E-26	1.72E-24	8.784531313	9.169370643	8.59038503	6.054369667	6.889210391	5.888334403	A1-	snoRNA
AT5G01785	303.01485	2.1602463	0.245553524	8.797455781	1.40E-18	6.34E-17	8.892263047	9.278089131	8.700308217	6.332434805	6.420348952	7.188751486	A1+	snoRNA
AT5G01785	255.9516	2.4055148	0.263004783	9.146277881	5.89E-20	6.92E-18	8.686687998	9.074883686	8.498764447	6.87521402	5.958429508	5.616881481	A2-	snoRNA
AT5G02655	69.463632	2.962621	0.320365989	9.247613835	2.30E-20	1.10E-18	7.180555873	7.045376151	6.733650715	3.933736191	3.546623725	3.613294506	A1-	snoRNA
AT5G02655	72.836865	3.5030697	0.359862388	9.734470156	2.15E-22	1.31E-20	7.28780625	7.15348251	6.842851908	3.684038477	3.04536424	3.086509522	A1+	snoRNA
AT5G02655	66.059554	2.8998605	0.329177359	8.809416665	1.26E-18	1.31E-16	7.083181843	6.951459744	6.642675095	4.697193151	3.212236784	2.975939682	A2-	snoRNA
AT5G02665	63.359	2.8010918	0.33564973	8.34528247	7.10E-17	2.74E-15	6.723653183	7.201787115	6.560562384	3.689460601	3.546623725	3.83605124	A1-	snoRNA
AT5G02665	66.034581	3.4018933	0.379394753	8.966632385	3.06E-19	1.48E-17	6.830546154	7.309975108	6.669636406	3.480233365	3.04536424	3.086509522	A1+	snoRNA
AT5G02665	55.125681	3.5635035	0.377732947	9.433922988	3.95E-21	5.01E-19	6.626449718	7.107794648	6.469700304	0	2.575486135	2.148557953	A2-	snoRNA
AT5G07105	742.36408	2.5816635	0.184726019	13.97563537	2.20E-44	3.32E-42	10.34103725	10.49434011	10.08197048	7.468757335	8.12317979	7.498313193	A1-	snoRNA
AT5G07105	810.55759	2.4321818	0.150418454	16.16943756	8.29E-59	3.13E-56	10.4489247	10.60316807	10.19207106	7.895187087	8.007659435	7.970467384	A1+	snoRNA
AT5G07105	655.87564	3.0740365	0.246427552	12.47440272	1.03E-35	3.79E-33	10.24304205	10.39975107	9.990191344	7.235050545	6.03318807	7.182110658	A2-	snoRNA
AT5G08515	94.12318	2.4831312	0.31348531	7.921044783	2.36E-15	8.07E-14	7.280115706	7.763533112	6.85286003	4.56149373	5.26298084	4.351279944	A1-	snoRNA
AT5G08515	95.518639	3.0859001	0.345073613	8.942729766	3.80E-19	1.83E-17	7.387413924	7.871950996	6.96214034	4.414102287	4.164272639	3.753887089	A1+	snoRNA
AT5G08515	85.989308	2.4001167	0.353107012	6.79713702	1.07E-11	4.97E-10	7.182695048	7.669326401	6.761831764	4.697193151	4.943185652	2.975939682	A2-	snoRNA
AT5G09515	91.113066	2.5651593	0.356332226	7.198785717	6.08E-13	1.69E-11	7.260744581	7.927874425	6.470220707	4.324976877	4.792504907	4.277198875	A1-	snoRNA
AT5G09515	93.529152	3.1949514	0.395324653	8.081842005	6.38E-16	2.32E-14	7.368034977	8.036344295	6.579222035	3.480233365	4.164272639	3.881635851	A1+	snoRNA
AT5G09515	81.800904	2.7088379	0.364302065	7.435691978	1.04E-13	6.78E-12	7.163333974	7.833619255	6.379423521	3.219377994	4.262230145	3.764554301	A2-	snoRNA

AT5G13225	84.200146	2.621689	0.376736791	6.958940695	3.43E-12	8.99E-11	7.206097323	7.756822631	6.36383995	3.933736191	5.26298084	3.487531741	A1-	snoRNA
AT5G13225	84.792521	3.3910591	0.407478556	8.322055455	8.65E-17	3.36E-15	7.31336029	7.865238264	6.472749626	3.862584211	3.416037926	3.086509522	A1+	snoRNA
AT5G13225	75.989401	2.6297157	0.362723089	7.249926371	4.17E-13	2.49E-11	7.108711022	7.662618018	6.273124571	3.751761308	4.262230145	3.498446379	A2-	snoRNA
AT5G46315	253.96666	3.7418728	0.218331935	17.13845857	7.67E-66	2.37E-63	8.918805325	8.843325624	8.945910989	4.997461935	4.792504907	5.074348265	A1-	snoRNA, U6 small nucleolar RNA29
AT5G46315	277.8219	3.4462011	0.228530775	15.0798118	2.20E-51	5.95E-49	9.026558028	8.951997912	9.055894306	5.192160237	4.654502272	5.958938819	A1+	snoRNA, U6 small nucleolar RNA29
AT5G46315	232.7394	4.3088034	0.255900862	16.83778397	1.29E-63	1.68E-60	8.82094156	8.748881747	8.854236664	4.697193151	3.830719935	4.089549378	A2-	snoRNA, U6 small nucleolar RNA29
AT5G51174	228.85452	3.1853596	0.260259757	12.23915524	1.92E-34	1.90E-32	8.246218933	9.016241821	8.756314475	5.373818996	5.617177427	5.117444234	A1-	snoRNA, SNO30, Encodes a C/D box snoRNA (snoR30)
AT5G51174	242.41172	3.5039781	0.274734398	12.7540567	2.96E-37	4.13E-35	8.353843953	9.124939907	8.866267573	5.192160237	5.476812514	4.767143513	A1+	snoRNA, SNO30, Encodes a C/D box snoRNA (snoR30)
AT5G51174	214.39405	2.981479	0.264606008	11.26761631	1.90E-29	4.55E-27	8.148479683	8.921773889	8.664667159	4.911618862	5.613343285	5.276953745	A2-	snoRNA, SNO30, Encodes a C/D box snoRNA (snoR30)
AT5G66564	122.99509	3.805936	0.290495111	13.10154908	3.23E-39	3.95E-37	7.819586838	7.992136787	7.832169608	3.689460601	2.665086523	4.028969492	A1-	snoRNA
AT5G66564	137.2616	3.4216382	0.266602206	12.83424562	1.05E-37	1.50E-35	7.927093939	8.100625429	7.941902437	4.29471016	4.654502272	4.391288416	A1+	snoRNA
AT5G66564	115.6202	3.7827074	0.296086617	12.77567835	2.24E-37	9.17E-35	7.72196256	7.89786412	7.740719132	3.751761308	3.652487504	3.344390632	A2-	snoRNA
snRNAs														
AT1G04263	852.78262	2.0146602	0.214093264	9.410198954	4.95E-21	2.48E-19	10.20070252	10.14581845	10.83930763	8.031448215	8.630654304	8.334564326	A1-	snRNA
AT1G04263	929.47497	1.9429112	0.200435434	9.693451748	3.21E-22	1.93E-20	10.30858178	10.25462653	10.94944819	8.371524085	8.525969037	8.69936184	A1+	snRNA
AT1G04263	708.82589	2.9498799	0.296059444	9.963809444	2.19E-23	3.41E-21	10.10271532	10.05124794	10.74749275	7.066322111	5.958429508	7.515650348	A2-	snRNA
AT1G05853	806.75193	2.0871132	0.211957303	9.846856855	7.07E-23	3.98E-21	10.12706734	10.08818113	10.77046823	7.964284092	8.508984911	8.123525489	A1-	snRNA
AT1G05853	878.29863	2.0091702	0.207564118	9.679757007	3.68E-22	2.19E-20	10.23494197	10.19698544	10.88060596	8.165743217	8.365964742	8.623717717	A1+	snRNA
AT1G05853	674.46391	2.9883551	0.298422822	10.01382896	1.33E-23	2.12E-21	10.02908465	9.993614144	10.67865588	6.973930171	5.796179779	7.393293768	A2-	snRNA
AT4G03995	923.19148	2.7653183	0.220577911	12.53669649	4.70E-36	1.82E-33	10.63877723	10.80693664	10.58077071	7.522814926	7.227101262	8.199777056	A2-	snRNA
AT4G04185	36.417973	1.986113	0.37500583	5.296218969	1.18E-07	1.88E-06	5.832072401	5.67001866	6.193595463	2.526213436	4.483532941	3.935732613	A1-	snRNA
AT4G04185	36.282964	2.3952139	0.413396006	5.79399373	6.87E-09	1.14E-07	5.93821284	5.776857722	6.302343639	2.133098153	3.04536424	3.998987077	A1+	snRNA
AT4G04185	28.939961	2.7656996	0.402518134	6.870993716	6.38E-12	3.09E-10	5.735779293	5.577281985	6.103024215	0	0	2.975939682	A2-	snRNA
AT4G04615	262.51767	3.8433552	0.219782271	17.48710291	1.80E-68	6.41E-66	8.962921844	8.911376517	9.005022865	4.94268382	4.483532941	5.074348265	A1-	snRNA
AT4G04615	288.70951	3.4698713	0.226421445	15.32483526	5.22E-53	1.57E-50	9.070681021	9.020059328	9.11501482	5.257479592	4.654502272	5.987621232	A1+	snRNA
AT4G04615	241.35049	4.3696455	0.254708728	17.15546027	5.72E-66	1.05E-62	8.865051765	8.816922827	8.91334082	4.445238744	3.9893347	4.089549378	A2-	snRNA
AT4G07875	262.49943	3.8433706	0.219716036	17.49244462	1.64E-68	6.00E-66	8.965915207	8.911376517	9.001801647	4.94268382	4.483532941	5.074348265	A1-	snRNA
AT4G07875	288.68953	3.4698485	0.226320695	15.3315564	4.71E-53	1.45E-50	9.073674816	9.020059328	9.11179314	5.257479592	4.654502272	5.987621232	A1+	snRNA
AT4G07875	241.33268	4.3698242	0.254643826	17.16053451	5.24E-66	1.05E-62	8.868044707	8.816922827	8.910120014	4.445238744	3.9893347	4.089549378	A2-	snRNA
AT4G09135	186.42738	4.6067339	0.29771503	15.47363566	5.23E-54	1.09E-51	8.377906668	8.645009697	8.448531371	3.549829232	4.483532941	3.027056186	A1-	snRNA
AT4G09135	206.4111	3.7731713	0.24862295	15.17627915	5.08E-52	1.48E-49	8.485561581	8.753648327	8.558426113	4.414102287	4.786788781	4.831847463	A1+	snRNA
AT4G09135	176.42014	4.102493	0.282282904	14.53326764	7.46E-48	5.31E-45	8.280138268	8.550597202	8.35693621	4.697193151	3.9893347	3.171895698	A2-	snRNA
AT5G04465	131.59793	2.6045921	0.250223738	10.40905292	2.25E-25	1.44E-23	7.796232554	7.666621214	8.099583006	5.197878395	4.483532941	5.199956346	A1-	snRNA
AT5G04465	156.67836	1.8401108	0.278126205	6.616099981	3.69E-11	8.35E-10	7.903732137	7.775005547	8.209394629	5.492673666	5.625572377	6.602556983	A1+	snRNA
AT5G04465	122.44718	2.5558965	0.261836278	9.761430108	1.65E-22	2.35E-20	7.698615605	7.572445774	8.008062125	3.751761308	5.090491598	5.233721953	A2-	snRNA
AT5G40395	67.327168	3.0354024	0.343574808	8.834764133	1.00E-18	4.34E-17	6.921566334	6.558810884	7.282579923	3.395221171	4.089833736	3.487531741	A1-	snRNA U6 acat
AT5G40395	74.309724	2.6265867	0.353380812	7.432737269	1.06E-13	3.16E-12	7.028675623	6.666598517	7.392096801	4.021446993	3.04536424	4.767143513	A1+	snRNA U6 acat
AT5G40395	61.627352	3.0887031	0.352874732	8.752973195	2.08E-18	2.10E-16	6.824329795	6.465191369	7.191322375	3.751761308	2.106732017	3.344390632	A2-	snRNA U6 acat
tRNAs														
AT2G07754	44.52511	2.171487	0.327509596	6.630300419	3.35E-11	8.03E-10	6.363880002	6.15142592	6.281227452	3.689460601	3.546623725	4.116544802	A1-	tRNA-Ser (anticodon: GCT)
AT2G07754	48.195904	2.2837394	0.334587185	6.825543535	8.76E-12	2.14E-10	6.470584043	6.258850205	6.39006114	3.862584211	3.955228997	3.998987077	A1+	tRNA-Ser (anticodon: GCT)
AT2G07754	38.659715	2.6722019	0.353461632	7.560090544	4.03E-14	2.80E-12	6.267038232	6.058144708	6.190579894	2.366511377	2.575486135	3.344390632	A2-	tRNA-Ser (anticodon: GCT)
AT2G07759	41.422103	2.5272826	0.348869021	7.24421628	4.35E-13	1.22E-11	6.270122728	6.109901683	6.248986003	3.222033331	3.546623725	3.487531741	A1-	tRNA-Ser (anticodon: GCT)
AT2G07759	43.986995	2.7181401	0.368379455	7.378641969	1.60E-13	4.68E-12	6.376741883	6.217282833	6.357788832	3.480233365	3.04536424	3.458449401	A1+	tRNA-Ser (anticodon: GCT)
AT2G07759	35.452878	3.1029167	0.382435525	8.11356828	4.92E-16	4.19E-14	6.173363621	6.01666062	6.158365983	0	1.407936067	2.749120822	A2-	tRNA-Ser (anticodon: GCT)

Supplementary Table 3: List of non-coding RNAs with at least log2-fold increases (negative log2-fold change) or decreases (positive log2-fold change) of 2.5 in at least one of the four lines A1+, A1-, A2+ or A2-.

	No of genes	Genes with heritable changes	Percentage heritable changes
non-coding RNAs			
miRNAs	4	4	100
NATs	10	5	50
ncRNA	50	41	82
rRNAs	2	0	0
snoRNAs	57	56	98.2
snRNAs	8	8	100
tRNAs	2	2	100

Supplementary Table 4: Summary of non-coding RNAs with altered transcript levels and their heritability rates. Data were compiled for different categories of genes expressing non-coding RNAs (S3 Table) that showed at least log₂-fold changes of +/- 2.5 in line A1+ compared to wildtype. For each gene, the values in A1+ and A1- were compared to score the heritability of expression changes.

	baseMean	log2Fold	lfcSE	stat	pvalue	padj	1	2	3	4	5	6	Line	Description
AT1G01060	421.85555	2.947925538	0.43507898	6.77561	1.24E-11	2.96E-10	10.0700886	9.27175784	9.31875631	6.817077	5.76041692	5.26573414	A1+	LHY1, LATE ELONGATED HYPOCOTYL 1, LHY encodes a myb-related putative transcription factor involved in circadian rhythm along with another myb transcription factor CCA1
AT1G01060	394.55683	3.184763053	0.25067777	12.70461	5.57E-37	6.25E-35	9.96222523	9.16304015	9.20873716	6.22475323	6.24407167	5.91300539	A1-	
AT1G01060	373.66459	2.960935856	0.2586256	11.44873	2.39E-30	6.13E-28	9.86425353	9.06855394	9.11703081	6.59409018	6.03318807	5.94637	A2-	
AT1G01680	220.77449	4.44029318	0.30586609	14.51711	9.44E-48	2.29E-45	8.44683167	8.76089953	8.97309852	4.626795	1.77337038	4.10750664	A1+	plant U-box 54 (PUB54); FUNCTIONS IN: ubiquitin-protein ligase activity; INVOLVED IN: response to stress, protein ubiquitination; LOCATED IN: ubiquitin ligase complex
AT1G02380	136.04545	1.022072363	0.22449132	4.552837	5.29E-06	5.53E-05	7.58078636	7.43763045	7.57634055	6.90123459	6.15252779	6.24686126	A1+	Transmembrane protein
AT1G02380	129.1293	0.839139584	0.2027848	4.138079	3.50E-05	0.00036278	7.47340418	7.32938212	7.46674197	6.57018063	6.02484804	6.71708414	A1-	
AT1G02380	89.270544	2.768546336	0.27245078	10.16164	2.94E-24	4.99E-22	7.37590169	7.23533343	7.37541144	4.13977271	4.59395234	4.08954938	A2-	
AT1G02520	59.715478	2.783904615	0.36050934	7.722143	1.14E-14	3.72E-13	6.996005	6.94647136	6.89625809	3.86258421	2.54523522	4.10750664	A1+	ARCB11 ATP-binding cassette B11, P-glycoprotein 11 (PGP11); FUNCTIONS IN: ATPase activity, coupled to transmembrane movement of substances; Encodes an ATP-binding cassette (ABC) transporter. Expressed in the vascular tissue of primary stem
AT1G03445	16.947858	2.868191299	0.55767467	5.143126	2.70E-07	3.55E-06	4.32110939	4.6394544	5.83987211	0	0	1.80658324	A1+	BSU1, BRI1 SUPPRESSOR 1 (BSU1); FUNCTIONS IN: protein binding, protein serine/threonine phosphatase activity; INVOLVED IN: brassinosteroid mediated signaling pathway, regulation of protein localization, encodes a serine-threonine protein phosphatase with an N-terminal Kelch-repeat domain, which is nuclear localized and expressed preferentially in elongating cells. Genetic evidence suggest that this gene plays a redundant role (along with other members of the same gene family) in modulating growth in response to brassinosteroid
AT1G06137	17.77101	3.373150534	0.53910072	6.256995	3.92E-10	7.71E-09	5.38438681	5.07139443	5.02412426	1.42937086	0	0	A1+	Transmembrane protein
AT1G08630	321.55366	-3.62596957	0.25276195	-14.3454	1.14E-46	2.40E-44	5.84316659	5.4399702	4.91005617	9.79650239	9.56604578	9.23314	A1+	THA1 threonine aldolase 1
AT1G08630	510.04162	-4.29613354	0.25840863	-16.6254	4.57E-62	1.23E-59	5.7371505	5.33367291	4.80366153	9.3016882	10.4409625	9.57387113	A1-	
AT1G08630	318.83918	-3.65672986	0.2631786	-13.8945	8.84E-44	4.20E-41	5.64097839	5.24143997	4.71518724	8.61379335	9.4891466	9.44011431	A2-	
AT1G08860	18.312015	2.567995031	0.51271648	5.008606	5.48E-07	6.85E-06	4.54470746	4.99965037	5.62167163	2.13309815	1.77337038	1.80658324	A1+	BON3, BONZAI 3 (BON3); Encodes a copine-like protein, which is a member of a newly identified class of calcium-dependent, phospholipid binding proteins that are present in a wide range of organisms. Overexpression of this gene suppresses bon1-1 phenotypes. Double mutant analyses with bon1-1 suggest that BON1 and BON3 have overlapping functions in maintaining cellular homeostasis and inhibiting cell death.
AT1G09932	148.00755	3.853735542	0.34746279	11.09107	1.39E-28	1.23E-26	8.05681467	7.83463835	8.46809348	4.89656107	2.54523522	3.2844326	A1+	Phosphoglycerate mutase family protein; CONTAINS InterPro DOMAIN/s: Histidine phosphatase superfamily, clade-1
AT1G09950	59.672902	4.106685521	0.4665702	8.789	1.51E-18	6.80E-17	6.62550015	6.31903844	7.44425745	2.13309815	1.77337038	1.80658324	A1+	RESPONSE TO ABA AND SALT 1
AT1G09950	69.427418	1.227763154	0.35078805	3.500014	4.65E-04	4.50E-03	6.42170048	6.11821652	7.24343721	5.66911504	5.51243115	4.27156266	A2-	
AT1G10070	2134.618	-4.74987205	0.14541544	-32.6642	5.05E-234	6.48E-230	7.40653601	7.21285235	6.91855481	11.8752588	12.1654607	11.9744991	A1+	Encodes a chloroplast branched-chain amino acid aminotransferase. Complements the yeast leu/iso-leu/val auxotrophy mutant. Involved in cell wall development.
AT1G10070	2333.6892	-4.90686239	0.17949758	-27.3366	1.56E-164	8.00E-161	7.29922898	7.10471398	6.80930265	12.1144867	12.4206346	11.8470555	A1-	
AT1G10070	1321.8585	-4.05648753	0.21832473	-18.5801	4.66E-77	5.14E-73	7.20179973	7.01076774	6.71828152	10.7393559	11.4893007	11.5368664	A2-	
AT1G11810	5.3324159	-2.56091953	0.58929127	-4.34576	1.39E-05	0.00013428	0.64014872	0	0	2.95850299	3.41603793	3.99889708	A1+	F-box associated ubiquitination effector family protein;
AT1G11810	5.3033588	-2.24263711	0.51475078	-4.35674	1.32E-05	0.00014887	0.60238038	0	0	4.32497688	3.41603793	3.7289679	A1-	
AT1G11810	5.9180957	-2.17693813	0.45418536	-4.79306	1.64E-06	3.15E-05	0.56964858	0	0	3.21937799	4.38148219	2.97593968	A2-	
AT1G13310	49.92424	3.205134777	0.39406541	8.13351	4.17E-16	1.54E-14	6.35721808	6.63537675	6.66963641	3.68403848	0	0	A1+	BRO1 Endosomal targeting BRO1-like domain-containing protein
AT1G15040	91.736687	-1.87546259	0.283232	-6.62162	3.55E-11	8.06E-10	5.45955343	5.4033698	4.68576835	7.03764045	7.58543433	6.91779169	A1+	GAT1_2_1, Class I glutamine amidotransferase-like superfamily protein; FUNCTIONS IN: hydrolase activity; INVOLVED IN: glutamine metabolic process; overlaps with NAT antisense AT1G15047
AT1G15040	137.10092	-2.53789379	0.28530132	-8.89549	5.82E-19	2.55E-17	5.35413127	5.29713935	4.58001253	7.66764055	8.46603619	7.38824596	A1-	
AT1G15040	138.01983	-2.37944847	0.36374743	-6.54149	6.09E-11	2.52E-09	5.2585368	5.20496851	4.49210629	6.16325204	8.42328211	8.32863943	A2-	
AT1G15380	63.70528	-2.93836372	0.35519458	-8.27255	1.31E-16	5.04E-15	4.36068592	4.33122513	2.84483429	6.68085238	7.16684068	6.69241692	A1+	GLY1 4 Lactoylglutathione lyase / glyoxalase I family protein
AT1G15380	63.094372	-2.86759648	0.36266889	-7.90693	2.64E-15	9.00E-14	4.25834422	3.33277285	2.75048837	6.12986766	7.07217374	7.17021492	A1-	
AT1G15380	113.12957	-3.85633258	0.29356462	-13.1362	2.04E-39	9.80E-37	4.16556389	3.24779332	2.67264875	7.58660415	7.98866549	7.67765904	A2-	
AT1G15580	35.151853	3.379716437	0.46264902	7.305141	2.77E-13	7.86E-12	5.61596949	6.19604123	6.35778883	2.13309815	1.77337038	2.24707457	A1+	IAA5 indole-3-acetic acid inducible 5; ATAUX2-27, AUXIN-INDUCIBLE 2-27, AUX2-27; FUNCTIONS IN: sequence-specific DNA binding transcription factor activity; INVOLVED IN: response to auxin stimulus, response to cyclopentenone, response to brassinosteroid stimulus;
AT1G15580	34.385857	2.55772591	0.39226635	6.5205	7.01E-11	1.61E-09	5.50991359	6.0886826	6.248986	3.0251823	2.66508652	3.02705619	A1-	
AT1G15580	34.267955	2.089987389	0.36826608	5.67521	1.39E-08	3.95E-07	5.41406557	5.99546251	6.15836598	4.13977271	2.57548613	3.34439063	A2-	
AT1G17380	58.489424	2.605026251	0.34122747	7.634281	2.27E-14	7.17E-13	6.50647594	6.83408558	6.77114728	4.29471016	2.54523522	4.10750664	A1+	JAZ5 jasmonate-zim-domain protein 5
AT1G17960	63.331991	2.772214712	0.37511712	7.390264	1.47E-13	4.31E-12	6.44306671	6.86132772	7.16226418	4.41410229	1.77337038	3.88163585	A1+	Threonyl-tRNA synthetase
AT1G18050	5.5811015	-2.51173559	0.58268996	-4.31059	1.63E-05	0.00015502	0	0.62641448	0.69458906	3.48023337	3.41603793	3.75388709	A1+	SWAP/surp RNA-binding domain protein, SWAP (Suppressor-of-White-APRicot)/surp RNA-binding domain-containing protein; FUNCTIONS IN: RNA binding; INVOLVED IN: RNA processing
AT1G20310	18.869329	2.583215164	0.51255244	5.039904	4.66E-07	5.88E-06	5.15487351	5.1397391	5.20431899	3.24282533	0	0	A1+	syringolide-induced protein
AT1G20520	31.405853	3.41382565	0.49895789	6.841911	7.81E-12	1.93E-10	5.74141419	5.4399702	6.46266906	2.60404218	0	0	A1+	DUF241 domain protein, putative (DUF241), overlaps with NAT AT1G20515
AT1G21400	3048.3443	-2.51199741	0.13130172	-19.1315	1.38E-81	1.36E-78	9.90173588	9.75288559	9.74817618	12.1027894	12.5434907	12.3576396	A1+	Thiamin diphosphate-binding fold (THDP-binding) superfamily protein; FUNCTIONS IN: oxidoreductase activity, acting on the aldehyde or oxo group of donors, disulfide as acceptor, 3-methyl-2-oxobutanoate dehydrogenase (2-methylpropanoyl-transferring) activity
AT1G21400	3360.1468	-2.77084392	0.1454299	-19.0528	6.23E-81	3.41E-78	9.79388542	9.64411601	9.63811087	12.4596271	12.7764133	12.2973678	A1-	
AT1G21400	2514.6632	-2.36864814	0.17309511	-13.6841	1.26E-42	7.34E-40	9.6959263	9.54958141	9.54636326	11.6743441	12.0790668	12.3366094	A2-	
AT1G21850	34.031045	3.423515795	0.4815372	7.109556	1.16E-12	3.15E-11	5.69550873	5.74795637	6.55095461	1.42937086	1.77337038	2.24707457	A1+	SKS8, SKUS similar 8 (sks8); FUNCTIONS IN: oxidoreductase activity, copper ion binding; INVOLVED IN: oxidation reduction
AT1G22240	18.839789	3.399326976	0.54058848	6.288197	3.21E-10	6.41E-09	4.7974027	5.42178607	5.44861069	1.42937086	0	0	A1+	PUM8, pumilio 8, Encodes a member of the Arabidopsis Pumilio (APUM) proteins containing PUF domain (eight repeats of

																				approximately 36 amino acids each). PUF proteins regulate both mRNA stability and translation through sequence-specific binding to the 3' UTR of target mRNA transcripts.
AT1G24260	10.928146	-2.7080859	0.56376718	-4.80355	1.56E-06	1.80E-05	1.08200738	0.62641448	1.16146642	2.60404218	5.12346883	4.62831981	A1+							AGAMOUS-LIKE 9, AGL9, SEP3, SEPALLATA3 Member of the MADs box transcription factor family, SEP3 is redundant with SEP1 and 2. Flowers of SEP1/2/3 triple mutants show a conversion of petals and stamens to sepals. SEP3 forms heterotrimeric complexes with other MADs box family members and binds to the CARG box motif.
AT1G24260	10.701727	-2.92776225	0.48300425	-6.06157	1.35E-09	2.74E-08	1.0260486	0.58898859	1.10157598	4.82646308	3.54662372	4.6145692	A1-							
AT1G27570	25.341114	-3.46767743	0.5660269	-6.12635	8.99E-10	1.69E-08	1.08200738	1.06173972	0	2.60404218	6.33648057	6.04333002	A1+							Phosphatidylinositol 3- and 4-kinase family protein;
AT1G30190	80.657804	3.33861717	0.42556309	7.845176	4.32E-15	1.46E-13	6.9526569	6.92080442	7.73969719	4.52436469	1.77337038	2.24707457	A1+							Cotton fiber protein
AT1G30370	62.944797	2.567707051	0.3839564	6.687496	2.27E-11	5.27E-10	6.47964108	6.82026915	7.10508681	4.52436469	0	4.302755	A1+							DLAH alpha/beta-Hydrolases superfamily protein Encodes a mitochondria-localized class III phospholipase A1 that plays a role in seed viability.
AT1G31095	4.9571189	-2.62521578	0.59218065	-4.43313	9.29E-06	9.27E-05	0	0	0	2.60404218	3.41603793	3.99898708	A1+							Lactate/malate dehydrogenase, NAD-binding domain protein
AT1G32080	393.66224	2.625581472	0.21679548	12.11087	9.25E-34	8.80E-32	9.09593325	9.43619354	9.70599131	6.64070742	6.13861985	6.93751624	A1-							Lrg8 membrane protein, putative. Encodes a plant LrgAB/CidAB protein localized to the chloroplast envelope that is involved in chloroplast development, carbon partitioning and leaf senescence. The gene may have evolved from gene fusion of bacterial LrgA and lrg8.
AT1G32910	13.446124	2.838225066	0.56591766	5.015262	5.30E-07	6.64E-06	4.50976567	4.06763741	5.40716122	1.42937086	0	0	A1+							HXXXD-type acyl-transferase family protein; FUNCTIONS IN: transferase activity, transferring acyl groups other than amino-acyl groups, transferase activity
AT1G33720	197.60122	2.523362541	0.3328352	7.581417	3.42E-14	1.06E-12	8.19244906	8.32022307	8.73422477	6.53041085	4.65450227	5.16887455	A1+							CYP76C6 cytochrome P450, family 76, subfamily C, polypeptide 6' (CYP76C6); FUNCTIONS IN: electron carrier activity, monooxygenase activity, iron ion binding, oxygen binding, heme binding
AT1G33760	146.81846	4.268422494	0.36499634	11.69443	1.36E-31	1.44E-29	8.03240252	7.796335	8.53456426	4.41410229	1.77337038	2.8570496	A1+							ETHYLENE RESPONSE FACTOR2, ERF2, encodes a member of the DREB subfamily A-4 of ERF/AP2 transcription factor family. The protein contains one AP2 domain. There are 17 members in this subfamily including TINY.
AT1G36060	26.955035	-1.5041823	0.37941084	-3.96452	7.35E-05	6.06E-04	4.10401826	3.10637019	3.92825069	5.31996921	5.47681251	5.39982454	A1+							RAP2.4/TRANSLUCENT GREEN, TG Integrase-type DNA-binding superfamily protein, encodes a member of the DREB subfamily A-6 of ERF/AP2 transcription factor family. The protein contains one AP2 domain. There are 8 members in this subfamily including RAP2.4. Overexpression results in increased drought tolerance and vitrified leaves. Binds to DRE/GCC promoter elements and activates expression of aquaporin genes AtTIP1.1, AtTIP2.3, and AtTIP2.2
AT1G36060	50.899524	-2.61465431	0.31002659	-8.43365	3.35E-17	1.32E-15	4.0025554	3.01054461	3.82555491	6.33520582	6.6796267	6.48996466	A1-							
AT1G42980	14.401981	2.527846059	0.54177664	4.665845	3.07E-06	3.38E-05	4.23815049	4.70106583	5.27514959	2.13309815	1.77337038	0	A1+							Actin-binding FH2 (formin homology 2) family protein; FUNCTIONS IN: actin binding
AT1G43910	394.42426	3.041107271	0.54663834	5.563289	2.65E-08	4.03E-07	9.15930773	9.07345248	10.182122	4.89656107	3.04536424	5.95893882	A1+							P-loop containing nucleoside triphosphate hydrolases superfamily protein; FUNCTIONS IN: nucleoside-triphosphatase activity, ATPase activity, nucleotide binding.
AT1G44130	20.558726	2.685495329	0.48509639	5.536004	3.09E-08	4.68E-07	5.08537786	5.22610318	5.5280995	2.60404218	0	2.24707457	A1+							Eukaryotic aspartyl protease family protein; FUNCTIONS IN: aspartic-type endopeptidase activity; INVOLVED IN: proteolysis
AT1G47590	10.52504	2.998700306	0.57241215	5.238708	1.62E-07	2.20E-06	4.32110939	4.43706106	4.61471504	0	0	0	A1+							PUP20, Member of a family of proteins related to PUP1, a purine transporter. May be involved in the transport of purine and purine derivatives such as cytokinins, across the plasma membrane.
AT1G48285	17.556816	-3.282025	0.5880518	-5.58118	2.39E-08	3.66E-07	0	0	0	1.42937086	5.31093132	6.04333002	A1+							GRF zinc finger protein
AT1G51850	116.09549	2.61073402	0.57228222	4.561969	5.07E-06	5.31E-05	7.65462057	7.43763045	8.19728676	4.626795	0	3.08650952	A1+							Leucine-rich repeat protein kinase family protein; FUNCTIONS IN: kinase activity; INVOLVED IN: protein amino acid phosphorylation
AT1G55390	13.565131	2.621425176	0.53315789	4.91679	8.80E-07	1.06E-05	4.57882294	4.60763305	4.99644157	1.42937086	0	1.80658324	A1+							Cysteine/Histidine-rich C1 domain family protein; FUNCTIONS IN: zinc ion binding
AT1G57650	24.791551	3.03993756	0.48959777	6.209051	5.33E-10	1.03E-08	5.4224596	5.28764416	5.95939724	2.60404218	0	1.80658324	A1+							ATP binding protein; FUNCTIONS IN: ATP binding; INVOLVED IN: apoptosis, defense response
AT1G59920	83.406609	-4.07194081	0.37050456	-10.9903	4.26E-28	3.62E-26	3.04620597	2.41948197	3.17624359	7.17921099	7.90949191	6.62098232	A1+							QSX19 MADs-box family protein
AT1G59920	264.36151	-3.35886639	0.16817948	-19.9719	9.67E-89	6.43E-85	3.7210802	3.06206738	3.85318425	8.7477845	9.33197473	8.91237284	A2+							
AT1G59930	171.47592	-4.6002686	0.37818128	-12.1642	4.82E-34	5.66E-32	3.66996625	2.26485625	3.60070039	8.39348439	8.9565094	7.42728597	A1+							MADS-box family protein
AT1G59930	481.38601	-3.66340969	0.16779881	-21.8322	1.15E-105	1.02E-101	4.37066785	2.89389119	4.29466969	9.60687286	10.2234705	9.76695616	A2+							
AT1G60590	76.765807	1.00523313	0.24956056	4.028013	5.63E-05	4.74E-04	6.54149654	6.87475828	6.67837384	5.74125297	5.76041692	5.52250498	A1+							Pectin lyase-like superfamily protein; FUNCTIONS IN: polygalacturonase activity; INVOLVED IN: carbohydrate metabolic process
AT1G60590	52.981932	2.656145851	0.33015276	8.045203	8.61E-16	3.06E-14	6.43473192	6.76682115	6.56929303	3.6894606	2.66508652	3.83605124	A1-							
AT1G61800	69.440077	2.685835027	0.42893995	4.261564	3.81E-10	7.53E-09	7.15277078	6.11913152	7.40794396	3.68403848	1.77337038	4.62831981	A1+							GPT2, ATGPT2, ARABIDOPSIS GLUCOSE-6-PHOSPHATE/PHOSPHATE TRANSLOCATOR 2, glucose-6-phosphate/phosphate translocator 2 (GPT2); FUNCTIONS IN: antiporter activity, glucose-6-phosphate transmembrane transporter activity;
AT1G62580	18.541913	-2.13404986	0.46119362	-4.62723	3.71E-06	4.01E-05	1.69330149	2.91163087	2.9639655	5.49267367	4.65450227	4.83184746	A1+							NOG1 nitric oxide-dependent guanylate cyclase 1, Flavin-binding monooxygenase family protein; FUNCTIONS IN: NADP or NADPH binding, monooxygenase activity, FAD binding, flavin-containing monooxygenase activity;
AT1G62580	25.507512	-2.63652322	0.40154293	-6.56598	5.17E-11	1.22E-09	1.61959049	2.81768511	2.86836947	5.10114755	5.61717743	5.86323418	A1-							
AT1G65390	74.177788	3.998164215	0.39530626	10.11409	4.78E-24	3.30E-22	7.09500687	7.07420579	7.32690788	3.86258421	0	1.80658324	A1+							ATPP2-AS, PHLOEM PROTEIN 2 AS, PP2-AS, FUNCTIONS IN: carbohydrate binding; INVOLVED IN: signal transduction, defense response, innate immune response;
AT1G65481	16.237047	3.501551686	0.55653324	6.291721	3.14E-10	6.29E-09	5.01236438	4.81691609	5.32050896	0	0	0	A1+							Transmembrane protein
AT1G65610	24.46579	2.800766342	0.47273391	5.45E-08	5.32532476	1.13E-09	5.4399702	5.82421041	2.13309815	0	2.8570496	0	A1+							KOR2, KORRIGAN 2, UNCTIONS IN: hydrolase activity, hydrolyzing O-glycosyl compounds, catalytic activity; INVOLVED IN: carbohydrate metabolic process
AT1G67856	52.363097	2.571485439	0.39529874	6.50517	7.76E-11	1.69E-09	6.32742784	6.28925818	6.96214034	4.41410229	1.77337038	3.6137176	A1+							RING/U-box superfamily protein; FUNCTIONS IN: zinc ion binding
AT1G68050	102.66285	-3.34656876	0.31573836	-10.5992	3.01E-26	2.30E-24	3.46634215	4.15829113	4.33421961	6.92152868	7.83504327	7.80305538	A1+							FLAVIN-BINDING, KELCH REPEAT, F BOX 1", ADO3, FK1, a flavin-binding kelch repeat F box protein, is clock-controlled, regulates transition to flowering. Forms a complex with GI on the CO promoter to regulate CO expression.
AT1G68050	100.08165	-3.45475441	0.26759391	-12.9104	3.93E-38	4.59E-36	3.36848215	4.05571171	4.22968725	7.80449888	7.38043732	7.4144016	A1-							

AT1G68050	81.596309	-3.18803458	0.25590639	-12.4578	1.27E-35	4.59E-33	3.28020153	3.96692572	4.14286763	7.23505054	7.22710126	7.24877322	A2-	
AT1G68765	65.979225	3.592629122	0.38322175	9.374805	6.93E-21	3.73E-19	7.16965839	6.94009731	6.81142231	3.86258421	0	2.8570496	A1+	IDA, INFLORESCENCE DEFICIENT IN ABCISSION, Putative membrane lipoprotein , encodes a small protein of 77 amino acids. Loss of

AT2G19800	1233.9243	-1.78389795	0.44572138	-4.00227	6.27E-05	0.00052358	8.13914393	9.07345248	9.07917436	10.2727504	11.6892446	10.5590142	A1+	development including curled leaves and reduced stature. A maternally expressed imprinted gene.
AT2G19800	2490.6113	-3.26415631	0.22669463	-14.3989	5.26E-47	8.94E-45	8.03157389	8.96476175	8.9691876	12.2103562	12.366197	11.8410417	A1-	MIOX2, MYO-INOSITOL OXYGENASE 2
AT2G19850	33.818679	-4.56683636	0.41707284	-10.9497	6.66E-28	4.91E-26	1.0260486	1.32916698	0	6.02829941	6.24407167	5.96111666	A1-	Transcription repressor
AT2G20350	17.897106	-2.652202672	0.52940128	5.009815	5.45E-07	6.82E-06	4.70774793	5.68835652	4.7200244	2.60404218	0	1.16932484	A1+	Integrase-type DNA-binding superfamily protein; FUNCTIONS IN: DNA binding, sequence-specific DNA binding transcription factor activity; INVOLVED IN: regulation of transcription, DNA-dependent. encodes a member of the ERF (ethylene response factor) subfamily B-6 of ERF/AP2 transcription factor family. The protein contains one AP2 domain. There are 12 members in this subfamily including RAP2.11
AT2G20720	266.75968	4.505572761	0.28452861	15.83522	1.78E-56	6.01E-54	8.77576671	9.05881817	9.18413037	3.68403848	3.41603793	4.89377362	A1+	Pentatricopeptide repeat (PPR) superfamily protein
AT2G21660	2116.1192	-2.7842902	0.23958866	-11.6211	3.22E-31	3.28E-29	8.32900314	9.4650628	8.86626757	11.5628244	11.9424875	12.052082	A1+	GLYCINE-RICH RNA-BINDING PROTEIN 7, cold, circadian rhythm, and rna binding 2" (CCR2); FUNCTIONS IN: double-stranded DNA binding, RNA binding, single-stranded DNA binding; Encodes a small glycine-rich RNA binding protein that is part of a negative-feedback loop through which AtGRP7 regulates the circadian oscillations of its own transcript. Gene expression is induced by cold. GRP7 appears to promote stomatal opening and reduce tolerance under salt and dehydration stress conditions, but, promotes stomatal closing and thereby increases stress tolerance under conditions of cold tolerance.
AT2G21660	1652.7774	-2.48384597	0.23312316	-10.6547	1.66E-26	1.15E-24	8.22138407	9.35632217	8.75631447	11.6965862	11.3458888	11.3522328	A1-	
AT2G21660	1938.0129	-2.77963843	0.23486678	-11.8349	2.58E-32	8.01E-30	8.12365063	9.26181456	8.66466716	11.8356312	11.6729347	11.7378327	A2-	
AT2G21900	77.133761	4.397807122	0.41085716	10.70398	9.75E-27	7.73E-25	7.15842198	7.10302156	7.45446703	2.60404218	0	2.58406216	A1+	WRKY DNA-binding protein 59 (WRKY59);
AT2G22470	200.03114	3.113374023	0.3114891	9.99513	1.60E-23	1.07E-21	8.44452073	8.15392552	8.86626757	5.87213781	3.955229	5.01018029	A1+	AGP2 Encodes arabinogalactan-protein (AGP2)
AT2G23030	51.488796	-1.72462103	0.31403167	-5.49187	3.98E-08	5.90E-07	4.98718166	4.20156765	4.24292849	6.17229309	6.57473948	6.29355404	A1+	SNF1-related protein kinase 2.9 (SNRK2.9); FUNCTIONS IN: protein serine/threonine kinase activity, protein kinase activity, kinase activity, ATP binding; INVOLVED IN: protein amino acid phosphorylation, response to osmotic stress; EXPRESSED IN: hypocotyl, root
AT2G23030	48.438047	-1.73155631	0.30864587	-5.61017	2.02E-08	3.55E-07	4.88274439	4.09880182	4.13876548	6.51492659	6.13861985	6.13896187	A1-	
AT2G23030	80.550242	-2.6326441	0.26817824	-9.81677	9.53E-23	1.38E-20	4.78810675	4.00984341	4.05227356	6.87521402	7.37814109	7.18211066	A2-	
AT2G23270	40.564177	2.559245933	0.47375406	5.402056	6.59E-08	9.50E-07	6.07596656	6.18530198	6.4216273	1.42937086	0	4.302755	A1+	Transmembrane protein
AT2G25460	71.059387	2.503553978	0.35154204	7.121635	1.07E-12	2.89E-11	6.83054615	7.21285235	6.81934414	5.05191825	3.71067778	3.4584494	A1+	EEIG1/EHBP1 protein amino-terminal domain protein, CONTAINS InterPro DOMAIN/s: C2 calcium-dependent membrane targeting
AT2G27080	178.91183	2.988879615	0.32010415	9.33721	9.89E-21	5.21E-19	8.21160172	7.95964247	8.75088865	5.82981529	4.16427264	4.83184746	A1+	Late embryogenesis abundant (LEA) hydroxyproline-rich glycoprotein family; CONTAINS InterPro DOMAIN/s: Late embryogenesis abundant protein, group 2
AT2G27660	53.824162	2.535964241	0.40183306	6.310989	2.77E-10	5.61E-09	6.67365048	6.39557205	6.70427307	4.72243246	0	3.4584494	A1+	Cysteine/Histidine-rich C1 domain family protein; FUNCTIONS IN: zinc ion binding
AT2G27690	132.63774	3.564015813	0.34201992	10.42049	2.00E-25	1.48E-23	7.6940635	7.56736362	8.4655718	4.41410229	3.955229	3.88163585	A1+	CYP94C1, cytochrome P450, family 94, subfamily C, polypeptide 1, Encodes a CYP94C1. Has highest omega-hydroxylase activity with 9,10-epoxystearic acid, while also metabolized lauric acid (C12:0) and C18 unsaturated fatty acids. Gene expression is induced in response to wounding and jasmonic acid treatment
AT2G32020	52.539428	2.696036325	0.3762845	7.164888	7.79E-13	2.14E-11	6.27636832	6.45042037	6.92591112	3.68403848	2.54523522	3.99898708	A1+	Acyl-CoA N-acyltransferases (NAT) superfamily protein; FUNCTIONS IN: N-acetyltransferase activity; INVOLVED IN: response to abscisic acid stimulus, metabolic process
AT2G32810	285.30387	3.109293374	0.21424878	14.51254	1.01E-47	2.42E-45	8.87692035	9.17329494	8.96240678	5.25747959	6.20076121	5.89980442	A1+	BGAL9, beta galactosidase 9 (BGAL9); FUNCTIONS IN: sugar binding, cation binding, beta-galactosidase activity, hydrolase activity, hydrolyzing O-glycosyl compounds, catalytic activity; INVOLVED IN: lactose catabolic process, using glucoside 3-dehydrogenase, carbohydrate metabolic process, lactose catabolic process via UDP-galactose, lactose catabolic process
AT2G32810	258.60633	3.423076975	0.2164553	15.81424	2.48E-56	5.69E-54	8.76919114	9.06459018	8.85243787	5.28852909	5.45092181	5.35204435	A1-	
AT2G33830	8176.0517	-2.46363084	0.15152067	-16.2594	1.92E-59	7.35E-57	11.4492732	10.9358639	11.3406461	13.8349075	13.8692431	13.5671133	A1+	Dormancy/auxin associated family protein
AT2G33830	8691.8351	-2.65841067	0.16985111	-15.6514	3.25E-55	7.01E-53	11.3413457	10.827021	11.2304918	14.1081301	13.8709234	13.6327646	A1-	
AT2G33830	6308.2105	-2.20207206	0.18708031	-11.7707	5.52E-32	1.67E-29	11.2433114	10.732418	11.1386647	13.1556804	13.1902866	13.6665211	A2-	
AT2G34130	79.886095	-6.3430864	0.46794237	-13.5553	7.37E-42	1.32E-39	0	0.62641448	0	7.33862744	7.70730679	6.79334513	A1+	MEE19 maternal effect embryo arrest 19; hypothetical protein
AT2G34130	3.8502539	-1.85505238	0.51127945	-3.62826	0.0002853	0.00237993	0	0.58898859	0	2.52621344	3.54662372	3.02705619	A1-	
AT2G34130	147.32616	-2.97018227	0.17873414	-16.6179	5.17E-62	1.06E-58	0	0.94032516	0	7.71636699	8.64221298	8.10948759	A2+	
AT2G35820	258.82682	2.070846629	0.2114287	9.794539	1.19E-22	7.38E-21	8.87004865	8.58822318	8.7067286	7.03764045	6.20076121	6.38263676	A1+	Ureidoglycolate hydrolases; FUNCTIONS IN: ureidoglycolate hydrolase activity; INVOLVED IN: allantoin catabolic process;
AT2G35820	229.70695	2.535910766	0.20136815	12.59341	2.30E-36	2.50E-34	8.76232058	8.47961638	8.59680419	5.86113479	6.43433558	5.93726157	A1-	
AT2G35930	93.085353	3.343311505	0.32516482	10.2819	8.50E-25	6.10E-23	7.37290417	7.27494913	7.65812289	4.41410229	2.54523522	3.88163585	A1+	PUB23, plant U-box 23, Encodes a cytoplasmically localized U-box domain containing E3 ubiquitin ligase that is involved in the response to water stress and acts as a negative regulator of PAMP-triggered immunity
AT2G36270	16.381569	-2.69176041	0.46794979	-5.75224	8.81E-09	1.44E-07	2.12132674	1.39570492	2.23589253	4.52436469	5.12346883	5.1178917	A1+	ABA INSENSITIVE 5 (ABIS), Encodes a member of the basic leucine zipper transcription factor family, involved in ABA signalling during seed maturation and germination. The Arabidopsis abscisic acid (ABA)-insensitive abi5 mutants have pleiotropic defects in ABA response, including decreased sensitivity to ABA inhibition of germination and altered expression of some ABA-regulated genes. Comparison of seed and ABA-inducible vegetative gene expression in wild-type and abi5-1 plants indicates that ABIS regulates a subset of late embryogenesis-abundant genes during both developmental stages
AT2G36750	36.425532	3.876054014	0.52065982	7.444504	9.73E-14	2.91E-12	5.24261498	6.3768159	6.61607048	0	0	1.80658324	A1+	UGT73C1, UDP-glucosyl transferase 73C1
AT2G36790	980.09842	2.783866682	0.56146439	4.958225	7.11E-07	8.74E-06	10.4948763	10.8466692	11.1849541	7.67380434	4.90795769	5.31182967	A1+	UGT73C6, UDP-glucosyl transferase 73C6, The At2g36790 gene encodes a UDP-glucose:flavonol-3-O-glycoside-7-O-
AT2G36790	2253.8655	0.788484544	0.17104274	4.609868	4.03E-06	3.68E-04	11.2417392	11.6034789	11.9273331	9.62198026	10.6900972	10.6978771	A2+	glucosyltransferase [UGT73C6]attaching a glucosyl residue to the 7-O-position of the flavonols kaempferol, quercetin and their 3-O-glycoside derivatives. Overexpression of the UGT73C6 alters brassinosteroid glucoside formation in Arabidopsis thaliana
AT2G36790	1237.7828	0.864754363	0.24409756	3.542659	0.0003961	0.00393956	10.2889886	10.6432303	10.9829822	9.99357091	9.9060547	9.08322057	A2-	
AT2G36800	511.21857	2.822011587	0.21804137	12.94255	2.59E-38	3.89E-36	9.44244867	9.92171522	10.0393574	7.17921099	6.37902412	6.99044986	A1+	D0GT1, don-glucosyltransferase 1, Encodes a DON-Glucosyltransferase. The UGT73C5 glucosylates both brassinolide and

AT2G36800	1139.4215	0.74521948	0.1576785	4.726196	2.29E-06	0.00022048	10.1888773	10.6782374	10.781434	9.11113897	9.67873079	9.82024547	A2+	castasterone in the 23-O position. The enzyme is presumably involved in the homeostasis of those steroid hormones hence regulating BR activity.
AT2G37125	10.498296	-3.34626037	0.58357844	-5.73404	9.81E-09	1.58E-07	0	0	0	2.60404218	4.65450227	5.1178917	A1+	GRF zinc finger protein
AT2G39490	30.721134	2.826242406	0.44495097	6.351806	2.13E-10	4.37E-09	5.75639705	5.67306373	6.06977307	3.48023337	1.77337038	1.80658324	A1+	F-box family protein
AT2G40750	75.170034	3.089316235	0.37400997	8.259984	1.46E-16	5.59E-15	7.15842198	6.73447092	7.41841284	4.29471016	0	3.99898708	A1+	WRKY54 WRKY DNA-binding protein 54, member of WRKY Transcription Factor; Group III
AT2G41280	4.2455762	-1.70335166	0.51508339	-3.30694	0.0009432	0.0068504	0.60238038	1.00603493	0.65346813	3.6894606	2.66508652	2.83386398	A1-	Glutamyl-tRNA (Gln) amidotransferase subunit C
AT2G42065	28.972692	3.634022154	0.4913134	7.396546	1.40E-13	4.13E-12	5.75639705	5.71846419	6.04296064	1.42937086	0	1.80658324	A1+	DnaJ domain protein, DnaJ is a member of the hsp40 family of molecular chaperones, which is also called the J-protein family, the members of which regulate the activity of hsp70s
AT2G42065	35.059782	1.135247087	0.34261975	3.313432	9.22E-04	8.14E-03	5.55444735	5.51905269	5.84418141	4.91161886	4.68949991	3.34439063	A2-	
AT2G42530	516.01361	-2.76008522	0.26902372	-10.2596	1.07E-24	7.67E-23	7.00377848	6.68957927	7.0522874	8.94267517	10.1852551	10.0787386	A1+	Cold regulated 15b (COR15B); INVOLVED IN: response to cold, defense response to fungus
AT2G42530	500.60416	-2.70094105	0.30029404	-8.99432	2.38E-19	2.66E-17	6.79946214	6.48813817	6.85185558	10.5682203	9.22385629	9.17178014	A2-	
AT2G44070	26.306646	2.550744945	0.44801448	5.693443	1.25E-08	1.98E-07	5.67987648	5.76247942	5.34266482	3.24282533	0	2.8570496	A1+	NagB/RpiA/CoA transferase-like superfamily protein; FUNCTIONS IN: GTP binding, translation initiation factor activity; INVOLVED IN: translational initiation, cellular metabolic process; LOCATED IN: eukaryotic translation initiation factor 2B complex
AT2G44840	26.568378	3.063932879	0.50564122	6.0595	1.37E-09	2.51E-08	5.47774872	5.11731537	6.25640028	1.42937086	0	2.58406216	A1+	ERF13, EREBP, ATERF13, ETHYLENE-RESPONSIVE ELEMENT BINDING FACTOR 13, encodes a member of the ERF (ethylene response factor) subfamily B-3 of ERF/AP2 transcription factor family. The protein contains one AP2 domain. There are 18 members in this subfamily including ATERF-1, ATERF-2, AND ATERF-5
AT2G47000	981.79182	3.243590978	0.21804213	14.87598	4.72E-50	1.25E-47	10.3670996	10.9706785	10.9999869	7.78873798	6.98598828	7.43771761	A1+	ABC84, ATP binding cassette subfamily B4, MDR4, ARABIDOPSIS P-GLYCOPROTEIN 4, AtABC84, MULTIDRUG RESISTANCE 4, ATPGP4, PGP4, P-GLYCOPROTEIN 4, Encodes an auxin efflux transmembrane transporter that is a member of the multidrug resistance P-glycoprotein (MDR/PGP) subfamily of ABC transporters. Functions in the basipetal redirection of auxin from the root tip. Exhibits apolar plasma membrane localization in the root cap and polar localization in tissues above and is involved in root hair elongation.
AT3G01345	198.40494	-7.0759132	0.38343906	-18.4538	4.86E-76	3.57E-73	1.41979204	1.39570492	0	8.92267842	8.46802692	8.45424982	A1+	Expressed protein;(source:Araport11)
AT3G01345	176.26334	-6.82859757	0.34752016	-19.6495	5.84E-86	3.85E-83	1.35313044	1.32916698	0	8.45492618	8.42176956	8.50652787	A1-	
AT3G01345	16.680528	-0.88251328	0.16358525	-5.39482	6.86E-08	7.93E-06	1.93072218	1.90953583	0	4.55903547	5.5227663	4.79820712	A2+	
AT3G01760	25.029187	3.225284501	0.50159649	6.430038	1.28E-10	2.70E-09	5.2637412	5.626188	5.91572749	0	0	2.58406216	A1+	LHT6, lysine-histidine-like transporter 6, Encodes an amino acid transporter expressed in the root that is involved in the uptake of acidic amino acids, glutamine and alanine, and probably phenylalanine.
AT3G05320	81.684093	2.60864553	0.32216043	8.097349	5.62E-16	2.06E-14	7.10088846	6.97168962	7.41841284	5.05191825	3.71067778	3.99898708	A1+	O-fucosyltransferase family protein
AT3G05320	91.88521	0.992453481	0.28089022	3.533243	4.10E-04	4.07E-03	6.89645991	6.76987284	7.2176151	5.98536134	6.3286119	5.18915455	A2-	
AT3G06890	51.594123	3.665209796	0.43310882	8.462561	2.62E-17	1.07E-15	6.46146979	6.31903844	7.04554951	2.60404218	1.77337038	2.58406216	A1+	Transmembrane protein, downregulated in RETARDED GROWTH OF EMBRYO1 mutant, which has small seeds
AT3G07195	119.26219	2.635947743	0.54390092	4.846375	1.26E-06	1.48E-05	7.9630577	7.74971596	7.70591056	5.12374266	1.77337038	3.2844326	A1+	RP1M1-interacting protein 4 (RIN4) family protein; CONTAINS InterPro DOMAIN/s: RP1M1-interacting protein 4, defence response
AT3G09870	27.548028	3.304197803	0.52593206	6.282556	3.33E-10	6.62E-09	5.77122591	4.78881395	6.34686895	2.13309815	0	1.16932484	A1+	SMALL AUXIN UPREGULATED RNA 48, SAUR48, SAUR-like auxin-responsive protein family ; FUNCTIONS IN: molecular_function unknown; INVOLVED IN: response to auxin stimulus
AT3G10986	33.471661	3.853168454	0.51041212	7.549132	4.38E-14	1.35E-12	5.80043405	5.68835652	6.5414077	2.13309815	0	0	A1+	LURP-one-like protein (DUF567)
AT3G10986	73.974473	0.789824288	0.18017547	4.383639	1.17E-05	0.00099509	6.53719807	6.43401673	7.27779066	4.42763923	5.5272663	5.57567307	A2+	
AT3G12900	23.922549	3.08509547	0.53606529	5.755074	8.66E-09	1.41E-07	4.85421964	5.02396364	6.32477806	0	1.77337038	1.80658324	A1+	2-oxoglutarate (2OG) and Fe(II)-dependent oxygenase superfamily protein; FUNCTIONS IN: oxidoreductase activity, acting on paired donors, with incorporation or reduction of molecular oxygen, 2-oxoglutarate as one donor, and incorporation of one atom each of oxygen into both donors, oxidoreductase activity;
AT3G13080	2455.4568	2.999607444	0.44789637	6.697102	2.13E-11	4.95E-10	11.6752511	12.3290028	12.351337	9.24199598	7.43224682	8.31972345	A1+	ABC3 ATP-binding cassette C3, MRP3, MRP3, MULTIDRUG RESISTANCE PROTEIN 3, multidrug resistance-associated protein 3, multidrug resistance-associated protein 3 (MRP3); FUNCTIONS IN: chlorophyll catabolite transmembrane transporter activity, ATPase activity, coupled to transmembrane movement of substances, glutathione S-conjugate-exporting ATPase activity; INVOLVED IN: transport, transmembrane transport
AT3G13080	5721.0748	0.694298481	0.16674503	4.163833	3.13E-05	0.00241297	12.4223399	13.0860179	13.0938542	11.2550077	12.1356886	12.1233354	A2+	
AT3G13100	55.057165	2.612473331	0.3937771	6.634396	3.26E-11	7.43E-10	6.05187904	6.61150886	7.05899397	4.29471016	3.04536424	3.4584494	A1+	ABC7, ATP-binding cassette C7 multidrug resistance-associated protein 7 (MRP7); MRP7, multidrug resistance-associated protein 7, MRP7, multidrug resistance-associated protein 7, ATMRP7 FUNCTIONS IN: ATPase activity, coupled to transmembrane movement of substances; INVOLVED IN: response to other organism;
AT3G13600	82.231872	2.787312942	0.30366215	9.178994	4.35E-20	2.21E-18	7.06523381	7.2597371	7.25279528	4.626795	4.50885002	3.6137176	A1+	Calmodulin-binding family protein;
AT3G14450	50.242147	1.474114021	0.33028665	4.463135	8.08E-06	8.15E-05	6.11136015	6.2588502	6.44229412	4.29471016	4.16427264	5.21811706	A1+	CID9, CTC-interacting domain 9, CTC-interacting domain 9 (CID9); FUNCTIONS IN: RNA binding, nucleotide binding, nucleic acid binding;
AT3G14450	38.127377	2.778216741	0.37868967	7.336394	2.19E-13	6.35E-12	6.00501318	6.15142592	6.33341193	3.54982923	0	2.61074174	A1-	
AT3G14735	241.001	4.368041804	0.25462994	17.15447	5.82E-66	1.05E-62	8.86355296	8.81692283	8.90850691	4.44523874	3.9893347	4.08954938	A2-	ATALD1
AT3G15440	38.605375	-3.32773352	0.397758	-8.36623	5.95E-17	2.36E-15	3.14059174	1.89476658	2.41385498	5.87213781	6.61088694	5.98762123	A1+	RING/U-box protein
AT3G15440	39.885208	-3.40677985	0.36487448	-9.33685	9.92E-21	4.92E-19	3.04528097	1.81596854	2.32498747	6.51492659	6.24407167	5.93726157	A1-	
AT3G15440	19.245766	-2.77118429	0.38853731	-5.84547	5.05E-09	1.55E-07	2.95944895	1.74883288	2.25192843	5.0982599	4.86347939	5.3993805	A2-	
AT3G16860	102.5916	2.586518617	0.26999858	9.579749	9.73E-22	5.59E-20	7.47606788	7.40096989	7.59952678	5.19216024	3.955229	4.83184746	A1+	COBL8; COBRA-like protein 8 precursor
AT3G17609	24.899406	3.122319303	0.4808336	6.493555	8.38E-11	1.82E-09	5.69550873	5.4399702	5.6574648	1.42937086	0	2.58406216	A1+	HYH, HYS-homolog, Encodes a homolog of HYS (HYH). Involved in <i>phsB</i> signaling pathway
AT3G18610	47.291031	2.766682983	0.39850741	6.942614	3.85E-12	9.79E-11	6.27636832	6.58723944	6.44229412	4.29471016	0	3.08650952	A1+	PARL1L, NUC2, nucleolin like 2, PARALLEL1-LIKE 1, nucleolin 2, ATNUC-L2, nucleolin like 2 (NUC-L2); FUNCTIONS IN: nucleotide binding, nucleic acid binding

AT3G19390	45.848893	-2.48073004	0.32932297	-7.53282	4.97E-14	1.52E-12	3.39153771	3.91998967	3.74076218	5.99212983	6.71419343	6.19860657	A1+	Granulin repeat cysteine protease family protein; FUNCTIONS IN: cysteine-type endopeptidase activity, cysteine-type peptidase activity; INVOLVED IN: proteolysis
AT3G19390	61.896596	-2.81378877	0.3399715	-8.27654	1.27E-16	4.83E-15	3.29421364	3.81854263	3.63910454	6.4574718	7.51293966	6.13896187	A1-	
AT3G19390	45.630384	-2.44454444	0.35690144	-6.84935	7.42E-12	3.55E-10	3.20644851	3.73080312	3.55483128	4.91161886	6.92731345	6.55018935	A2-	
AT3G20340	165.36213	-2.91160591	0.31440446	-9.2607	2.03E-20	1.06E-18	5.54831838	4.541804	5.02412426	7.78873798	8.79307821	7.85067324	A1+	Expression of the gene is downregulated in the presence of paraquat, an inducer of photooxidative stress.
AT3G20340	136.90471	-2.77028727	0.25018053	-11.0732	1.69E-28	1.30E-26	5.44274445	4.43775147	4.9174408	7.84239886	8.12317979	7.80552781	A1-	
AT3G20340	163.71946	-2.93090502	0.29839634	-9.82219	9.04E-23	1.31E-20	5.34700241	4.34760177	4.82870952	8.78670799	7.67517685	7.98193947	A2-	
AT3G21080	109.90144	4.683714386	0.40618704	11.53093	9.21E-31	9.07E-29	7.52500908	7.49528577	8.15409065	2.95850299	1.77337038	2.24707457	A1+	ABC transporter-like protein
AT3G21570	9.1891304	-3.45057726	0.57864985	-5.96315	2.47E-09	4.39E-08	0	0	0	3.24282533	4.65450227	4.55355437	A1+	Proline-rich nuclear receptor coactivator
AT3G21570	3.3005793	-1.94878505	0.50665271	-3.84639	0.0001199	0.00110669	0	0	0	3.22203333	2.66508652	2.83386398	A1-	
AT3G24542	38.685197	-5.55137252	0.50821671	-10.9232	8.93E-28	7.50E-26	0	0	0	5.64689647	6.57473948	6.48677716	A1+	Beta-galactosidase related protein
AT3G24542	31.852727	-4.88911448	0.46233684	-10.5748	3.90E-26	2.63E-24	0	0	0	5.45434691	6.60240584	5.73073232	A1-	
AT3G27150	12.153752	2.637236802	0.54511271	4.837966	1.31E-06	1.54E-05	4.50976567	4.541804	4.68576835	1.42937086	1.77337038	0	A1+	Galactose oxidase/kelch repeat superfamily protein;Target gene of MIR2111-5p
AT3G27473	12.828131	-2.98424919	0.51966515	-5.74264	9.32E-09	1.51E-07	1.08200738	0.62641448	1.79647046	5.05191825	4.16427264	4.62831981	A1+	Cysteine/Histidine-rich C1 domain family protein
AT3G27473	6.5104928	-1.79671071	0.51325828	-3.5006	0.0004642	0.00367044	1.0260486	0.58898859	1.71886773	3.54982923	0	4.67351385	A1-	
AT3G28193	12.671876	-3.8231251	0.55087996	-6.94003	3.92E-12	9.95E-11	0	0	0.69458906	4.41410229	5.12346883	4.47470153	A1+	Transmembrane protein
AT3G28193	23.234293	-4.47698895	0.46079601	-9.71577	2.58E-22	1.41E-20	0	0	0.65346813	5.60305581	5.76623828	5.27800355	A1-	
AT3G28580	54.002216	3.078237266	0.39685658	7.756548	8.73E-15	2.86E-13	6.32742784	6.89467256	6.72128447	3.24282533	0	3.88163585	A1+	P-loop containing nucleoside triphosphate hydrolases superfamily protein; FUNCTIONS IN: nucleoside-triphosphatase activity, ATPase activity, nucleotide binding, ATP binding; INVOLVED IN: response to abscisic acid stimulus
AT3G28917	7.9901805	-2.85207742	0.57760138	-4.9378	7.90E-07	9.61E-06	0.64014872	0.62641448	0	4.81212227	3.04536424	3.75388709	A1+	Mini zinc finger protein 2
AT3G29250	100.0304	4.008993665	0.40369995	9.930627	3.06E-23	1.99E-21	7.32847823	7.06251638	8.16034127	2.95850299	4.31603793	2.8570496	A1+	SDR4 short-chain dehydrogenase reductase 4, NAD(P)-binding Rossmann-fold superfamily protein; FUNCTIONS IN: oxidoreductase activity, copper ion binding; INVOLVED IN: oxidation reduction, metabolic process
AT3G29250	111.80531	1.261240597	0.35995438	3.50389	4.59E-04	4.45E-03	7.12381447	6.86059344	7.9590341	5.66911504	6.57370237	4.71047703	A2-	
AT3G30165	28.095123	-5.09190701	0.52422841	-9.71315	2.65E-22	1.59E-20	0	0	0	6.30179705	5.76041692	5.26573414	A1+	Zinc ion-binding protein
AT3G30720	311.0296	-4.18498005	0.18175136	-23.0259	2.57E-117	5.50E-114	4.90888351	4.97492033	5.02412426	9.04333885	9.19544847	9.37558921	A1+	QQS qua-quine starch
AT3G30720	253.0322	-3.95130953	0.19072375	-20.7174	2.41E-95	2.21E-92	4.80464288	4.86961204	4.9174408	9.08983702	8.79584563	8.80559757	A1-	
AT3G30720	79.406869	-0.74802691	0.16612109	-4.5029	6.70E-06	5.92E-04	5.63660448	5.71319536	5.74880253	6.73715322	6.83030173	6.73206822	A2+	
AT3G30751	37.718115	-5.59277317	0.50491903	-11.0766	1.63E-28	1.43E-26	0	0	0	6.2384977	5.82338964	6.60255698	A1+	Putative uncharacterized protein
AT3G30770	35.712351	-5.09746376	0.51469785	-9.9038	4.01E-23	2.57E-21	0.64014872	0	0	6.85976936	5.39625474	5.86930272	A1+	Eukaryotic aspartyl protease family protein
AT3G30770	36.671413	-5.14908705	0.44265561	-11.6323	2.83E-31	2.44E-29	0.60238038	0	0	6.12986766	5.76623828	6.61552448	A1-	
AT3G30775	1990.5298	-1.20501986	0.21129008	-5.70315	1.18E-08	1.88E-07	10.4546776	9.80379883	10.2822403	11.40602133	11.8117421	11.0349219	A1+	EARLY RESPONSIVE TO DEHYDRATION 5 (ERD5); CONTAINS InterPro DOMAIN/s: Proline dehydrogenase (InterPro:IPR002872),
AT3G30775	4479.6745	-2.71852901	0.21110366	-12.8777	6.01E-38	6.99E-36	10.3467898	9.69502471	10.1721338	12.6705281	13.355068	12.6886406	A1-	Proline oxidase. Encodes a proline oxidase that is predicted to localize to the inner mitochondrial membrane, its mRNA expression induced by high levels of A1 and by osmotic stress. The promoter contains an L-proline-inducible element.
AT3G31910	31.326196	-4.85468126	0.48209751	-10.0699	7.50E-24	5.10E-22	1.08200738	0.62641448	0	6.30179705	5.55310897	5.98762123	A1+	Ulp1 protease family protein (DUF1985)
AT3G31910	16.358621	-3.7091329	0.46699348	-7.94258	1.98E-15	6.84E-14	1.0260486	0.58898859	0	4.88574345	5.26298084	4.98490969	A1-	
AT3G42060	108.18227	-6.52370125	0.40624346	-16.0586	4.98E-58	1.18E-55	0	0	0.65346813	8.0893335	7.74621963	7.36160737	A1-	Myosin heavy chain-like protein
AT3G42723	33.615858	-4.20525915	0.53000245	-7.93441	2.11E-15	7.40E-14	0	0.62641448	1.51362724	7.03764045	5.01973368	5.26573414	A1+	ATP binding / aminoacyl-tRNA ligase/ nucleotide binding protein
AT3G42723	10.651867	-2.8695191	0.49134996	-5.84007	5.22E-09	9.87E-08	0	0.58898859	1.44298843	4.700053	4.48353294	4.02896949	A1-	
AT3G44070	62.394514	-5.70907579	0.51940222	-10.9916	4.19E-28	3.58E-26	0	0	0	7.8429441	6.46052296	5.89980442	A1+	Glycosyl hydrolase family 35 protein
AT3G44070	55.27904	-5.61657919	0.442475	-12.6936	6.42E-37	7.17E-35	0	0	0	6.51492659	7.38043732	6.25929154	A1-	
AT3G44265	87.006571	-6.3759127	0.44867291	-14.2106	7.87E-46	1.57E-43	0.64014872	0.62641448	0	7.68571859	7.56715209	7.00455248	A1+	Beta-galactosidase-like protein
AT3G44265	66.43804	-5.86554841	0.40575965	-14.4557	2.31E-47	3.95E-45	0.60238038	0.58898859	0	6.94935831	7.18241068	7.04187066	A1-	
AT3G44265	7.6799656	-0.54900155	0.13981763	-3.92655	8.62E-05	6.11E-03	0.95418637	0.94032516	0	3.35532952	4.09707691	4.31291624	A2+	
AT3G44350	55.201534	2.831427114	0.40420626	7.004907	2.47E-12	6.41E-11	6.96560812	6.71966171	6.23286803	4.29471016	0	3.4584494	A1+	NAC61, NAC domain containing protein 61, DOMAIN/s: No apical meristem (NAM) protein (InterPro:IPR003441);
AT3G45090	60.226327	-1.829316156	0.30055986	6.086362	1.18E-09	2.14E-08	6.56721516	6.68957927	6.57922203	4.626795	3.955229	5.06504098	A1+	P-loop containing nucleoside triphosphate hydrolases superfamily protein
AT3G45090	50.232254	2.533035585	0.32531316	7.786453	6.89E-15	2.26E-13	6.46042928	6.58177406	6.47022071	3.93373619	2.66508652	3.7289679	A1-	
AT3G45300	3240.7532	-2.84119786	0.16339953	-17.388	1.02E-67	5.80E-65	9.9159845	9.38871428	9.38163373	12.2973362	12.5809892	12.5475008	A1+	Isovaleryl-CoA-dehydrogenase (IVD); FUNCTIONS IN: isovaleryl-CoA dehydrogenase activity, ATP binding; INVOLVED IN: leucine catabolic process
AT3G45300	2673.6069	-2.61836042	0.17855531	-14.6641	1.09E-48	1.95E-46	9.80813289	9.27998234	9.27160694	12.2168632	12.3632741	11.9226559	A1-	
AT3G45300	2154.1126	-2.34520997	0.18769114	-12.495	7.94E-36	3.02E-33	9.71017265	9.18548285	9.17989375	11.5756261	11.826646	12.0520163	A2-	
AT3G45700	37.283393	4.09896825	0.52707206	7.778665	7.43E-15	2.46E-13	6.08786116	5.47566499	6.81934414	0	0	1.16932484	A1+	Major facilitator superfamily protein; FUNCTIONS IN: transporter activity; INVOLVED IN: oligopeptide transport
AT3G45960	37.737164	2.955114566	0.46941799	6.295273	3.07E-10	6.16E-09	6.03968276	5.4033698	6.72128447	3.24282533	2.54523522	1.80658324	A1+	EXLA3, EXPL3, expansin-like A3, ATEXLA3, ATEXPL3, ATHEXP BETA 2.3, expansin-like A3 (EXLA3); INVOLVED IN: plant-type cell wall organization, unidimensional cell growth, plant-type cell wall loosening;
AT3G48640	39.361501	3.511199299	0.45653635	7.690952	1.46E-14	4.69E-13	5.84316659	6.45042037	6.39006114	2.95850299	1.77337038	1.16932484	A1+	transmembrane protein
AT3G50770	76.348205	2.81603224	0.35774192	7.871686	3.50E-15	1.19E-13	6.69713612	7.31491012	7.25279528	4.81212227	3.04536424	3.6137176	A1+	CML41, calmodulin-like 41 FUNCTIONS IN: calcium ion binding
AT3G50770	191.06441	-0.94782585	0.2534824	-3.73922	0.0001846	0.00162621	6.59024651	7.20671969	7.14334748	7.55345777	7.85008742	8.44444186	A1-	
AT3G53910	20.870582	-4.68239315	0.53931387	-8.68213	3.88E-18	1.70E-16	0	0	0	5.43737123	4.65450227	5.89980442	A1+	Malate dehydrogenase-like protein

AT3G53910	12.982538	-3.70054128	0.49604041	-7.46016	8.64E-14	2.61E-12	0	0	0	4.32497688	5.26298084	4.48892248	A1-	
AT3G54730	65.514678	-5.2215664	0.38583882	-13.533	9.98E-42	1.39E-39	0.60238038	1.32916698	1.44298843	7.03039938	7.38043732	6.56971052	A1-	Putative transmembrane protein
AT3G54730	11.031955	-0.58180543	0.15132913	-3.84464	1.21E-04	8.23E-03	0.95418637	1.90953583	2.03712832	3.84180415	5.00688535	3.99110709	A2+	
AT3G55150	17.323637	2.65395901	0.52044228	5.09943	3.41E-07	4.39E-06	4.96155155	4.94975896	5.25192365	2.95850299	0	0	A1+	EXO70H1, exocyst subunit exo70 family protein H1, INVOLVED IN: exocytosis, vesicle docking involved in exocytosis; A member of EXO70 gene family, putative exocyst subunits, conserved in land plants. Arabidopsis thaliana contains 23 putative EXO70 genes, which can be classified into eight clusters on the phylogenetic tree.
AT3G56380	14.09531	3.055770317	0.55425541	5.513289	3.52E-08	5.28E-07	4.76813249	4.47282702	5.20431899	0	0	1.16932484	A1+	RR17, response regulator 17 (RR17); CONTAINS InterPro DOMAIN/s: CheY-like (InterPro:IPRO11006), Signal transduction response regulator
AT3G56380	13.302527	2.028922074	0.43801633	4.632069	3.62E-06	6.38E-05	4.5701966	4.27908139	5.00812498	2.36651138	2.10673202	0	A2-	
AT3G56891	137.1618	4.778637782	0.39260152	12.17172	4.40E-34	5.21E-32	8.19244906	7.60007556	8.33903492	3.68403848	0	2.24707457	A1+	Heavy metal transport/detoxification superfamily protein, FUNCTIONS IN: metal ion binding; INVOLVED IN: metal ion transport
AT3G57460	35.344597	2.621200845	0.45240181	5.793966	6.87E-09	1.14E-07	5.38438681	6.08487224	6.44229412	3.24282533	0	3.4584494	A1+	Catalytic/metal ion binding; FUNCTIONS IN: catalytic activity, metal ion binding
AT3G57520	4407.3092	-3.51273244	0.14179102	-24.774	1.71E-135	5.49E-132	9.5036663	9.47722036	9.28482951	12.9700734	13.2226405	12.7323058	A1+	ATSI2 encodes a raffinose-specific alpha-galactosidase that catalyzes the breakdown of raffinose into alpha-galactose and sucrose. This enzyme may function in unloading raffinose from the phloem as part of sink metabolism. Although it was originally predicted to act as a raffinose synthase (RS), that activity was not observed for recombinant S1P2.
AT3G57520	5030.6531	-3.74333637	0.19314187	-19.3813	1.11E-83	6.48E-81	9.39585307	9.36847839	9.17481462	12.9235266	13.641671	12.9158099	A1-	
AT3G57520	2290.8142	-2.5441048	0.23673288	-10.7467	6.14E-27	1.26E-24	9.29799028	9.27396953	9.08311208	11.203334	12.1384763	12.3144106	A2-	
AT3G59330	31.875399	2.317159449	0.41386605	5.598815	2.16E-08	3.33E-07	6.00246284	5.64198308	5.83987211	2.95850299	1.77337038	3.88163585	A1+	Solute carrier family 35 protein (DUF914)
AT3G59330	28.207032	2.824278081	0.41356084	6.829172	8.54E-12	2.15E-10	5.89624286	5.53534589	5.73167162	2.52621344	2.66508652	2.02322194	A1-	
AT3G59930	57.04168	-2.77303026	0.35138355	-7.89175	2.98E-15	1.02E-13	4.10401826	3.63438369	3.27171359	7.21253469	6.24743409	6.40407374	A1-	Defensin-like protein
AT3G59930	55.835697	-2.81790061	0.30534553	-9.22856	2.74E-20	1.31E-18	4.0025554	3.53456329	3.17332391	6.78781484	6.82267564	6.33427423	A1-	
AT3G61060	633.47327	-2.30533791	0.29577578	-7.79421	6.48E-15	2.16E-13	8.04770845	7.20755493	7.41841284	9.15038946	10.4918704	10.2468479	A1+	ATPP2-A13, PHLOEM PROTEIN 2-A13, PP2-A13, phloem protein 2-A13
AT3G61060	513.35701	-2.08127432	0.25012637	-8.32089	8.73E-17	3.36E-15	7.94016442	7.09941936	7.30888365	9.2923583	10.193576	9.54456606	A1-	
AT3G61060	814.37409	-2.93694097	0.21595521	-13.5998	4.02E-42	2.27E-39	7.84250413	7.00547573	7.2176151	10.2854922	10.5403367	10.6865884	A2-	
AT3G61190	134.7409	3.063202057	0.34286586	8.934112	4.10E-19	1.97E-17	7.97911312	7.45561721	8.29710267	5.37986412	3.41603793	4.302755	A1+	BAP, BON association protein 1, Encodes a protein with a C2 domain that binds to BON1 in yeast two hybrid analyses. Its ability to bind to phospholipids is enhanced by calcium ions. Involved in maintaining cell homeostasis.
AT3G62210	15.668434	3.207685238	0.57207494	5.607107	2.06E-08	3.18E-07	4.54470746	4.2844107	5.75980592	0	0	0	A1+	EDA32 embryo sac development arrest 32, Putative endonuclease or glycosyl hydrolase
AT4G00130	23.708583	2.452290707	0.45388513	5.402888	6.56E-08	9.47E-07	5.28456251	5.36581665	5.62167163	3.24282533	2.54523522	1.80658324	A1+	DNA-binding storekeeper protein-related transcriptional regulator
AT4G00130	236.04993	-3.35489884	0.20005157	-16.7702	4.03E-63	1.14E-60	5.17946829	5.25965655	5.51379711	8.64276785	8.571110185	9.02799996	A1-	
AT4G02160	21.19472	3.348455911	0.57262854	5.847518	4.99E-09	8.42E-08	5.1773142	3.97090311	6.29099423	0	0	0	A1+	Cotton fiber protein
AT4G02170	64.83101	3.978809484	0.47833219	8.181088	8.94E-17	3.47E-15	6.7874325	6.07326928	7.68004098	1.42937086	1.77337038	2.58406216	A1+	
AT4G03950	18.922543	-3.24635367	0.5807513	-5.58992	2.27E-08	3.49E-07	6.64014872	6.62641448	0	6.53041085	3.04536424	3.88163585	A1+	Nucleotide/sugar transporter family protein
AT4G03950	11.742448	-3.24952041	0.49436674	-6.5731	4.93E-11	1.16E-09	6.60238038	0.58898859	0	3.81676229	4.79250491	4.9367521	A1-	
AT4G04030	46.391975	-4.9760323	0.40853633	-12.1801	3.97E-34	3.83E-32	6.60238038	1.59300347	0	6.7563961	6.60240584	6.20038087	A1-	Ovate family protein 9 (OPF9)
AT4G04510	18.129615	2.758811326	0.52217153	5.283343	1.27E-07	1.76E-06	4.54470746	5.52760398	5.20431899	1.42937086	0	2.24707457	A1+	CRK38, cysteine-rich RLK (RECEPTOR-like protein kinase) 38, FUNCTIONS IN: kinase activity; INVOLVED IN: protein amino acid phosphorylation;
AT4G08190	10.27703	-3.31241483	0.50567027	-6.55054	5.73E-11	1.34E-09	0	0	0	3.93373619	5.0468368	4.02896949	A1-	P-loop containing nucleoside triphosphate hydrolases superfamily protein;
AT4G08691	65.548556	-5.7213473	0.41643476	-13.7389	5.94E-43	8.62E-41	0.60238038	0.58898859	0	6.51492659	7.23452333	7.25949526	A1-	Putative uncharacterized protein
AT4G09430	9.9297132	-2.53057544	0.53370214	-4.74155	2.12E-06	2.40E-05	1.08200738	1.39570492	1.51362724	4.41410229	3.41603793	4.69940081	A1+	Disease resistance protein (TIR-NBS-LRR class) family; with Natural antisense transcript At4G09432, FUNCTIONS IN: transmembrane receptor activity, ATP binding;
AT4G09430	11.928288	-2.72057747	0.468818	-5.80306	6.51E-09	1.21E-07	1.0260486	1.32916698	1.44298843	4.88574345	4.48353294	4.19910693	A1-	
AT4G11000	83.123977	2.877310357	0.36997764	7.776984	7.43E-15	2.46E-13	6.91976087	7.21285235	7.52881931	4.97632986	3.41603793	3.08650952	A1+	Ankyrin
AT4G11250	7.2448848	2.556009438	0.58454973	4.372612	1.23E-05	1.20E-04	4.10401826	3.8124332	3.92825069	0	0	0	A1+	AGL52, AGAMOUS-like 52 (AGL52); FUNCTIONS IN: sequence-specific DNA binding transcription factor activity; INVOLVED IN: regulation of transcription, DNA-dependent
AT4G13540	67.594726	-2.63371295	0.36226215	-7.27019	3.59E-13	1.01E-11	4.05638537	4.5077277	3.27171359	6.30179705	7.43224682	6.79334513	A1+	Golgin family A protein, unknown protein; INVOLVED IN: N-terminal protein myristoylation
AT4G13540	69.997725	-2.67426255	0.3408067	-7.84686	4.27E-15	1.43E-13	3.95514036	4.40379085	3.17332391	6.90706414	7.51293966	6.27840572	A1-	
AT4G13540	31.996499	-1.63136643	0.34300515	-4.7561	1.97E-06	3.70E-05	3.86359518	4.31374833	3.09193373	5.26349776	5.83848469	5.89179208	A2-	
AT4G14130	4892.7225	-2.60060431	0.23501389	-11.0657	1.84E-28	1.61E-26	10.497108	9.93299364	10.5183221	12.4981728	13.5254312	12.9469674	A1+	XTR7, xyloglucan endotransglucosylase 7, xyloglucan endotransglucosylase/hydrolase 15 (XTH15); FUNCTIONS IN: hydrolase activity, acting on glycosyl bonds, xyloglucan:xyloglucosyl transferase activity, hydrolase activity, hydrolyzing O-glycosyl compounds; INVOLVED IN: N-terminal protein myristoylation, carbohydrate metabolic process, cellular glucan metabolic process
AT4G14130	8997.8162	-3.69538578	0.17239948	-21.435	6.30E-102	6.47E-99	10.3892179	9.82420868	10.4082017	14.1114321	14.1493791	13.825294	A1-	
AT4G15530	2035.4536	-2.17280903	0.11394671	-19.0686	4.60E-81	4.08E-78	9.59713705	9.55331938	9.37895617	11.672414	11.8472142	11.5881028	A1+	pyruvate orthophosphate dikinase (PPDK); FUNCTIONS IN: kinase activity, pyruvate, phosphate dikinase activity; INVOLVED IN: phosphorylation, response to absence of light. The product of this long transcript was shown to be targeted to the chloroplast, whereas the shorter transcript (no targeting sequence) accumulates in the cytosol. They were also found in slightly different tissues.
AT4G15530	2493.316	-2.56277733	0.19838549	-12.9182	3.55E-38	4.17E-36	9.48931413	9.44456926	9.26892969	11.7150901	12.5289362	11.8382267	A1-	
AT4G15530	2054.2744	-2.3433641	0.19293666	-12.1458	6.04E-34	2.02E-31	9.39138189	9.35005279	9.17721678	11.2849141	12.0779636	11.8177711	A2-	
AT4G16250	95.038696	2.697492529	0.27529796	9.798447	1.14E-22	7.11E-21	7.28780625	7.4511415	7.45446703	4.81212227	3.955229	4.69940081	A1+	PHYD, phytochrome D, Encodes a phytochrome photoreceptor with a function similar to that of phyB that absorbs the red/far-red part of the light spectrum and is involved in light responses. It cannot compensate for phyB loss in Arabidopsis but can substitute for tobacco phyB in vivo.
AT4G16250	85.33817	2.962200571	0.28747503	10.3042	6.74E-25	4.23E-23	7.18055587	7.34288709	7.34492132	4.32497688	3.54662372	4.02896949	A1-	
AT4G16820	27.779976	3.964851424	0.51617149	7.681268	1.58E-14	5.03E-13	5.80043405	5.74795637	5.8706945	1.42937086	0	0	A1+	PLA-1[beta]2, phospholipase A 1 beta 2, alpha/beta-Hydrolases superfamily protein; DAD1-Like Lipase 1, DALL1, Encodes a lipase

AT4G18150	49.639822	-5.6599251	0.46687824	-12.1229	7.99E-34	9.29E-32	1.08200738	0	0	6.30179705	6.74704798	6.82547753	A1+	that hydrolyzes phosphatidylcholine, glycolipids as well as triacylglycerols FUNCTIONS IN: galactolipase activity, triglyceride lipase activity, phospholipase A1 activity; INVOLVED IN: lipid metabolic process
AT4G18150	50.777458	-5.3882543	0.42287294	-12.742	3.45E-37	3.91E-35	1.0260486	0	0	6.64070742	7.01372669	6.27840572	A1-	Serine/Threonine-kinase, putative
AT4G21680	117.3354	3.126205488	0.3406135	9.178161	4.39E-20	2.22E-18	7.20285189	7.62413179	8.2509894	4.52436469	3.955229	4.47470153	A1+	NRT1.8, NITRATE TRANSPORTER 1.8, NRT1/ PTR family 7.2, NPF7.2, AtNPF7.2, Encodes a nitrate transporter (NRT1.8). Functions in nitrate removal from the xylem sap. Mediates cadmium tolerance.
AT4G21680	103.67261	2.69304547	0.35300123	7.628997	2.37E-14	1.69E-12	6.99831337	7.42168197	8.04963608	4.91161886	4.68949991	2.97593968	A2-	
AT4G22590	120.33706	2.535735923	0.37997522	6.673424	2.50E-11	5.78E-10	7.6940635	7.49528577	7.98127222	5.87213781	3.04536424	4.39128842	A1+	TPPG Haloacetal dehalogenase-like hydrolase (HAD) superfamily protein; FUNCTIONS IN: catalytic activity, trehalose-phosphatase activity; INVOLVED IN: trehalose biosynthetic process, metabolic process;
AT4G23070	16.049594	3.202106202	0.54974073	5.824757	5.72E-09	9.59E-08	4.82609085	4.70106583	5.44861069	0	0	1.16932484	A1+	RBL7, RHOMBOID-like protein 7 (RBL7); FUNCTIONS IN: serine-type endopeptidase activity;
AT4G24570	111.61367	2.893124774	0.27157608	10.65309	1.69E-26	1.32E-24	7.75873667	7.46007907	7.71017741	4.89656107	4.34682445	4.55355437	A1+	DIC2 dicarboxylate carrier 2 (DIC2); FUNCTIONS IN: binding, dicarboxylic acid transmembrane transporter activity
AT4G25530	983.3379	-10.3163052	0.446696975	-23.0805	7.26E-118	2.12E-114	0	0	0	0	11.172183	11.3504313	A1+	FLOWERING WAGENINGEN, FWA, HDG6, HOMEODOMAIN GLABROUS 6
AT4G25530	104.45451	-3.85787677	0.50802234	0	3.10E-14	9.74E-13	0	0	0	6.53358073	8.61107536	7.19053793	A1-	
AT4G25530	84.596732	-2.50267411	0.1801412	-13.8928	7.00E-44	8.46E-41	0	0	0	7.10288148	7.8644139	7.13013113	A2+	
AT4G25580	63.812785	-5.29688893	0.4297685	-12.325	6.65E-35	8.33E-33	1.08200738	1.06173972	1.51362724	6.30179705	7.28341303	7.20105069	A1+	Putative uncharacterized protein
AT4G25580	69.81524	-5.25573844	0.38751893	-13.5625	6.68E-42	9.48E-40	1.0260486	1.00603493	1.44298843	6.7563961	7.63428961	6.79878427	A1-	
AT4G25580	82.954602	-5.57653952	0.33777995	-16.5094	3.14E-61	3.65E-58	0.97696772	0.95928517	1.38559459	7.23505054	7.36372912	7.50659804	A2-	
AT4G27654	39.756524	2.965474185	0.43548448	6.809598	9.79E-12	2.37E-10	5.9642572	6.15259609	6.50257548	3.86258421	0	2.24707457	A1+	Transmembrane protein
AT4G27654	44.714233	1.274260556	0.338319	3.766447	0.0001656	0.00186436	5.76175919	5.95210834	6.30290054	5.41174015	4.59395234	3.63762718	A2-	
AT4G29200	124.64548	-6.96814846	0.42550825	-16.3761	2.84E-60	1.16E-57	0	0.62641448	0.69458906	7.97502982	8.02115358	7.89676951	A1+	Beta-galactosidase related protein;(source:Araport11)
AT4G29200	85.43925	-5.79169256	0.42574655	-13.6036	3.81E-42	5.47E-40	0	0.58898859	0.65346813	6.67471869	8.09526687	7.11811844	A1-	
AT4G29200	13.500262	-0.84429995	0.15745271	5.36224	8.22E-08	9.47E-06	0	0.94032516	1.02485808	4.84311283	5.18784947	4.07853495	A2+	
AT4G30280	775.45996	3.328055775	0.51889166	6.413778	1.42E-10	2.99E-09	10.3111209	10.2750288	10.935849	6.99996539	4.78678878	5.1178917	A1+	XYL18, xyloglucan endotransglucosylase/hydrolase 18, Encodes a xyloglucan endotransglucosylase/hydrolase with only the endotransglucosylase (XET; EC 2.4.1.207) activity towards xyloglucan and non-detectable endohydrolytic (XH; EC 3.2.1.151) activity. Expressed in the mature or basal regions of both the main and lateral roots, but not in the tip of these roots where cell division occurs.
AT4G30430	33.132379	3.278773186	0.47622801	6.884881	5.78E-12	1.44E-10	5.74141419	5.6576071	6.48276025	2.13309815	0	2.58406216	A1+	TET9, Tetraspanin9 (TET9); FUNCTIONS IN: molecular_function unknown; INVOLVED IN: aging;
AT4G31800	218.36826	2.503573765	0.31001968	8.075532	6.72E-16	2.43E-14	8.30881787	8.486916	8.86626757	6.53041085	4.50885002	5.86930272	A1+	WRKY DNA-binding protein 18 (WRKY18)
AT4G33150	1769.7907	-3.77889042	0.12217258	-30.9308	4.61E-210	3.95E-206	8.05983735	7.87529569	7.66253323	11.6505442	11.75533	11.6655877	A1+	LKR/SDH locus. Encodes two proteins. One protein is the monofunctional saccharopine dehydrogenase involved in lysine degradation. The longer protein from the same LKR/SDH locus is bifunctional and also has saccharopine dehydrogenase activity.
AT4G33150	1266.7159	-3.28256763	0.19358003	-16.9572	1.70E-64	5.09E-62	7.95228977	7.76687668	7.55289987	11.0364585	11.5626917	10.8358009	A1-	The monofunctional SDH functions mainly to enhance the flux of lysine catabolism. Gene expression is induced by abscisic acid, jasmonate, and under sucrose starvation.
AT4G33150	1530.6515	-3.70622686	0.15403528	-24.0609	6.42E-128	1.42E-123	7.85462602	7.67266893	7.46153827	11.2631185	11.5894667	11.5692894	A2-	
AT4G33465	67.312894	-4.00565346	0.45496597	-8.80429	1.32E-18	6.01E-17	2.71916111	2.41948197	1.79647046	5.43737123	7.70730679	7.15121196	A1+	SCR-LIKE 22, SCRL22, Encodes a member of a family of small, secreted, cysteine rich proteins with sequence similarity to SCR (S locus cysteine-rich protein).
AT4G33465	31.170814	-3.1974906	0.37634063	-8.49627	1.96E-17	7.87E-16	2.62811916	2.3315719	1.71886773	5.80081296	6.24407167	5.55377989	A1-	
AT4G33465	88.605696	-4.6406246	0.32829845	-14.1354	2.30E-45	1.49E-42	2.54636852	2.25622116	1.65553269	7.27432006	7.02213107	7.90134866	A2-	
AT4G34410	294.07078	2.927365822	0.27902055	10.49158	9.44E-26	7.16E-24	9.00319506	9.30562138	8.78364987	6.63242758	5.12346883	5.63556587	A1+	RRTF1, ERF109, ethylene response factor 109, redox responsive transcription factor 1 (RRTF1); CONTAINS InterPro DOMAIN/s: DNA-binding, integrase-type (InterPro:IPRO16177), Pathogenesis-related transcriptional factor/ERF, DNA-binding
AT4G34410	647.43606	0.787481005	0.16507306	4.7705	1.84E-06	1.80E-04	9.74932518	10.0618198	9.52496045	8.22181499	9.15025765	8.48239181	A2+	
AT4G37220	132.91322	-2.2069466	0.33305332	-6.62641	3.44E-11	7.82E-10	5.28456251	5.42178607	5.5280995	6.83858109	4.88760066	7.65892076	A1+	Cold acclimation protein WCOR413 family, early CK response gene
AT4G37220	215.88843	-3.14886742	0.21554192	-14.6091	2.46E-48	4.36E-46	5.17946829	5.31552177	5.42038057	8.32174183	9.02025045	8.42310676	A1-	
AT4G37220	91.87239	-1.91481018	0.24479621	-7.82206	5.20E-15	3.98E-13	5.08419255	5.22331949	5.33072716	6.76924384	7.12825324	7.62006655	A2-	
AT4G38560	123.66808	2.561696699	0.30040443	8.527493	1.50E-17	6.25E-16	7.6304266	7.61615753	7.99532626	5.74125297	4.50885002	4.47470153	A1+	Phospholipase-like protein (PEARL1 4) family protein. Overlaps with NAT AT4G09715
AT4G39030	273.63436	2.525423793	0.23679884	10.66485	1.49E-26	1.16E-24	8.6062531	8.79308635	9.19482705	6.65684315	5.82338964	6.14868187	A1+	EDDS ENHANCED DISEASE SUSCEPTIBILITY 5 (EDDS);SCORD3, SID1, susceptible to coronatine-deficient Pst DC3000 3, SALICYLIC ACID INDUCTION DEFICIENT 1 Encodes an orphan multidrug and toxin extrusion transporter. Essential component of salicylic acid-dependent signaling for disease resistance. Member of the MATE-transporter family. Expression induced by salicylic acid. Mutants are salicylic acid-deficient
AT4G39070	50.596541	-1.56648574	0.32629676	-4.8008	1.58E-06	1.82E-05	4.82609085	4.06763741	4.84945148	6.6075917	6.29264424	5.89980442	A1+	Encodes BZS1, a brassinosteroids-regulated BZR1 target (BRBT) gene. BZS1 is a putative zinc finger transcription factor. Expression of BZS1 was increased under BR-deficient condition and repressed by BR. Transgenic Arabidopsis plants overexpressing BZS1 showed a hypersensitivity to the BR biosynthetic inhibitor brassinazole (BRZ). In contrast, transgenic plants expressing reduced level of BZS1 had longer hypocotyls than wild type when grown on BRZ. B-box zinc finger family protein; FUNCTIONS IN: sequence-specific DNA binding transcription factor activity, zinc ion binding; INVOLVED IN: response to karrikin, response to chitin, regulation of transcription;
AT4G39070	92.245303	-2.70869377	0.26665548	-10.158	3.05E-24	1.84E-22	4.72207007	3.96546697	4.74321981	7.63346001	7.12834486	7.24984372	A1-	
AT5G01080	10.052266	-2.55025532	0.58688177	-4.34543	1.39E-05	0.00013443	0.64014872	0.62641448	0.69458906	1.42937086	4.16427264	5.35649789	A1+	Beta-galactosidase related protein
AT5G01080	22.361071	-4.21792242	0.448412	-9.40635	5.14E-21	2.57E-19	0.60238038	0.58898859	0.65346813	5.67203104	5.45092181	5.35204435	A1-	
AT5G01380	19.558548	3.117262195	0.51129561	6.09679	1.08E-09	2.02E-08	5.08537786	5.42178607	5.29800753	1.42937086	0	1.80658324	A1+	Homeodomain-like superfamily protein; CONTAINS InterPro DOMAIN/s: SANT, DNA-binding (InterPro:IPRO1005), MYB-like
AT5G10250	32.345702	1.98945362	0.38315291	5.192323	2.08E-07	2.78E-06	6.00246284	5.5777379	5.69239139	3.48023337	3.71067778	3.6137176	A1+	DOT3 DEFECTIVELY ORGANIZED TRIBUTARIES 3 (DOT3), Encodes a protein with an N-terminal BTB/POZ domain and a C-terminal

AT5G10250	27.550389	2.51078304	0.40296113	6.230832	4.64E-10	9.83E-09	5.89624286	5.4712037	5.58440579	2.7971628	2.66508652	2.61074174	A1-	NPH3 family domain. dot3 mutants have defects in shoot and primary root growth and produce an aberrant parallel venation pattern in juvenile leaves.
AT5G13170	54.231122	1.815432322	0.37472143	4.844752	1.27E-06	1.72E-05	5.66530953	6.93675849	6.60369669	4.88574345	4.08983374	3.83605124	A1-	SAG29, senescence-associated gene 29, Encodes a member of the SWEET sucrose efflux transporter family proteins
AT5G13170	43.821205	2.846084079	0.39718626	7.165616	7.74E-13	4.43E-11	5.56923443	6.84289997	6.51280503	0	2.92870966	2.74912082	A2-	
AT5G13320	812.59623	2.536724107	0.56629758	4.47949	7.48E-06	7.62E-05	10.5550248	10.4618187	10.720621	7.4121823	3.71067778	6.58389328	A1+	PBS3, AVRPPHB SUSCEPTIBLE 3, AtGH3.12, GDG1, GH3.12, GH3-LIKE DEFENSE GENE 1, GRETCHEN HAGEN 3.12, WIN3, HOPW1-1-INTERACTING 3, Encodes an enzyme capable of conjugating amino acids to 4-substituted benzoates. 4-HBA (4-hydroxybenzoic acid) and pABA (4-aminobenzoate) may be targets of the enzyme in Arabidopsis, leading to the production of pABA-Glu, 4HBA-Glu, or other related compounds. This enzyme is involved in disease-resistance signaling. It is required for the accumulation of salicylic acid, activation of defense responses, and resistance to Pseudomonas syringae. Salicylic acid can decrease this enzyme's activity in vitro and may act as a competitiveinhibitor.
AT5G13930	177.64877	0.735271732	0.20759302	3.54189	0.0003973	0.00270848	7.51182528	7.91483857	7.95274664	7.24510602	7.09209032	6.80950079	A1+	TT4, TRANSPARENT TESTA 4, ATCHS, CHALCONE SYNTHASE, CHS, Encodes chalcone synthase (CHS), a key enzyme involved in the biosynthesis of flavonoids. Required for the accumulation of purple anthocyanins in leaves and stems. Also involved in the regulation of auxin transport and the modulation of root gravitropism.
AT5G13930	118.34823	2.746380743	0.26882886	10.21609	1.68E-24	1.03E-22	7.40447177	7.80640655	7.84301032	4.700053	5.45092181	4.55311326	A1-	
AT5G13930	108.2862	2.781966252	0.27823858	9.998492	1.55E-23	2.44E-21	7.30699721	7.71218666	7.75155673	4.91161886	3.9893347	4.71047703	A2-	
AT5G14920	1149.3031	-1.41374148	0.20844614	-6.78229	1.18E-11	2.84E-10	9.17611944	8.88389072	9.62364628	10.8652035	10.8987597	10.3303972	A1+	GASA14, A-stimulated in Arabidopsis 14, Gibberellin-regulated family protein; INVOLVED IN: response to gibberellin Stimulus
AT5G14920	2058.1372	-2.50623275	0.22549052	-11.1146	1.07E-28	8.29E-27	9.06834557	8.77522947	9.51359298	11.6476559	12.2203752	11.3818077	A1-	
AT5G15360	47.798425	-4.21413157	0.56252793	-7.49142	6.81E-14	2.06E-12	0.64014872	0	0.69458906	2.95850299	7.16684068	7.09958974	A1+	Transmembrane protein
AT5G15360	73.341129	-6.02113899	0.40151677	-14.996	7.80E-51	1.50E-48	0.60238038	0	0.65346813	7.14401612	7.18241068	7.27860676	A1-	
AT5G17460	89.599698	-2.9729055	0.31978622	-9.29654	1.45E-20	7.59E-19	4.05638537	4.1136762	4.37778648	6.53041085	7.63893074	7.62280649	A1+	Glutamyl-tRNA (Gln) amidotransferase subunit C
AT5G17460	38.23128	-1.70122265	0.32909855	-5.16934	2.35E-07	3.56E-06	3.95514036	4.01129486	4.27308589	6.33520582	5.90133004	5.45643433	A1-	
AT5G17460	84.103257	-2.78812138	0.32821768	-8.49473	1.98E-17	1.89E-15	3.86359518	3.92269205	4.18611696	7.94403054	6.3286119	7.08814715	A2-	
AT5G20260	15.016385	-2.02485671	0.4994604	-4.05409	5.03E-05	4.29E-04	3.14059174	1.89476658	1.51362724	4.29471016	4.78678878	5.06504098	A1+	Exostosin family protein
AT5G20260	22.745821	-2.63763323	0.42277905	-6.2388	4.41E-10	9.37E-09	3.04528097	1.81596854	1.44298843	5.53061657	5.61717743	5.02992519	A1-	
AT5G22380	85.45932	4.140996733	0.38201548	10.83987	2.23E-27	1.81E-25	7.2617914	7.23384966	7.61326173	3.24282533	0	3.08650952	A1+	NAC090, NAC domain containing protein 90 (NAC090); FUNCTIONS IN: sequence-specific DNA binding transcription factor activity; INVOLVED IN: multicellular organismal development, regulation of transcription
AT5G22680	23.38055	3.01395056	0.48238615	6.248004	4.16E-10	8.14E-09	5.32532476	5.61021808	5.54730575	2.60404218	0	1.80658324	A1+	F-box protein
AT5G23240	131.49702	-2.88144895	0.2544157	-11.3258	9.78E-30	9.18E-28	4.88181046	4.541804	5.20431899	7.52258607	7.86528529	8.17135078	A1+	ATDC17, DUC7E, DNA J PROTEIN C7E, DNAJ heat shock N-terminal domain-containing protein;
AT5G23240	103.41809	-2.54394015	0.27307225	-9.316	1.21E-20	5.96E-19	4.77764034	4.43775147	5.09722326	7.86466996	7.47011028	7.05301304	A1-	
AT5G23240	130.60801	-3.04555181	0.22516401	-13.5259	1.10E-41	5.92E-39	4.68326202	4.34760177	5.00812498	7.64769193	8.06191227	7.92871554	A2-	
AT5G24080	13.986962	2.753350104	0.55114855	4.995659	5.86E-07	7.30E-06	4.43723593	4.40038584	5.36448556	1.42937086	0	1.16932484	A1+	Protein kinase superfamily protein; FUNCTIONS IN: protein serine/threonine kinase activity, protein kinase activity, kinase activity, ATP binding; INVOLVED IN: protein amino acid phosphorylation;
AT5G24150	22.582887	3.09099771	0.52373227	5.901866	3.59E-09	6.18E-08	4.70774793	5.88699943	5.56625967	2.13309815	1.77337038	0	A1+	SQP1 squalene monooxygenase gene homolog, FUNCTIONS IN: squalene monooxygenase activity; INVOLVED IN: sterol biosynthetic process;
AT5G24150	22.547028	2.204167194	0.44176054	4.989507	6.05E-07	8.63E-06	4.60406405	5.78000894	5.45847607	2.19233088	2.66508652	2.83386398	A1-	
AT5G24240	48.621449	-4.14428579	0.54668537	-7.58075	3.44E-14	1.06E-12	0.64014872	1.39570492	0.69458906	3.48023337	7.19092088	7.07306901	A1+	ATP4Ky3 Encodes P4K3, localizes to the nucleus and has autophosphorylation activity, but no lipid kinase activity. Overexpression mutants display late-flowering phenotype.
AT5G24240	44.037252	-4.52354256	0.44592866	-10.1441	3.52E-24	2.12E-22	0.60238038	1.32916698	0.65346813	5.1978784	6.60240584	7.03064156	A1-	
AT5G26270	181.76099	-3.46970054	0.57880781	-5.99456	2.04E-09	3.68E-08	2.45099173	2.26485625	2.03284735	5.54593423	9.11592871	8.90881485	A1+	Transmembrane protein
AT5G26270	131.78805	-5.4112406	0.32024317	-16.8973	4.71E-64	1.38E-61	2.36338304	2.17930179	1.95036556	7.55345777	8.32894059	8.09685545	A1-	
AT5G26270	26.010065	-1.09839815	0.17851947	-6.15282	7.61E-10	1.07E-07	3.08744471	2.89389119	2.62615782	5.35807838	5.59295787	5.66312425	A2+	
AT5G28235	15.780963	-4.01914835	0.48984858	-8.20488	2.31E-16	8.56E-15	0	0	5.6379556	4.48353294	4.67351385	0	A1-	Ulp1 protease family protein
AT5G28235	8.6186294	-0.67585414	0.14446884	-4.6782	2.89E-06	2.74E-04	0	0	0	3.84180415	4.49088377	4.16096601	A2+	
AT5G28810	7.4244365	-3.06318733	0.51077939	-5.99708	2.01E-09	4.02E-08	0	0	0	4.04193303	3.54662372	4.27719887	A1-	
AT5G28810	18.29304	-1.20014933	0.16850073	-7.12252	1.06E-12	2.01E-10	0	0	0	5.20597357	5.49326367	4.94501561	A2+	
AT5G34780	116.67902	-2.3831593	0.20581137	-11.5793	5.24E-31	5.26E-29	5.1773142	5.16181962	5.25192365	7.60017557	7.78845734	7.49877138	A1+	Thiamin diphosphate-binding fold (THDP-binding) superfamily protein, FUNCTIONS IN: oxidoreductase activity, acting on the aldehyde or oxo group of donors, disulfide as acceptor, 2-dehydropanoate 2-reductase activity; INVOLVED IN: pantothenate biosynthetic process
AT5G34780	129.73309	-2.60427704	0.2121349	-12.2765	1.21E-34	1.22E-32	5.07244149	5.05607532	5.14472731	7.76557634	8.09526687	7.57761133	A1-	
AT5G34780	93.485269	-2.19949274	0.24437892	-9.00034	2.25E-19	2.53E-17	4.97738096	4.96435614	5.05553944	6.71318926	7.36372912	7.65325752	A2-	
AT5G34850	944.32802	7.955572999	0.36435753	21.83452	1.09E-105	1.75E-102	10.8638483	10.8782684	10.904541	0	0	2.8570496	A1+	Purple acid phosphatase 26
AT5G34850	874.99348	7.971465872	0.35623171	22.37719	6.56E-111	8.43E-108	10.7559408	10.7694278	10.7944023	1.13102597	0	1.01552275	A1-	
AT5G35375	24.187825	-3.3787582	0.57451982	-5.88101	4.08E-09	6.96E-08	1.08200738	0	0.69458906	2.13309815	6.20076121	6.09696739	A1+	Transmembrane protein
AT5G35375	6.5867773	-2.39768249	0.50898728	-4.71069	2.47E-06	3.16E-05	1.0260486	0	0.65346813	3.6894606	3.54662372	4.02896949	A1-	
AT5G37490	45.765071	3.024021674	0.41139248	7.350697	1.97E-13	5.69E-12	6.25542754	6.61950878	6.36862668	4.02144699	0	2.58406216	A1+	ARM repeat superfamily protein; FUNCTIONS IN: ubiquitin-protein ligase activity, binding; INVOLVED IN: response to chitin; LOCATED IN: ubiquitin ligase complex
AT5G38190	10.995175	-3.29884404	0.5863684	-5.52527	3.29E-08	4.95E-07	0	0	0	2.13309815	5.12346883	4.89377362	A1+	Myosin heavy chain-like protein
AT5G38700	33.545355	3.637127063	0.47726541	7.620764	2.52E-14	7.93E-13	6.05187904	5.74795637	6.29099423	2.13309815	0	1.80658324	A1+	Cotton fiber protein
AT5G39580	104.34109	2.599660144	0.35529524	7.316901	2.54E-13	7.25E-12	7.75501157	7.64387669	7.13077913	5.54593423	3.41603793	4.20843131	A1+	Peroxidase superfamily protein; FUNCTIONS IN: peroxidase activity, heme binding
AT5G41080	238.09943	-2.99889183	0.27380384	-10.9527	6.45E-28	4.76E-26	5.44274445	5.4380305	5.60153091	8.03799581	9.3739288	8.54254921	A1-	ATGDPD2, GDPD2, GLYCEROPHOSPHODIESTER PHOSPHODIESTERASE 2

AT5G41730	32.138556	3.617690398	0.47286316	7.650607	2.00E-14	6.35E-13	5.89824294	5.95179862	6.09609626	2.13309815	0	1.80658324	A1+	Protein kinase family protein; FUNCTIONS IN: protein serine/threonine/tyrosine kinase activity, kinase activity; INVOLVED IN: protein amino acid phosphorylation
AT5G42900	53.911358	3.72340193	0.39379189	-9.45525	3.22E-21	1.77E-19	2.83660846	2.91163087	2.03284735	6.13801551	6.42034895	7.27272211	A1+	COR27 cold regulated protein 27
AT5G42900	81.185868	-4.34402624	0.32579968	-13.3334	1.48E-40	1.94E-38	2.74425034	2.81768511	1.95036556	7.30468494	6.6257266	6.82502086	A1-	
AT5G42900	41.134378	-3.44235731	0.32840454	-10.4821	1.04E-25	1.95E-23	2.66124385	2.73683811	1.88283617	6.07704679	6.20471195	6.5677036	A2-	
AT5G44440	28.154109	-2.50095074	0.54151284	-4.61845	3.87E-06	4.17E-05	3.3126415	1.39570492	1.51362724	3.86258421	6.61088694	5.56118482	A1+	FAD-binding Berberine family protein; FUNCTIONS IN: electron carrier activity, oxidoreductase activity, FAD binding, catalytic activity
AT5G44440	27.099033	-2.78998043	0.43591836	-6.40024	1.55E-10	3.44E-09	3.21591338	1.32916698	1.44298843	5.97470154	5.76623828	5.19995635	A1-	
AT5G45570	297.16681	-4.7586928	0.56749137	-8.38549	5.05E-17	2.01E-15	0	0.62641448	1.16146642	3.24282533	9.68949857	9.89032466	A1+	Ulp1 protease family protein
AT5G45570	14.76882	-3.48682875	0.48212627	-7.23219	4.75E-13	1.33E-11	0	0.58898859	1.10157598	5.5672908	4.08983374	4.67351385	A1-	
AT5G45570	23.843422	-1.28999413	0.1729219	-7.45998	8.65E-14	1.95E-11	0	0.94032516	1.61801232	5.35807838	5.98427431	5.27615855	A2+	
AT5G45630	32.889554	-2.731748773	0.4358359	-6.267838	3.66E-10	7.25E-09	5.91168966	5.49318658	6.27955484	2.60404218	2.54523522	3.08650952	A1+	Senescence regulator (Protein of unknown function, DUF584)
AT5G47240	85.708358	-2.65904018	0.26187882	-10.1537	3.19E-24	2.23E-22	4.32110939	4.32411403	4.78618885	6.92152868	7.3490875	7.39553072	A1+	ATNUDT8, NUDIX HYDROLASE HOMOLOG 8, NUDT8, NUDX8
AT5G47240	65.642137	-2.25974846	0.29657505	-7.61948	2.55E-14	8.06E-13	4.21873955	4.22084958	4.68013474	7.20347287	6.75292342	6.35242641	A1-	
AT5G47240	117.24561	-3.31849837	0.21871803	-15.1725	5.38E-52	4.75E-49	4.12610626	4.13142977	4.59196332	7.73473151	7.74356126	7.80125719	A2-	
AT5G47850	41.329649	-2.777573796	0.41238081	-6.735458	1.63E-11	3.84E-10	5.95129379	6.44142257	6.31360446	4.02144699	1.77337038	2.58406216	A1+	CCR4, CRINKLY4 related 4 (CCR4); FUNCTIONS IN: kinase activity; INVOLVED IN: protein amino acid phosphorylation;
AT5G49160	621.24181	-2.65610947	0.23121494	-11.4876	1.52E-30	1.49E-28	6.85162926	7.72397513	6.33343334	10.3040046	10.2031247	9.66247896	A1+	Methyltransferase 1;
AT5G49160	4864.8109	-3.9411864	0.14971499	-26.3246	1.00E-152	2.67E-148	7.59383749	8.47831575	7.9974661	13.2507733	13.2298542	13.1413712	A2+	
AT5G51000	22.132615	3.746536459	0.55244669	6.781716	1.19E-11	2.85E-10	4.85421964	5.4399702	5.98779291	0	0	0	A1+	F-box and associated interaction domains-containing protein
AT5G52050	153.84908	3.01565808	0.32467389	9.288264	1.57E-20	8.19E-19	8.25971467	8.07467382	8.05021207	5.78621359	3.955229	4.10750664	A1+	MATE efflux family protein; FUNCTIONS IN: antiporter activity, drug transmembrane transporter activity; INVOLVED IN: drug transmembrane transport, transmembrane transport;
AT5G52310	634.27801	-2.36746606	0.43361792	-5.4598	4.77E-08	7.01E-07	7.26703204	7.52965372	7.09206701	8.9866795	10.0337226	10.7984041	A1+	RD29A, LTI78, LOW-TEMPERATURE-INDUCED 78, cold regulated gene, the 5' region of cor78 has cis-acting regulatory elements that can impart cold-regulated gene expression
AT5G52310	912.7899	-2.60889079	0.40505965	-6.44076	1.19E-10	4.76E-09	7.06242817	7.32727884	6.89159079	11.5756261	10.0556176	9.89681577	A2-	
AT5G52760	227.39833	3.408524221	0.25280876	13.48262	1.98E-41	3.39E-39	8.75166842	8.56148066	8.84119729	5.64689647	3.71067778	5.31182967	A1+	Copper transport protein family; BEST Arabidopsis thaliana protein match is: Heavy metal transport/detoxification superfamily protein (TAIR:AT5G52750.1).
AT5G54030	30.081129	3.817521017	0.53469357	7.139643	9.36E-13	2.55E-11	5.71097342	5.204992	6.5317972	1.42937086	0	0	A1+	Cysteine/Histidine-rich C1 domain protein
AT5G54030	32.621718	1.468889532	0.41912314	5.504673	4.57E-04	4.44E-03	5.50915439	5.00734922	6.33207437	4.69719315	3.83071993	1.71774955	A2-	
AT5G54710	17.21434	-2.91830967	0.54076751	-3.96607	6.79E-08	9.78E-07	9.00319506	9.07199571	9.57066007	6.06691588	3.04536424	4.47470153	A1+	Ankyrin repeat family protein
AT5G54720	124.54916	4.251240816	0.34855051	12.19691	3.23E-34	3.86E-32	7.84186202	6.68638708	8.17276186	4.02144699	2.54523522	2.8570496	A1+	
AT5G56870	3218.9635	-2.5523556	0.21911143	-11.6487	2.33E-31	2.41E-29	10.2790567	9.37460283	9.56242359	12.2312983	12.6990305	12.3441864	A1+	Beta-galactosidase 4 (BGAL4); INVOLVED IN: lactose catabolic process, using glucoside 3-dehydrogenase, carbohydrate metabolic process, lactose catabolic process via UDP-galactose, lactose catabolic process
AT5G56870	3255.3293	-2.64618991	0.22650787	-11.6826	1.57E-31	1.38E-29	10.1711792	9.26587255	9.45237657	12.2930832	12.8079266	12.252461	A1-	
AT5G56870	3536.1097	-2.73357111	0.27205923	-10.0477	9.40E-24	1.54E-21	10.0731938	9.1713746	9.36064531	11.8776745	12.8511952	12.9216918	A2-	
AT5G56970	17.34139	2.564109355	0.5072071	5.05535	4.30E-07	5.46E-06	4.85421964	4.84448128	5.38598118	2.60404218	0	1.80658324	A1+	CKX3 cytokinin oxidase 3 (CKX3); FUNCTIONS IN: primary amine oxidase activity, cytokinin dehydrogenase activity; INVOLVED IN: cytokinin catabolic process, It encodes a protein whose sequence is similar to cytokinin oxidase/dehydrogenase, which catalyzes the degradation of cytokinins
AT5G57010	26.819181	2.834448122	0.45553799	6.222199	4.90E-10	9.52E-09	5.7859039	5.6576071	5.56625967	2.13309815	0	3.08650952	A1+	Calmodulin-binding family protein
AT5G57640	45.988995	-2.84965525	0.40269648	-7.07643	1.48E-12	3.94E-11	3.6052331	2.91163087	3.07400535	5.49267367	7.04001448	6.27039654	A1+	GCK domain-containing protein
AT5G57640	36.547487	-2.612454	0.34523101	-7.56726	3.81E-14	1.18E-12	3.50644834	2.81768511	2.97734197	6.10513807	6.34233788	5.61520612	A1-	
AT5G57640	21.095763	-1.82454873	0.37221626	-4.90185	9.49E-07	1.92E-05	3.41727736	2.73683811	2.89746984	4.91161886	4.77911066	5.65014497	A2-	
AT5G58610	18.135488	2.607943255	0.51217469	5.091902	3.54E-07	4.55E-06	4.57882294	5.1397391	5.5086341	2.13309815	0	2.24707457	A1+	PHD finger transcription factor, putative; FUNCTIONS IN: RNA binding, DNA binding, zinc ion binding; INVOLVED IN: N-terminal protein myristoylation, regulation of transcription, DNA-dependent, response to chitin;
AT5G58750	35.853928	4.145916297	0.5182061	8.000516	1.24E-15	4.39E-14	5.74141419	5.97692474	6.64310204	1.42937086	0	0	A1+	Disease resistance protein (TIR-NBS-LRR class) family; FUNCTIONS IN: transmembrane receptor activity, nucleoside-triphosphatase activity, nucleotide binding, ATP binding; INVOLVED IN: signal transduction, defense response, apoptosis, innate immune response
AT5G58750	83.544962	0.694360839	0.1799485	3.858664	1.14E-04	0.00789776	6.47773795	6.72467098	7.37991092	4.84311283	6.03244207	5.69113504	A2+	
AT5G60100	101.21354	-3.23509598	0.29770894	-10.8666	1.66E-27	1.36E-25	4.19481075	4.36275392	3.8060034	6.92152868	7.83504327	7.72002383	A1+	Encodes pseudo-response regulator 3 (APRR3/PRR3). PRR3 transcript levels vary in a circadian pattern with peak expression at dusk under long and short day conditions. PRR3 affects the period of the circadian clock and seedlings with reduced levels of PRR3 have shorter periods, based on transcriptional assays of clock-regulated genes. PRR3 is expressed in the vasculature of cotyledons and leaves where it may help stabilize the TOC1 protein by preventing interactions between TOC1 and the F-box protein ZTL.
AT5G60100	73.01443	-2.85778932	0.25982639	-10.9988	3.87E-28	2.89E-26	4.09295198	4.2593408	3.70396919	7.09462095	7.07217374	6.94949098	A1-	
AT5G60100	77.164918	-2.93346609	0.28443554	-10.3133	6.14E-25	1.10E-22	4.00081328	4.16978335	3.61936292	6.92541626	6.78313965	7.57747433	A2-	
AT5G62480	155.57501	4.743709873	0.34720111	13.66272	1.70E-42	3.11E-40	8.15901254	8.10062543	8.47563218	3.48023337	0	3.4584494	A1+	GST14, ATGSTU9, GST14B, GLUTATHIONE S-TRANSFERASE 14B, glutathione S-transferase tau 9, GLUTATHIONE S-TRANSFERASE 14, Encodes glutathione transferase belonging to the tau class of GSTs
AT5G62480	368.82281	0.703960436	0.17658326	3.986564	6.70E-05	0.0048458	8.90423778	8.85560738	9.21662895	6.91939831	8.44286446	7.73202374	A2+	
AT5G64810	97.064133	3.331983388	0.31282743	10.65119	1.72E-26	1.34E-24	7.41127719	7.55906841	7.53844961	4.52436469	1.77337038	4.10750664	A1+	WRKY51 WRKY DNA-binding protein 51, member of WRKY Transcription Factor; Group II-c. Involved in jasmonic acid inducible defense responses
AT5G66620	78.807017	2.680791384	0.36757066	7.293268	3.03E-13	8.54E-12	6.9526569	7.22338921	7.25279528	5.12374266	1.77337038	3.88163585	A1+	DAR6, DA1-related protein 6 (DAR6); FUNCTIONS IN: zinc ion binding
AT5G66640	90.337731	2.736783793	0.40611597	6.738922	1.60E-11	3.75E-10	6.93958836	7.33933508	7.70163105	5.25747959	1.77337038	3.75388709	A1+	DAR3, DA1-related protein 3
AT5G67450	47.392557	3.592800662	0.42883906	8.37797	5.38E-17	2.14E-15	6.5240925	6.22778749	6.76295557	2.95850299	0	2.58406216	A1+	ZF1, zinc-finger protein 1, Encodes zinc-finger protein. mRNA levels are elevated in response to low temperature, cold temperatures and high salt. The protein is localized to the nucleus and acts as a transcriptional repressor

Supplementary Table 5: List of coding genes at least log₂-fold increases (negative log₂-fold change) or decreases (positive log₂-fold change) of 2.5 in at least one of the four lines A1+, A1, A2+ or A2-.

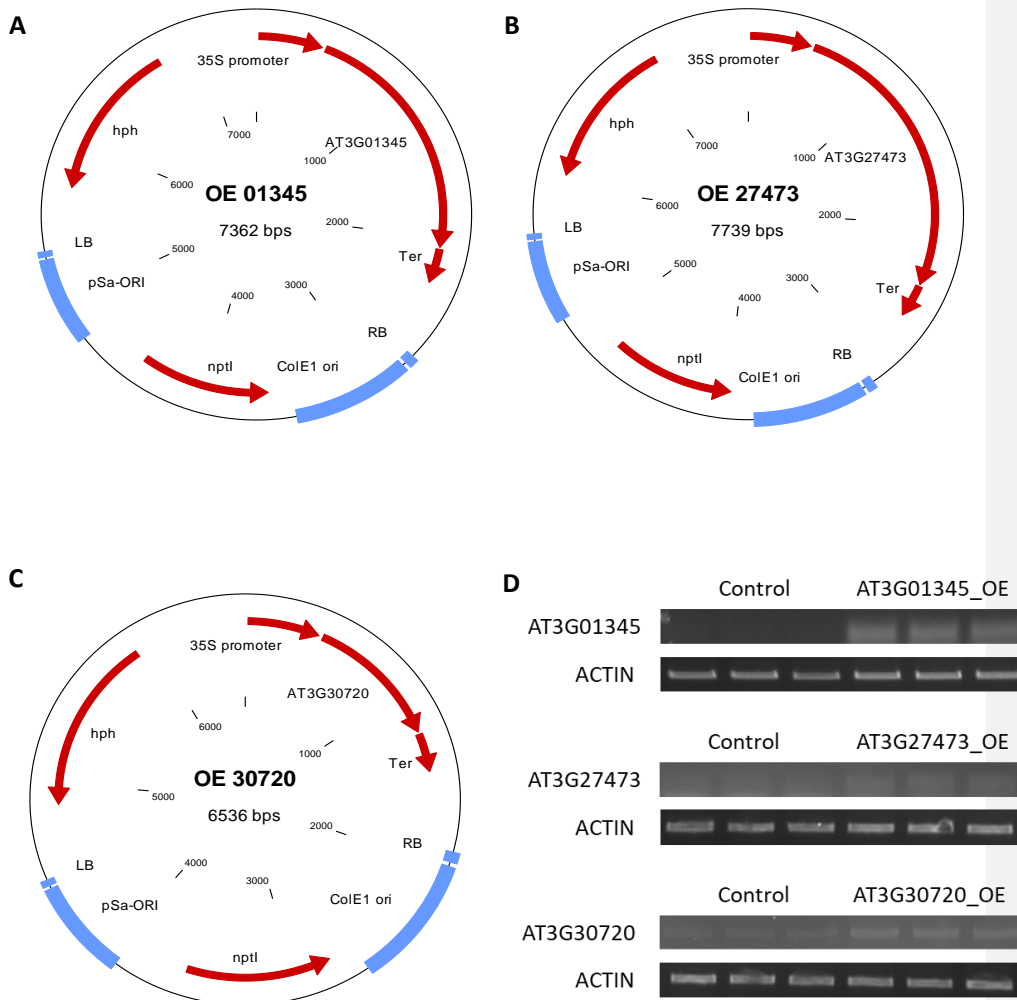
Gene ID	line	log ₂ -fold change	pvalue	Location of dense C methylation	Annotation
Increased transcript levels					
<i>AT2G34130</i>	A1+	-6.343	7.37E-42	genic	MEE19 maternal effect embryo arrest 19; hypothetical protein
	A1-	-1.855	0.000285		
	A2+	-2.970	5.17E-62		
<i>AT3G01345</i>	A1+	-7.076	4.86E-76	genic	Expressed protein
	A1-	-6.829	5.84E-86		
	A2+	-0.883	6.86E-08		
<i>AT3G21570</i>	A1+	-3.451	2.47E-09	genic	proline-rich nuclear receptor coactivator
	A1-	-1.949	0.000119		
<i>AT3G24542</i>	A1+	-5.551	8.93E-28	genic	Beta-galactosidase related protein
	A1-	-4.889	3.90E-26		
<i>AT3G53910</i>	A1+	-4.682	3.88E-18	genic	Malate dehydrogenase-like protein
	A1-	-3.701	8.64E-14		
<i>AT4G18150</i>	A1+	-5.660	7.99E-34	genic	Serine/Threonine-kinase, putative
	A1-	-5.388	3.45E-37		

<i>AT5G15360</i>	A1+	-4.214	6.81E-14	genic	Transmembrane protein
	A1-	-6.021	7.80E-51		
<i>AT5G26270</i>	A1+	-3.470	2.04E-09	genic	Transmembrane protein
	A1-	-5.411	4.71E-64		
<i>AT5G35375</i>	A1+	-3.379	4.08E-09	genic	Transmembrane protein
	A1-	-2.398	2.47E-06		
<i>AT5G01080</i>	A1+	-2.550	1.39E-05	upstream/ genic	Beta-galactosidase related protein
	A1-	-4.218	5.14E-21		
<i>AT3G27473</i>	A1+	-2.984	9.32E-09	upstream	Cysteine/Histidine-rich C1 domain family protein
	A1-	-1.797	0.000464		
<i>AT3G30775</i>	A1+	-1.205	1.18E-08	upstream	EARLY RESPONSIVE TO DEHYDRATION 5 (ERD5); Encodes a proline oxidase, its mRNA expression induced by high levels of AI and by osmotic stress. The promoter contains an L-proline-inducible element.
	A1-	-2.719	6.01E-38		
<i>AT4G09430</i>	A1+	-2.531	2.12E-06	upstream	Disease resistance protein (TIR-NBS-LRR class) family; with Natural antisense transcript At4G09432, FUNCTIONS IN: transmembrane receptor activity, ATP binding.
	A1-	-2.721	6.51E-09		
<i>AT4G25530</i>	A1+	-10.316	7.26E-118	upstream	FLOWERING WAGENINGEN, FWA, HDG6, HOMEODOMAIN GLABROUS6
	A1-	-3.858	3.10E-14		
	A2+	-2.503	7.00E-44		
<i>AT5G23240</i>	A1+	-2.881	9.78E-30	upstream	ATDJC17, DJC76, DNA J PROTEIN C76, DNAJ heat shock N-terminal domain-containing protein
	A1-	-2.544	1.21E-20		
	A2-	-3.046	1.10E-41		

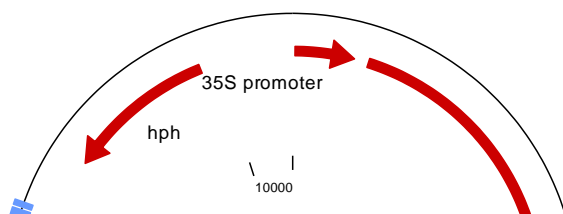
<i>AT5G24240</i>	A1+	-4.144	3.44E-14	upstream	Phosphoinositide 4-kinase PI4Kc3, Overexpression mutants display late-flowering phenotype.
	A1-	-4.524	3.52E-24		
<i>AT2G06904</i>	A1+	-5.267	1.48E-23	region	Nucleic acid / zinc ion binding protein
	A1-	-4.457	1.88E-20		
	A2+	-1.449	7.54E-17		
<i>AT2G07240</i>	A1+	-2.203	1.99E-04	region	Cysteine-type peptidase
	A1-	-3.788	2.22E-15		
<i>AT2G11778</i>	A1+	-9.461	1.53E-116	region	Transmembrane protein
	A1-	-8.981	6.08E-135		
	A2+	-2.911	2.75E-59		
<i>AT3G28193</i>	A1+	-3.823	3.92E-12	region	Transmembrane protein
	A1-	-4.477	2.58E-22		
<i>AT3G30720</i>	A1+	-4.185	2.57E-117	region	QQS qua-quine starch
	A1-	-3.951	2.41E-95		
	A2+	-0.748	6.70E-06		
<i>AT3G30770</i>	A1+	-5.097	4.01E-23	region	Eukaryotic aspartyl protease family protein
	A1-	-5.149	2.83E-31		
<i>AT3G31910</i>	A1+	-4.855	7.50E-24	region	Ulp1 protease family protein (DUF1985)
	A1-	-3.709	1.98E-15		
<i>AT3G42723</i>	A1+	-4.205	2.11E-15	region	ATP binding / aminoacyl-tRNA ligase/ nucleotide binding protein
	A1-	-2.870	5.22E-09		
<i>AT3G44070</i>	A1+	-5.709	4.19E-28	region	Glycosyl hydrolase family 35 protein

	A1-	-5.617	6.42E-37		
<i>AT3G44265</i>	A1+	-6.376	7.87E-46	region	Beta-galactosidase-like protein
	A1-	-5.866	2.31E-47		
	A2+	-0.549	8.62E-05		
<i>AT4G03950</i>	A1+	-3.246	2.27E-08	region	Nucleotide/sugar transporter family protein
	A1-	-3.250	4.93E-11		
<i>AT5G45570</i>	A1+	-4.759	5.05E-17	region	Ulp1 protease family protein
	A1-	-3.487	4.75E-13		
	A2+	-1.290	8.65E-14		
Reduced transcript levels					
<i>AT5G34850</i>	A1+	7.956	1.09E-105	upstream	Purple acid phosphatase 26
	A1-	7.971	6.56E-111		
Antagonistic transcript level changes in A1+ and A1-					
<i>AT3G50770</i>	A1+	2.816	3.50E-15	upstream	CML41, calmodulin-like 41 FUNCTIONS IN: calcium ion binding
	A1-	-0.948	0.00018459		
<i>AT4G00130</i>	A1+	2.452	6.56E-08	region	DNA-binding storekeeper protein-related transcriptional regulator

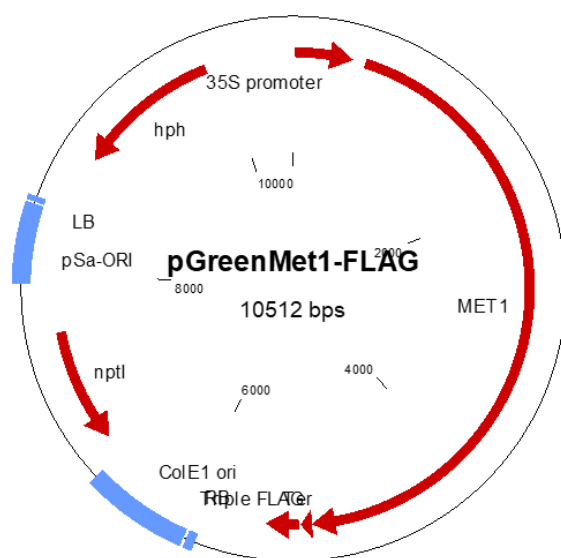
Supplementary Table 6: List of all coding genes with heritably increased (negative log₂-fold change) or reduced (positive log₂-fold change) transcript levels in the A1 lines with dense cytosine methylation in all three sequence contexts (CG, CHG, CHH).



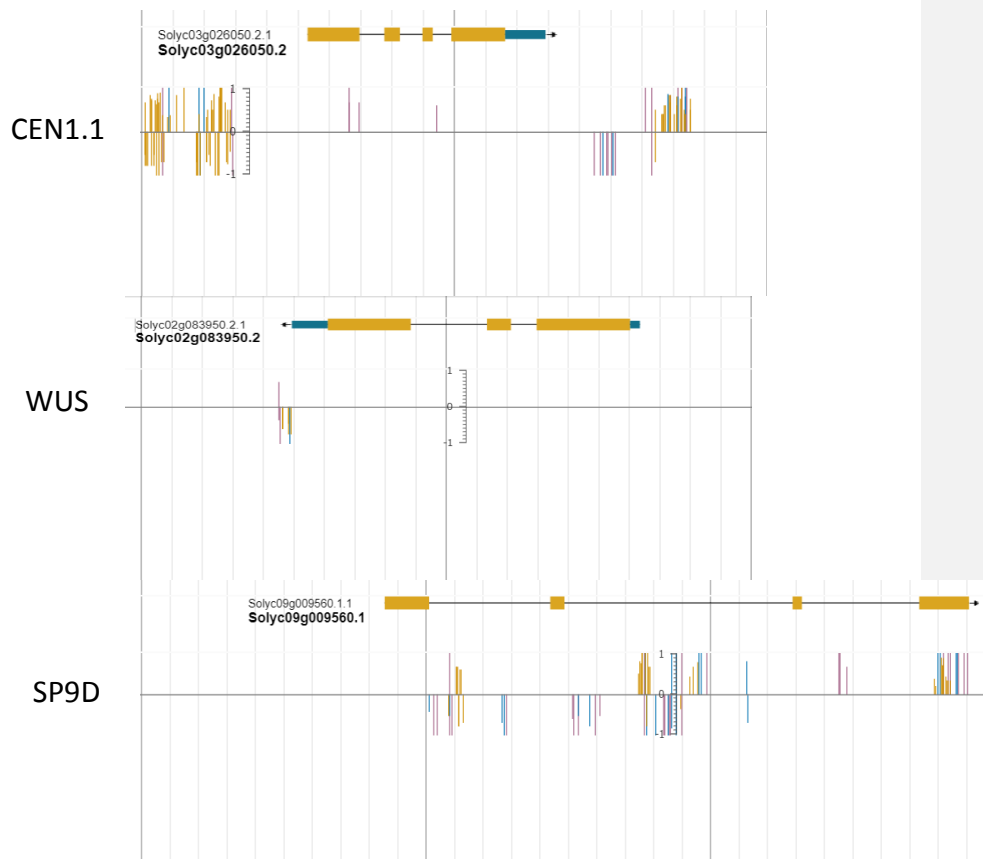
Supplementary Figure 1: Map and expression analysis of the three over-expression lines. A) AT3G01345 was inserted into the plant transformation vector 35S pGreen 0179, to produce the 35S AT3G01345 over-expression construct. B) AT3G27473 was inserted into the plant transformation vector 35S pGreen 0179, to produce the 35S AT3G27473 over-expression construct. C) AT3G30720 was inserted into the plant transformation vector 35S pGreen



0179, to produce the 35S AT3G30720 over-expression construct. D) cDNA was generated from seedlings 4 weeks after stratification. Greater transcript levels were detected for all over-expression lines (AT3G01345, AT3G27473, AT3G30720). EF1 α was used as a standardizing control to ensure equal concentration of input cDNA.



Supplementary Figure 2: Maps of the FLAG-tagged MET1. A triple FLAG sequence was inserted at the 3' end of the catalytically active MET1 construct.



Supplementary Figure 3: Bisulphite analysis of CEN1.1, WUS, SP9D. Methylation data from tomato epigenome database. Yellow bars indicate the presence of CG methylation, blue indicates the presence of CHG methylation and red indicate the presence of methylation in a CHH context. Two Genes, CEN1.1 and WUS, possess dense DNA methylation adjacent to the gene. SP9D contains dense methylation within the gen. Methylation profiles in the three genes were extracted from <http://epigenome.genetics.uga.edu/PlantMethylome/>.